Western Australian School of Mines

Orebody Characterization using Measure-While-Drilling Data

Daniel Goldstein

0000-0001-6140-6942

This thesis is presented for the Degree of

Doctor of Philosophy

of

Curtin University

September 2025

Declaration

To the best of my knowledge and belief this thesis contains no material previously published by any other person except where due acknowledgment has been made.

This thesis contains no material which has been accepted for the award of any other degree or diploma in any university.

Signature: *Daniel Goldstein*

Date: *30 September 2025*

Abstract

Enhancing orebody knowledge through real-time data acquisition and advanced analytics is critical for optimizing mine planning and production efficiency. This research investigates the integration of Measure-While-Drilling (MWD) data with machine learning (ML) techniques to improve geotechnical, geophysical and geochemical characterization in open-pit mining. Traditional methods rely on sparse and costly exploration drill holes, leading to significant uncertainties in subsurface geological models. By leveraging MWD data, which provides continuous, cost-effective drilling performance metrics, this study applies feature selection algorithms and ML models to predict key geotechnical, geophysical and geochemical properties, including rock strength, stratigraphic units and mineral compositions. Decision Trees, Support Vector Machines, Random Forests and Gaussian Processes were evaluated, with Random Forests achieving the highest predictive accuracy (up to $R^2 = 0.98$). Additionally, novel MWD-derived variables, such as the ratio of bit air pressure to penetration rate, were identified as significant predictors of ore quality. The findings demonstrate the potential for MWD-driven ML models to provide high-resolution, real-time orebody characterization, reducing the reliance on resource-definition drilling and enhancing operational decision-making. This research contributes to the advancement of data-driven orebody intelligence, subsurface modelling and mine-grade control strategies in the mining industry.

Acknowledgements

I would like to sincerely thank my supervisors Professor Chris Aldrich, Dr Quanxi Shao and Dr Louisa O'Connor for all their support, encouragement and guidance throughout the project.

I would also like to thank Kim le Roux and James Jung for their professional support during this project.

Thank you also to my wonderful family, Amanda, Jackson, Oliver and Ashton.

List of Publications Included in this Thesis

Paper	Publication	Cite-Score	Ranking
A	Goldstein, D. M., Aldrich, C., & O'Connor, L. (2024). A Review of Orebody Knowledge Enhancement Using Machine Learning on Open-Pit Mine Measure-While-Drilling Data. *Machine Learning and Knowledge Extraction*, *6(2),* 1343-1360. https://doi.org/10.3390/make6020063	9.9	Q1 (Engineering (misc.))
B	Goldstein, D., Aldrich, C., Shao, Q., & O'Connor, L. (2025). A Field-Scale Framework for Assessing the Influence of Measure-While-Drilling Variables on Geotechnical Characterization Using a Boruta-SHAP Approach. *Mining*, 5(1), 20. https://doi.org/10.3390/mining5010020	4.0	Q2 (Geology)
C	Goldstein, D., Aldrich, C., Shao, Q., & O'Connor, L. (2025). A Machine Learning Classification Approach to Geotechnical Characterization Using Measure-While-Drilling Data. *Geosciences*, 15(3), 93. https://doi.org/10.3390/geosciences15030093	5.3	Q1 (General Earth and Planetary Sciences)
D	Goldstein, D., Aldrich, C., Shao, Q., & O'Connor, L. (2025). Unlocking Subsurface Geology: A Case Study with Measure-While-Drilling Data and Machine Learning. *Minerals, 15(3),* 241. https://doi.org/10.3390/min15030241	4.4	Q1 (Geology)
E	Goldstein, D. M., Aldrich, C., & O'Connor, L. (2024). Enhancing Orebody Knowledge using Measure-While-Drilling Data: A Machine Learning Approach. *IFAC-PapersOnLine, 58(22)*, 72-76. https://doi.org/10.1016/j.ifacol.2024.09.293.	1.8	N/A

Co-Authorship Statement

This thesis includes published manuscripts that have been co-authored with members of the PhD supervision team and contributions of each author are detailed below:

Daniel Goldstein was responsible for the conceptualization, methodology, data collection, data analysis, machine learning model development, interpretation of results and manuscript drafting. He conducted all experiments, implemented computational models and synthesized findings into the final manuscripts.

Prof. Chris Aldrich, Dr. Louisa O'Connor and Dr. Quanxi Shao provided supervision, guidance and academic oversight throughout the research. Their contributions were primarily in the form of reviewing and providing feedback on manuscript drafts prior to submission.

All authors have read and approved the final versions of the manuscripts submitted for publication as part of this thesis. The primary responsibility for the research, analysis and writing lies with Daniel Goldstein, while the supervision team provided essential academic mentorship and manuscript review.

Copyright

I have obtained permission from the copyright owners where necessary to use any third-party copyright material reproduced in the thesis (e.g. questionnaires, artwork, unpublished letters), or to use any of my own published work (e.g. journal articles) in which the copyright is held by another party (e.g. publisher, co-author).

Open Access Statement

All papers included in this thesis have been published under open access licenses, ensuring unrestricted access to the research findings for the global scientific community. These publications are freely available in accordance with the policies of the respective journals and publishers.

The open access status of these papers aligns with the commitment to promoting transparency, knowledge dissemination and accessibility in research. By making the findings openly available, this thesis contributes to the broader scientific discourse and facilitates the application of data-driven orebody characterization methods in the mining industry and related fields.

The open access licenses allow for the reuse and distribution of the research, provided proper attribution is given to the original authors. The full texts of all included papers can be accessed through their respective journal websites or institutional repositories.

Acknowledgement of Country

We acknowledge that Curtin University works across hundreds of traditional lands and custodial groups in Australia and with First Nations people around the globe. We wish to pay our deepest respects to their ancestors and members of their communities, past, present and to their emerging leaders. Our passion and commitment to work with all Australians and peoples from across the world, including our First Nations peoples are at the core of the work we do, reflective of our institutions' values and commitment to our role as leaders in the Reconciliation space in Australia.

Contents

Chapter 1: Introduction

1.1 Background and Context

The mining industry is undergoing a rapid digital transformation, driven by increasing demands for automation, real-time data and improved decision-making across the resources value chain. Orebody Knowledge (OBK) is a critical enabler of efficient mine planning, grade control and processing optimization. Accurate, high-resolution characterization of subsurface geological, geotechnical and geochemical properties enables better control over each step of the mining value chain, from blast design and fragmentation to processing recovery and waste management. Improved OBK not only reduces operational uncertainty and cost but also supports safer, more sustainable and adaptive mine planning practices, which are critical in the context of rising social, environmental and regulatory pressures.

Among the digital tools available, Measure-While-Drilling (MWD) technology presents a significant opportunity to advance OBK through the real-time collection of drilling response data during blast hole drilling. MWD systems provide continuous measurements such as rate of penetration, torque, weight on bit and air pressure, at minimal additional cost.

Despite MWD systems having been used in open-pit mining for decades, their analytical potential remains largely untapped. Most sites interpret MWD signals only at a broad scale to flag major lithological changes or drilling issues. Broader use has been restricted because: (i) the data are high-frequency and highly variable due to rig, operator and condition effects, demanding advanced analytics, (ii) integrating MWD with geotechnical, geophysical and geochemical data requires precise spatial alignment that operations rarely achieve and (iii) conventional statistics cannot model the nonlinear links between drilling mechanics and rock properties. As a result, systematic orebody characterization from MWD has been limited. This thesis addresses that gap using machine-learning methods capable of capturing these complex, operational-scale interactions.

This research addresses this gap by leveraging an unusually comprehensive, production-scale dataset from a large open-pit iron ore operation in Western Australia. The dataset integrates thousands of MWD records across multiple rigs with high-quality, spatially aligned geotechnical logs, geophysical wireline logs and laboratory-based geochemical assays representing a rare field-scale resource for machine learning-based orebody characterization.

Another digital tool, machine learning (ML), has demonstrated value in modelling complex, non-linear relationships within geoscientific data. When combined with large volumes of MWD observations, ML offers a pathway to automate and scale subsurface characterization, potentially replacing or augmenting traditional exploratory drilling and laboratory testing. This thesis explores the intersection of leveraging MWD data and ML algorithms.

This research is novel and advances the state-of-the-art by:

- Developing and validating a unified, model-agnostic analytical framework that integrates MWD data with machine learning to predict geotechnical, geophysical and geochemical properties at sub-meter resolution.
- Applying and comparing feature importance techniques across multiple domains to identify the most influential MWD inputs and improve model interpretability for operational use.

Demonstrated through five peer-reviewed studies, real-time MWD data can augment or replace traditional exploration methods to deliver enhanced OBK across the mining value chain.

1.2 Research Aim and Objectives

The aim of this thesis is to develop and validate a data-driven framework that leverages MWD data and ML techniques to enhance orebody knowledge in open-pit mining. By integrating geotechnical, geophysical and geochemical analysis, this research seeks to establish a scalable and cost-effective methodology for subsurface characterization, ultimately improving mine planning, resource estimation and operational decision-making.

To operationalize this aim, the research was structured around the following objectives:

1. Review existing applications of MWD data and ML techniques in subsurface characterization to identify gaps and limitations.

2. Develop regression models for predicting geotechnical properties using interpretable feature-importance approaches.
3. Develop classification models capable of identifying stratigraphy and geotechnical domains from MWD responses.
4. Establish ML frameworks for predicting geophysical properties from MWD data and assess their capacity to serve as surrogates for wireline logs.
5. Evaluate the potential of MWD data to approximate geochemical assay results and quantify predictive performance across multiple impurity elements.
6. Synthesize findings across all modelling domains to produce a unified, operationally scalable framework for MWD-driven orebody intelligence.

These objectives align directly with the five peer-reviewed papers that form the core of the thesis.

Although geological classification is an important component of orebody characterisation, the available dataset for this study contained substantially higher-quality and more spatially consistent measurements for geotechnical, geophysical and geochemical properties. In contrast, the geological labels exhibited greater uncertainty due to variable logging practices, inconsistent stratigraphic boundaries and fewer intervals with high-confidence lithological control.

These limitations reduce the reliability of supervised geological modelling at operational scale. For this reason, the thesis focuses on the domains where data density, label quality and operational relevance are strongest, while geological classification is addressed in Paper C in a constrained and methodologically appropriate manner.

A key focus is the application of feature importance techniques alongside supervised ML models to identify the most influential MWD variables and to quantify their predictive relationship with subsurface properties. By identifying the most influential MWD parameters, this research aims to enhance interpretability and provide actionable insights into the underlying geological, geotechnical and geochemical conditions.

This thesis is distinguished by its use of a rare, multivariate dataset collected at full operational scale and by the systematic application of explainable ML techniques across diverse orebody attributes. The methodological rigor and domain breadth strengthen the reliability, generalizability and operational relevance of the findings.

1.3 Significance

This study holds significant value in advancing the use of MWD data and ML techniques to enhance orebody knowledge in open-pit mining. The mining industry increasingly relies on data-driven approaches to optimize orebody characterization, reducing operational costs while improving efficiency. Traditional subsurface characterization methods rely heavily on sparse and costly exploration drilling, leading to uncertainties in mine planning and operational decision-making.

By leveraging MWD data with predictive ML models and feature importance techniques, this research provides a high-resolution, data-driven approach to understanding geotechnical, geophysical and geochemical properties in real time. Moreover, it establishes a scalable framework for orebody characterization that can be adapted across various mining environments. The findings contribute to both academic knowledge and industry practice, offering a pathway towards more efficient and sustainable mining operations.

This significance of this study contributes to the mining industry by:

- Improving mine planning and resource estimation by integrating MWD data with ML models.
- Better predictive insights into subsurface conditions, reducing geological uncertainty and optimizing resource allocation and supporting more informed decision-making in open-pit mining.
- Enhancing operational efficiency and safety through the real-time application of MWD-based predictive models, which can support decision-making in drilling, blasting and excavation
- Reducing costs and improving sustainability via a data-driven approach minimizes reliance on expensive exploration drilling

and laboratory testing while maximizing the value of existing MWD datasets.

- Advancing digital transformation in mining by contributing to the broader shift towards automation and digitalization in the mining industry, promoting the adoption of AI-driven decision-support systems.

1.4 Structure of the Thesis

This thesis is structured as a collection of five published, peer-reviewed journal papers, each addressing a key aspect of orebody knowledge enhancement using MWD data:

- Chapter 1 - Background, Context, Research Aims and Objectives, Significance and Thesis Structure
- Chapter 2 - Data and Methodology
- Chapter 3 - Literature Review of MWD and ML in mining (Paper A)
- Chapter 4 - Feature importance and development of geotechnical regression ML models (Paper B).
- Chapter 5 - Feature importance and classification of geotechnical conditions using ML (Paper C).
- Chapter 6 - Feature importance and prediction of geophysical properties from MWD data using ML (Paper D).
- Chapter 7 - Feature importance and estimation of geochemical composition using MWD and ML (Paper E).
- Chapter 8 - Synthesis of findings, implications for industry and recommendations for future research.
- References - A list of all works cited in the publications
- Appendix: Peer review comments and responses for publications

While each published paper is self-contained, the chapters collectively implement a progressive analytical framework. Paper A synthesises the broader literature and situates the research within the state of knowledge. Paper B establishes the foundations for geotechnical regression and interpretable feature importance, Paper C extends these insights into categorical geotechnical classification, Paper D expands the framework to geophysical property prediction, and Paper E applies similar techniques to geochemical analysis. This structure reflects a logical progression from understanding MWD behaviour, to applying predictive models across increasingly complex subsurface domains.

While the analytical framework is consistent across Papers B-E, the specific modelling and feature-selection methods differ to reflect domain-specific challenges:

- Boruta-SHAP was chosen for Paper B because it provides model-agnostic variable importance suitable for high-noise geotechnical labels.
- Paper C employed MRMR and ReliefF, which are effective for multi-class categorical classification where redundancy and local neighbourhood structure strongly influence separability.
- Papers D and E used MARS and PPR to capture non-linear additive behaviours in geophysical and geochemical responses.

Similarly, differences in dataset selection (one pit versus two pits) reflect the availability of validated reference measurements in each domain. These methodological divergences ensure that each task uses the most technically appropriate approach while remaining aligned with the overarching framework.

This research demonstrates that certain MWD variables are important for prediction of orebody properties and multivariate MWD data. Combined with ML, a scalable and cost-effective solution is presented for improving orebody knowledge and optimizing mining operations.

Chapter 2: Data and Methodology

The analytical approach developed in this thesis is model agnostic and designed to flexibly integrate MWD data with multiple subsurface property domains via ML. The framework prioritizes generalizability, interpretability and practicality for implementation in real mining operations.

The framework comprises five sequential stages (Figure 2.1). While feature selection and importance analysis are shown as preceding model training, these stages can also be an iterative process. Model-derived importance measures obtained after initial training can be used to refine the features and improve subsequent modelling cycles.

1. Input data aggregation, during which raw MWD metrics are combined with domain-specific reference data:
    a. Geotechnical measurements, including Unconfined Compressive Strength, Fractures per Meter, Geological Strength Index
    b. Wireline geophysical logs, including gamma radiation, density, magnetic susceptibility and caliper
    c. Geochemical assays, including iron percentage, phosphorous, sulfur, alumina and silica
2. Preprocessing and feature engineering, which includes cleaning erroneous values, smoothing noise and computing derived variables, such as MWD ratios and a moving standard deviation. Spatial alignment with reference datasets is performed for supervised learning compatibility.
3. Feature selection and importance analysis, during which model-independent methods rank the predictive relevance of each MWD metric. These algorithms include Boruta-SHAP (Paper B), ReliefF (Paper C) MARS (Papers D and E) and PPR (Paper D).
4. Model training and selection, in which a suite of ML models is implemented for both regression and classification, including Decision Trees, Random Forests, Support Vector Machines, Gaussian Processes and Neural Networks. Models are trained using 80/20 splits and 10-fold cross-validation.
5. Model evaluation and deployment, during which performance metrics include R^2 and RMSE for regression and accuracy and confusion matrices for classification. Results are interpreted statistically and operationally.

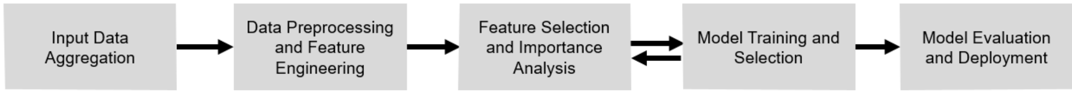

Figure 2.1 Analytical framework for MWD-based subsurface characterization. Feature selection and variable importance analysis can occur before and after model training, allowing for an iterative workflow in which modelling outcomes inform subsequent feature refinement.

This workflow is applied consistently across four modelling domains, including geotechnical regression (Paper B), geotechnical classification (Paper C), geophysical regression (Paper D) and geochemical regression (Paper E). The generalized workflow illustrated in Figure 2.1 serves as the methodological foundation for this thesis. The next sections describe the datasets and modelling approach used to implement this framework across four domains (geotechnical regression, geotechnical classification, geophysical regression and geochemical regression), each corresponding to a distinct research objective.

2.1 Introduction

This chapter outlines the data sources, preprocessing steps and modelling methodologies employed to integrate MWD data with ML techniques for enhanced orebody characterization in open-pit mining. The research employs a combination of statistical analysis, ML algorithms, feature importance techniques and supervised learning algorithms across geotechnical, geophysical and geochemical domains.

Given the thesis by compilation format, the methods are structured around the five core research objectives. Each objective targets a distinct modelling challenge and is addressed through an associated peer-reviewed journal publication. Table 2.1 summarizes these objectives and the corresponding peer-reviewed, published papers.

Table 2.1: Summary of research objectives, focus areas and corresponding peer-reviewed, published papers.

Research Objectives	Output Type and Domain	Summary	Paper	Publication	Cite-Score	Ranking
1. To review existing applications of MWD data and ML algorithms in subsurface characterization	Literature Review MWD	Review of intersections between MWD and ML for open-pit rock characterization	A	Goldstein, Aldrich and O'Connor 2024a	9.9	Q1 (Engineering (misc.))
2. To develop regression models for predicting geotechnical properties, such as rock strength and fracture frequency, using feature-importance techniques	Regression Geotechnical	Predict rock strength parameters (UCS, FPM, GSI) from MWD using Boruta-SHAP for feature ranking	B	Goldstein, Aldrich, Shao and O'Connor 2025c	4.0	Q2 (Geology)
3. To classify rock mass conditions and geotechnical categories based on MWD responses	Classification Geotechnical	Classify rock types, stratigraphy and strength classes using interpretable ML classifiers	C	Goldstein, Aldrich, Shao and O'Connor 2025b	5.3	Q1 (General Earth and Planetary Sciences)
4. To establish predictive models for geophysical attributes, including density, gamma radiation and magnetic susceptibility	Regression Geophysical	Model gamma, density and magnetic logs using nonparametric regression with MWD inputs	D	Goldstein, Aldrich, Shao and O'Connor 2025a	4.4	Q1 (Geology)
5. To apply ML techniques to estimate orebody geochemical properties, including iron, phosphorus and sulfur content, using MWD data	Regression Geochemical	Predict ore chemistry (e.g., %Fe, P, S, Al_2O_3, SiO_2) from drilling response data using MARS	E	Goldstein, Aldrich and O'Connor 2024b	1.8	N/A

Acronyms: a) rop = rate of penetration, b) tor = torque, c) wob = weight on bit, d) bap = bit air pressure and e) rpm = rotations per minute.

The remainder of this chapter is organized as follows: Section 2.2 describes the study area, MWD exploration datasets and data preprocessing. Section 2.3 introduces the ML models used for feature importance, regression and classification predictions. Section 2.4 details model validation procedures and performance metrics. Section 2.5 documents the software and computational infrastructure used in this study.

2.2 Data Collection and Preprocessing

2.2.1 Study Area and Data Sources

Data for this study were sourced from an open-pit iron ore mine in the Pilbara region of Western Australia. The deposit is hosted within a banded iron formation (BIF) sequence typical of Pilbara iron ore operations, comprising interlayered hematite-goethite mineralisation, chert bands and structurally deformed shale units. The near-surface profile includes a well-developed detrital and CID (channel iron deposit) horizon, underlain by variably weathered BIF transitioning into fresh, competent material at depth. Local folding and faulting contribute to lithological variability and influence both rock mass strength and geophysical responses. This geological context provides the structural and stratigraphic framework within which MWD responses and target properties must be interpreted.

Due to commercial confidentiality requirements associated with the operational dataset, the precise number of MWD records, blast holes and exploration intervals cannot be disclosed. However, the dataset is sufficiently large to support model training, validation and testing across all domains, with each blasthole contributing on the order of tens to hundreds of depth-resolved measurements per variable. All modelling results presented in this thesis reflect the full operational dataset provided, and only aggregated outcomes—not raw counts or identifiable operational metrics—are reported. Predictor and target variables were selected based on their data completeness, spatial reliability and operational relevance, ensuring that each supervised learning task was built on the highest-quality labels available within the constraints of the confidential dataset.

The key data sources include:

- MWD sensor readings from open pit blasthole drilling rigs capturing

  - Penetration rate (*rop*) is the drilling speed, which is influenced by rock strength and other drilling variables
  - Torque (*tor*) is the rotational pressure on the drill bit, which is sensitive to lithological changes and rock fractures
  - Force on bit (*wob*) is the downward force applied on the bit
  - Bit air pressure (*bap*) is the pneumatic pressure to clear cuttings from the bottom of the drillhole
- Wireline geophysical measurements from exploration diamond and Reverse Circulation (RC) drillholes, including density (*dens*), gamma radiation (*gamma*), magnetic susceptibility (*magsus*), resistivity (*res*) and hole diameter (*cal*).
- Laboratory assays for geochemical composition from exploration RC drilled holes, including percent iron (%Fe), phosphorus (P), sulfur (S), alumina (Al_2O_3) and silica (SiO_2).
- Geotechnical field logs from exploration diamond drilled core holes containing fracture frequency per meter (FPM) and categorial Stratigraphic Unit, Rock/Soil Strength, Rock Type and Weathering,
- Laboratory testing results from exploration diamond drilled core samples for Uniaxial Compressive Strength (UCS)
- Calculated rock mass classification system scores and categories from exploration diamond drilled core holes for Geological Strength Index (GSI)

An important consideration in this study is the integration of datasets with inherently different temporal and spatial resolutions. MWD sensor readings are captured at high frequency during blasthole drilling, with measurements recorded at approximately 0.1 m intervals along each hole. For a typical 10 m production hole, around 100 records per variable are recorded in minutes. In contrast, laboratory geochemical assays from exploration drilling are generally collected at much coarser intervals consisting of a 2 m composite of rock chips, often years prior to production drilling in the same area. Similarly, geotechnical logs from core drilling are recorded at 0.01m scale while geotechnical laboratory samples are limited to selective intervals based on the logger’s judgement. Wireline geophysical responses are continuously recorded at 0.01m spacing from the bottom of the hole to the collar at the beginning.

These discrepancies necessitate careful spatial alignment and interpolation or aggregation of high-frequency operationally-sourced MWD data to match the coarser, irregularly spaced exploration-sourced reference measurements. Such integration challenges influence label density for supervised learning and can affect model generalization, particularly in zones where reference data are sparse or highly variable.

2.2.2 Data Preprocessing

To ensure data consistency and accuracy, the following preprocessing steps were applied:

1. Feature engineering by computing derived variables, such as force-on-bit ratios and moving standard deviations.
2. Noise removal by filtering unreliable MWD readings (e.g., negative values, extreme outliers) using interquartile range detection and smoothing.
3. Fusion of MWD data with spatially aligned exploration drilling results for supervised ML training.

The engineered features were selected to capture drilling mechanics behaviors that are not directly observable from raw measurements. For example, ratios such as bap/rop highlight cuttings removal efficiency relative to penetration rate, while moving standard deviations emphasize short-scale transitions associated with fractures, voids or material changes. These transformations provide physically interpretable signals that improve predictive performance. “Fusion” refers specifically to the spatial integration of depth-matched MWD observations with exploration-derived labels so that each training instance contains both predictor and response variables.

2.3 ML methodology

2.3.1 Feature Selection versus Feature Importance

Feature selection and feature importance serve complementary roles within the modelling workflow. Feature selection methods, such as MRMR and ReliefF identify subsets of variables that maximize predictive relevance while reducing redundancy that ultimately improve stability of classification models. In contrast, feature importance algorithms such as Boruta-SHAP, MARS and PPR quantify the relative contribution of each variable to model outputs without necessarily removing predictors.

The choice of algorithm in each paper reflects the characteristics of the target domain:

- Classification tasks benefit from reduced feature redundancy
- Regression tasks emphasize interpretability via importance ranking

2.3.2 ML Models

The ML models used in this thesis span several families chosen to balance predictive performance, interpretability and operational feasibility across the prediction tasks in Papers B-E.

- Decision Trees and Random Forests offer transparent, rule-based structures suited to heterogeneous inputs
- Support Vector Machines handle high-dimensional decision boundaries
- Gaussian Processes provide smooth, probabilistic functional estimates
- Neural Networks model complex feature interactions with appropriate tuning.

Each paper applies the following common analytical framework

- An 80/20 data split
- A consistent cross-validation strategy
- Shared performance metrics that differ in the specific output variable, data source and domain-specific challenge addressed.

2.3.3 Geotechnical Regression (Paper B)

- Target OBK characteristics included UCS, FPM, GSI.
- Feature importance analysis using Boruta-SHapley Additive Explanations (Boruta-SHAP) identified key MWD variables contributing to model performance and all measured and engineered variables outperformed shadow variables.
- Decision Trees (DT), Random Forest (RF), Support Vector Regression (SVR), Gaussian Process Regression (GPR) and Neural Networks (NN) were trained to predict UCS rock strength, FPM fracture frequency and GSI rock mass classification scores.
- Model performance was assessed using Coefficient of determination (R^2) and root mean square error (RMSE) values for validation and testing data.

2.3.4 Geotechnical Classification (Paper C)

- Target OBK characteristics included lithology, stratigraphic unit, rock strength class and weathering intensity.
- Feature selection analysis using Minimum Redundancy Maximum Relevance and ReliefF identified all measured MWD variables as contributing to model performance.
- DT, RF, SVM, K-Nearest Neighbors (KNN), Linear Discriminant Analysis (LDA) and Naïve Bayes (NB) were trained to predict Categorial geotechnical properties, including Lithology, Stratigraphic Unit, Rock/Soil Strength, Rock Type and Weathering.
- Model performance was assessed using validation and testing accuracies, validation costs and confusion matrices.

2.3.5 Geophysical Regression (Paper D)

- Target OBK characteristics included gamma, density, magnetic susceptibility, resistivity and caliper.
- Feature importance was performed using Multivariate Adaptive Regression Splines (MARS) and Project Pursuit Regression (PPR) to identify critical MWD features.

- Downhole wireline sonde geophysical measurements, including density, gamma, magnetic susceptibility, resistivity and caliper, were predicted using DT, RF, SVM, GP and NN.
- Model performance was assessed using R^2 and RMSE values for validation and testing data.

2.3.6 Geochemical Regression (Paper E)

- Target OBK characteristics included %Fe, P, S, Al_2O_3, SiO_2.
- MARS was applied to determine the most important MWD variables for geochemical predictions.
- %Fe as well as geochemical impurities, such as P, S, Al_2O_3 and SiO_2, were modelled using Linear Regression (LR), DT, RF, SVM, GP and NN.
- Model performance was assessed using R^2 and RMSE values for validation and testing data.

While the framework evaluates a diverse suite of ML models for each prediction task, the adequacy of different model families for MWD-based orebody characterization has been considered. Linear models are interpretable and computationally efficient. On the other hand, they are generally limited in capturing the highly non-linear and interacting relationships between drilling responses and subsurface properties observed in this dataset. Non-linear models, such as RF, GP and NN, provide higher predictive accuracy by modelling complex interactions. However, they occur at the cost of increased computational need and reduced interpretability.

From an operational perspective, there is also a trade-off between optimizing model performance for each domain (geotechnical, geophysical, geochemical) and deploying a single, general-purpose model across all tasks. For example, a multilayer perceptron could be adapted to predict all property types from MWD inputs. This approach simplifies maintenance, integration and training pipelines. However, domain-specific models often achieve superior accuracy by tailoring hyperparameters, feature sets and architectures to the characteristics of the target property. In production operations, the decision between these approaches will depend on the relative importance of predictive performance, interpretability, ease of deployment and maintenance overhead.

2.4. Model Evaluation and Validation

To ensure robustness, ML models were built using:

- An 80/20 split was used, with 80% of the data allocated to training and validation and 20% reserved for independent testing.
- A 10-fold cross-validation procedure was applied within the training/validation portion to ensure model tuning and evaluation on independent subsets.
- Regression model were evaluated using Coefficient of determination (R^2) and root mean square error (RMSE) as performance metrics.
- Classification models were evaluated using validation accuracy, testing accuracy, validation costs and confusion matrices as performance metrics.
- In the Boruta framework, shadow variables are randomly permuted duplicates of the predictors that establish a baseline for determining whether a real variable carries meaningful signal beyond noise. In Chapter 4, this method is applied to assess the feature importance of MWD variables, using SHAP scores to compare each predictor against its shadow counterpart.
- Feature importance rankings were validated for stability across folds and modelling approaches. Transparency and interpretability were prioritized to support operational uptake.

2.5. Software and Hardware

- MATLAB was used for data processing, calculation of Boruta-SHAP values as well as ML predictive model development using the Regression Learner and Classification Learner toolboxes
- The earth and stats packages in R were used to compute the MARS and PPR feature importance scores, respectively
- Computations were performed on a Pawsey Supercomputer Nimbus cloud Ubuntu instance with 8 vCPUs and 32 GB of memory.

Chapter 3: Paper A

A Review of Orebody Knowledge Enhancement Using Machine Learning on Open-Pit Mine Measure-While-Drilling Data.

Goldstein, D. M., Aldrich, C., & O'Connor, L. (2024). A Review of Orebody Knowledge Enhancement Using Machine Learning on Open-Pit Mine Measure-While-Drilling Data. *Machine Learning and Knowledge Extraction*, *6(2),* 1343-1360. https://doi.org/10.3390/make6020063 *machine learning & knowledge extraction*

Review

A Review of Orebody Knowledge Enhancement Using Machine Learning on Open-Pit Mine Measure-While-Drilling Data

Daniel M. Goldstein *, Chris Aldrich and Louisa O'Connor

Western Australian School of Mines: Minerals, Energy and Chemical Engineering, Curtin University, GPO Box U1987, Perth, WA 6845, Australia; chris.aldrich@curtin.edu.au (C.A.); louisa.oconnor@riotinto.com (L.O.)
* Correspondence: 20878119@student.curtin.edu.au

Abstract: Measure while drilling (MWD) refers to the acquisition of real-time data associated with the drilling process, including information related to the geological characteristics encountered in hard-rock mining. The availability of large quantities of low-cost MWD data from blast holes compared to expensive and sparsely collected orebody knowledge (OBK) data from exploration drill holes make the former more desirable for characterizing pre-excavation subsurface conditions. Machine learning (ML) plays a critical role in the real-time or near-real-time analysis of MWD data to enable timely enhancement of OBK for operational purposes. Applications can be categorized into three areas, focused on the mechanical properties of the rock mass, the lithology of the rock, as well as, related to that, the estimation of the geochemical species in the rock mass. From a review of the open literature, the following can be concluded: (i) The most important MWD metrics are the rate of penetration (rop), torque (tor), weight on bit (wob), bit air pressure (bap), and drill rotation speed (rpm). (ii) Multilayer perceptron analysis has mostly been used, followed by Gaussian processes and other methods, mainly to identify rock types. (iii) Recent advances in deep learning methods designed to deal with unstructured data, such as borehole images and vibrational signals, have not yet been fully exploited, although this is an emerging trend. (iv) Significant recent developments in explainable artificial intelligence could also be used to better advantage in understanding the association between MWD metrics and the mechanical and geochemical structure and properties of drilled rock.

Keywords: measure-while-drilling (MWD); logging-while-drilling (LWD); open-pit mining; subsurface characterization; machine learning (ML); data acquisition; rock properties; geochemical analysis; artificial intelligence (AI); predictive modelling; feature importance

check for updates

Citation: Goldstein, D.M.; Aldrich, C.; O'Connor, L. A Review of Orebody Knowledge Enhancement Using Machine Learning on Open-Pit Mine Measure-While-Drilling Data. *Mach. Learn. Knowl. Extr.* **2024**, *6*, 1343–1360. https://doi.org/10.3390/make6020063

Academic Editors: Liang Zhao, Liang Zou and Boxiang Dong

Received: 22 February 2024
Revised: 1 June 2024
Accepted: 5 June 2024
Published: 18 June 2024

1. Introduction

Measurement while drilling (MWD) originated from Schlumberger's downhole electrical logging system in 1911, which was exclusively successful within the oil industry [1]. They described MWD as a system of sensors collecting performance data during rock drilling of open-pit mining production blast holes that can be correlated with pre-excavation subsurface conditions. Using MWD as a characterization system is desirable due to the low cost and high resolution of blast holes. On the other hand, exploration drill holes are expensive and are rarely collected in comparison.

While MWD was introduced to the open-pit mining environment in the 1970s, its use to characterize the subsurface was limited due to the high volume of analogue data to manually analyse. To address this limitation, computerized data acquisition of MWD variables to broadly determine lithological boundaries in open-pit mining was introduced around the 1980s [2–7]. Evolving from this initial use of computerized MWD rock recognition, this literature review focuses on the progression of advancing analytics, including machine learning (ML) algorithms, in MWD data to determine the geotechnical, geological, and geochemical subsurface characteristics before open-pit mining.

To perform the above correlations, multiple MWD metrics are collected by researchers. Depending on the manufacturer system setup, MWD datapoints are generated as time series or depth series in blast holes ranging from 10 m deep in surface iron ore mines to over 60 m in open-pit coal mines [8]. The most common variables acquired in open-pit mining MWD systems are time, depth, rate of penetration (rop), torque or rotational pressure (tor), bit air pressure (bap; also called flushing air pressure), weight on bit (wob; also called weight on rods, thrust, or feed pressure), and rotary speed or revolutions per minute (rpm) [9]. Other less commonly collected variables are the drilling acoustic changes and vibrations of the drill rods [10].

Due to the continuous nature of drill and blast cycles for excavation in open-pit operations, enormous quantities of MWD datapoints are collected. Due to this sheer volume of data to analyse, researchers have recently begun applying artificial intelligence to MWD datasets to understand nonlinear trends between drill responses and subsurface composition. For instance, a single productive rig at an open-pit iron ore mine may drill around one hundred 10–12 m blast holes per day, generating a minimum of 10,000 MWD observations with several responses per observation, including rop, tor, wob, bap, and rpm [11]. Many major iron ore mines employ around a dozen simultaneously operating blast drills. Despite the abundance of data, as shown in Section 2 most studies have focused on broad classification of rock types or hardness using rop to denote lithological boundaries rather than detailed characterization of each rock type. In industry, mine technical services professionals are not necessarily appropriately skilled to analyse large volumes of data in the brief time period between drilling blast holes and loading of explosives.

The objective of this study is to present a systematic and thorough examination of the existing body of research pertaining to the utilization of ML algorithms in the analysis of MWD data for the purpose of characterizing rock in mining operations. Furthermore, this study incorporates a comprehensive analysis of algorithms employed for assessing the significance of each metric related to the MWD technique, in relation to variations in the subsurface, such as rock strength, fracture frequency, elemental composition, and density. Additionally, it explores the potential of ML algorithms and their prospective utilization in forthcoming applications. Figure 1 presents a flowchart that describes the research framework of this study. Section 2 presents a concise summary of the dissemination of scholarly literature through journals and the prevailing patterns in publications. Section 3 details the development of ML models from MWD data. In Section 4, this study presents the pragmatic implementations of data analysis derived from MWD techniques in the domains of geology identification using density; gamma; magnetic susceptibility and resistivity responses; assessment of rock mass characteristics, including rock strength, fracture frequency and rock mass classification scores; and geochemical composition, such as iron percentage as well as primary and secondary contaminants. These applications are expounded upon in Sections 4.1–4.3, respectively. Section 5 presents an exposition on the challenges and potential associated with the application of ML techniques for rock characterization utilizing MWD data. The concluding remarks are presented in Section 6.

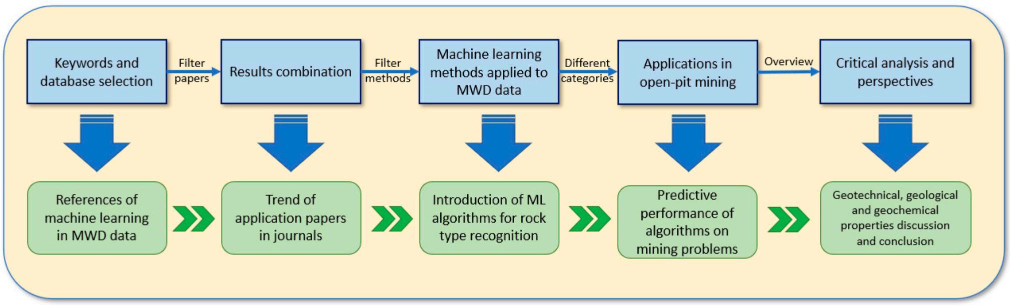

Figure 1. Research framework for review of machine learning (ML) of mining MWD data.

2. Literature Sources and Dissemination

As indicated by the literature review process, the publication of papers on this topic spans around thirty years. A total of 537 research articles mentioning "Measure-While-Drilling" or "Measurement-While-Drilling" have been indexed in Google Scholar (GS) from the late 1980s to the present, as shown in Figure 2's yellow bars. Nonetheless, when the search results are filtered to studies employing MWD to strictly characterize the rock being drilled, there are just 129 publications. The 129 articles are organized according to the year of publication, as shown in Figure 2's green bars. Indeed, the use of MWD data for rock characterization is limited in the first decade of the twenty-first century, whereas the number of papers has expanded dramatically in the last decade, with twenty-six publications expected in 2022. When the search parameters are restricted to using MWD to strictly characterize the rock being drilled using ML approaches, there are just 32 publications with a rapid employment of ML algorithms since 2016, shown in blue in Figure 2.

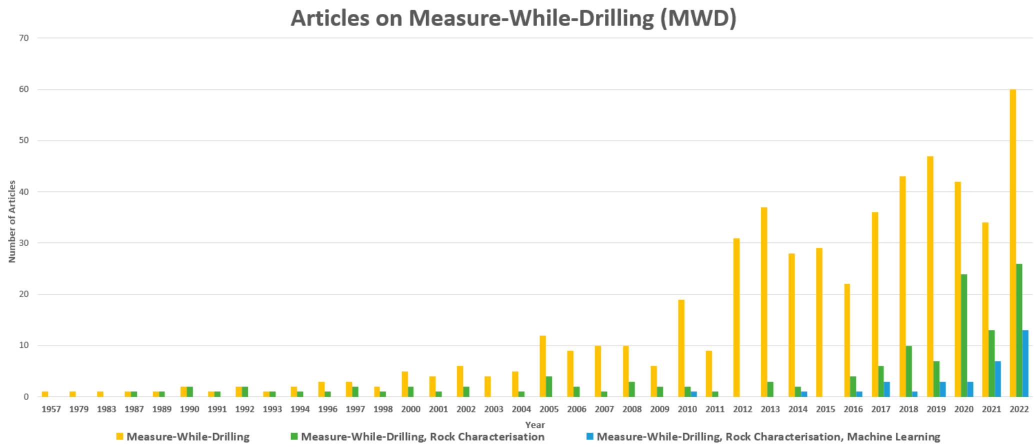

Figure 2. Annual distribution of published journal papers mentioning MWD for rock characterization in all excavation types using ML from 1997 to 2022.

To address readers' academic interests in characterizing rock types using ML techniques on MWD data in open-pit mining, more journal articles than conference papers have been published. While master's and doctorate dissertations were not featured on GS, a few of them have been published [12–17]. The leading journals are Mathematical Geosciences and Minerals, which have published over 22% of the discoveries concentrating on the use of ML on MWD data for open-pit mining rock characterization. Each of the remaining journals has published one paper.

Several ML techniques were applied to characterize rock conditions using MWD data in the reports identified with the GS search parameters. There are generally two types of ML techniques used in those findings: neural networks (NNs) [12,16,18–20] and Gaussian process (GP) [8,11,21]. Other approaches, including support vector machines (SVMs), random forests (RFs), boosting, self-organizing maps (SOMs), and fuzzy logic, have been compared to NNs in various studies [19,20]. Generally, the selection of any particular ML model would depend on its predictive power, its interpretability, and, to some extent, also the complexity of the data to be processed. Relevant studies to ML analysis of open-pit mining MWD data is presented in Table 1.

Table 1. Summary of ML applications on MWD data for open-pit mining rock characterization.

Approach	Application	Model *	Commodity	Holes	Target	Comment **	References
Supervised	Classification	HOP	Coal	35	Rock Type	Input of full-waveform sonic velocity	[22]
		LB	Iron Ore	28	Rock Type	2D analysis; drill data averaged per hole	[20]
		FIS	Iron Ore	28	Rock Type	2D analysis; drill data averaged per hole	[20]
		GP	Iron Ore	31	Rock Type	Labels exclusive of 1 m from contact	[8]
			Iron Ore	N/A	Rock Type	BIF and shale in Brockman Formation	[11]
			Iron Ore	N/A	Rock Type	CWT preprocessing of MWD data	[8]
		LoR	Marble	204	Grade	6 classes of marble quality tested	[23]
		NN	Coal	17	Rock Type	Backpropagation	[16]
			Iron Ore	33	Rock Type	Feedforward and Backpropagation	[12]
			Iron Ore	28	Rock Type	2D analysis; drill data averaged per hole	[20]
		RF	Coal	35	Rock Type	ANN compares thresholding of SEM	[18]
			Marble	204	Grade	6 classes of marble quality tested	[23]
	Regression	GP RF SVM	Iron Ore	7000	Grade	Iron percentage, Phosphorous, Sulphur, Aluminum Oxide, Silicon Dioxide	[24]
Unsupervised	Feature Importance	PCA	Coal	17	Rock Type	Used as validation of 3 input features	[16]
			Iron Ore	33	Rock Type	To investigate specific fracture energy	[12]
			Iron ore	302	Rock Type	Used for individual index calculation	[25]
	Change Detection	PCA	Marble	4	Rock Type	Intrusion detection of marble	[26]
	Clustering	AS	Coal	35	Rock Type	Seam roof detection to cease drilling	[27]
		KMC	Coal	17	Rock Type	4 class clusters identified	[16]
		GP	Iron Ore	138	Rock Type	2D analysis; drill data averaged per hole	[21]
			Iron Ore	14,340	Grade	Gaussian kernel	[28]
		HMM	Marble	3	Rock Type	Sudden material type transition	[29]
		NN	Iron Ore	33	Rock Type	Simple competitive learning	[12]
		SOM	Coal	17	Rock Type	3, 4 and 5 class maps for rock types	[16]
			Iron Ore	33	Rock Type	3 class maps for 3 major rock types	[12]
		SVM	Iron Ore	14,340	Grade	2D analysis; drill data averaged per hole	[28]

* HOP: higher order polynomial, LB: LogitBoost, FIS: fuzzy inference system, GP: Gaussian process, LoR: logistic regression, NN: neural network, RF: random forest, SVM: support vector machines, PCA: principal component analysis, AS: adaptive sampling, KMC: K-means clustering, HMM: hidden Markov model and SOM: self-organizing maps. ** BIF: banded iron formation and CWT: continuous wavelet transformation.

For example, while linear models or simple decision trees may not have the same predictive power as multilayer perceptrons or support vector machines, it may be easier to interpret the results generated by these models. Likewise, deep learning models, such as convolutional neural networks or vision transformers may be better able to analyse more complex signals and images than traditional multilayer perceptrons or random forests and can also be coupled with explanatory models, where required. Further investigations of these trade-offs could yield significant advances in the field.

3. Development of Machine Learning Models from MWD Data

The development of machine learning models comprises multiple discrete stages, depicted in Figure 3. The process begins with data in its unrefined state, a phase commonly known as data preprocessing (Figure 3A). Here, the focus is on improving the consistency and integrity of the data. In the case of sequential data, such as time-series data, it is often necessary to adjust or eliminate identifiable patterns and trends. Furthermore, to provide a cohesive basis for the following stages, any discrepancies resulting from different intervals of data recording are reconciled.

Feature engineering is the segment that follows preprocessing. In this phase, data is transformed into a form that computer algorithms can easily understand (Figure 3B). When confronted with complex data types, such as images or sound signals, it is necessary to perform transformations to convert them into a structured format. Depending on the ML model, a crucial aspect of this stage could entail reducing redundancy by replacing groups of interconnected variables with a more succinct set that encompasses most of the initial information. After suitably structuring the data, it is segregated into distinct subsets known as training, validation, and test datasets (Figure 3C). The training data functions as the fundamental dataset upon which the model is initially constructed. The utilisation of a validation set facilitates the process of refining the model, whilst the test set is specifically put aside to act as a benchmark for assessing the model's performance in real-world situations.

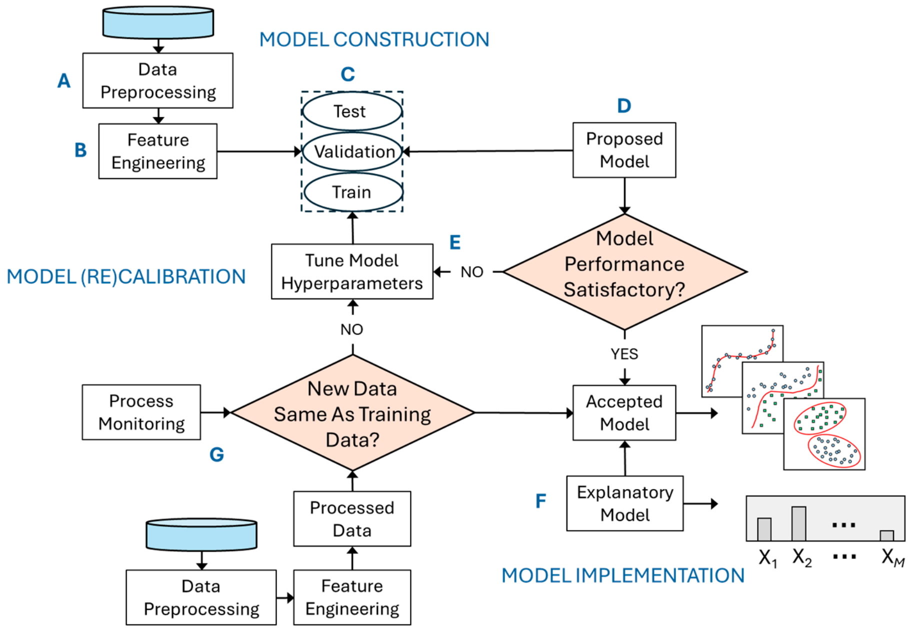

Figure 3. A general methodology for the building of ML models for the interpretation of data, including data preprocessing (A), feature engineering (B), structuring of training, validation and test sets (C) model validation (D), model optimisation (E), construction of a complementary explanatory model (F) validation of new data (G) prior to implementation of the model.

After data partitioning, the focus shifts to the training of the model itself (Figure 3D). There is a wide array of models available for this purpose, encompassing neural networks, decision trees, and support vector machines. The selection of a model is primarily contingent upon the characteristics of the data and the goals of the research. If the proposed model's performance is not acceptable, then the model's hyperparameters can be tuned (Figure 3E), then trained, validated, and tested (Figure 3C) before acceptable predictions can be made. In situations where it is necessary to explain the reasoning behind a model's decisions, particularly in diagnostic contexts, an additional explanatory model can be developed (Figure 3F). Nevertheless, if the decisions made by the primary model possess intrinsic transparency, this step may be deemed unnecessary.

Ultimately, when novel datasets are introduced, they undergo identical preliminary phases of preprocessing and feature engineering as the initial training data (Figure 3G). An essential component of this phase involves determining the statistical similarity between the newly acquired data and the first training dataset, although this is not necessarily always done in practice. Several analytical techniques, such as principal component analysis and t-stochastic neighbour approaches, offer valuable insights into this congruence. If a noticeable discrepancy exists between the datasets, it may be necessary to recalibrate the model.

4. Practical Applications

4.1. Geology Recognition from MWD

This part pertains to the utilization of ML techniques on MWD data to understand the intricate relationships between drilling metrics and forecast subsurface geological conditions before commencing mining operations. For example, a banded iron formation (BIF) deposit might have classification zones of shale and BIF. These broad categorization of geological zones from MWD data are useful for identifying the contacts between highly contrasting material types to update a deposit-scale model and increase its accuracy within localized areas [8]. This increased accuracy leads to improved blasting outcomes, in terms of achieving fragmentation around geological boundaries. However, these nongranular assortments do not necessarily provide resolution within each lithological unit that are required to optimize mining operations downstream of the drill and blast process, including excavation, haulage, and beneficiation.

First, an overview of the various types of geological deposits in which MWD data have been used to identify geology in open-pit mining operations is presented. The next section critically reviews the types of analysis performed by researchers to understand which MWD metrics are important to describe changing subsurface conditions from a data science perspective, including lithology, density, rock strength, and weathering or fracture intensity. Several authors have used principal component analysis (PCA) to interpret feature importance [12,16,25]. However, it is worth noting that PCA is generally not an effective approach for rating the significance of input variables. The final section details the application of ML to categorize rock types from MWD data. The classification methods employed by previous studies can be improved upon gaining a granular comprehension of the changing subsurface geological conditions.

4.1.1. Mined Commodities

Most researchers delineating lithologies from MWD data in open-pit mining have focused on sedimentary commodities, predominantly iron ore and coal. In these deposits, the resource geology has been reasonably defined by exploration drilling at hole spacings of 50 m grids in iron ore and 100–200 m grids in coal. The use of MWD data attempts to add local accuracies in between the exploration drillholes through blast holes located at approximately 5 m burden and spacing. Most of the research to recognize subsurface geology from drilling metrics has taken place in Canada [7,12,16] and Australia [8,11,18,20–22,27]. These countries have had strong research collaboration between the mining industry and universities.

The initial findings to link six open-pit blast hole drilling responses with the subsurface geology via the use of downhole geophysical responses was the basis for later work [7]. Nearly 20 years later, postgraduate research applied NN for open-pit geological classification from MWD datasets in coal and iron ore mining blast holes [12,16]. Since these earlier Canadian-based studies, research on open-pit classification of geology has been entirely within Australian coal and iron ore deposits. The research in coal geology recognition aimed to accurately predict coal roof locations to prevent blast damage in open-pit mining with several reports presenting the results of various ML classification methods on the same MWD dataset from 35 blast holes in the Australian Hunter Valley coal region [18,22,27]. A few years later, coal seams in six gas wells were identified with 96% accuracy from the Surat Basin using five categorization algorithms [19]. In the iron ore industry, various classification methods were used on datasets of 28 holes and approximately 120 holes were utilized [20,21]. Both studies successfully distinguished BIF rock from shale in the Pilbara region to improve fragmentation by tailoring explosive loading for each rock unit. Nearly a decade later, multiple findings from the University of Sydney presented successful classification of BIF and shale units from a significantly larger dataset of several thousand blast holes [8,11].

While the majority of rock type recognition has occurred in open-pit mining in Canada and Australia, examples from civil engineering, tunnelling, oil and gas, and other mining industries have also been investigated. MWD data were used to distinguish geological zones in an urban construction project from Hong Kong. In the tunnelling industry, MWD data were also used to predict geology ahead of blasting in the Norwegian Loren, Swedish Stockholm Bypass, and the Chinese Jiuding Shan projects [30–32]. The use of MWD data within the oil and gas sector has demonstrated their efficacy in the classification of lithology within narrow targets [33–36]. This classification aids to attain precise directional drilling, hence optimizing the selection of well locations. In the underground coal mining industry, linear correlation and ML algorithms were applied to MWD data from roof support drills to determine geological zones and adjust locations and spacings of rock bolts and cable bolts to improve ground support [37–40]. In the open-pit quarry industry, successful use of MWD metrics to observe sill and marble boundaries was reported in four blast holes and altered explosive loading practices to achieve optimal fragmentation, which prevented unnecessary rock breaking off boulders from under-blasting [29]. More recently, six classes of marble qualities were predicted using Logistical Regression and RF [23]. All the above examples establish the wider applicability of determining geology from MWD data outside of open-pit mining of sedimentary deposits.

4.1.2. MWD Metrics

MWD metrics (rop, tor, fob, wob, rpm, etc.) have shown varying levels of feature importance when correlated with subsurface geological conditions [41]. Feature importance refers to methods that calculate a score for each of the MWD metrics in a particular model. The resulting scores represent the contribution of each feature in the prediction of the target variable.

A high score indicates that the characteristic will have a greater influence on the model used to forecast a particular subsurface geological variable. Initial manual attempts to interpret the feature importance of open-pit mining MWD variables with wireline gamma responses identified local minimum and maximum variations; the changes in rop, tor, wob, and SED parameters were associated with different lithological factors [7]. They also reported that rpm did not significantly correlate with any rock type, due to being controlled by the operator at a relatively constant rate. However, these univariate experiments each focused on an isolated, individual drilling parameter. Indeed, all other drilling metrics were required to be maintained near constant in these studies, which is unrealistic for common production blast hole drilling. An example of a surface blast hole drill rig is presented in Figure 4 (left), together with the typical MWD variables collected (Figure 4, right).

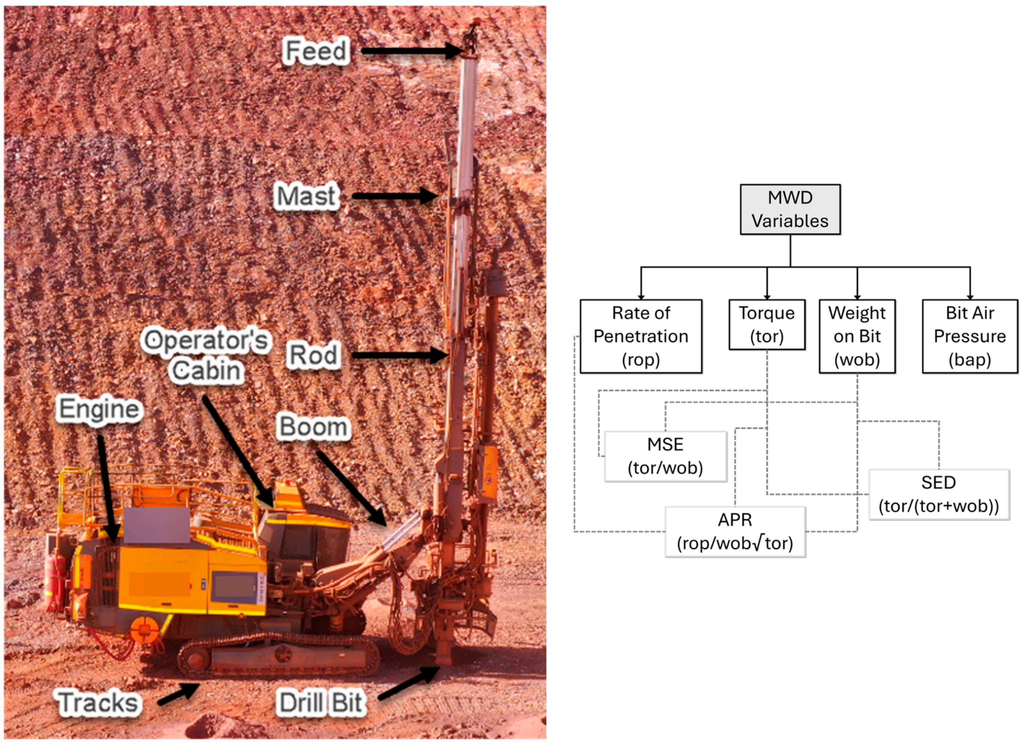

Figure 4. Typical layout of a surface mining blast drill rig (Type: Epiroc D65) (**left**) and MWD variables (**right**).

Early attempts to manually interpret the feature importance for each MWD input metric on rock type recognition models have given way to more advanced analytical methods, primarily principal component analysis (PCA). PCA aims to show patterns in multivariate data by reducing the dimensionality of these datasets and creating new variables, called principal components [42]. The principal components are a set of orthogonal vectors that are linear combinations of the input variables and best describe which of these inputs represent the most variation to the data. The rop and tor were identified as the MWD metrics that were most closely linked with subsurface geological conditions, while rpm was the least significant [12,16]. Both researchers identified feature importance by using the loading plots that detailed the most variation (the first and second principal components), although this may not necessarily account for most of the variation in the target variable. PCA has also been applied to determine coal vs. non-coal rock types by including gamma response and hole diameter as inputs along with the MWD metrics of rop, wob, and tor [19]. This work also applied a fit-for-purpose feature importance algorithm based on random forests and determined that the rate of penetration was the single most important MWD metric to classify coal vs. non-coal rock types in the investigated holes. The wob, tor, and rpm were presented as relatively insignificant compared to rop [19].

Several studies introduced derived drilling metrics calculated from the collected MWD variables to determine if derived features were more important than the raw drilling metrics. Modulated specific energy (MSE) takes advantage of the variations in the ratio of tor to wob to identify rock type in coal blast holes [18]. SEM is calculated by modifying the specific energy of drilling (SED) with a rotational work fraction, which is determined by dividing the tor by the sum of the tor and the wob. They reported SEM as an important feature from the drilling metrics to detect boundaries of multiple coal seams amongst predominantly sandstone units. A second novel drilling parameter called adjusted penetrate rate (APR) was developed to account for variations between drilling operators in manually operated rigs as well as between manual and autonomous drilling rigs in iron ore blast holes [21]. APR is calculated by dividing the rop by the product of the wob the square root of tor. Their finding reported APR was a more important feature than SED for the categorization of iron ore rock types of BIF waste, mineralized BIF and shale. rule-based labelling of geology from multiple drilling metrics outperformed the univariate APR method of rock type recognition [8]. However, not all variables are consistently collected in open-pit iron ore production drilling conditions due to sensor faults or breakdowns [8]. As a result, the missing data have resulted in up to 90% of blast hole observations not being able to be used for APR and SED.

Determination of feature importance reveals which variables are essential to collect for accurate prediction of rock type. Conversely, feature importance should identify which features may be discarded during selection of variables to include for subsequent analysis using ML algorithms. As mentioned previously, the use of PCA on MWD data for the selection of features with the highest variation as the most important predictors may not be effective. In contrast, developments in interpretable and explainable AI have opened significantly more advanced approaches for this purpose. This could include Shapley value regression, permutation analysis, interpretation of model structures, kernel SHAP, LIME, etc., and in the case of deep learning models, also even direct interpretation of image or signal data, where applicable [43–45].

4.1.3. Machine Learning Classification

Classification of geology using ML methods on open-pit blast hole MWD data has been demonstrated on mostly small datasets of a few dozen holes. Feature engineering has consistently been applied to clean noisy MWD data, including filtering, smoothing, normalizing, and removing outliers to prepare the raw data for ML analysis. Although a range of different ML models have been used, multilayer perceptrons and Gaussian process regression have featured prominently in recent studies, as discussed in Section 2.

NN algorithms have demonstrated the probability of geological recognition in both iron ore and coal deposits. The classification accuracy for five rock types reached 95% using back propagation neural network (BPNN) algorithms on 17 blast holes from a Canadian coal mine [16]. The classification accuracy for three rock types in an iron ore deposit averaged 57% based on 33 blast holes in the United States [12]. One study used NN as an assessment tool to determine if the SEM metric was superior to APR to identify lithologies, while another study demonstrated a prediction accuracy of 96% using NN to classify coal and non-coal rock types [18,19]. A multilayer perceptron NN algorithm classified four BIF rock types at 78% accuracy [20].

GPs have been exclusively used at the Pilbara BIF iron ore mines to classify geology. GP clustering of hardness values (approximated by regression modelling of APR) was used to categorize three types of iron ore units (waste BIF, mineralized ore, and shale) [21]. The figures presented are two-dimensional, indicating the researchers used an average MWD value for each hole to classify geology. This two-dimensional method provides a singular rock type, and thus, a limited perspective for mine planning. In a novel three-dimensional method, MWD datapoints were labelled with categorized units from downhole gamma responses [11]. The GP approximations resulted in a thresholding strategy that classified two BIF units in the Dales Gorge Member in three blast patterns at 87%, 84%, and 81% accuracy, respectively. GP-derived results were reported as only 62% accurate to classify two rock types (unmineralized shale and mineralized iron ore) [8]. They attributed this poor performance to noisy data requiring further data cleaning.

The use of NN and GP algorithms on MWD metrics has been largely successful in classifying rock types. Several findings reported other ML algorithms, including fuzzy inference systems (FISs), SVM, random forest (RF), and boosting to compare results with NNs, but none demonstrated significantly better performance to NNs [19,20]. Despite ML classification accuracy being greater than 90%, the prediction of a handful of broad geological categories does not adequately capture subtle differences within each geological unit. An increased resolution of rock type (including subcategories, such as massive, fractured, or deformed rock) is required for informed and effective mine planning.

4.2. Rock Mass Properties from MWD

Rock mass quality has been correlated with drilling response data [41]. As with determining geological zones, the geotechnical properties are categorized rather than predicted from discrete values using ML analytical techniques. The main rock mass properties under investigation are rock strength, discontinuities or fractures, and rock mass categorization scores, such as, rock mass rating (RMR), the geological strength index (GSI), Q-system, and rock quality designation (RQD) [46–49]. These geotechnical conditions are traditionally determined by logging and laboratory testing of diamond drill cores from holes that are spaced hundreds of meters apart without any regular pattern. Rock mass characterization data collection from exploration drilling is sparse due to the expense of drilling. This low-resolution data capture requires interpolation and broad geotechnical domaining to classify a rock mass with significant uncertainty between holes. Surface mine ML applications on MWD data were generally focused on geotechnical characterization to improve fragmentation, or rock breakage from blasting [1,6,25,50]. The focus of understanding rock mass properties from MWD data in underground mining- and tunnelling-based research is to reduce strata failure by adjusting the spacing and locations of ground support equipment [13,51–59].

First, an overview of the various environments and mined commodities in which MWD data have been used to identify rock mass properties is presented. Next, the types of feature importance analysis conducted by researchers to understand which MWD metrics are useful to describe changing geotechnical conditions, such as strength and fracture state, are critically reviewed from a data science perspective. Finally, the application of ML in characterizing rock mass zones from MWD data is surveyed. As with the geology-based findings in the previous section, these broad rock mass zone classifications are useful but do not accurately predict the complex fabric of a rock mass.

4.2.1. Commodities

As discussed in Section 2, there are considerably fewer studies on the ML classification of MWD data for rock mass characteristics in open-pit mining than for geological types. However, the use of ML algorithms on MWD data to characterize a rock mass has been demonstrated in other industries. These include tunnelling [51,53,54] and underground mining [52,57–60], which employ drilling prior to excavation. Exploration and laboratory-based activities [61–63] have also correlated rock mass properties with drilling metrics

In a series of classic studies, Schunnesson' (1990, 1996, 1997, 1998) drill monitoring was used in underground Scandinavian iron ore and copper mines to distinguish changing conditions in each investigated rock mass [57–60]. More than two decades later, potential blasting issues in the underground Swedish Malmberget iron ore mine were predicted by assessing trends in MWD data [52]. In the tunnelling space, rock mass classification zones, including RMR and rock mass quality, were predicted from intelligent MWD data analysis to improve ground support patterns [51,53,54].

Exploration drilling, and laboratory experiments also support the use of ML methods to predict geotechnical properties from drilling metrics. Rock strength could be predicted from an exploration drill rig's MWD data in the seven holes of diamond core in Turkey [61]. In laboratory experiments involving drilling through prepared samples, it was demonstrated that rock properties, including density, porosity, P-wave velocity, Schmidt hardness, UCS, tensile strength, and elasticity modulus, could be successfully predicted from acoustics produced during the drilling of laboratory samples [62]. On the other hand, in the tunnelling space, simulated fractures were detected in the rock mass from MWD data trends during the excavation of a 20 m wide tunnel [53]. More recently, several Chinese tunnel excavations have used regression- and classification-based methods to determine rock properties from MWD data. NNs were used to predict rock strength values, including UCS, elasticity modulus, and Poisson's ratio, from MWD data [64]. In terms of a classification approach, a bi-directional long short-term memory NN was used to predict trimodal rock mass classes [65].

However, few studies have attempted to characterize rock mass conditions from MWD data in the open-pit mining environment utilizing thresholding or simple correlation. It was observed that high and low rop correlated with weak and strong rock strength zones in 1267 blast holes from the Aitik copper mine in Sweden [66]. To determine fracture locations from MWD data, downhole geophysical televiewer logs were interpreted to correlate fracture locations in eight blast holes from the Canadian Highland Valley copper mine [50]. Also using televiewer logs to calibrate their findings, two novel rock description indexes were developed based exclusively on MWD data from 302 production blast holes at the Erzberg mine [25]. These systems categorized rock mass zones for structural condition and strength properties and were corroborated by highwall mapping via photogrammetrically generated models. However, no studies were identified that used ML analytical methods on MWD data to characterize subsurface geotechnical properties in open-pit operations.

4.2.2. Feature Importance

As with the determination of geological zones from MWD data, research has attempted to identify the feature importance that each MWD metric has in predicting subsurface geotechnical conditions. Determination of feature importance using advanced analytical methods has almost entirely taken place within underground mining and tunnelling operations [51,52,57]. Multiple studies have utilized manual correlation in open-pit mining to identify feature importance for drillability or blastability. These are outside the scope of this review due to their focus on other aspects that are not directly related to subsurface geotechnical conditions [1,6,14,55,66–68] (Ghosh et al., 2014; Khorzoughi, 2011; Liu and Yin, 2001; Manzoor et al., 2019; Navarro et al., 2018; Scoble and Peck 1987; Segui and

Higgins, 2001). PCA has only been used on open-pit mining MWD data to determine feature importance for a novel MWD-based rock mass classification system (drilling rock factor—DRF) [25].

PCA has been used to determine the feature importance of MWD metrics for geotechnical properties in underground mining and tunnelling projects. Specifically, the features ranking highly on the first principal component have generally been interpreted to be the most important. As discussed, the variables with the most variation are not necessarily the most important (Section 4.1). Schunnesson determined that the rop was most important from PCA loading plots showing rop as low in higher rock strength zones and, conversely, the rop was observed to be higher in weaker rock strength zones [57]. A later study focusing on the link between rock mass conditions and chargeability issues in underground blast holes employed PCA to identify ropS, torS, rop, and tor highly in terms of the first principal component, accounting for 62% of data variability [52]. Using a combination of PCA and ordered weighted average (OWA), Galende-Hernández et al. determined the top three features to select for predictive analysis were wob, damper pressure, and tor [51]. The inconsistent feature importance results between these two findings may be attributed to discrepancies with data collection, data cleaning equipment, or geological settings. It is also likely that the results do not support one another because PCA is not a statistically appropriate method for feature selection.

PCA has also been used on an open-pit mining MWD dataset from 286 blast holes at the Erzberg Mine in central Europe to interpret the feature importance of drilling metrics for input to their DRF [25]. The DRF rock mass classification system is composed of a structural factor and strength-grade factors. The structural factor consists of huge, fractured, and extensively fractured zones, while the strength-grade factor has soft-waste, hard-waste, transition zone, and hard-ore categories. Navarro et al. reported that the metrics rop, ropS, and torS ranked highly on PC1, the first principal component, for the structural factor evaluation, while tor dominated the positive side of PC2, the second principal component [25]. The first two main components of the structural factor explain a combined 66.02% of the entire variation, with PC1 contributing 47.47% and PC2 contributing 18.55%. In contrast, for the strength-grade factor, rop and wob dominated the positive sides of PC1 and PC2, respectively. The results of the study demonstrate that the strength-grade PC1 outcomes can differentiate between two distinct regions characterized by varying rock strength. Specifically, the schisted sandstone exhibits a uniaxial compressive strength (UCS) value of 30 MPa, while the limestone displays a UCS value of 125 MPa [25]. These results correlate well with digital photogrammetry reconstructions of the pit walls after blasting and excavation [25]. However, the DRF results are heavily dependent on calibration with manually interpreted televiewer logs. In addition, since the rock factor zones are also based on the local iron ore geology of the Erzberg Mine, adapting DRF to different mineral deposits would require intensive re-calibration. A deposit-agnostic approach without manual calibration would be more readily adopted to determine geotechnical properties from open-pit mining MWD data.

4.2.3. Machine Learning Classification

Classification of rock mass properties using ML methods on open-pit blast hole MWD data has not been demonstrated, despite an exhaustive search. It was discovered that while many reports claim to characterize rock mass conditions using ML on MWD data, what was reported was often rock type, with an assumption of strong vs. weak UCS values for contrasting rock types. The results of these are discussed in Section 4. No studies were found that attempted to predict geotechnical properties using ML methods in the open-pit mining, underground mining, or construction industries.

4.3. Geochemical Properties from MWD

Very few studies attempt to predict geochemical properties from MWD data [24,25,57]. Commonly reported geochemical properties of ore included aluminium oxide (Al_2O_3), calcium oxide (CaO), iron (Fe), total loss of ignition (LOI), magnesium oxide (MgO), manganese (Mn), phosphorus (P), sulfur (S), silica oxide (SiO_2), and titanium oxide (TiO_2). All findings reporting geochemical properties from mining MWD data were located within an iron ore deposit and listed grade or iron ore percentage.

Fe was reported as the only ore quality investigated [25,57]. Partial least squares (PLS) analysis was applied on MWD data from an underground mine and closely predicted iron content against assays of drill cuttings in areas of high and low phosphorus geology [57]. The ore grade prediction of Navarro et al. was split into two simple categories of (1) waste consisting of less than 20% iron and (2) ore consisting of greater than 20% iron [25]. These waste and ore class results appear equivalent to the DRF results. However, there is no explicit mention of the ore grade prediction accuracy, which suggests it is probable that no validation of results was conducted against laboratory assays.

Only one study reported the use of ML classification for geochemical properties from MWD and drill cutting assay data from two Australian iron ore mines [24]. Unlike previous studies that only reported the investigated ore properties were Al_2O_3, CaO, Fe, LOI, MgO, Mn, P, S, SiO_2, and TiO_2. Fe was predicted with acceptable R^2 values of 0.79, 0.79, and 0.78 in the first mine and 0.64, 0.64, and 0.63 in the second mine for the GP, SVM, and RF algorithms, respectively. The datasets were combined to predict P and S. Acceptable R^2 values for P were 0.79, 0.78, and 0.81, and S were 0.91, 0.90, and 0.92 for the GP, SVM, and RF algorithms, respectively. The report also identified that several of the geochemical properties correlated with each other. Based on this, cross-assay predictive models showed improved results for the remaining ore properties. For example, the R^2 value for Al_2O_3 of 0.65 on MWD data alone in an RF model was improved to 0.90 and 0.85 when adding the cross-assay results for Fe and SiO_2, respectively. The primary benefit of this result is that if one assay can be directly measured with a sensor or strongly predicted from a model, these measurements can be utilized to enhance estimates for other geochemical properties.

5. Discussion

5.1. Current Challenges

This summary makes it clear that the motivation behind these findings is to circumvent the limitations of conventional subsurface characterization prior to excavation. NNs and GPs are the two primary categories of ML algorithms utilized with MWD data for rock categorization. While some artificial intelligence algorithms have been applied to the same datasets, different ML architectures produced different outcomes [18,22,27]. Thus, no model has been proposed as optimal for characterizing geological, geotechnical, and geochemical features from MWD data, as model selection depends on underlying aims, scientific objectives, and model restrictions. Notably, some ML approaches are more attractive (NN and RF) than others (GP) due to their computational efficiency [19]. In addition to there being no accepted, optimal ML modelling algorithm to characterize subsurface conditions from MWD data, there is no uniformly consistent approach to MWD data collection and processing.

There are still some challenges in data collection and processing that must be overcome. First, most of the investigated projects featured limited amounts of data from blast holes, making it difficult to extensively analyse and interpret the subsurface. Second, the quality of the output is dependent not just on the model but also on the condition of the gathered data. Quality assurance and quality control processes are not commonplace with open-pit MWD data acquisition. During the development of predictive models, the robustness of the model may be affected due to the existence of missing values or outliers within the dataset. In addition, the feature importance among MWD variables may also affect the modelling robustness. Existing studies [16,25,52] disagree as to which metrics should be utilized to characterize rock properties under different environmental situations, as they vary based on deposit-specific conditions. To identify the feature importance of drilling variables, PCA has been used to choose input variables from the MWD data. A statistically suitable strategy for determining feature relevance should enhance feature selection to improve computational precision and speed. In conclusion, the subsurface characterization applications of ML techniques applied to MWD data are in an escalating stage of development.

In summary, the relative frequencies of machine learning methods used in the analysis of MWD data reported are shown in Figure 5. The analysis is based on a keyword search of the Scopus database. Interestingly, convolutional neural networks (tied with SVM at 16%) are comparatively high up the list, despite being a relative new approach focused on image analysis.

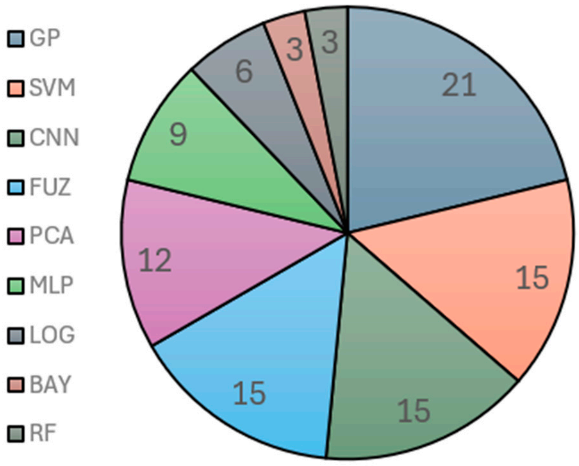

Figure 5. Relative frequency of machine learning methods reported in the in the analysis of MWD data in the Scopus database (GP—Gaussian processes, SVM—support vector machines, CNN—convolutional neural networks, FUZ—fuzzy systems, PCA—principal component analysis, MLP—multilayer perceptron, LOG—logistic regression, BAY—Bayes modelling, RF—random forest).

5.2. Future Developments

Even though non-traditional approaches to comprehend mining subsurface conditions require further development, they are gaining popularity. ML methods can be utilized as a supplement to conventional theory [8,25]. They have the potential to extract insights about a vast array of spatial data, which can then be narrowed down to investigate areas of interest in greater detail. However, despite the widespread use of ML classification algorithms for categorizing geology in MWD data, ML analytical methods have seldom been applied. A common assumption has been that it is far more crucial to understand the boundaries between dissimilar rock types than the variation within each rock type [11,18,25]. As a result, the categorization of 'strong' and 'weak' rock types, such as BIF and shale, respectively, has dominated projects by investigating univariate relationships, mainly rop and tor [69]. In contrast, existing multivariate ML regression algorithms have significant prospects for solving the complicated challenge of variance within each rock type.

To interpret subsurface properties using MWD data, supervised [8,18,22,25] and unsupervised learning [12,16] techniques have been implemented. Supervised learning can use all available information to make predictions and classifications, while unsupervised learning may identify potential relationships and extract features from a substantial volume of unlabelled data. In the context of both supervised and unsupervised learning applications, it is essential to employ suitable data preprocessing approaches. These techniques encompass the removal of noise, outliers, and false attributes. This necessity arises from the considerable geographic variability observed in measurements while considering the data related to MWD and subsurface conditions [70].

Existing techniques of MWD data processing and analysis rely heavily on manual interpretation, such as determining the most critical rock-property-dependent metrics [31]. Consequently, it is difficult to repeatedly process data from new sources and places. A pertinent aim of applied research is therefore to design an automated workflow in which

ML methods and available input data, connected with specific conditions, can correlate, process, and select drilling variables for subsequent estimation of rock properties. In the interim, the gathering of a training dataset during algorithm execution could facilitate data collecting for future applications operating under comparable conditions.

The implementation of ML techniques is dependent on the training data set accurately representing the connection between the input datasets, MWD, and subsurface properties, respectively. It is crucial to select attributes for the training set that accurately represent the population. As a result, ML training progress is impeded by the challenges of overfitting, extended training time, and a notable inclination to become trapped in local minima [12]. As demonstrated in the tunnelling sector, these obstacles may be overcome with optimization algorithms, including genetic algorithms, particle swarm optimization and imperialist competition algorithms [54]. Due to their ability to rapidly analyse massive and complex MWD datasets, ML methods provide an effective solution to provide accurate and relevant predictions of subsurface properties in open cut mining operations.

Interpretation of MWD features can benefit considerably from recent advances in explainable artificial intelligence, as discussed among other by Saranya and Subshini [71] and Lundberg and Lee [72]. Moreover, although having emerged only recently, deep learning models have significant potential in the analysis and interpretation of measure-while-drilling (MWD) data in hard-rock mining [73,74]. These models are particularly well suited to deal with complex data, such as associated with panoramic borehole imaging, for example [73,75,76], or vibrational data [77]. In addition, they could also better support the processing of MWD metrics when considered as time series data [78].

6. Conclusions

The mining industry is increasingly using methods of artificial intelligence to overcome the uncertainty associated with data on geological objects. ML algorithms have been applied on mining MWD datasets to understand pre-excavation subsurface conditions. Numerous studies have been conducted on the collection, processing, analysis, and application of MWD variables for the characterization of rock type, rock mass, and ore properties.

From this review of the literature, the following conclusions can be made:

- The most commonly measured MWD variables measured together with the depth of drilling in open-pit mines are rate of penetration (rop), torque or rotational pressure (tor), bit air pressure (bap), weight on bit (wob), and rotary speed or revolutions per minute (rpm).
- Several studies have analysed the relative importance of each of these variables related to the identification of rock types and characteristics with mixed results. This is an emerging area that can benefit from recent significant advances in machine learning, where models are interpreted or explained. This would particularly be the case where other MWD variables, such as image, vibrational or acoustic signals are included in models.
- In most studies, ML models could successfully categorize geological zones or rock types from MWD data, but further work is required to capture more subtle differences within geological units.
- Classification of discrete rock mass properties, including rock strength and fracture count, using ML methods on open-pit blast hole MWD data does not appear to have been demonstrated yet. Instead, rock type is typically identified as a proxy for rock strength based on assumptions associated with each type.
- Only one study considered the prediction of geochemical properties using ML classification on MWD and drill cutting assay datasets. ML analytical methods applied to MWD data resulting in discrete values for geotechnical, geological, and geochemical will enable a low-cost, high-resolution comprehension of subsurface conditions beyond simple rock type classification.
- Overall, these studies have not yet taken full advantage of recent developments in deep learning and, as more data are collected, these ML approaches are likely to play

a more important role in MWD data analysis for enhanced comprehension of geology, rock mass characteristics, and ore attributes for enhanced sustainability, efficiency, and safety of mining operations.

Author Contributions: Conceptualization, D.M.G.; methodology, D.M.G.; software, D.M.G.; validation, D.M.G.; formal analysis, D.M.G.; investigation, D.M.G.; resources, D.M.G.; data curation, D.M.G.; writing—original draft preparation, D.M.G.; writing—review and editing, D.M.G., C.A. and L.O.; visualization, D.M.G. and C.A.; supervision, C.A. and L.O.; project administration, D.M.G.; funding acquisition, D.M.G. All authors have read and agreed to the published version of the manuscript.

Funding: This research was funded by the MRIWA Postgraduate Research Scholarship and the Australasian Institute of Mining and Metallurgy Education Endowment Fund Postgraduate Scholarship.

Acknowledgments: The research was supported by the advanced computing resources provided by the Pawsey Supercomputing Research Centre in Perth, Australia.

Conflicts of Interest: The authors declare no conflicts of interest.

References

1. Segui, J.B.; Higgins, M. *Blast Design Using Measurement While Drilling Parameters*; Australasian Institute of Mining and Metallurgy: Melbourne, Australia, 2001; pp. 28–31.
2. Barr, M.V. Instrumented Horizontal Drilling for Tunnelling Site Investigation. Ph.D. Thesis, University of London: Imperial College of Science and Technology, London, UK, 1984.
3. Barr, M.V.; Brown, E.T. A Site Exploration Trial Using Instrumented Horizontal Drilling. In Proceedings of the 5th ISRM Congress, Melbourne, Australia, 10–15 April 1983; International Soceity of Rock Mechanics: Lisbon, Portugal, 1983; pp. 51–58.
4. Brown, E.T.; Barr, M.V. Instrumented Drilling as an Aid to Site Investigations. In Proceedings of the 3rd International Congress of the International Association of Engineering Geology, Madrid, Spain, 4–8 September 1978; pp. 21–28.
5. Leighton, J.C. Development of a Correlation between Rotary Drill Performance and Controlled Blasting Powder Factors. Master's Thesis, University of British Columbia, Vancouver, BC, Canada, 1982.
6. Scoble, M.J.; Peck, J. A Technique for Ground Characterization Using Automated Production Drill Monitoring. *Int. J. Surf. Min. Reclam. Environ.* **1987**, *1*, 41–54. [CrossRef]
7. Scoble, M.J.; Peck, J.; Hendricks, C. Correlation between Rotary Drill Performance Parameters and Borehole Geophysical Logging. *Min. Sci. Technol.* **1989**, *8*, 301–312. [CrossRef]
8. Silversides, K.L.; Melkumyan, A. Boundary Identification and Surface Updates Using MWD. *Math. Geosci.* **2020**, *53*, 1047–1071. [CrossRef]
9. Basarir, H.; Wesseloo, J.; Karrech, A.; Pasternak, E.; Dyskin, A. The Use of Soft Computing Methods for the Prediction of Rock Properties Based on Measurement While Drilling Data. In *Deep Mining 2017: Proceedings of the Eighth International Conference on Deep and High Stress Mining*; Australian Centre for Geomechanics: Perth, Australia, 2017; pp. 537–551. [CrossRef]
10. Lucifora, D.J.; Rafezi, H. State of the Art Review: Monitoring-While-Drilling for Mining Applications. In Proceedings of the World Mining Congress (WMC), Montreal, QC, Canada, 11–15 August 2013; Volume 4.
11. Silversides, K.L.; Ball, A.; Melkumyan, A. BIF-Hosted Deposit Unit Differentiation Using Multivariate Gaussian Processes on Measure While Drilling Data. *Appl. Earth Sci.* **2020**, *129*, 164–175. [CrossRef]
12. Beattie, N. Monitoring-While-Drilling for Open-Pit Mining in a Hard Rock Environment. Master's Thesis, Queen's University, Kingston, ON, Canada, 2009.
13. Ghosh, R. Assessment of Rock Mass Quality and Its Effects on Chargeability Using Drill Monitoring Technique. Ph.D. Thesis, Lulea University of Technology, Luleå, Sweden, 2017.
14. Khorzoughi, M.B. Use of Measurement While Drilling Techniques for Improved Rock Mass Characterization in Open-Pit Mines. Master's Thesis, University of British Columbia, Vancouver, BC, Canada, 2011.
15. Liu, J. Study on Intelligent Prediction Models of Geological Conditions ahead of Tunnel Face Using Measurement-While-Drilling Data. Ph.D. Thesis, Nagasaki University, Nagasaki, Japan, 2021.
16. Martin, J. Application of Pattern Recognition Techniques to Monitoring-While-Drilling on a Rotary Electric Blasthole Drill at an Open-Pit Coal Mine. Master's Thesis, Queen's University, Kingston, ON, Canada, 2007.
17. Navarro Miguel, J. The Use of Measure While Drilling for Rock Mass Characterization and Damage Assessment in Blasting. Ph.D. Thesis, Universidad Politechnica de Madrid, Madrid, Spain, 2018.
18. Leung, R.; Scheding, S. Automated Coal Seam Detection Using a Modulated Specific Energy Measure in a Monitor-While-Drilling Context. *Int. J. Rock Mech. Min. Sci.* **2015**, *75*, 196–209. [CrossRef]
19. Zhong, R.; Johnson, R.L.; Chen, Z. Using Machine Learning Methods to Identify Coals from Drilling and Logging-While-Drilling LWD Data. In *Asia Pacific Unconventional Resources Technology Conference, Brisbane, Australia, 18–19 November 2019*; Society of Petroleum Engineers: Richardson, TX, USA, 2019. [CrossRef]

20. Kadkhodaie-Ilkhchi, A.; Monteiro, S.T.; Ramos, F.; Hatherly, P. Rock Recognition from MWD Data: A Comparative Study of Boosting, Neural Networks, and Fuzzy Logic. *IEEE Geosci. Remote Sens. Lett.* **2010**, *7*, 680–684. [CrossRef]
21. Zhou, H.; Hatherly, P.; Monteiro, S.T.; Ramos, F.; Oppolzer, F.; Nettleton, E.; Scheding, S. Automatic Rock Recognition from Drilling Performance Data. In Proceedings of the 2012 IEEE International Conference on Robotics and Automation, Saint Paul, MN, USA, 14–18 May 2012; pp. 3407–3412. [CrossRef]
22. Hatherly, P.; Leung, R.; Scheding, S.; Robinson, D. Drill Monitoring Results Reveal Geological Conditions in Blasthole Drilling. *Int. J. Rock Mech. Min. Sci.* **2015**, *78*, 144–154. [CrossRef]
23. Akyildiz, O.; Basarir, H.; Vezhapparambu, V.S.; Ellefmo, S. MWD Data-Based Marble Quality Class Prediction Models Using ML Algorithms. *Math. Geosci.* **2023**, *55*, 1059–1074. [CrossRef]
24. Khushaba, R.N.; Melkumyan, A.; Hill, A.J. A Machine Learning Approach for Material Type Logging and Chemical Assaying from Autonomous Measure-While-Drilling (MWD) Data. *Math. Geosci.* **2021**, *54*, 285–315. [CrossRef]
25. Navarro, J.; Seidl, T.; Hartlieb, P.; Sanchidrián, J.A.; Segarra, P.; Couceiro, P.; Schimek, P.; Godoy, C. Blastability and Ore Grade Assessment from Drill Monitoring for Open Pit Applications. *Rock Mech. Rock Eng.* **2021**, *54*, 3209–3228. [CrossRef]
26. Vezhapparambu, V.S.; Eidsvik, J.; Ellefmo, S.L. Rock Classification Using Multivariate Analysis of Measurement While Drilling Data: Towards a Better Sampling Strategy. *Minerals* **2018**, *8*, 384. [CrossRef]
27. Ahsan, N.; Scheding, S.; Monteiro, S.T.; Leung, R.; McHugh, C.; Robinson, D. Adaptive Sampling Applied to Blast-Hole Drilling in Surface Mining. *Int. J. Rock Mech. Min. Sci.* **2015**, *75*, 244–255. [CrossRef]
28. Liaghat, S.; Gustafson, A.; Johansson, D.; Schunnesson, H. Ore Grade Prediction Using Informative Features of MWD Data. In *Mining Goes Digital, Proceedings of the 39th International Symposium on Application of Computers and Operations Research in the Mineral Industry, APCOM 2019, Wroclaw, Poland, 4–6 June 2019*; CRC Press: London, UK, 2019; pp. 226–234. [CrossRef]
29. Vezhapparambu, V.S.; Ellefmo, S.L. Estimating the Blast Sill Thickness Using Changepoint Analysis of MWD Data. *Int. J. Rock Mech. Min. Sci.* **2020**, *134*, 104443. [CrossRef]
30. Fang, Y.; Wu, Z.; Sheng, Q.; Tang, H.; Liang, D. Tunnel Geology Prediction Using a Neural Network Based on Instrumented Drilling Test. *Appl. Sci.* **2020**, *11*, 217. [CrossRef]
31. van Eldert, J.; Schunnesson, H.; Saiang, D.; Funehag, J. Improved Filtering and Normalizing of Measurement-While-Drilling (MWD) Data in Tunnel Excavation. *Tunn. Undergr. Space Technol.* **2020**, *103*, 103467. [CrossRef]
32. Hjelme, J.G. Drill Parameter Analysis in the Løren Tunnel. Master's Thesis, University of Oslo: Faculty of Mathematics and Natural Sciences, Oslo, Norway, 2010.
33. Gupta, I.; Tran, N.; Devegowda, D.; Jayaram, V.; Rai, C.; Sondergeld, C.; Karami, H. Looking Ahead of the Bit Using Surface Drilling and Petrophysical Data: Machine-Learning-Based Real-Time Geosteering in Volve Field. *SPE J.* **2020**, *25*, 990–1006. [CrossRef]
34. Klyuchnikov, N.; Zaytsev, A.; Gruzdev, A.; Ovchinnikov, G.; Antipova, K.; Ismailova, L.; Muravleva, E.; Burnaev, E.; Semenikhin, A.; Cherepanov, A.; et al. Data-Driven Model for the Identification of the Rock Type at a Drilling Bit. *J. Pet. Sci. Eng.* **2019**, *178*, 506–516. [CrossRef]
35. Litvinenko, V.S.; Dvoinikov, M.V. Justification of the Technological Parameters Choice for Well Drilling by Rotary Steerable Systems. *PMI* **2019**, *235*, 24–29. [CrossRef]
36. Romanenkova, E.; Zaytsev, A.; Klyuchnikov, N.; Gruzdev, A.; Antipova, K.; Ismailova, L.; Burnaev, E.; Semenikhin, A.; Koryabkin, V.; Simon, I.; et al. Real-Time Data-Driven Detection of the Rock-Type Alteration During a Directional Drilling. *IEEE Geosci. Remote Sens. Lett.* **2020**, *17*, 1861–1865. [CrossRef]
37. Finfinger, G.; Peng, S.; Gu, Q.; Wilson, G.; Thomas, B. An Approach to Identifying Geological Properties from Roof Bolter Drilling Parameters. In Proceedings of the 19th International Conference on Ground Control in Mining, Morgantown, WV, USA, 8–10 August 2000; pp. 1–12.
38. Kahraman, S.; Rostami, J.; Naeimipour, A. Review of Ground Characterization by Using Instrumented Drills for Underground Mining and Construction. *Rock Mech. Rock Eng.* **2016**, *49*, 585–602. [CrossRef]
39. Rostami, J.; Kahraman, S.; Naeimipour, A.; Collins, C. Rock Characterization While Drilling and Application of Roof Bolter Drilling Data for Evaluation of Ground Conditions. *J. Rock Mech. Geotech. Eng.* **2015**, *7*, 273–281. [CrossRef]
40. Utt, W.K. Neural Network Technology for Strata Strength Characterization. In Proceedings of the IJCNN'99. International Joint Conference on Neural Networks. Proceedings (Cat. No.99CH36339), Washington, DC, USA, 10–16 July 1999; IEEE: Washington, DC, USA, 1999; Volume 6, pp. 3806–3809.
41. Teale, R. The Concept of Specific Energy in Rock Drilling. *Int. J. Rock Mech. Min. Sci.* **1965**, *2*, 57–73. [CrossRef]
42. Wold, S.; Esbensen, K.; Geladi, P. Principal Component Analysis. *Chemom. Intell. Lab. Syst.* **1987**, *2*, 37–52. [CrossRef]
43. Herwig, N.; Borghesani, P. Explaining Deep Neural Networks Processing Raw Diagnostic Signals. *Mech. Syst. Signal Process.* **2023**, *200*, 110584. [CrossRef]
44. Loh, W.-Y.; Zhou, P. Variable Importance Scores. *J. Data Sci.* **2021**, *19*, 569–592. [CrossRef]
45. Wei, P.; Lu, Z.; Song, J. Variable Importance Analysis: A Comprehensive Review. *Reliab. Eng. Syst. Saf.* **2015**, *142*, 399–432. [CrossRef]
46. Barton, N.; Lien, R.; Lunde, J. Engineering Classification of Rock Masses for the Design of Tunnel Support. *Rock Mech.* **1974**, *6*, 189–236. [CrossRef]

47. Bieniawski, Z.T. Geomechanics Classification (Rock Mass Rating System). In *Engineering Rock Mass Classifications: A Complete Manual for Engineers and Geologists in Mining, Civil, and Petroleum Engineering*; Wiley-Interscience: New York, NY, USA, 1989.
48. Deere, D.U. Technical Description of Rock Cores. *Rock Mech. Eng. Geol.* **1963**, *1*, 18–22.
49. Hoek, E.; Brown, E.T. Practical Estimates of Rock Mass Strength. *Int. J. Rock Mech. Min. Sci.* **1997**, *34*, 1165–1186. [CrossRef]
50. Khorzoughi, M.B.; Hall, R.; Apel, D. Rock Fracture Density Characterization Using Measurement While Drilling (MWD) Techniques. *Int. J. Min. Sci. Technol.* **2018**, *28*, 859–864. [CrossRef]
51. Galende-Hernández, M.; Menéndez, M.; Fuente, M.J.; Sainz-Palmero, G.I. Monitor-While-Drilling-Based Estimation of Rock Mass Rating with Computational Intelligence: The Case of Tunnel Excavation Front. *Autom. Constr.* **2018**, *93*, 325–338. [CrossRef]
52. Ghosh, R.; Gustafson, A.; Schunnesson, H. Development of a Geological Model for Chargeability Assessment of Borehole Using Drill Monitoring Technique. *Int. J. Rock Mech. Min. Sci.* **2018**, *109*, 9–18. [CrossRef]
53. Liu, J.; Jiang, Y.; Ishizu, S.; Sakaguchi, O. Estimation of Tunnel Support Pattern Selection Using Artificial Neural Network. *Arab. J. Geosci.* **2020**, *13*, 321. [CrossRef]
54. Liu, J.; Jiang, Y.; Han, W.; Sakaguchi, O. Optimized ANN Model for Predicting Rock Mass Quality Ahead of Tunnel Face Using Measure-While-Drilling Data. *Bull. Eng. Geol. Environ.* **2021**, *80*, 2283–2305. [CrossRef]
55. Navarro, J.; Sanchidrián, J.A.; Segarra, P.; Castedo, R.; Costamagna, E.; López, L.M. Detection of Potential Overbreak Zones in Tunnel Blasting from MWD Data. *Tunn. Undergr. Space Technol.* **2018**, *82*, 504–516. [CrossRef]
56. Navarro, J.; Segarra, P.; Sanchidrián, J.A.; Castedo, R.; López, L.M. Assessment of Drilling Deviations in Underground Operations. *Tunn. Undergr. Space Technol.* **2019**, *83*, 254–261. [CrossRef]
57. Schunnesson, H. Drill Process Monitoring in Percussive Drilling: A Multivariate Approach for Data Analysis. Licentiate Thesis, Lulea University of Technology, Lulea, Sweden, 1990.
58. Schunnesson, H. RQD Predictions Based on Drill Performance Parameters. *Tunn. Undergr. Space Technol.* **1996**, *11*, 345–351. [CrossRef]
59. Schunnesson, H. Rock Characterization Using Percussive Drilling. *Int. J. Rock Mech. Min. Sci.* **1998**, *35*, 711–725. [CrossRef]
60. Schunnesson, H. Drill Process Monitoring in Percussive Drilling for Location of Structural Features, Lithological Boundaries and Rock Properties, and for Drill Productivity Evaluation. Ph.D. Thesis, Lulea University of Technology, Lulea, Sweden, 1997.
61. Basarir, H.; Karpuz, C. Preliminary Estimation of Rock Mass Strength Using Diamond Bit Drilling Operational Parameters. *Int. J. Min. Reclam. Environ.* **2016**, *30*, 145–164. [CrossRef]
62. Rajesh Kumar, B.; Vardhan, H.; Govindaraj, M.; Vijay, G.S. Regression Analysis and ANN Models to Predict Rock Properties from Sound Levels Produced during Drilling. *Int. J. Rock Mech. Min. Sci.* **2013**, *58*, 61–72. [CrossRef]
63. Liu, W.; Rostami, J.; Ray, A.; Elsworth, D. Statistical Analysis of the Capabilities of Various Pattern Recognition Algorithms for Fracture Detection Based on Monitoring Drilling Parameters. *Rock Mech. Rock Eng.* **2020**, *53*, 2265–2278. [CrossRef]
64. Zhao, R.; Shi, S.; Li, S.; Guo, W.; Zhang, T.; Li, X.; Lu, J. Deep Learning for Intelligent Prediction of Rock Strength by Adopting Measurement While Drilling Data. *Int. J. Geomech.* **2023**, *23*, 04023028. [CrossRef]
65. Cheng, X.; Tang, H.; Wu, Z.; Liang, D.; Xie, Y. BILSTM-Based Deep Neural Network for Rock-Mass Classification Prediction Using Depth-Sequence MWD Data: A Case Study of a Tunnel in Yunnan, China. *Appl. Sci.* **2023**, *13*, 6050. [CrossRef]
66. Ghosh, R.; Schunnesson, H.; Kumar, U. Evaluation of Rock Mass Characteriztics Using Measurement While Drilling in Boliden Minerals Aitik Copper Mine, Sweden. In *Mine Planning and Equipment Selection*; Drebenstedt, C., Singhal, R., Eds.; Springer International Publishing: Cham, Switzerland, 2014; pp. 81–91. ISBN 978-3-319-02677-0.
67. Liu, H.; Yin, K.K. Analysis and Interpretation of Monitored Rotary Blasthole Drill Data. *Int. J. Surf. Min. Reclam. Environ.* **2001**, *15*, 177–203. [CrossRef]
68. Manzoor, S.; Liaghat, S.; Gustafson, A.; Johansson, D.; Schunnesson, H. Rock Mass Characterization Using MWD Data and Photogrammetry. In *Mining Goes Digital, Proceedings of the 39th International Symposium on Application of Computers and Operations Research in the Mineral Industry, APCOM 2019, Wroclaw, Poland, 4–6 June 2019*; CRC Press: London, UK, 2019; pp. 217–225. [CrossRef]
69. Rai, P.; Schunesson, H.; Lindqvist, P.A.; Kumar, U. An Overview on Measurement-While-Drilling Technique and Its Scope in Excavation Industry. *J. Inst. Eng. India Ser. D* **2015**, *96*, 57–66. [CrossRef]
70. Khorzoughi, B.M.; Hall, R. Processing of Measurement While Drilling Data for Rock Mass Characterization. *Int. J. Min. Sci. Technol.* **2016**, *26*, 989–994. [CrossRef]
71. Saranya, A.; Subhashini, R. A systematic review of Explainable Artificial Intelligence models and applications: Recent developments and future trends. *Decis. Anal. J.* **2023**, *7*, 100230. [CrossRef]
72. Lundberg, S.; Lee, S.-I. A Unified Approach to Interpreting Model Predictions. *arXiv* **2017**, arXiv:1705.07874. [CrossRef]
73. Liu, X.; Zhang, X.; Wang, L.; Qu, F.; Shao, A.; Zhao, L.; Wang, H.; Yue, X.; Li, Y.; Yan, W.; et al. Research Progress and Prospects of Intelligent Technology in Underground Mining of Hard Rock Mines. *Green Smart Min. Eng.* **2024**, *1*, 12–26. [CrossRef]
74. Su, R.; Zhao, Q.; Zheng, T.; Han, G.; Jiang, J.; Hu, J. A Framework for RQD Calculation Based on Deep Learning. *Min. Metall. Explor.* **2023**, *40*, 1567–1583. [CrossRef]
75. Wang, C.Y.; Wang, Y.T.; Zou, X.J.; Han, Z.Q.; Zhong, S. Study of a Borehole Panoramic Stereopair Imaging System. *Int. J. Rock Mech. Min. Sci.* **2018**, *104*, 174–181. [CrossRef]
76. Jin, C.Y.; Wang, K.; Han, T.; Lu, Y.; Liu, A.X.; Liu, D. Segmentation of Ore and Waste Rocks in Borehole Images using the Multi-Module Densely Connected U-net. *Comput. Geosci.* **2022**, *159*, 105018. [CrossRef]

77. Chen, G.; Chen, M.; Hong, G.; Lu, Y.; Zhou, B.; Gao, Y. A New Method of Lithology Classification Based on Convolutional Neural Network Algorithm by Utilizing Drilling String Vibration Data. *Energies* **2020**, *13*, 888. [CrossRef]
78. Yang, M.; Hu, Y.; Liu, B.; Wang, L.; Zhou, Z.; Jia, M. Application of Artificial Neural Networks for Identification of Lithofacies by Processing of Core Drilling Data. *Appl. Sci.* **2023**, *13*, 11934. [CrossRef]

Chapter 4: Paper B

A Field-Scale Framework for Assessing the Influence of Measure-While-Drilling Variables on Geotechnical Characterization Using a Boruta-SHAP Approach

Goldstein, D., Aldrich, C., Shao, Q., & O'Connor, L. (2025). A Field-Scale Framework for Assessing the Influence of Measure-While-Drilling Variables on Geotechnical Characterization Using a Boruta-SHAP Approach. *Mining*, 5(1), 20. https://doi.org/10.3390/mining5010020 *mining*

Article

A Field-Scale Framework for Assessing the Influence of Measure-While-Drilling Variables on Geotechnical Characterization Using a Boruta-SHAP Approach

Daniel Goldstein [1,*], Chris Aldrich [1], Quanxi Shao [2] and Louisa O'Connor [1]

[1] Western Australia School of Mines, Curtin University, Kalgoorlie, WA 6430, Australia
[2] CSIRO Data61, P.O. Box 1130, Bentley, WA 6102, Australia
* Correspondence: daniel.goldstein@postgraduate.curtin.edu.au

Abstract: This study presents an application of Boruta-SHapley Additive ExPlanations (*Boruta-SHAP*) for geotechnical characterization using Measure-While-Drilling (*MWD*) data, enabling a more interpretable and statistically rigorous assessment of feature importance. Measure-While-Drilling data collected at the scale of an open-pit mine was used to characterize geotechnical properties using regression-based machine learning models. In contrast to previous studies using *MWD* data to recognize rock type using Principal Component Analysis (*PCA*), which only identifies the directions of maximum variance, the *Boruta-SHAP* method quantifies the individual contribution of each Measure-While-Drilling variable. This method ensures interpretable and reliable geotechnical characterization as well as robust feature selection by comparing predictors against randomized 'shadow' features. The *Boruta-SHAP* analysis revealed that bit air pressure and torque-to-penetration ratio were the most significant predictors of rock strength, contradicting previous assumptions that rate of penetration was the dominant factor. Moreover, feature importance was conducted for fracture frequency and Geological Strength Index (*GSI*), a rock mass classification system. A comparative analysis of prediction performance was also performed using a range of different machine learning algorithms that resulted in strong coefficient of determinations of actual field or laboratory results versus predicted values. The results are plausible, confirming that *MWD* data could provide a high-resolution description of geotechnical conditions prior to mining, leading to a more confident prediction of subsurface geotechnical properties. Therefore, the fragmentation from blasting as well as downstream operational phases, such as digging, hauling, and crushing, could be improved effectively.

Keywords: measure-while-drilling (MWD) geotechnical characterization; Boruta-SHAP feature importance; rock mass prediction; machine learning in mining; subsurface geotechnical modeling

Academic Editor: Hossein Masoumi

Received: 24 February 2025
Revised: 4 March 2025
Accepted: 18 March 2025
Published: 20 March 2025

Citation: Goldstein, D.; Aldrich, C.; Shao, Q.; O'Connor, L. A Field-Scale Framework for Assessing the Influence of Measure-While-Drilling Variables on Geotechnical Characterization Using a Boruta-SHAP Approach. *Mining* **2025**, *5*, 20. https://doi.org/10.3390/mining5010020

1. Introduction

Geotechnical characterization provides information about the conditions of the rock mass, such as the type of rock, geomechanical properties, average ore grade, ore boundary, etc. This data is essential for mine planning, fragmentation optimization, and equipment selection to achieve efficient mineral extraction. The most used systems include Geological Strength Index (*GSI*), Q-System (*Q*), Rock Mass Rating (*RMR*) and Rock Quality Designation (*RQD*) [1–4]. These rock mass characterization systems describe the mechanical and structural characteristics of the rock through logging diamond drill core and laboratory testing, respectively [5]. However, determining geotechnical conditions via diamond core drilling is costly and destructive to the rock core [6]. In addition, the limited core samples obtained via diamond drilling do not provide a representative description of a complex rock mass on the scale of a pit in a surface mine [7,8]. Consequently, an economic technique with widespread data capture is necessary to characterize geotechnical conditions in high resolution.

Measure-While-Drilling (*MWD*) is a well-known drill monitoring technology that originated in the petroleum industry and was adopted in the 1970s for open pit mining blast hole drilling systems [9]. This technique involves equipping a blast hole drill rig with *MWD* sensors that collect drilling data that can be used to assess subsurface penetration performance [10]. Because of the continuous nature of drill and blast cycles for excavation in open-pit and underground mining, construction and tunnelling environments, enormous quantities of *MWD* datapoints are collected from blast rigs [11–13]. More specifically, in the open pits examined in this paper, a single, productive blast rig at an open-pit iron ore mine may generate around 10,000 *MWD* observations per day. Many major iron-ore mines employ around over a dozen simultaneously operating blast drills, resulting in hundreds of thousands of drilling response datapoints every day [14].

Due to this sheer volume of data to be analyzed and the complicated, multivariate, as well as nonlinear responses between the drill responses and subsurface composition, advanced analytical techniques, such as Machine Learning (*ML*), have been applied on *MWD* datasets across multiple excavation industries, including open pit mining, underground mining, and tunnelling [15]. Research on open pit mining applications of *MWD* data has generally focused on rock type recognition to improve fragmentation from blasting [9,14,16–26]. In contrast, few reports have applied analytical methods on *MWD* responses to determine changing subsurface geophysical [27] and geochemical conditions [24,28]. In underground excavations, rock type recognition from *MWD* data can assist decision making for placement of ground support equipment to reduce strata failure in underground metalliferous mining [12,29–34], underground coal mining [35–37] and tunnelling [22,38–46]. In summary, each industry uses rock type recognition from *MWD* data for various purposes.

Nevertheless, the dominant output across all excavation industries using *MWD* data is the classification of rock types often using univariate methods, which is useful to delineate lithological boundaries. These broad classifications of contrasting rock types, such as BIF and shale, may improve blasting around rock type contacts [25,47,48]. However, general rock type recognition does not characterize geotechnical conditions in enough detail to optimize open pit blasting within a particular geological unit. Despite an exhaustive search, no studies were identified that aimed to investigate the relationship between *MWD* data and geotechnical properties, such as rock strength and fracturing, rather than rock type recognition [15]. Additionally, no studies were found that utilized an appropriate method to evaluate the feature importance of multivariate *MWD* features in predictive modelling of the geotechnical conditions.

A common approach in prior studies has been the use of Principal Component Analysis (*PCA*) to assess feature importance in *MWD* datasets [25,29,32]. *PCA* is a well-established dimensionality reduction technique that identifies orthogonal principal components explaining the greatest variance in data [49]. However, *PCA* is not inherently designed for feature importance ranking; instead, it highlights directions of maximum variance amongst all features, some of which may not correspond to the most predictive features for geotechnical conditions. This fundamental limitation can lead to misleading interpretations, as *PCA*-derived components often mix multiple variables and fail to preserve the individual explanatory power of each *MWD* parameter [7].

Existing methods for geotechnical characterization using MWD data lack a rigorous feature selection framework. To address this gap, our study employs Boruta-SHapley Additive ExPlanations (*Boruta-SHAP*), a game-theoretic approach that quantifies the contribution of each feature to a model's predictions that has been used in other mining areas, such as metallurgy [50,51]. *Boruta-SHAP* was applied to determine the most influential MWD parameters for geotechnical property prediction. Previous studies have relied on *PCA* or simple correlation metrics, which fail to account for feature interactions and non-linear dependencies. *Boruta-SHAP*, on the other hand, provides a mathematically robust measure of feature importance, ensuring transparency and reliability in model interpretation. By using this method, we ensure that only statistically significant variables are retained, providing a principled approach to feature selection that has not been previously applied to MWD data.

While prior research has identified relationships between MWD parameters and geotechnical categorical properties [52], this study goes further by using *Boruta-SHAP* to quantify feature contributions and to eliminate spurious correlations. By integrating *Boruta-SHAP*-based feature importance analysis with advanced ML models—including Decision Trees (*DT*), Support Vector Machines (*SVM*), Random Forests (*RF*), Gaussian Process Regression (*GP*), and Neural Networks (*NN*)—this study establishes a high-resolution framework for predicting subsurface geotechnical properties to provide a data-driven, interpretable, and scalable framework for integrating *MWD* technology into mine geotechnical workflows, ultimately enhancing decision-making for excavation and resource management.

2. Methods

The data used in this paper are the same as in Goldstein et al. [28,52,53] which aimed to predict wireline geophysical measurements, geochemical assay values and geotechnical categories from the same *MWD* dataset. For the sake of self-completeness, the site and data are briefed as below:

2.1. Mine Site Geotechnical Data

The Pilbara region in Western Australia is Australia's primary supplier of iron-ore, producing 874 million tons in 2021 [54]. The Marra Mamba Formation and Brockman Formation of the Hammersley Group were the deposits analyzed in this study, as they are the greatest sources of economic Pilbara iron ore [55]. Both Formations consist of extensive sequences of mineralized Banded Iron Formation (BIF) interlayered with shale bands that were deposited about 2.5 billion years ago [56]. The Marra Mamba Formation is contained within the Mount Newman Member and is overlain by the shale dominated West Angelas Member. The Brockman Formation consists of mineralized Dales Gorge BIF and shales.

Two pits were selected for this study, with each pit's geology representing the Marra Mamba and Brockman Formations, respectively. Each pit's geotechnical conditions were characterized by exploration drilling data. The Brockman Pit (*BR*) contained 12 diamond cored holes totaling 1089 m at an average depth of 90 m per hole. The Marra Mamba Pit (*MM*) consisted of 14 diamond cored holes totaling 1431 m at an average depth of 102 m per hole. The exploration data from the *BR* and *MM* diamond cored holes consisted of laboratory results for Unconfined Compressive Strength (*UCS*; measured in MPa) to approximate rock strength, field observed fracture frequency logs (*FPM*; measured in fractures per meter) and several rock mass classification systems scored by the logging geotechnical engineer, including *GSI*, *Q*, *RMR* and *RQD*. The exploration dataset has been scrutinized in the mining company's Quality Assurance and Quality Control (*QA*/*QC*) process and does not require further data engineering.

For the present analysis, rock strengths, fracture frequencies and rock mass classification system scores were considered. Rock strength (*UCS*) is measured from laboratory testing of diamond drilled core samples. Fracture frequency (*FPM*) is recorded from counting naturally occurring discontinuities of diamond drilled core. Scores from a rock mass classification system (*GSI*) operate as an index of the rock's mechanical and structural properties. *GSI* scores were determined from field observations and laboratory test findings and were the only reported rock mass classification system.

2.2. Mine Site MWD Systems and Data

Twenty-two rotary blast hole rigs equipped with tricone Tungsten Carbide Insert bits acquired *MWD* data for this study. Ten Atlas Copco (Epiroc) PV271 rigs, two Terex SKS 12 rigs, one Bucyrus SKS 13 rig, and two Sandvik 460 rigs were employed to drill production blast holes with a 0.229 m hole diameter (Figure 1a). For 0.165 m wall control blast holes, one Cubex QXR 920, one Sandvik 560, and five Atlas Copco (Epiroc) D65 drill rigs were used (Figure 1b). The bench height in the investigated iron-ore pits averaged 10 m, while the sub drilling was approximately 2 m below the bench floor. The burden and spacing of the production blast holes averaged 7 m and 8 m, respectively.

Figure 1. Examples of blasthole drill rigs used for collecting *MWD* data [52]: (**a**) Terex SKS 12, utilized for the drilling of 0.229 m production blast holes and (**b**) Epiroc D65, used in the creation of 0.165 m wall control blast holes.

The Measure-While-Drilling system on the drills at the iron-ore mines monitored the rate of penetration (*rop*; m/s), the torque or rotary pressure (*tor*; Nm), the force on bit (*fob*; kgf), also known as weight on bit, thrust or pulldown pressure, the bit air pressure, or flushing air medium (*bap*; kgf/cm), and the rotary speed (*rpm*). Due to the instability of the onboard sensor, less than 25 percent of sample points included *rpm*. This uneven data collection led to the elimination of *rpm* as a drilling parameter in this study. Metrics for *MWD* were collected by a combination of rigs operated by onboard workers and semi-autonomous equipment remotely managed by an off-site Operations Centre. The drilling system recorded the *MWD* time-series data at approximately 0.1 m intervals along the depth of the blast hole.

The *MWD* data used in this study originated from two pits in different geological environments: the *BR* pit's dataset contained 75,470 blast holes totaling 844,855 m, while the *MM* pit's dataset had 18,887 holes totaling 208,707 m. For this investigation, the *MWD* data from 2 m below the hole collars to the bottom of the blast holes were analyzed. The reason for choosing this depth is that the first two meters of the borehole may not be typical of the rock mass characteristics since this region was likely impacted by the toe charge during blasting of the prior bench and is likely to not be representative of in situ geotechnical properties. This hole collar filtering resulted in 4486 and 3239 datapoints for *BR* and *MM*, respectively.

2.3. MWD Data Pre-Processing

Due to the heterogenous nature of rock, the drill rig control system, and external factors affecting *MWD* responses, production *MWD* data contains unrealistically high and poor performance values [57]. As a result, these variables can result in an inaccurate measurement and an incorrect interpretation of geotechnical properties [58]. Consequently, the mining *MWD* dataset examined in this paper contains a high ratio of noise to signal that is typical of *MWD* data. Such noise could be the result of sensor anomalies, operational inconsistency or geomechanical irregularities. To ensure robust analysis, a structured data preprocessing workflow was applied, addressing noise filtration, feature engineering, and data validation.

Since these noisy *MWD* datapoints in this paper have not been thoroughly examined in any *QA*/*QC* process, they require feature engineering in preparation for use in later experiments. The *MWD* data was first cleaned by removing the initial 2 m of each blast drillhole which may not represent the in situ rock mass for two reasons: (1) the effects of collaring at the beginning of a hole so that the hole remains open, and (2) inclusion of data points with blast damage from the bottom of the last bench's holes. Then, all blasthole data points in which the *rop*, *tor*, *fob*, or *bap* were negative were eliminated. Next, missing *MWD* data points were filled using linear interpolation with the quartile detection method and a threshold factor of 1.5. To limit the localized influence of noise, the blast hole data was subsequently smoothed using a Gaussian filter with a smoothing factor of 0.3. While alternative methods are available, a Gaussian filter was selected as the optimal approach, balancing noise reduction, computational efficiency, and geological signal retention.

Both the *MWD* and exploration drill datasets were converted from drillhole interval formats to point data, consisting of the geospatial coordinates of each data point and the corresponding values from the relevant dataset. The exploration geotechnical hole point data was calculated utilizing downhole wireline logged desurvey data that recorded the azimuth and dip of each hole at every 10 m until the end depth. The blast hole *MWD* data were not desurveyed due to the production nature of the holes and the calculation of point locations assumed of straight holes from the hole collar. The two datasets were then combined using a K-Nearest Neighbor distance-based search algorithm that determines the distance between each point. To facilitate supervised *ML*, each geotechnical drilling data point was queried and matched with the closest *MWD* data point. The results were then filtered to only include points that were within three-dimensional proximity.

2.4. Feature Engineering–MWD Variables

Accurate prediction of geotechnical properties from *MWD* data requires careful selection of input variables. While prior studies have primarily relied on raw *MWD* parameters (*rop*, *tor*, *fob*, *bap*) for rock type classification, this study investigates the role of engineered features, particularly ratio-based and moving standard deviation (*MSD*) features, in improving predictive performance for *UCS*, *FPM*, and *GSI*. Geotechnical properties such as rock strength and fracture density are influenced by multi-variable interactions rather than single metrics. For example, interactions between *fob* and other MWD variables capture drill resistance variations across different lithologies.

The *MWD* values that were derived from the cleaned *MWD* data are shown in Table 1. Derived variables included ratios of the four original variables (such as the rate of penetration divided by the torque, labelled as *roptor*) and a moving standard deviation across 0.5 m for the four original variables (e.g., the moving standard deviation for the rate of penetration is *ropS*). Due to the fragility of the onboard sensor, rotary speed (*rpm*) was unavailable for the majority of blastholes and hence was not included in the analysis. The Specific Energy of Drilling (*SED*) could not be estimated and was also omitted from the analysis due to the absence of rotary speed [59].

Table 1. Measure-While-Drilling variables investigated in this study.

Type	*MWD* Features			
Recorded	*rop*	*tor*	*fob*	*bap*
Ratio	*roptor* *ropfob* *ropbap*	*torrop* *torfob* *torbap*	*fobrop* *fobtor* *fobbap*	*baprop* *baptor* *bapfob*
Moving Standard Deviation	*ropS*	*torS*	*fobS*	*bapS*

It is also important to evaluate whether additional engineered MWD features would strengthen the prediction performance of regression-based ML models. To do this, the NN method was used to compare the performance of only Measured data with additional Engineered data (Measured plus ratios and MSD). Engineered features incorporate additional interactions between drilling parameters (e.g., torque-to-penetration ratios), which improve the predictive model's ability to capture non-linear relationships. The measured features alone do not fully describe rock variability, while engineered features reduce noise and enhance feature differentiation, improving model accuracy.

A preliminary investigation was conducted using the *NN* method to determine if additional engineered *MWD* features would strengthen the prediction performance of regression-based *ML* models. Two feature sets were evaluated, including the Measured (*rop*, *tor*, *fob* and *bap)* and Engineered (Measured plus ratios and *MSD*).

The results of this comparison (Table 2) demonstrate all models performed better with the Engineered features, increasing R^2 by 10–40% and reducing RMSE by up to 40%. The improvement was particularly notable in *MM*, where geological heterogeneity made raw features less effective. The decision was made to incorporate all Measured and Engineered *MWD* features in all the investigated predictive *ML* models.

Table 2. Prediction performance testing results of *NN* using the four measured *MWD* features and all 20 investigated *MWD* features. Higher performing models are bold.

Geotechnical Measurements	*BR*				*MM*			
	Measured		Engineered		Measured		Engineered	
	RMSE	R^2	RMSE	R^2	RMSE	R^2	RMSE	R^2
Unconfined Compressive Strength (MPa)	14.38	0.86	**9.31**	**0.94**	23.56	0.38	**13.95**	**0.78**
Fracture Per Meter	2.88	0.82	**1.32**	**0.96**	4.98	0.61	**2.87**	**0.87**
Geological Strength Index	7.96	0.79	**2.56**	**0.98**	6.78	0.43	**3.23**	**0.87**

2.5. Feature Importance–Boruta-SHAP

In contrast to the commonplace practice of using *PCA* on *MWD* data, this study utilized a deliberate feature importance methodology to establish the relative importance of each *MWD* variable on the various geotechnical values. *Boruta-SHAP* is derived from cooperative game theory, where the contribution of each feature is computed as the marginal contribution across all possible feature subsets [50]. It assigns each feature an importance score based on Shapley values, which quantify the average contribution of a feature across all possible combinations of features.

The *Boruta-SHAP* framework ensures consistency and local accuracy, making it a robust method for feature importance analysis. The Kernel-*SHAP* method was used, as it is computationally efficient for low-dimensional data, and defined by the objective function as:

$$\arg min_{\Phi} \sum_{S \subseteq N} w(S)[f(s) - (\Phi_0) - (\Phi_0 + \sum_{i \in S} \Phi_i]^2 \quad (1)$$

where ϕ_0 is the baseline *SHAP* prediction (expected model output with no features), ϕ_i is the *SHAP* value for feature *i*, *f(S)* is the model prediction using only subset *S*, *N* is the total number of features and $w(S)$ is the Shapley kernel weight, computed as:

$$w(S) = \frac{(|N| - 1)}{\binom{|N|}{|S|} \left| S \right| (|N| - |S|)} \quad (2)$$

This weight ensures that smaller feature subsets receive appropriate consideration. The *SHAP* value for a feature x_i was computed as:

$$\Phi_i = \sum_{S \subseteq N\{i\}} \frac{|S|!(|N| - |S| - 1)!}{|N|!} [f(S \cup \{i\} - f(S)] \quad (3)$$

where $f(S \cup \{i\})$ is the model prediction after adding feature *i* [60].

The *Boruta-SHAP* method was applied to assess the statistical significance of each feature by generating randomized shadow variables:

$$X_{shadow,i} = shuffle(X_i), \quad \forall i \in \{1, 2, \ldots, d\} \quad (4)$$

where Xi is the original feature, $X_{shadow,i}$ is the corresponding shadow feature (randomized version). Shuffling ensures that shadow features have no relationship to the target variable. The dataset is then augmented to include both original and shadow features [61]:

$$X' = [X_1, X_2, \ldots, X_d, X_{shadow,1}, X_{shadow,2}, \ldots, X_{shadow,d}] \quad (5)$$

SHAP values were computed using the *shapley* function from the MATLAB Statistics (2024) and Machine Learning Toolbox (2024) using default hyperparameters and no optimization [62].

Unlike PCA, which assumes linear relationships, *Boruta-SHAP* can handle complex, nonlinear interactions between drilling parameters and rock properties. Principal Component Analysis has been used in previous studies to estimate the importance of Measure-While-Drilling parameters in geotechnical characterization across various excavation environments [25,29,32]. However, such use is incorrect since *PCA* is not specifically designed for the purpose of feature importance. Instead, the method identifies the underlying structure in a high-dimensional dataset and projects it onto a lower-dimensional space. This dimensionality-reduction technique is accomplished by determining the principal components, which are linear combinations of the original attributes that capture the most data variance [7]. However, the most varied features are not necessarily the most important. *PCA* is not a statistically adequate strategy for selecting features, and the *PCA*-based feature importance conclusions from *MWD* data do not corroborate one another [15,28,52,53].

2.6. Regression-Based ML Methods

Regression-based *ML* algorithms, such as *DT, SVM, RF, GP*, and *NN*, have been used in many applications to solve geotechnical engineering problems [63]. Using the most informative characteristics, decision trees (*DT*) divide the data into smaller subsets via recursion [64]. They can capture nonlinear interactions although may be susceptible to overfitting if not pruned properly. *SVM* attempt to identify the hyperplane that maximally separates data into classes [65]. Using a kernel method, they are effective for high-dimensional data and can handle nonlinear relationships. Random forests (*RF*) are ensembles of decision trees that mix multiple models to improve predictive performance and minimize overfitting [66]. They can represent nonlinear relationships and are less susceptible to overfitting than individual *DT*. *GP* models the output variable as a Gaussian distribution and searches for the function that best matches the data [67]. This method captures nonlinear interactions and delivers a probabilistic output estimate. Finally, *NN* are a flexible, nonlinear model composed of layers of interconnected neurons based upon the human brain [68]. They may capture complex correlations and are excellent for high-dimensional data. However, if not adequately regularized, they are susceptible to overfitting.

This study compared the predictive performance of the *DT*, *SVM*, *RF*, *GP*, and *NN* algorithms on *MWD* data for predicting geotechnical conditions. A Pawsey Supercomputer Nimbus cloud Ubuntu instance with 8 vCPUs and 32 GB RAM performed the computations. The Regression Learner Toolbox in MATLAB was used with default hyperparameters and no optimization for each respective regression-based *ML* method to generate models and assess prediction performance [69].

A 10-fold cross-validation technique revealed the training dataset's prediction strength. Datasets were split into 80% Training and 20% Testing. Testing results reported in Root Mean Square Error (RMSE) and R^2 being the average of the 10 folds during cross validation were calculated as follows to compare findings:

$$R^2 = 1 - \frac{RSS}{TSS} = 1 - \left(\frac{\sum_{i=1}^{N} (y_i - f(x_i))^2}{\sum_{i=1}^{N} (y_i - \bar{y})^2} \right) \tag{6}$$

$$MSE = \sqrt{\frac{1}{N} * \sum_{i=1}^{N} (y_i - x_i)^2} \tag{7}$$

where:

R^2 = coefficient of determination
RSS = sum of squares of residuals
TSS = total sum of squares
N = the number of samples
y_i = the measured value,
x_i = the predicted value
$\bar{y}$ = the mean value.

3. Results

This section presents the *SHAP*-based feature importance analysis, including the *Boruta-SHAP* variable selection process, and the predictive performance of regression-based machine learning models.

3.1. MWD Exploratory Data Analysis

Initially, a statistical analysis was conducted for the *rop*, *tor*, *fob* and *bap* *MWD* variables collected by sensors on the drill rigs in both *BR* and *MM* pits. The *rop* followed a right-skewed distribution in both *BR* and *MM* (Figures 2a and 3a). The similar skewness in both formations suggests variable penetration resistance, likely due to bit wear, operator variability, and changing rock properties along the borehole. *tor* follows a normal distribution in both the normal distributions, indicating consistent torque requirements, likely because torque is automatically regulated based on drilling conditions, resulting in a more stable response (Figures 2b and 3b).

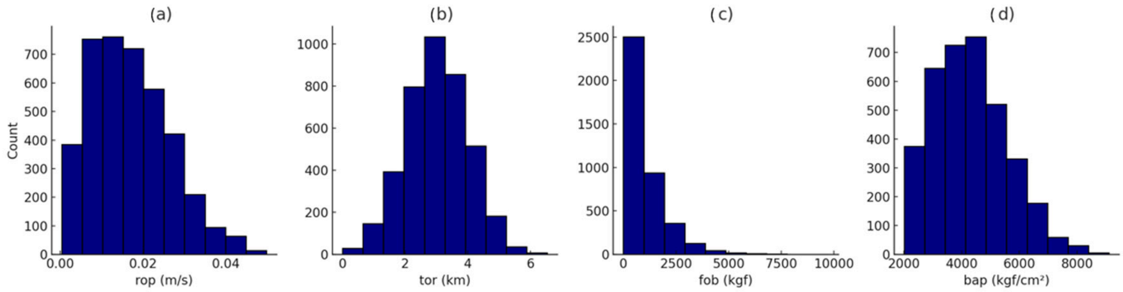

Figure 2. Distribution of *BR* data for (**a**) *rop*, (**b**) *tor*, (**c**) *fob* and (**d**) *bap*.

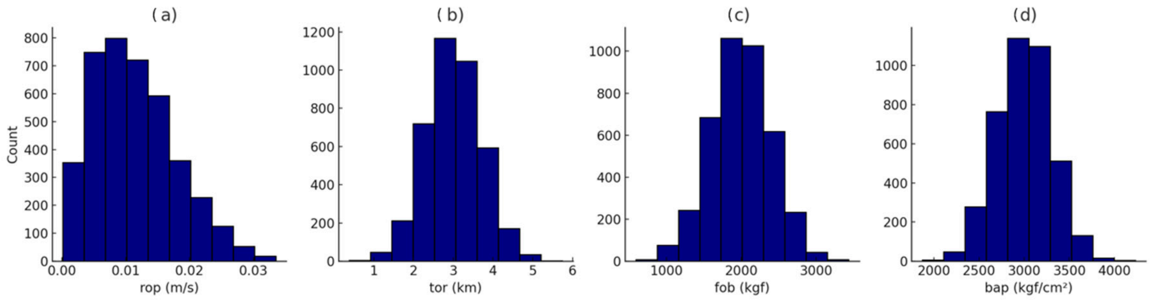

Figure 3. Distribution of *MM* data for (**a**) *rop*, (**b**) *tor*, (**c**) *fob* and (**d**) *bap*.

Key differences in *MWD* variables emerged between the *BR* and *MM* Formations in the *fob* and *bap* distributions. In the *BR* Formation, *fob* (Figure 2c) and *bap* (Figure 2d) followed right-skewed distributions, suggesting the presence of harder, banded lithologies interbedded with softer sediments, requiring variable forces for penetration. In contrast, the *fob* and *bap* (Figures 3c and 3d, respectively), in the *MM* Formation followed normal distributions indicating a more homogeneous rock type with less variability in hardness. The *MM* Formation, deposited in a more stable sedimentary environment, lacks the extensive structural banding and alternating hardness levels of the *BR* Formation, leading to a more consistent force requirement during drilling.

These findings underscore the importance of considering geological context when analyzing *MWD* data, as linear statistical assumptions may not capture the complex interactions between rock mass properties and drilling responses. Moreover, univariate examination of these variables may not describe non-linear relationships between the *MWD* responses and the geotechnical outputs.

Partial dependence plots provide a powerful tool for analyzing the relationship between *MWD* variables and target geotechnical properties across different deposit types. By isolating the effect of individual *MWD* parameters while averaging out other influences, the plots reveal how variables such as *rop*, *fob*, *tor* and *bap* contribute to predicting *UCS*, *FPM*, and *GSI*. This study applies partial dependence to compare these relationships between *BR* and *MM* formations, highlighting formation-specific differences in mechanical resistance, fracturing behavior, and rock mass quality. Understanding these dependencies improves the interpretability of *MWD*-based geotechnical models, supporting formation-specific feature selection and predictive accuracy.

Partial dependence analysis reveals key *UCS* differences between *BR* (Figure 4) and *MM* (Figure 5). In *BR*, *UCS* is driven by mechanical resistance, with *fob* and *tor* as strong predictors, reflecting higher rock competency. In *MM*, these relationships are weaker, suggesting fracturing and mineralogy play a greater role. *rop* inversely correlates with *UCS* in *BR*, indicating harder rock slows drilling, whereas in *MM*, *rop* is a weaker predictor, implying structural factors govern penetration speed. *bap* increases *UCS* in *BR* but declines at high values, suggesting flushing inefficiencies, while in *MM*, *bap* stabilizes earlier, indicating faster drilling optimization. These findings highlight formation-specific *UCS* controls, with *BR* dominated by mechanical resistance and *MM* influenced by additional geological factors.

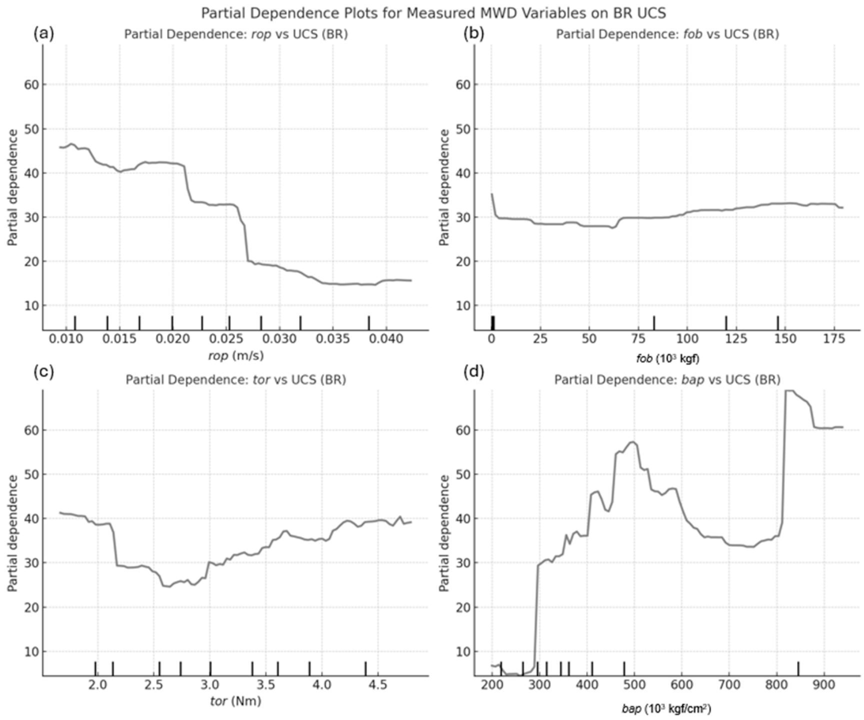

Figure 4. Partial Dependence Plot of Measured Measure-While-Drilling variables of *UCS* in the Brockman deposit pit.

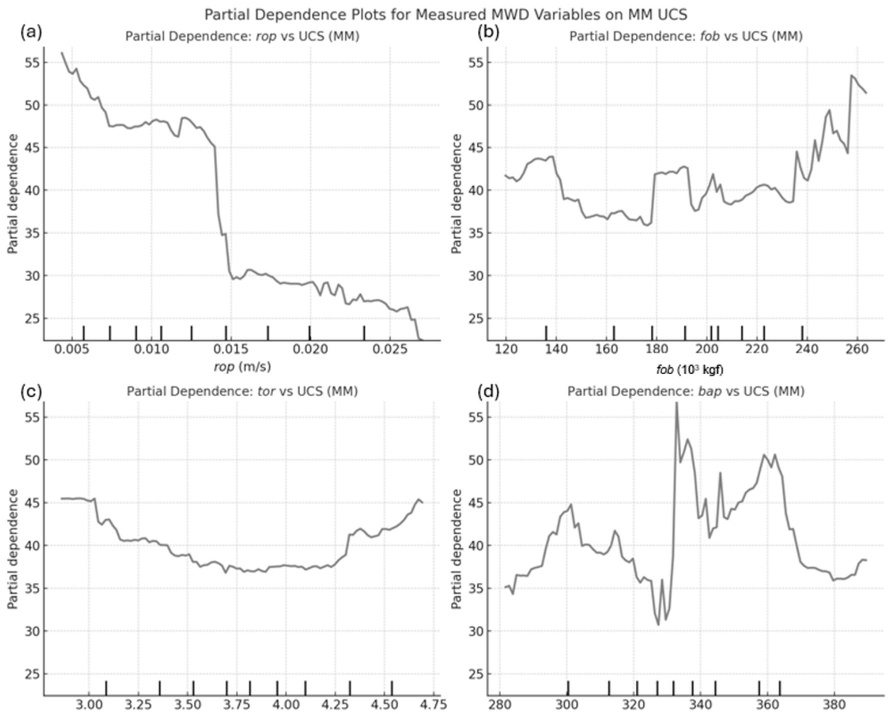

Figure 5. Partial Dependence Plot of Measured Measure-While-Drilling variables of *UCS* in the Marra Mamba deposit pit.

Distinct *FPM* controls in *BR* and *MM* in the partial dependence analysis were observed (Figures 6 and 7, respectively). In *BR*, *FPM* demonstrates a strong inverse correlation with *rop*, indicating fractured rock masses enhance penetration, whereas in *MM*, this relationship is weaker, suggesting fracturing plays a lesser role. *fob* and *tor* are stronger predictors in *BR*, implying fractures are more mechanically induced, while in *MM*, structural factors likely dominate. The Marra Mamba formation is characterized by a greater presence of pre-existing structural discontinuities (e.g., bedding planes, joints), which influence rock mass behavior more than mechanical drilling resistance. In contrast, the Brockman Formation has more competent, homogeneous rock where mechanical resistance dictates fracture behavior. Moreover, *bap* increases *FPM* in *BR* but stabilizes in *MM*, indicating flushing efficiency has less influence on fracture frequency in *MM*. These findings highlight formation-specific differences, with *BR* fracturing driven by drilling resistance, whereas in *MM*, geological discontinuities are more influential.

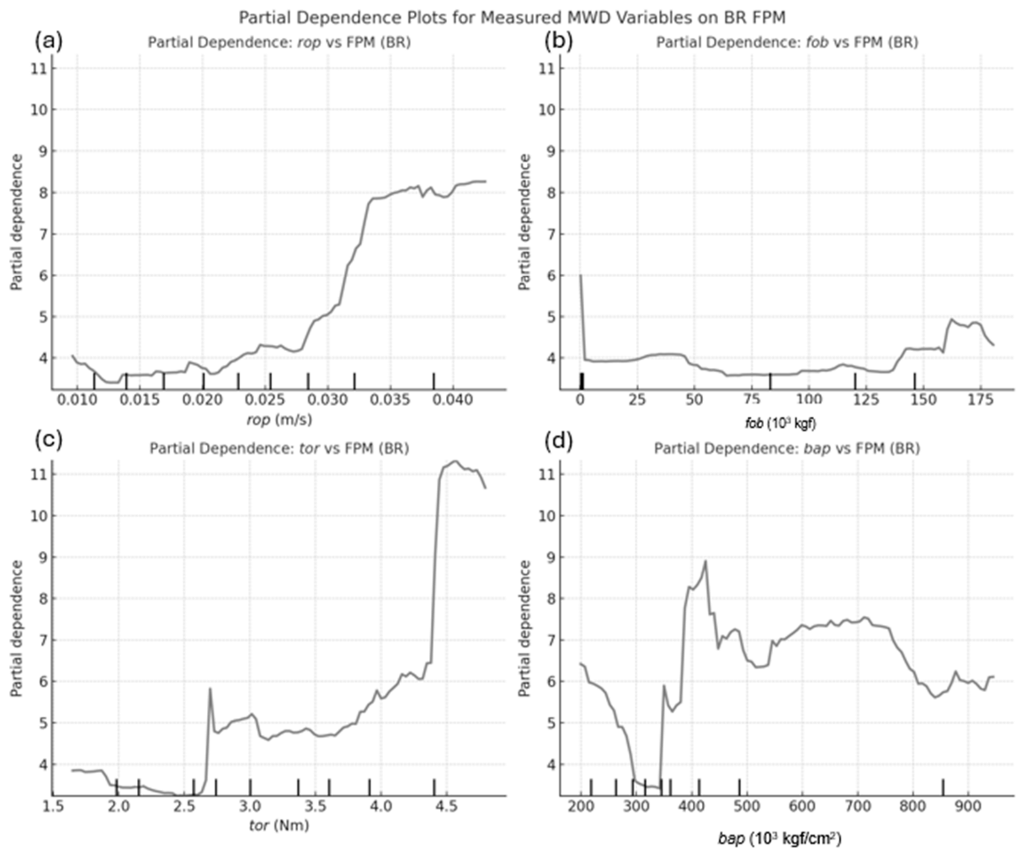

Figure 6. Partial Dependence Plot of Measured Measure-While-Drilling variables of *FPM* in the Brockman deposit pit.

Figures 8 and 9 demonstrate the partial dependence analysis on *GSI* in *BR* and *MM*, respectively. In *BR*, *rop* is strongly inversely related to *GSI*, suggesting higher-quality rock resists penetration, whereas in *MM*, this relationship is weaker, indicating structural factors may play a greater role. *fob* and *tor* exhibit stronger positive correlations with *GSI* in *BR*, implying mechanical resistance is a key indicator of rock mass quality, while in *MM*, these effects are less pronounced, suggesting *GSI* is less constrained by drilling force. *bap* influences *GSI* in both formations, but in *BR*, higher *bap* is more predictive, likely due to differences in air flushing dynamics in competent rock. These results suggest *MWD*-based *GSI* predictions require formation-specific adjustments, with *BR* dominated by mechanical controls and *MM* potentially influenced by additional geological factors.

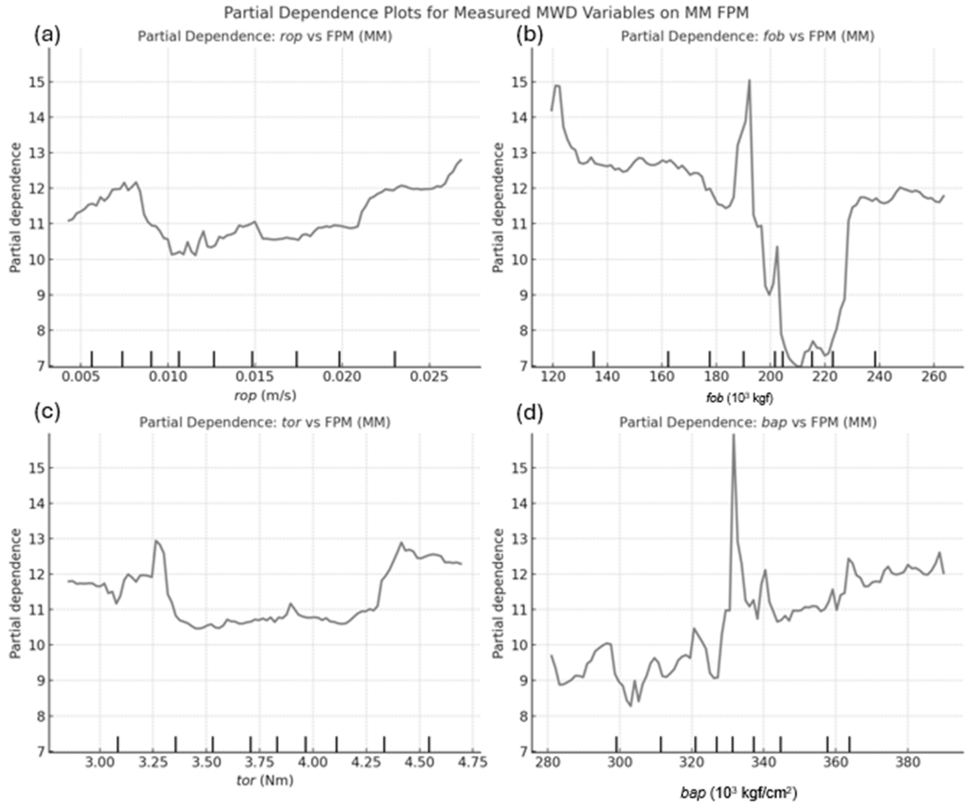

Figure 7. Partial Dependence Plot of Measured Measure-While-Drilling variables of *FPM* in the Marra Mamba deposit pit.

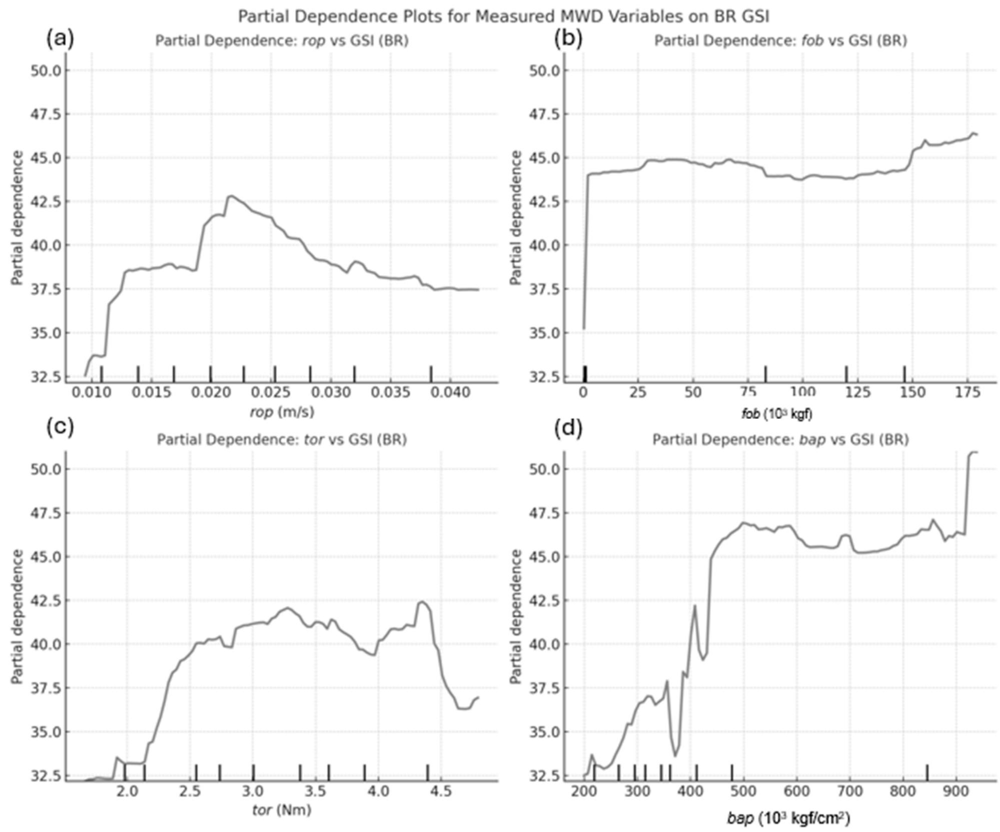

Figure 8. Partial Dependence Plot of Measured Measure-While-Drilling variables of *GSI* in the Brockman deposit pit.

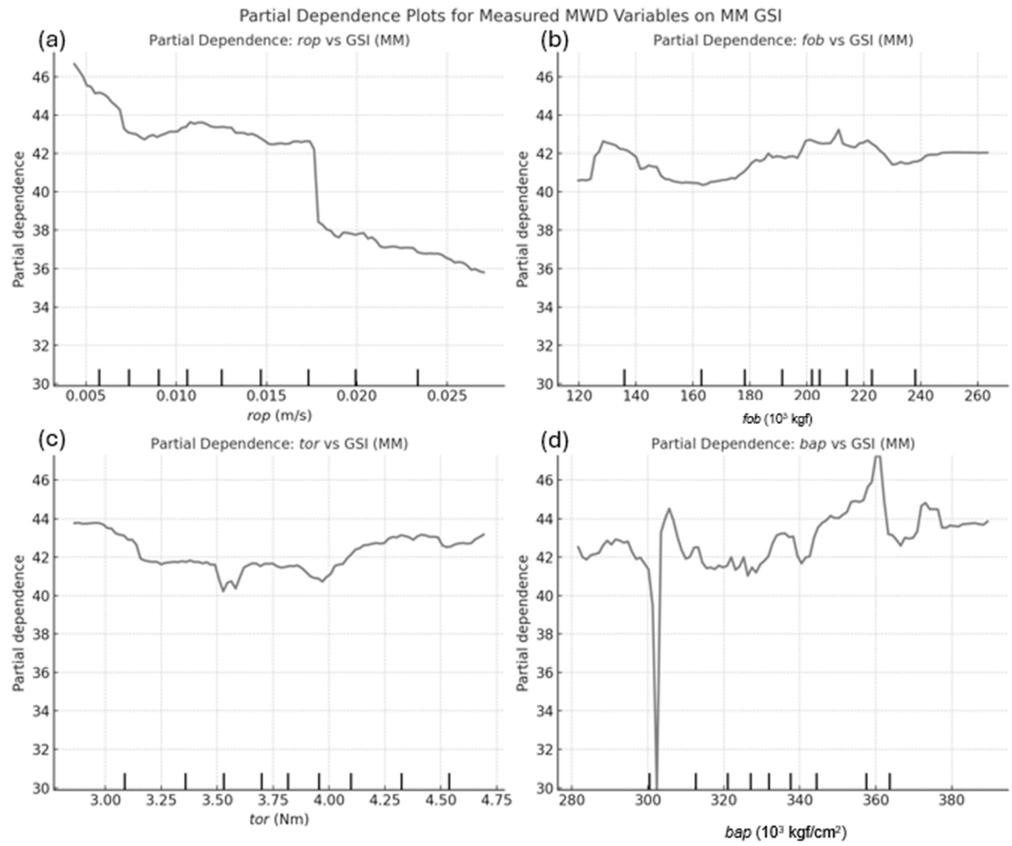

Figure 9. Partial Dependence Plot of Measured Measure-While-Drilling variables of *GSI* in the Marra Mamba deposit pit.

The Measured *MWD* variables influence *UCS*, *FPM*, and *GSI* differently in *BR* and *MM*. In *BR*, *UCS* and *FPM* are strongly controlled by mechanical resistance, with *fob* and *tor* as key predictors, while in *MM*, weaker correlations suggest fracturing and mineralogy play a greater role. *rop* inversely correlates with *UCS* and *GSI* in *BR*, indicating higher-quality rock resists penetration, whereas in *MM*, this relationship is weaker, implying structural controls dominate. *bap* affects *UCS* and *FPM* more in *BR*, while in *MM*, it stabilizes earlier, suggesting flushing efficiency is less critical. These results highlight formation-specific controls, with *BR* driven by mechanical resistance and *MM* influenced by broader geological factors.

3.2. Feature Importance

To determine the statistical significance of MWD predictors, a *Boruta-SHAP* approach was applied. This involved augmenting the predictor set with shadow variables (randomly permuted versions of each feature) and then applying *SHAP* analysis to the expanded feature set. Negative SHAP values indicate that the corresponding feature reduces the predicted value of the target variable, while positive SHAP values increase the predicted outcome. The magnitude of SHAP values reflects the strength of influence on the model's prediction.

This section compares the significance of the numerous features employed for the prediction of rock mass conditions to determine the importance of each *MWD* parameter to describe geotechnical properties. The results of the *Boruta-SHAP* analysis reveal distinct trends in the influence of *MWD* variables on *UCS*, *FPM*, and *GSI* for the *BR* and *MM* Formations, including:

i. Ratio-based features (*baprop*, *fobrop*, *torrop*) ranked higher than raw features in *UCS* and *GSI* prediction;

ii. *MSD* features (ropS, torS) were critical for *FPM*, indicating their effectiveness in detecting fracture-related variability;

iii. *bap* emerged as the most significant raw feature, reinforcing the role of flushing pressure in geotechnical characterization.

These results challenge the conventional assumption that *rop* and *tor* are the primary indicators of geotechnical conditions, highlighting the need for multi-variable analysis.

3.2.1. Feature Importance Boruta-SHAP—UCS

The *Boruta-SHAP* values for *UCS* prediction in *BR* (Figure 10) indicate that *bap*, *bapfob*, *torbap*, and *torS* are the most influential features, suggesting that *UCS* in *BR* is primarily controlled by pressure-related variables rather than purely force-based parameters. This challenges the initial assumption that *fob* and *tor* would dominate, instead highlighting that higher *bap* correlates with increased *UCS*, implying a pressure-dominated response where greater air pressure is required to penetrate stronger rock. While *rop* and *fob* still contribute, their role appears secondary to *bap*-related variables, suggesting that mechanical resistance remains a factor but is overshadowed by pressure effects.

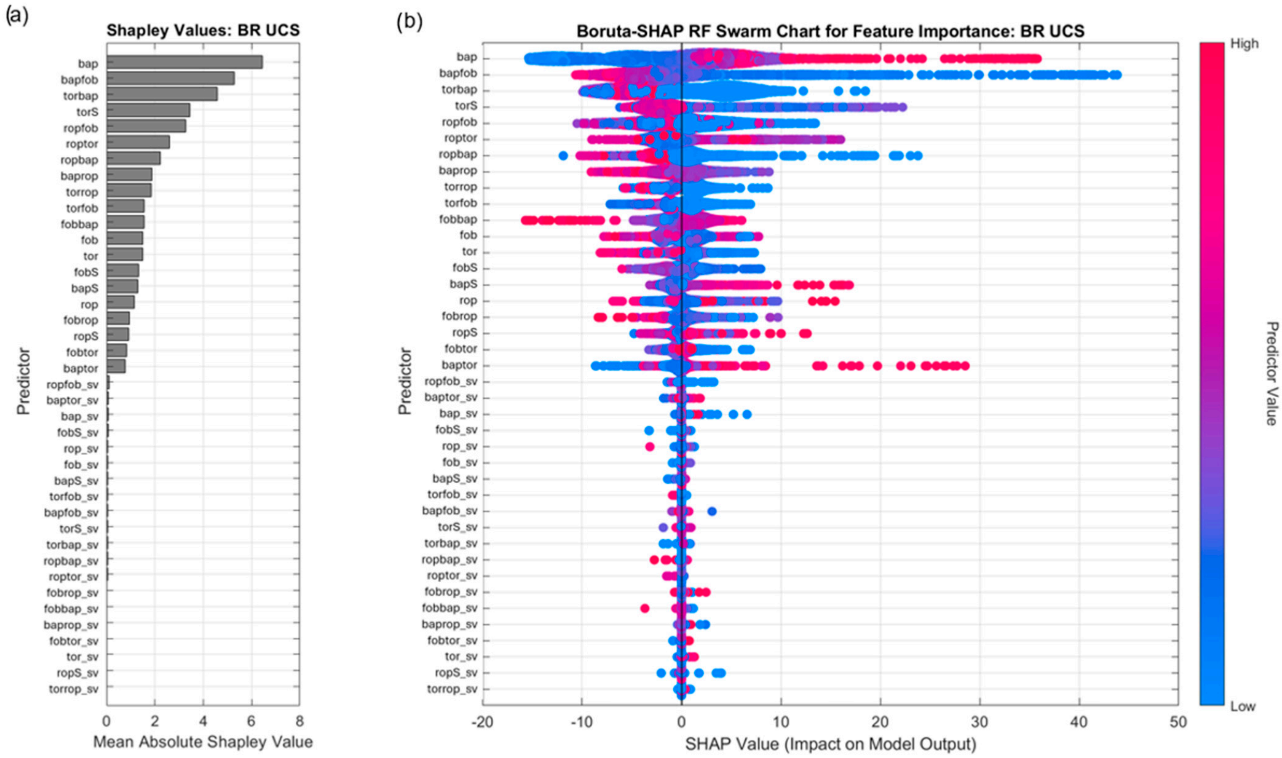

Figure 10. Feature importance analysis for Unconfined Compressive Strength in the Brockman Formation using the *Boruta-SHAP* method with a random forest model. (**a**) The bar plot illustrates the mean absolute *SHAP* values for each Measure-While-Drilling parameter, highlighting the most influential variables in predicting fracture occurrence. (**b**) The swarm chart provides a detailed view of how each parameter affects the model's output, indicating the relative contribution of key drilling responses such as torque, bit air pressure, and rate of penetration.

Boruta-SHAP values for *BR* range from −20 to +50, reflecting high *UCS* variability across different sections of the pit, which aligns with the geological complexity of *BR*, characterized by interbedded high-strength chert and quartz layers. This high variability emphasizes the importance of drilling efficiency and airflow management in *UCS* interpretation from *MWD* data. The pressure-driven nature of *UCS* estimation implies that rock breakage and drill performance are more affected by air pressure regulation than direct force application, reinforcing the critical role of pressure-based drilling adjustments in *BR* formations.

The *Boruta-SHAP* analysis for *MM UCS* (Figure 11) reveals that *fobtor*, *bapfob*, *fobS*, and *rop* are the most important variables, indicating a stronger influence of force-based interactions in *MM* compared to *BR*. While *bap* remains a key factor, *MM* shows greater importance of *fobtor* and *fobS*, suggesting that *UCS* in *MM* is controlled by both applied forces and pressure effects. Additionally, *rop* and *ropS* hold greater significance in *MM* than in *BR*, indicating a higher sensitivity of penetration rate variations to rock strength. This suggests that *UCS* in *MM* is not purely pressure-driven but also strongly influenced by drilling force and mechanical loading, which reflects the more homogeneous nature of *MM* lithologies.

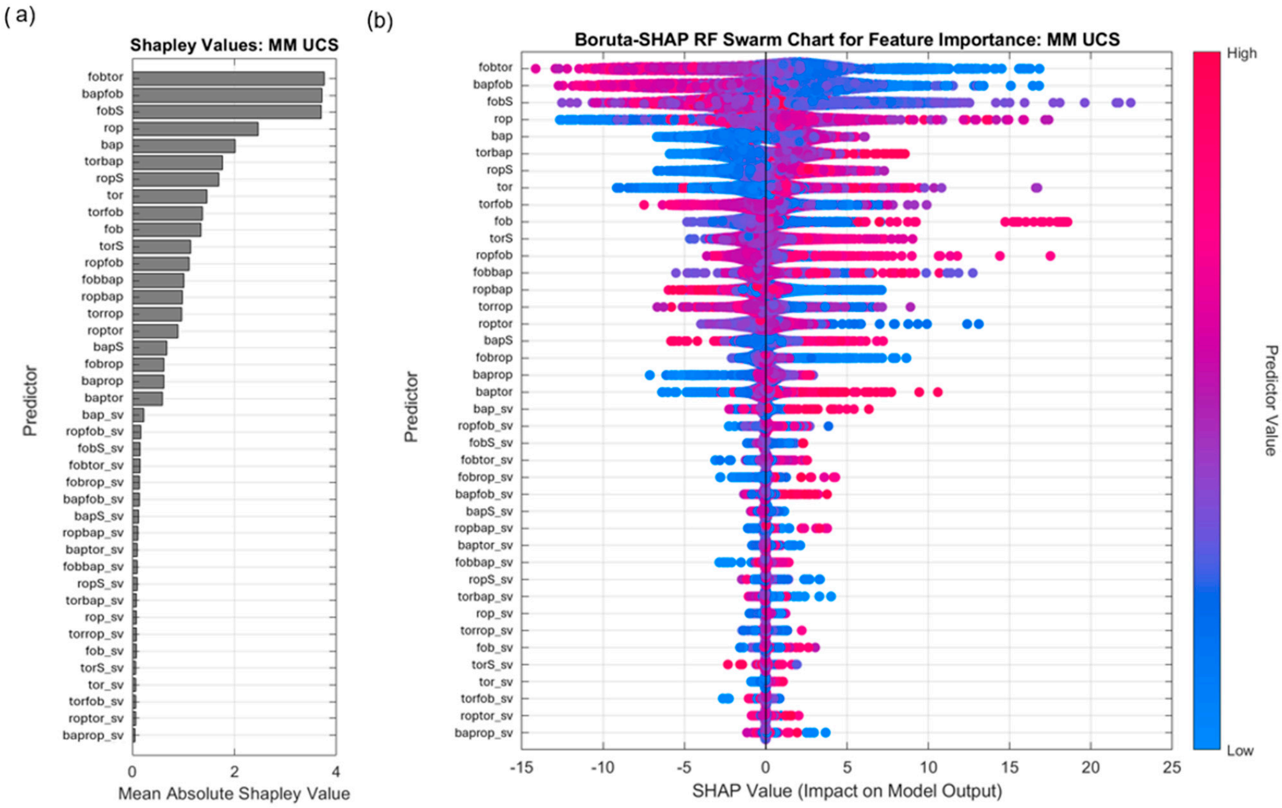

Figure 11. Feature importance analysis for Unconfined Compressive Strength in the Marra Mamba Formation using the *Boruta-SHAP* method with a random forest model. (**a**) The bar plot illustrates the mean absolute *SHAP* values for each Measure-While-Drilling parameter, highlighting the most influential variables in predicting fracture occurrence. (**b**) The swarm chart provides a detailed view of how each parameter affects the model's output, indicating the relative contribution of key drilling responses such as torque, bit air pressure, and rate of penetration.

The Boruta shadow variables (_sv) confirm these trends, reinforcing the reliability of the primary predictors. In *BR*, *ropfob_sv, torfob_sv,* and *bapfob_sv* exhibit low *SHAP* values, confirming that *bap* and its interactions are genuine *UCS* predictors. The lower significance of force-related shadow variables further supports the dominance of pressure-based controls in *BR UCS* estimation. *bap_sv, ropfob_sv,* and *fobtor_sv* also exhibit low influence for *MM*, reinforcing that while pressure effects remain important, force-based variables play a more significant role in *MM UCS* predictions. The weaker impact of *bap*_sv in *MM* compared to *BR* suggests that *UCS* in *MM* is less affected by pressure-driven variability, instead relying more on mechanical resistance and penetration efficiency.

3.2.2. Feature Importance Boruta-SHAP—FPM

Unlike PCA-based feature selection, which primarily identifies directions of maximum variance without necessarily ranking feature importance for predictive modeling, *Boruta-SHAP* ensures statistical robustness by comparing real MWD variables against shadow features. The method's reliance on Shapley values allows for the quantification of nonlinear feature interactions, preserving only the most informative variables while eliminating redundant or weak predictors. This enhances model interpretability, enabling the reliable identification of key MWD parameters that govern geotechnical conditions, ultimately supporting more effective decision-making in slope stability assessments.

The *Boruta-SHAP* analysis of *FPM* highlights distinct fracture detection mechanisms between *BR* and *MM*, reflecting their fundamentally different geomechanical behaviors. Figure 12 displays the most influential features in *BR* are *baptor*, *ropS*, *torS*, and *torbap*, indicating that fracture detection is primarily controlled by rotational force and penetration rate fluctuations. The dominance of torque-based variables (*torS*, *torbap*) suggests that fractures in *BR* are influenced by rotational resistance, likely due to the deposit's high rock competency and existing fracture networks. In *MM* (Figure 13), *ropfob*, *rop*, *torfob*, and *torbap* emerge as the most significant predictors, suggesting that fracturing is driven more by penetration efficiency and applied force rather than rotational resistance, highlighting a greater dependence on mechanical loading rather than pre-existing structural controls.

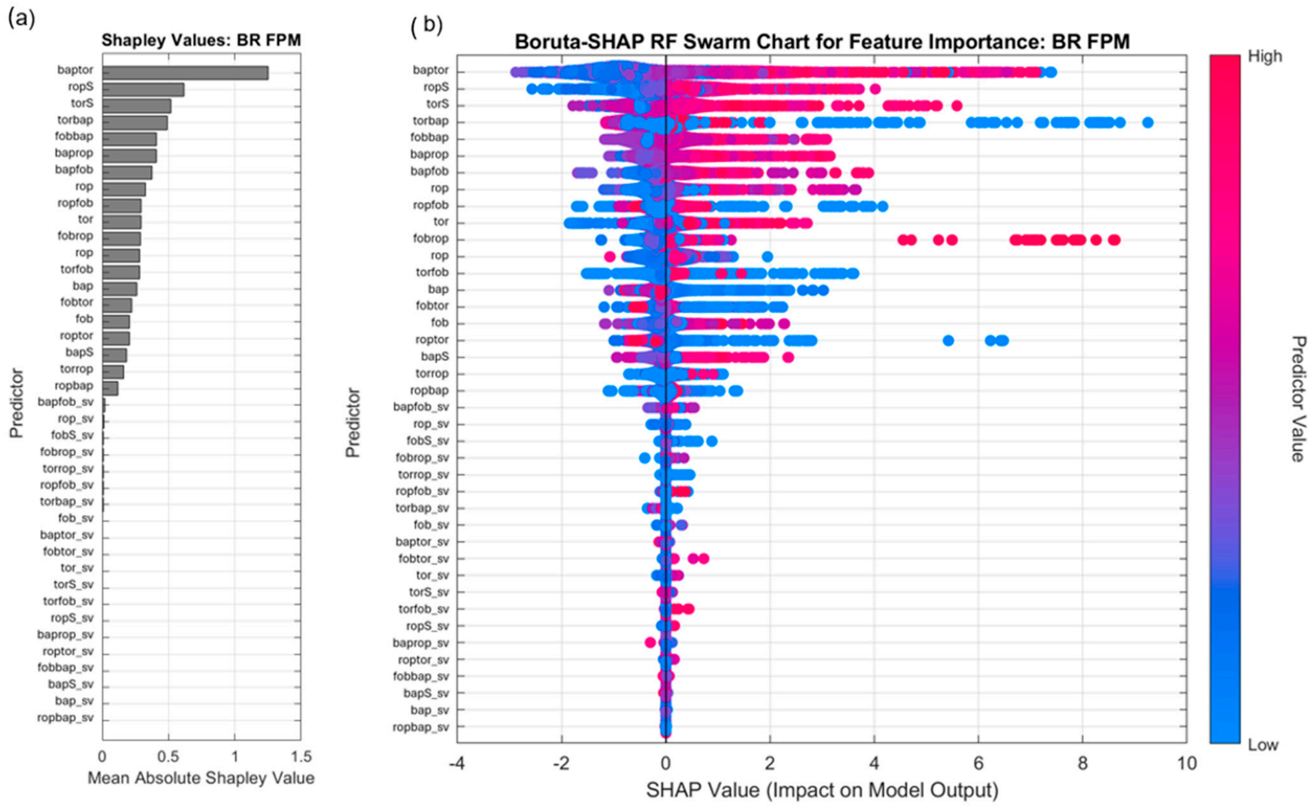

Figure 12. Feature importance analysis for fracture frequency per meter in the Brockman Formation using the *Boruta-SHAP* method with a random forest model. (**a**) The bar plot illustrates the mean absolute *SHAP* values for each Measure-While-Drilling parameter, highlighting the most influential variables in predicting fracture occurrence. (**b**) The swarm chart provides a detailed view of how each parameter affects the model's output, indicating the relative contribution of key drilling responses such as torque, bit air pressure, and rate of penetration.

Fracture behavior is influenced by the combined effects of multiple drilling variables rather than individual metrics alone. In the Brockman Formation, torque-related interactions (e.g., torque-to-penetration ratio) are dominant due to the rock's competency, where fractures develop primarily through mechanical resistance. In contrast, in the Marra Mamba Formation, interactions involving *fob* and *rop* play a larger role, as pre-existing structural discontinuities such as bedding planes and joints govern fracture propagation. These findings emphasize the non-linearity in fracture formation—while individual features provide some predictive power, their interactions enhance explanatory capability by capturing localized rock heterogeneity and stress redistribution. This supports previous research indicating that fracture initiation is a function of both drilling resistance and geological structure.

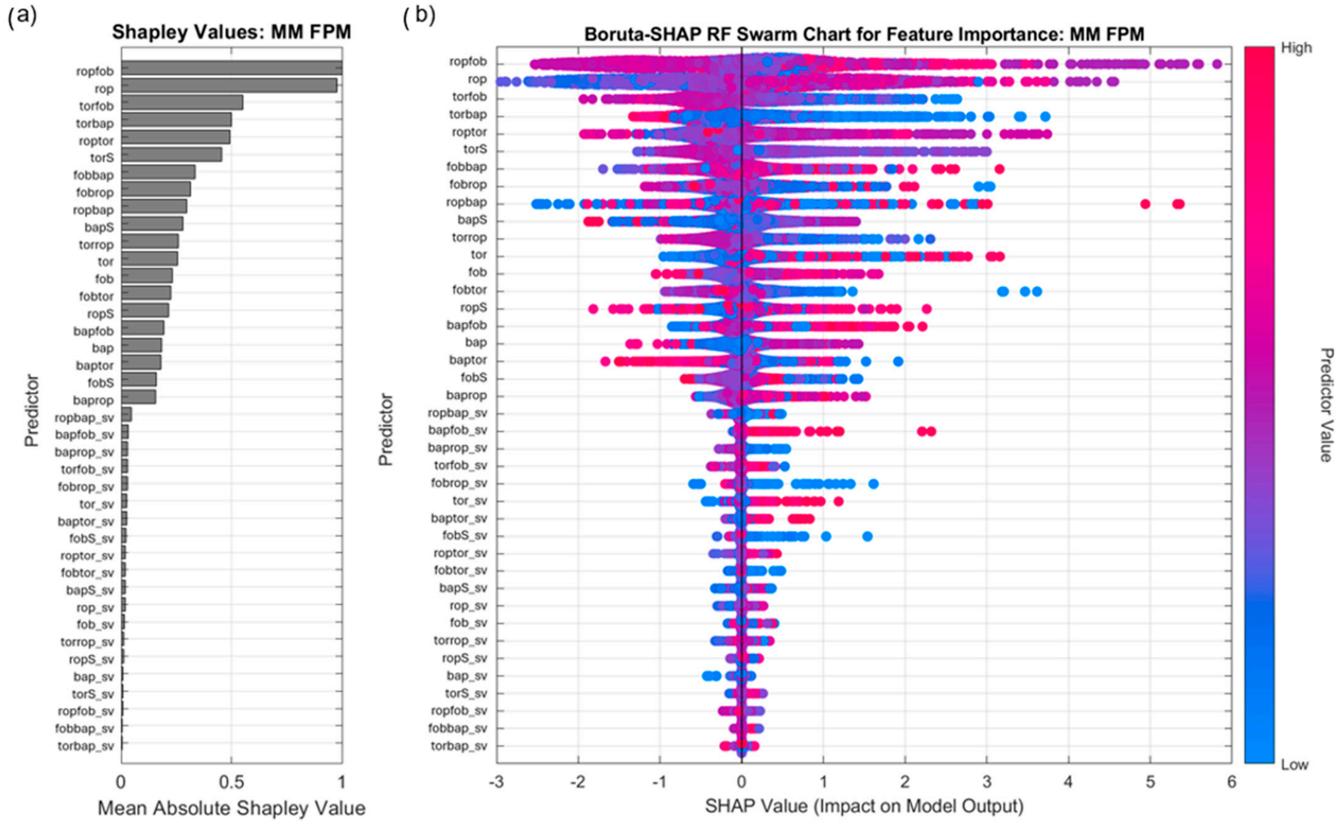

Figure 13. Feature importance analysis for fracture frequency per meter in the Marra Mamba Formation using the *Boruta-SHAP* method with a random forest model. (**a**) The bar plot illustrates the mean absolute *SHAP* values for each Measure-While-Drilling parameter, highlighting the most influential variables in predicting fracture occurrence. (**b**) The swarm chart provides a detailed view of how each parameter affects the model's output, indicating the relative contribution of key drilling responses such as torque, bit air pressure, and rate of penetration.

The role of interaction-based variables further underscores these contrasting fracture behaviors. In *BR*, *baptor* and *torbap* exhibited strong feature importance, emphasizing the role of pressure-assisted torque in controlling fracture initiation. This suggests that fracturing in *BR* is more dependent on dynamic drilling interactions, in which changes in penetration rate and torque signal structural weaknesses. In contrast, *MM* is more influenced by *ropfob* and *torfob*, indicating that fracture formation is primarily governed by the interplay of penetration rate and force-based responses rather than pressure alone. This implies that fracturing in *BR* is more dynamic and controlled by drilling efficiency, while *MM* is more sensitive to mechanical load variations and stress-induced fracturing.

The distribution of *Boruta-SHAP* values across both deposits further reinforces these differences in fracturing mechanisms. *ropS* and *torS* exhibited a wide range of *SHAP* values for *BR*, suggesting that fluctuations in penetration rate and torque can either enhance or suppress fracture formation depending on localized geological conditions. The presence of extreme *SHAP* values supports the idea that brittle failure mechanisms dominate *BR*, where abrupt energy release leads to rapid fracture propagation. On the other hand, *MM* exhibits a more uniform and progressive fracture development process, as seen in the tighter distribution of *SHAP* values for *ropfob* and *fob*. The lower variance in *SHAP* values in *MM* suggests that fractures are governed by stress-driven mechanisms, leading to gradual failure rather than abrupt mechanical breakdown.

The Boruta shadow variables (_sv) confirm the robustness of the key predictors. In *BR*, shadow variables such as *ropfob*_sv, *fobS*_sv, and *torfob*_sv exhibit minimal impact, reinforcing that the real counterparts (*ropfob*, *fobS*, *torfob*) are meaningful indicators of fracture formation. The low influence of force-based and penetration rate shadow variables suggests that fracturing in *BR* is governed by true drilling responses rather than random fluctuations.

Similarly, in *MM*, *bap*_sv, *torrop*_sv, and *fobtor*_sv show negligible influence, confirming that the primary features—*ropfob, rop, torfob*—are legitimate predictors of *FPM* in *MM*. The lower impact of shadow variables for *MM* compared to *BR* aligns with its more stable geomechanical behavior, suggesting that fracture development in *MM* is more predictable and less influenced by drilling variability. The limited significance of air pressure-related shadow variables in both deposits further support fracturing is primarily driven by penetration rate and force-based interactions rather than pressure alone.

3.2.3. Feature Importance Boruta-SHAP—GSI

The *Boruta-SHAP* results for *GSI* in *BR* and *MM* illustrate distinct patterns in how *MWD* variables correlate with rock mass quality. In *BR*, *Boruta-SHAP* values are more widely distributed, ranging from approximately −8 to +10, reflecting high variability in rock strength due to localized geological heterogeneity, such as alternating iron-rich and siliceous bands. In contrast, *MM* exhibits a narrower *SHAP* value range (−15 to +10), with values focused around zero, indicating more uniform rock strength and less short-range variability. The reduced spread of *SHAP* values in *MM* suggests that *GSI* can be more reliably estimated using steady-state *MWD* variables, as opposed to the more dynamic drilling responses seen in *BR*.

Key feature importance rankings further highlight deposit-specific differences in *GSI* prediction. *torrop, bap*, and *fobS* emerge as the most influential variables in *BR*, with *torrop* exhibiting the highest importance (Figure 14). This suggests that rotational torque and its interaction with penetration rate strongly influence *GSI* in *BR*, likely due to banding, alteration, and fracturing effects. Other key features include *fobrop, ropbap*, and *bapfob*, highlighting the role of multiple variable interactions in determining *BR* geotechnical properties. The strong influence of force-based variables (*fob, tor*) suggests that rock mass quality in *BR* is more sensitive to mechanical resistance and drilling force fluctuations.

On the other hand, *MM* (Figure 15) shows a different feature importance hierarchy, with *rop, bapfob*, and *bap* as the dominant predictors. Unlike *BR*, *bap* has a stronger direct relationship with GSI, suggesting that air pressure-based variables are more predictive of rock strength in *MM* formations. Additionally, torque-related variables (*torrop, torbap*) have greater importance in *MM* than in *BR*, reinforcing the role of rotational drilling forces in characterizing the *MM* rock mass. The lower importance of force-based variables in *MM*, along with the reduced variance of *Boruta-SHAP* values, suggests that *MM* exhibits a more homogeneous geomechanical structure, resulting in more stable and predictable drilling responses compared to *BR*.

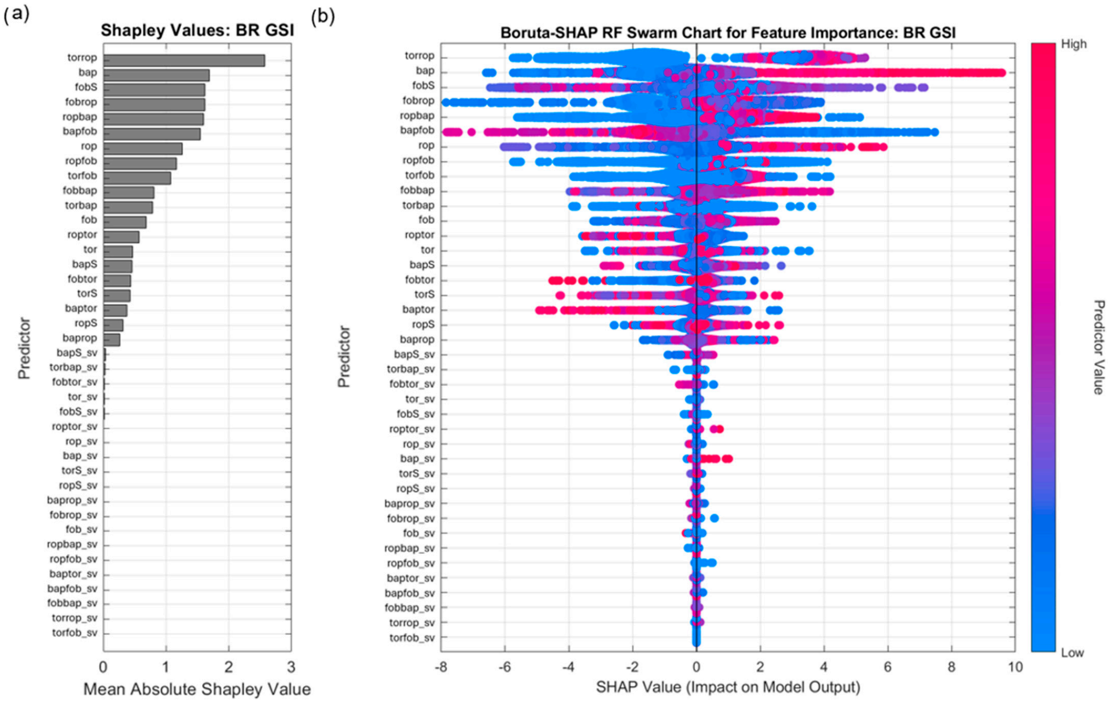

Figure 14. Feature importance analysis for Geological Strength Index in the Brockman Formation using the *Boruta-SHAP* method with a random forest model. (**a**) The bar plot illustrates the mean absolute *SHAP* values for each Measure-While-Drilling parameter, highlighting the most influential variables in predicting fracture occurrence. (**b**) The swarm chart provides a detailed view of how each parameter affects the model's output, indicating the relative contribution of key drilling responses such as torque, bit air pressure, and rate of penetration.

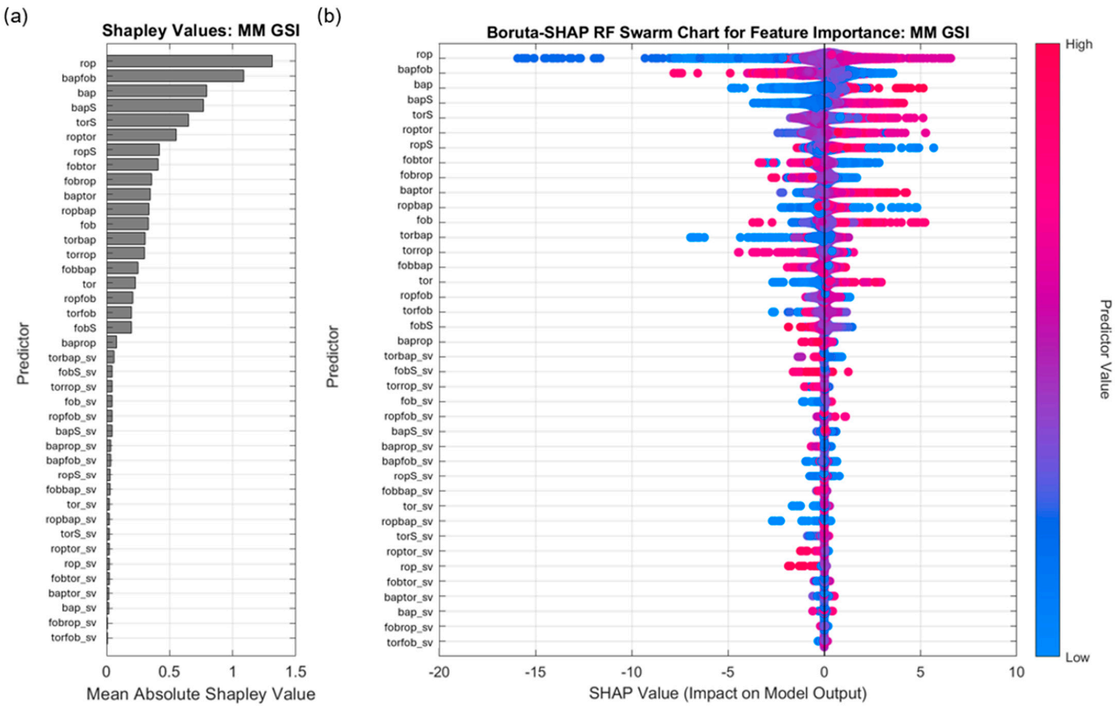

Figure 15. Feature importance analysis for Geological Strength Index in the Marra Mamba Formation using the *Boruta-SHAP* method with a random forest model. (**a**) The bar plot illustrates the mean absolute *SHAP* values for each Measure-While-Drilling parameter, highlighting the most influential variables in predicting fracture occurrence. (**b**) The swarm chart provides a detailed view of how each parameter affects the model's output, indicating the relative contribution of key drilling responses such as torque, bit air pressure, and rate of penetration.

The Boruta shadow variables (_sv) further validate the robustness of the *GSI* predictions by distinguishing genuine predictive features from statistical noise. For *BR*, *torbap_sv, fobS_sv*, and *torrop*_sv exhibited minimal importance, confirming that the real counterparts of these variables—such as *torrop*, *fobS*, and *bap*—are genuine indicators of rock mass quality. The presence of multiple interaction-based shadow variables with low significance reinforces the idea that *GSI* variations in *BR* are primarily controlled by actual drilling responses rather than random fluctuations.

In *MM*, *bap_sv, rop_sv*, and *torbap_sv* showed similarly low importance, supporting the conclusion that bap and rop remain the dominant drivers of *GSI* in *MM* formations. The weaker influence of shadow variables in *MM* compared to *BR* aligns with the observation that *GSI* prediction in *MM* is more stable and less influenced by short-range variability. This distinction highlights how *MWD*-based *GSI* estimation is more complex in *BR* due to geological heterogeneity, whereas *MM* allows for more reliable and consistent predictions using less variable drilling parameters.

3.3. Regression-Based ML Overview

The predictive performance of five regression-based ML models—*DT, SVM, RF, GP*, and *NN*—was evaluated for estimating *UCS*, *FPM*, and *GSI* from *MWD* data. The results revealed consistent trends across all models, with *NN* and *RF* outperforming other approaches in both datasets, particularly in *BR* where larger data volume and more homogeneous geotechnical conditions contributed to higher predictive accuracy.

Across all geotechnical parameters, *NN* consistently achieved the highest R^2 and lowest RMSE, followed closely by *RF*. The superior performance of *NN* can be attributed to its ability to model complex, nonlinear interactions between *MWD* variables and geotechnical properties. *RF* also demonstrated strong predictive capability, benefiting from its ensemble approach that reduces overfitting by averaging multiple *DTs*. Considering both R^2 and computational efficiency, *RF* was selected as the most balanced model, offering high accuracy with moderate computational time, making it suitable for operational deployment.

Conversely, *DT*, *SVM*, and *GP* exhibited lower predictive accuracy, particularly in *MM*, which is characterized by higher geological variability. *DT* was the least effective model, likely due to its sensitivity to noise in the *MWD* dataset and its tendency to overfit training data while failing to generalize well to test data.

The superior performance of *NN* and *RF* can be attributed to their ability to handle high-dimensional, multivariate datasets where complex interactions exist between input features. In contrast, simpler models like *DT* and *SVM* struggled because:

i. *DT* is prone to overfitting and lacks the ability to capture intricate geomechanical relationships;
ii. *SVM* relies on a fixed decision boundary, which is not well-suited to continuous, nonlinear geotechnical responses;
iii. *GP*, while effective in some cases, is computationally expensive and does not generalize well with the large, noisy datasets typical of *MWD* applications.

The comparison between *NN* and *RF* suggests a trade-off where *NN* provides the highest predictive accuracy but requires significantly longer training times and *RF* offers a strong balance between accuracy and computational efficiency, making it a practical choice for real-time mining applications. *GP* may be useful for smaller datasets but is not well-suited for large-scale *MWD* data due to its high computational cost.

Given these findings, future work should explore hybrid modeling approaches that combine the interpretability of *RF* with the high-dimensional learning capabilities of *NN*. Additionally, model uncertainty quantification should be incorporated to better assess prediction reliability in heterogeneous formations such as *MM*.

3.3.1. UCS Prediction

For the *BR* dataset, the *NN* model outperformed all other approaches, achieving an R^2 of 0.96 and the lowest RMSE of 7.7 MPa for both training and test datasets (Table 3). The *RF* model also exhibited strong predictive capabilities, with R^2 = 0.94 and RMSE = 9.3 MPa on the test set. *SVM* and *GP* demonstrated similar predictive accuracy, with R^2 values above 0.91 and RMSE values in the range of 10.4 to 11.9 MPa. *DT*, while computationally efficient, had the lowest predictive accuracy in *BR*, with R^2 = 0.90 and RMSE = 12.4 MPa.

Table 3. Regression-based *ML* 10-fold cross validation training and testing analytical coefficient of determination, RMSE (MPa) and training speed prediction results for *UCS* values from *MWD* data using all *MWD* features in *BR* and *MM* Formations.

Regression-Based *ML* Method	*BR*					*MM*				
	Train			Test		Train			Test	
	RMSE	R^2	Time (s)	RMSE	R^2	RMSE	R^2	Time	RMSE	R^2
DT	13.2	0.89	**8**	12.4	0.90	18.5	0.61	2.3	21.88	0.46
SVM	11.9	0.91	7	11.9	0.91	16.8	0.68	7.5	17.84	0.64
RF	9.7	0.94	60	9.3	0.94	13.3	0.8	66.1	13.95	0.78
GP	12.2	0.91	4	10.4	0.93	1.2	0.66	2.4	18.28	0.62
NN	7.7	0.96	517	7.7	0.96	10.3	0.88	184	11.95	0.84

In contrast, model performance was notably lower for the *MM* dataset, with a wider range of R^2 values (0.46 to 0.84) and higher RMSE values across all models. *NN* remained the best-performing model for *MM*, with R^2 = 0.84 and RMSE = 11.95 MPa. *RF* followed closely, achieving an R^2 of 0.78 and RMSE of 13.95 MPa. *SVM* and *GP* displayed moderate predictive ability, with R^2 values ranging from 0.62 to 0.68. *DT* performed the poorest, with an R^2 of 0.46 and the highest RMSE of 21.88 MPa, indicating important prediction errors for *MM* rock strength values. The higher RMSE values in *MM* suggest that *UCS* estimation in this formation is more challenging due to greater lithological variability. The lower performance of *GP* and *SVM* (R^2 = 0.62–0.68 for *MM*) suggests that these models struggle with the nonlinearity inherent in *MWD*-*UCS* relationships.

The training times for each model varied, with *NN* requiring the longest computation time (517 s for *BR* and 184 s for *MM*). Conversely, *GP* were the fastest models, taking only 4 s for *BR* and 2.4 s for *MM*. *DT* and *SVM* also demonstrated relatively fast training times, with *SVM* completing training in under 10 s for both deposits. *RF* had moderate computational demand, requiring 60 s for *BR* and 66.1 s for *MM*.

These results indicate that *NN* and *RF* offer the best compromise between predictive accuracy and robustness, particularly for the *BR* dataset. The *MM* dataset exhibits greater prediction uncertainty, likely due to increased geological heterogeneity or reduced data volume. Future work will focus on exploring the underlying causes of performance degradation in *MM* predictions, refining feature selection techniques, and integrating additional geotechnical parameters to improve model generalization.

3.3.2. FPM Prediction

The *BR* results presented in Table 4 demonstrate the *NN* model outperformed all other approaches, achieving an R^2 of 0.98 and the lowest RMSE of 1.0 for both training and test datasets, likely due to its ability to capture highly nonlinear fracture formation mechanisms. The *RF* model also exhibited strong predictive capabilities, with R^2 = 0.96 and RMSE = 1.3 on the test set. *SVM* and *GP* demonstrated similar predictive accuracy, with R^2 values above 0.93 and RMSE values ranging from 1.6 to 1.8. *DT*, while computationally efficient, had the lowest predictive accuracy in the *BR* dataset, with R^2 = 0.94 and RMSE = 1.7.

Table 4. Regression-based *ML* 10-fold cross validation training and testing analytical coefficient of determination, RMSE and training speed prediction results for *FPM* values from *MWD* data using all *MWD* features in *BR* and *MM* Formations.

Regression-Based *ML* Method	***BR***					***MM***				
	Train			**Test**		**Train**			**Test**	
	RMSE	**R^2**	**Time (s)**	**RMSE**	**R^2**	**RMSE**	**R^2**	**Time**	**RMSE**	**R^2**
DT	2.0	0.93	2	1.7	0.94	4.8	0.59	2	5.5	0.53
SVM	1.8	0.94	9	1.6	0.94	3.9	0.73	7	3.9	0.76
RF	1.3	0.97	77	1.3	0.96	3.1	0.84	59	2.9	0.87
GP	1.7	0.94	4	1.8	0.93	3.1	0.84	4	3.2	0.84
NN	1.0	0.98	279	1.0	0.98	2.4	0.9	206	2.2	0.93

Model performance was lower across all methods in *MM* models, with R^2 values ranging from 0.53 to 0.93. The *NN* model remained the best-performing approach, achieving R^2 = 0.93 and RMSE = 2.2, followed by *RF* (R^2 = 0.87, RMSE = 2.9). *SVM* and *GP* displayed moderate predictive ability, with R^2 values between 0.76 and 0.84, while *DT* exhibited the weakest performance, with R^2 = 0.53 and RMSE = 5.5, due to its tendency to oversimplify fracture-related interactions, leading to poor generalization.

The training times for each model varied, with *NN* requiring the longest computation time (Table 3). Conversely, *GP* were the fastest models, taking only 4 s for *BR* and *MM*. *DT* and *SVM* also demonstrated relatively fast training times, with *SVM* completing training in under 10 s for both datasets. *RF* had a moderate computational demand, requiring 77 s for *BR* and 59 s for *MM*.

Overall, these results indicate that *NN* and *RF* provide the most robust predictive performance for both *BR* and *MM* datasets, with *NN* yielding the highest accuracy but at a higher computational cost. The *MM* dataset exhibits greater prediction uncertainty, likely due to increased geological heterogeneity or reduced data volume. Future investigations will focus on identifying the sources of variability in *MM* predictions, optimizing feature selection, and integrating additional geotechnical parameters to enhance model generalization.

3.3.3. GSI Prediction

For the *BR* dataset, the *NN* model achieved the highest accuracy, with an R^2 of 0.99 and the lowest RMSE of 2.0 for both training and test datasets (Table 5). The *RF* model also performed well, with R^2 = 0.98 and RMSE = 2.6, followed by *SVM* (R^2 = 0.97, RMSE = 3.2) and *GP* (R^2 = 0.97, RMSE = 2.9). *DT* had the lowest accuracy among the models tested, with R^2 = 0.94 and RMSE = 4.3, but remained computationally efficient.

Table 5. Regression-based *ML* 10-fold cross validation training and testing analytical coefficient of determination, RMSE and training speed prediction results for *GSI* values from *MWD* data using all *MWD* features in *BR* and *MM* Formations.

Regression-Based *ML* Method	***BR***					***MM***				
	Train			**Test**		**Train**			**Test**	
	RMSE	**R^2**	**Time (s)**	**RMSE**	**R^2**	**RMSE**	**R^2**	**Time (s)**	**RMSE**	**R^2**
DT	4.3	0.94	2	4.3	0.94	5.9	0.64	2	5.1	0.68
SVM	3.7	0.95	8	3.2	0.97	4.6	0.78	8	3.8	0.82
RF	2.6	0.98	80	2.6	0.98	3.6	0.86	60	3.2	0.87
GP	3.2	0.96	5	2.9	0.97	3.6	0.86	3	3.0	0.89
NN	2.0	0.99	255	2.0	0.99	2.9	0.91	297	2.4	0.93

In contrast, *MM* model performance was comparatively lower across all methods, with R^2 values ranging from 0.68 to 0.93. *NN* remained the best-performing model, achieving R^2 = 0.93 and RMSE = 2.4, followed by *RF* (R^2 = 0.87, RMSE = 3.2). *SVM* and *GP* displayed moderate predictive ability, with R^2 values between 0.78 and 0.86, while *DT* exhibited the weakest performance (R^2 = 0.68, RMSE = 5.1). The performance gap in *MM* suggests that *GSI* estimation is more sensitive to variations in *MWD*-derived parameters, particularly *bap* and *torrop*.

The training times varied among models, with *NN* requiring the longest computation time (255 s for *BR* and 297 s for *MM*). In contrast, *DT* were the fastest models, requiring only 2 s for both datasets. *RF* had moderate computational demands (80 s for *BR*, 60 s for *MM*), while *GP* and *SVM* were relatively fast (5–8 s across both datasets). The high R^2 values of *GP* and *NN* (above 0.97 for *BR* and 0.91 for *MM*) suggest potential overfitting, particularly for *BR*, where geological variability may be lower.

Overall, *NN* and *RF* offer the best balance between predictive accuracy and robustness, particularly in *GSI* prediction for *BR* deposits. The *MM* dataset exhibits greater prediction uncertainty, which may necessitate further investigation into geological variability and dataset quality. Future work will focus on examining model generalization, refining feature selection techniques, and optimizing hyperparameters to mitigate overfitting while maintaining prediction accuracy.

4. Discussion

The results presented in this study suggest that leveraging *MWD* data through *ML* provides high predictive accuracy for *UCS, FPM*, and *GSI*. While this was demonstrated for these three parameters, the methodology can be applied to a broader range of geotechnical properties (excluded for brevity). However, since the findings are based on two iron ore pits in the Pilbara region of Western Australia, questions remain about their generalizability to other geological settings, mining operations, and commodity types.

In terms of feature importance, the *Boruta-SHAP* analysis with shadow variables provided new insights into the reliability of key predictors. Unlike previous studies where *rop* and *tor* were consistently identified as dominant *MWD* variables [18,19,22,25,32,70], this study found that derived ratio variables—such as *ropbap, torrop*, and *baprop*—exhibited stronger feature importance across *UCS, FPM*, and *GSI* estimations. Furthermore, bit-air-pressure was identified as a consistently high-ranking important feature. This drilling variable plays a crucial role in clearing cuttings from the borehole, reducing friction, and maintaining drilling efficiency. Variations in *bap* correlate strongly with rock mass competency, influencing both penetration efficiency and fracture response.

The lower significance of force-related shadow variables confirmed that pressure-based interactions (*bap, bapfob*) were genuinely important features of *UCS* in *BR*, contradicting prior assumptions that mechanical resistance (*fob, tor*) would be the primary controls. Additionally, the *MM* deposit showed a greater reliance on force-based metrics (*fobtor, torfob*) rather than pressure-driven responses, reinforcing the deposit-specific nature of *MWD*-based geotechnical predictions.

Porosity and *UCS* significantly influence rock mass behavior and joint stability, and while traditionally measured via core testing, they can be indirectly estimated using Measure-While-Drilling variables. High porosity typically correlates with lower rock strength, as increased void space weakens rock cohesion, often reflected in lower torque, penetration rate, and force-on-bit values. Conversely, low-porosity, high-strength rocks exhibit greater resistance, requiring higher drilling energy. These variations impact joint behavior, with porous, low-UCS rocks developing persistent, open joints prone to shear failure, while high-UCS formations exhibit tighter, more discontinuous fractures. By integrating MWD-derived estimates with geophysical data and site-specific calibration, mine operators can improve geotechnical risk assessments and slope stability management, enhancing excavation efficiency and safety.

The feasibility of estimating *GSI*, a calculated property, using Measure-While-Drilling data presents both opportunities and challenges. *MWD* variables, particularly bit air pressure, torque-to-penetration ratio, and force-on-bit, exhibit correlations with GSI, offering potential for real-time, high-resolution rock mass characterization. However, GSI is inherently a visual classification system, making direct numerical mapping challenging, especially when structural features like joint spacing and weathering are not explicitly captured by drilling responses. Additionally, bit wear, operational variability, and differences in spatial resolution between MWD datasets and traditional geotechnical logging introduce uncertainty in predictive models. To improve reliability, MWD-based GSI estimates should be validated against mapped discontinuities and geophysical data, with site-specific calibration of machine learning models. Despite these limitations, integrating MWD-derived GSI predictions into mine planning and slope stability models could enhance geotechnical decision-making by providing continuous, large-scale assessments of rock mass conditions.

The *ML* model performance differed significantly between *BR* and *MM*, largely due to geological variability. Prediction accuracy was higher in *BR*, consistently achieving R^2 values > 0.94, likely due to its more homogeneous BIF geology with relatively uniform mechanical properties. In contrast, *MM* exhibited greater lithological and structural heterogeneity, resulting in higher RMSE and lower R^2 values (0.78–0.87). The impact of shadow variables was also greater in *MM*, suggesting that higher geological complexity introduces greater uncertainty in *ML*-based predictions. This highlights that *ML* models trained in relatively uniform deposits may not generalize well to structurally complex formations without additional tuning or feature adjustments.

These findings emphasize the need for deposit-specific model training and validation before applying *MWD*-based geotechnical predictions to new sites. Further analysis of dataset distribution between the deposits revealed that differences in dataset volume contributed to disparities in model performance. The *MM* dataset contained fewer observations and exhibited greater geological heterogeneity, leading to higher prediction uncertainty. This reinforces the importance of training *ML* models with site-specific geomechanical data rather than assuming universal feature importance across deposits.

The methodology proposed in this study can be adapted for other orebody types (including copper, gold, nickel, and coal) and both open-pit and underground mining operations. Additionally, this study utilized data from multiple drill rig manufacturers (Epiroc, Terex, Bucyrus, and Sandvik), revealing that model performance remained consistent across rigs, though minor variations in sensor calibration and data resolution were observed. The impact of sensor calibration on *ML* predictions was further highlighted by shadow variable analysis, which showed that some rig-specific data variations may influence feature importance rankings. Ensuring standardization of *MWD* data processing across different drill rigs will be essential for improving model transferability.

Future studies should include:

i. Standardizing *MWD* data processing across different equipment types to improve the transferability of *ML* models to new operations;
ii. Evaluating the robustness of *MWD*-based geotechnical predictions across different drill bit designs, rig configurations, and automation levels;
iii. Training models on multi-site, multi-commodity datasets to differentiate universal vs. deposit-specific feature importance;
iv. Developing transfer learning techniques to allow pre-trained *ML* models to adapt to new sites with minimal re-training;
v. Integrating additional geological context variables (e.g., geophysical wireline logs, lithological logs) to enhance prediction accuracy across different orebody types;

vi. Validating model predictions against real-time operational outcomes, such as blast fragmentation and equipment performance, to ensure practical applicability.

By refining *MWD*-based *ML* models for broader geological settings, this approach could become a universal tool for real-time geotechnical assessment, enabling more efficient mine planning, optimized drill-and-blast operations, and improved slope stability management across diverse mining environments.

5. Conclusions

This study demonstrated the feasibility of estimating geotechnical properties using *MWD* data and *ML* techniques, showing that rock strength, fracture frequency, and rock mass classification scores can be predicted with high accuracy. A feature importance framework was developed using *Boruta-SHAP* algorithms, incorporating shadow variable analysis to validate key predictors. The results highlighted the dominance of bap and ratio-based metrics such as torrop in geotechnical characterization, while also confirming that pressure-driven responses are more significant in *UCS* estimation for *BR*, whereas force-based interactions play a larger role in *MM*. Comparative analyses across *DT, SVM, RF, GP,* and *NN* models showed strong correlations (up to R^2 = 0.98) between *MWD* features and geotechnical properties, reinforcing the robustness of *ML*-based geotechnical estimation, even in variable geological conditions.

The findings are highly relevant to the mining industry, as *MWD*-driven geotechnical characterization offers a pathway to more precise drill-and-blast design. The ability to optimize powder factor based on rock strength predictions and adjust stemming and detonation delays according to *FPM* results can lead to more efficient and controlled fragmentation. Furthermore, reducing oversized or inconsistent rock fragments can minimize over- and under-blasting effects, ultimately enhancing equipment longevity and reducing operational costs. Shadow variable analysis further confirmed the reliability of *MWD*-based feature selection, strengthening the case for integrating *ML* models into routine geotechnical assessments.

While this study demonstrates the feasibility of predicting geotechnical conditions from *MWD* data, further work is required to quantify the operational benefits, including:

i. Comparing *MWD*-based geotechnical predictions to actual fragmentation results, validating the impact on blast efficiency;
ii. Developing integrated *ML* models that link *MWD* data to downstream productivity metrics such as loader efficiency, cycle times, and crusher performance;
iii. Investigating real-time integration of *MWD* analytics into mine control systems, enabling dynamic adjustments to blast and excavation strategies.

By extending the application of *MWD*-based geotechnical characterization beyond prediction to real-time operational optimization, mining operations can achieve higher efficiency, lower costs, and improved safety in excavation and material processing. This study also underscores the need for deposit-specific model training, as demonstrated by the differing influence of shadow variables in *BR* and *MM*, further reinforcing the importance of site-specific calibration for *MWD*-based geotechnical estimation.

Author Contributions: Conceptualization, methodology, software, validation, formal analysis, investigation, resources, data curation, writing—original draft, and project administration were conducted by D.G. Writing—review and editing were carried out by D.G., C.A., Q.S. and L.O. Visualization was managed by D.G., while supervision was provided by C.A., Q.S. and L.O. All authors have read and agreed to the published version of the manuscript.

Funding: This study was conducted without any external funding support.

Data Availability Statement: The original contributions presented in this study are included in the article. Further inquiries can be directed to the corresponding author.

Acknowledgments: One of the authors (D.G.) received support through the MRIWA Postgraduate Research Scholarship and the AusIMM Education Endowment Fund Postgraduate Scholarship during his doctoral studies at Curtin University. Furthermore, the research was enabled by the advanced computing resources provided by the Pawsey Supercomputing Research Centre in Perth, Australia.

Conflicts of Interest: The authors declare no conflicts of interest.

References

1. Barton, N.; Lien, R.; Lunde, J. Engineering Classification of Rock Masses for the Design of Tunnel Support. *Rock Mech.* **1974**, *6*, 189–236. [CrossRef]
2. Bieniawski, Z.T. Geomechanics Classification (Rock Mass Rating System). In *Engineering Rock Mass Classifications: A Complete Manual for Engineers and Geologists in Mining, Civil, and Petroleum Engineering*; Wiley-Interscience: New York, NY, USA, 1989.
3. Deere, D.U. Technical Description of Rock Cores for Engineering Purpose. *Rock Mech. Eng. Geol.* **1963**, *1*, 18–22.
4. Hoek, E. Strength of Jointed Rock Masses. *Géotechnique* **1983**, *33*, 187–223. [CrossRef]
5. Howarth, D.F.; Rowlands, J.C. Quantitative Assessment of Rock Texture and Correlation with Drillability and Strength Properties. *Rock Mech. Rock Eng.* **1987**, *20*, 57–85. [CrossRef]
6. Elbaz, S.; Crawford, D.; Tuck, M. *A Method to Assess Rock Strength and Excavability of Diamondiferous Kimberlite Ore through In-Situ Rock Testing In Geotechnical and Geophysical Site Characterisation 5*; Springer International Publishing: Sydney, Australia, 2016.
7. Schunnesson, H. Drill Process Monitoring in Percussive Drilling for Location of Structural Features, Lithological Boundaries and Rock Properties, and for Drill Productivity Evaluation. Ph.D. Thesis, Lulea University of Technology, Lulea, Sweden, 1997.
8. Palleske, C.; Kalenchuk, K.; Hume, C.; Bawden, W. Strategic Use of Geotechnical Data for Maximised Value Added. In Proceedings of the Eighth International Conference on Deep and High Stress Mining, Australian Centre for Geomechanics, Perth, Australia, 28–30 March 2017; pp. 511–520.
9. Segui, J.B.; Higgins, M. Blast Design Using Measurement While Drilling Parameters. *Int. J. Blasting Fragm.* **2001**, *6*, 28–31. [CrossRef]
10. Hatherly, P.; Leung, R.; Scheding, S.; Robinson, D. Drill Monitoring Results Reveal Geological Conditions in Blasthole Drilling. *Int. J. Rock Mech. Min. Sci.* **2015**, *78*, 144–154. [CrossRef]
11. Khorzoughi, M.B.; Hall, R.; Apel, D. Rock Fracture Density Characterization Using Measurement While Drilling (MWD) Techniques. *Int. J. Min. Sci. Technol.* **2018**, *28*, 859–864. [CrossRef]
12. Navarro, J.; Sanchidrian, J.A.; Segarra, P.; Castedo, R.; Paredes, C.; Lopez, L.M. On the Mutual Relations of Drill Monitoring Variables and the Drill Control System in Tunneling Operations. *Tunn. Undergr. Space Technol.* **2018**, *72*, 294–304. [CrossRef]
13. Van Eldert, J.; Schunnesson, H.; Johansson, D.; Saiang, D. Application of Measurement While Drilling Technology to Predict Rock Mass Quality and Rock Support for Tunnelling. *Rock Mech. Rock Eng.* **2020**, *53*, 1349–1358. [CrossRef]
14. Kadkhodaie-Ilkhchi, A.; Monteiro, S.T.; Ramos, F.; Hatherly, P. Rock Recognition from MWD Data: A Comparative Study of Boosting, Neural Networks, and Fuzzy Logic. *IEEE Geosci. Remote Sens. Lett.* **2010**, *7*, 680–684. [CrossRef]
15. Goldstein, D.M.; Aldrich, C.; O'Connor, L. A Review of Orebody Knowledge Enhancement Using Machine Learning on Open-Pit Mine Measure-While-Drilling Data. *Mach. Learn. Knowl. Extr.* **2024**, *6*, 1343–1360. [CrossRef]
16. Peck, J.P. Performance Monitoring of Rotary Blasthole Drills. Ph.D. Thesis, McGill University, Montreal, Canada, 1989.
17. Scoble, M.J.; Peck, J.; Hendricks, C. Correlation between Rotary Drill Performance Parameters and Borehole Geophysical Logging. *Min. Sci. Technol.* **1989**, *8*, 301–312. [CrossRef]
18. Martin, J. Application of Pattern Recognition Techniques to Monitoring-While-Drilling on a Rotary Electric Blasthole Drill at an Open-Pit Coal Mine. Master's Thesis, Queen's University, Kingston, Canada, 2007.
19. Beattie, N. Monitoring-While-Drilling for Open-Pit Mining in a Hard Rock Environment. Master's Thesis, Queen's University, Kingston, ON, Canada, 2009.
20. Khorzoughi, M.B. Use of Measurement While Drilling Techniques for Improved Rock Mass Characterization in Open-Pit Mines. Master's Thesis, University of British Columbia, Vancouver, BC, Canada, 2011.
21. Basarir, H.; Wesseloo, J.; Karrech, A.; Pasternak, E.; Dyskin, A. The Use of Soft Computing Methods for the Prediction of Rock Properties Based on Measurement While Drilling Data. In *Deep Mining 2017: Proceedings of the Eighth International Conference on Deep and High Stress Mining*; Australian Centre for Geomechanics: Perth, Australia, 2017; pp. 537–551. [CrossRef]
22. Galende-Hernández, M.; Menéndez, M.; Fuente, M.J.; Sainz-Palmero, G.I. Monitor-While-Drilling-Based Estimation of Rock Mass Rating with Computational Intelligence: The Case of Tunnel Excavation Front. *Autom. Constr.* **2018**, *93*, 325–338. [CrossRef]

23. Klyuchnikov, N.; Zaytsev, A.; Gruzdev, A.; Ovchinnikov, G.; Antipova, K.; Ismailova, L.; Muravleva, E.; Burnaev, E.; Semenikhin, A.; Cherepanov, A.; et al. Data-Driven Model for the Identification of the Rock Type at a Drilling Bit. *J. Pet. Sci. Eng.* **2019**, *178*, 506–516. [CrossRef]
24. Khushaba, R.N.; Melkumyan, A.; Hill, A.J. A Machine Learning Approach for Material Type Logging and Chemical Assaying from Autonomous Measure-While-Drilling (MWD) Data. *Math. Geosci.* **2021**, *54*, 285–315. [CrossRef]
25. Navarro, J.; Seidl, T.; Hartlieb, P.; Sanchidrián, J.A.; Segarra, P.; Couceiro, P.; Schimek, P.; Godoy, C. Blastability and Ore Grade Assessment from Drill Monitoring for Open Pit Applications. *Rock Mech. Rock Eng.* **2021**, *54*, 3209–3228. [CrossRef]
26. Vezhapparambu, V.S.; Eidsvik, J.; Ellefmo, S.L. Rock Classification Using Multivariate Analysis of Measurement While Drilling Data: Towards a Better Sampling Strategy. *Minerals* **2018**, *8*, 384. [CrossRef]
27. Silversides, K.L.; Melkumyan, A. Machine Learning for Classification of Stratified Geology from MWD Data. *Ore Geol. Rev.* **2022**, *142*, 104737. [CrossRef]
28. Goldstein, D.; Aldrich, C.; O'Connor, L. Enhancing Orebody Knowledge Using Measure-While-Drilling Data: A Machine Learning Approach. *IFAC Pap.* **2024**, *58*, 72–76. [CrossRef]
29. Schunnesson, H. Drill Process Monitoring in Percussive Drilling: A Multivariate Approach for Data Analysis. Licentiate Thesis, Lulea University of Technology, Lulea, Sweden, 1990.
30. Schunnesson, H. RQD Predictions Based on Drill Performance Parameters. *Tunn. Undergr. Space Technol.* **1996**, *11*, 345–351. [CrossRef]
31. Schunnesson, H. Rock Characterisation Using Percussive Drilling. *Int. J. Rock Mech. Min. Sci.* **1998**, *35*, 711–725. [CrossRef]
32. Ghosh, R.; Gustafson, A.; Schunnesson, H. Development of a Geological Model for Chargeability Assessment of Borehole Using Drill Monitoring Technique. *Int. J. Rock Mech. Min. Sci.* **2018**, *109*, 9–18. [CrossRef]
33. Ghosh, R. Assessment of Rock Mass Quality and Its Effects on Chargeability Using Drill Monitoring Technique. Ph.D. Thesis, Lulea University of Technology, Lulea, Sweden, 2017.
34. Navarro, J.; Schunnesson, H.; Ghosh, R.; Segarra, P.; Johansson, D.; Sanchidrián, J.Á. Application of Drill-Monitoring for Chargeability Assessment in Sublevel Caving. *Int. J. Rock Mech. Min. Sci.* **2019**, *119*, 180–192. [CrossRef]
35. King, R.L.; Hicks, M.A.; Signer, S.P. Using Unsupervised Learning for Feature Detection in a Coal Mine Roof. *Eng. Appl. Artif. Intell.* **1993**, *6*, 565–573. [CrossRef]
36. Finfinger, G.; Peng, S.; Gu, Q.; Wilson, G.; Thomas, B. An Approach to Identifying Geological Properties from Roof Bolter Drilling Parameters. In Proceedings of the 19th Conference on Ground Control in Mining, Morgantown, WV, USA, 8–10 August 2000; pp. 1–12.
37. Peng, S. Evaluation of Roof Bolting Requirements Based on In-Mine Roof Bolter Drilling. Ph.D. Thesis, West Virgina University, Morgantown, WV, USA, 2004.
38. Van Eldert, J. Analysis of Excavation Damage, Rock Mass Characterisation and Rock Support Design Using Drilling Monitoring. Licentiate Thesis, Lulea University of Technology, Lulea, Sweden, 2018.
39. Van Eldert, J. Drill Monitoring for Rock Mass Assessment in Tunnelling. Ph.D. Thesis, Lulea University of Technology, Lulea, Sweden, 2020.
40. Liu, J. Jiankang Study on Intelligent Prediction Models of Geological Conditions Ahead of Tunnel Face Using Measurement-While-Drilling Data. Ph.D. Thesis, Nagasaki University, Nagasaki, Japan, 2021.
41. Liu, J.; Jiang, Y.; Han, W.; Sakaguchi, O. Optimized ANN Model for Predicting Rock Mass Quality Ahead of Tunnel Face Using Measure-While-Drilling Data. *Bull. Eng. Geol. Environ.* **2021**, *80*, 2283–2305. [CrossRef]
42. Liu, J.; Jiang, Y.; Ishizu, S.; Sakaguchi, O. Estimation of Tunnel Support Pattern Selection Using Artificial Neural Network. *Arab. J. Geosci.* **2020**, *13*, 321. [CrossRef]
43. Van Eldert, J.; Funehag, J.; Schunnesson, H.; Saiang, D. Drill Monitoring for Rock Mass Grouting: Case Study at the Stockholm Bypass. *Rock Mech. Rock Eng.* **2021**, *54*, 501–511. [CrossRef]
44. Navarro, J.; Sanchidrián, J.A.; Segarra, P.; Castedo, R.; Costamagna, E.; López, L.M. Detection of Potential Overbreak Zones in Tunnel Blasting from MWD Data. *Tunn. Undergr. Space Technol.* **2018**, *82*, 504–516. [CrossRef]
45. Costamagna, E.; Oggeri, C.; Vinai, R. Damage and Contour Quality in Rock Excavations for Quarrying and Tunnelling: Assessment for Properties and Solutions for Stability. In Proceedings of the IOP Conference Series: Earth and Environmental Science, Turin, Italy, 20–25 September 2021.
46. Zachos, D. Calculation of Penetration Depth of a Support Retaining System Anchored on the Top, for Underground Network and Buried Energy Pipelines. *Energy Syst.* **2024**, *15*, 1511–1526. [CrossRef]
47. Silversides, K.L.; Melkumyan, A. Multivariate Gaussian Process for Distinguishing Geological Units Using Measure While Drilling Data. In Proceedings of the Mining Goes Digitial; Taylor and Francis Group: London, UK, 2019; pp. 94–100.
48. Silversides, K.L.; Melkumyan, A. Boundary Identification and Surface Updates Using MWD. *Math. Geosci.* **2020**. [CrossRef]
49. Wold, S.; Esbensen, K.; Geladi, P. Principal Component Analysis. *Chemom. Intell. Lab. Syst.* **1987**, *2*, 37–52. [CrossRef]

50. Lundberg, S.; Lee, S.-I. A Unified Approach to Interpreting Model Predictions. In Proceedings of the Advances in Neural Information Processing Systems 30, Long Beach, CA, USA, 4–9 December 2017; pp. 1–10.
51. Liu, X.; Aldrich, C. Assessing the Influence of Operational Variables on Process Performance in Metallurgical Plants by Use of Shapley Value Regression. *Metals* **2022**, *12*, 1777. [CrossRef]
52. Goldstein, D.; Aldrich, C.; Shao, Q.; O'Connor, L. A Machine Learning Classification Approach to Geotechnical Characterisation Using Measure-While-Drilling Data. *Geosciences* **2025**, *15*, 93. [CrossRef]
53. Goldstein, D.; Aldrich, C.; Shao, Q.; O'Connor, L. Unlocking Subsurface Geology: A Case Study with Measure-While-Drilling Data and Machine Learning. *Minerals* **2025**, *15*, 241. [CrossRef]
54. Ker, P. Iron Ore Supply Slump as Rio Runs Late on New Mines. *Aust. Financ. Rev.* **2021**.
55. De-Vitry, C.; Vann, J.; Arvidson, H. Multivariate Iron Ore Deposit Resource Estimation—A Practitioner's Guide to Selecting Methods. *Appl. Earth Sci.* **2010**, *119*, 154–165. [CrossRef]
56. Jones, H.; Walraven, F.; Knott, G. Natural Gamma Logging as an Aid to Iron Ore Exploration in the Pilbara Region of Western Australia. In *Proceedings of the Australasian Institute of Mining and Metallurgy Annual Conference*; Australasian Institute of Mining and Metallurgy: Perth, Australia, 1973.
57. Khorzoughi, B.M.; Hall, R. Processing of Measurement While Drilling Data for Rock Mass Characterization. *Int. J. Min. Sci. Technol.* **2016**, *26*, 989–994. [CrossRef]
58. Van Eldert, J.; Schunnesson, H.; Saiang, D.; Funehag, J. Improved Filtering and Normalizing of Measurement-While-Drilling (MWD) Data in Tunnel Excavation. *Tunn. Undergr. Space Technol.* **2020**, *103*, 103467. [CrossRef]
59. Teale, R. The Concept of Specific Energy in Rock Drilling. *Int. J. Rock Mech. Min. Sci. Geomech. Abstr.* **1965**, *2*, 57–73. [CrossRef]
60. *MATLAB*; The MathWorks Inc.: Natick, MA, USA, 2024.
61. Kursa, M.B.; Rudnicki, W.R. Feature Selection with the Boruta Package. *J. Stat. Softw.* **2010**, *36*. [CrossRef]
62. *Statistics and Machine Learning Toolbox*; The MathWorks Inc.: Natick, MA, USA, 2024.
63. Zhang, W.; Li, H.; Li, Y.; Liu, H.; Chen, Y.; Ding, X. Application of Deep Learning Algorithms in Geotechnical Engineering: A Short Critical Review. *Artif. Intell. Rev.* **2021**, *54*, 5633–5673. [CrossRef]
64. Kotsiantis, S.B. Decision Trees: A Recent Overview. *Artif. Intell. Rev.* **2013**, *39*, 261–283. [CrossRef]
65. Hearst, M.A.; Dumais, S.T.; Osuna, E.; Platt, J.; Scholkopf, B. Support Vector Machines. *IEEE Intell. Syst. Their Appl.* **1998**, *13*, 18–28. [CrossRef]
66. Breiman, L. Random Forests. *Mach. Learn.* **2001**, *45*, 5–32. [CrossRef]
67. Schulz, E.; Speekenbrink, M.; Krause, A. A Tutorial on Gaussian Process Regression: Modelling, Exploring, and Exploiting Functions. *J. Math. Psychol.* **2018**, *85*, 1–16. [CrossRef]
68. Bishop, C.M. Neural Networks and Their Applications. *Rev. Sci. Instrum.* **1994**, *65*, 1803–1832. [CrossRef]
69. *Regression Learner Toolbox*; The MathWorks Inc.: Natick, MA, USA, 2024.
70. Scoble, M.J.; Peck, J. A Technique for Ground Characterization Using Automated Production Drill Monitoring. *Int. J. Surf. Min. Reclam. Environ.* **1987**, *1*, 41–54. [CrossRef]

Chapter 5: Paper C

A Machine Learning Classification Approach to Geotechnical Characterisation using Measure-While-Drilling Data

Goldstein, D., Aldrich, C., Shao, Q., & O'Connor, L. (2025). A Machine Learning Classification Approach to Geotechnical Characterization Using Measure-While-Drilling Data. *Geosciences*, 15(3), 93. https://doi.org/10.3390/geosciences15030093 geosciences

Article

A Machine Learning Classification Approach to Geotechnical Characterisation using Measure-While-Drilling Data

Daniel Goldstein[1]*, Chris Aldrich[1], Quanxi Shao[2], Louisa O'Connor[1]

[1] Western Australia School of Mines, Curtin University, Kalgoorlie, WA 6430, Australia
[2] CSIRO Data61, PO Box 1130, Bentley, WA, 6102, Australia
* Correspondance : daniel.goldstein@postgraduate.curtin.edu.au

Abstract: Due to limited exploration drilling and analogue mapping, bench-scale geotechnical characterization often suffers from high uncertainty, reducing confidence in geotechnical analysis. The Measure-While-Drilling (MWD) system uses sensors to collect drilling data from mining blast hole drill rigs. Historically, MWD studies have focused on penetration rates to identify rock formations during drilling. This study explores the effectiveness of Artificial Intelligence (AI) classification models using MWD data to predict geotechnical categories, including Stratigraphic Unit, Rock/Soil Strength, Rock Type, Geological Strength Index, and Weathering properties. Feature selection algorithms, Minimum Redundancy Maximum Relevance and ReliefF, identified all MWD responses as influential, leading to their inclusion in Machine Learning (ML) models. ML algorithms tested included Decision Trees, Support Vector Machines (SVMs), K-Nearest Neighbors (KNNs), Random Forests (RFs), Linear Discriminant Analysis, and Naive Bayes. KNN, SVMs, and RFs achieved up to 97% accuracy, outperforming other models. Prediction performance varied with class distribution, with balanced datasets showing wider accuracy ranges and skewed datasets achieving higher accuracies. The findings demonstrate a robust framework for applying AI in real-time orebody characterization, offering valuable insights for geotechnical engineers and geologists in improving orebody prediction and analysis.

Keywords: Measure-While-Drilling (MWD); Artificial Intelligence (AI); Machine Learning (ML); Geotechnical; Rock Mass; Real-time Orebody Analysis; Feature Importance

1. Introduction

Profiling a geological deposit is a critical task for mining production, requiring accuracy and precision to meet grade and tonnage requirements. However, traditional methods relying on resource-definition drill holes are often expensive and inefficient [1,2]. For example, the high costs of resource definition drilling result in large gaps between drill holes, leading to inaccurate subsurface depictions [3,4]. Moreover, the use of radioactive wireline instruments (sondes) in Reverse Circulation (RC) drill holes introduces physical limitations and potential risks to field personnel [5].

To address these challenges, engineers and geologists have turned to Measurement While Drilling (MWD) technology as a cost-effective and data-rich solution [6]. Originally developed for the petroleum sector, MWD sensors integrated into blast hole drill rigs in the 1970's to provide continuous data collection during operations, such as open-pit mining, construction, and tunnelling [7]. This technology generates a wealth of MWD data points, allowing for detailed insights into subsurface geological conditions [8–12].

Academic Editor: Firstname Lastname

Received: date
Revised: date
Accepted: date
Published: date

Citation: To be added by editorial staff during production.

Historically, manual methods were employed to interpret the abundant MWD data and its complex correlations with subsurface composition [9,10,13–17]. However, these methods were limited to rock-type detection, neglecting other essential geological attributes like stratigraphic unit, weathering intensity, and rock or soil strength [9,10,14,16–18]. In recent times, advancements in computing power and availability have enabled the application of Artificial Intelligence (AI) and Machine Learning (ML) approaches to MWD data interpretation predominantly for rock type identification using univariate methods [19–24]. Despite this progress, few studies have focused on applying ML methods to MWD data for geological boundary identification [25,25,26]. While some have taken a multivariate approach to predictive regression-based algorithms for geochemical or geophysical values [22,24,27], none have effectively evaluated the importance of individual MWD features for predicting categorical geotechnical features, such as rock type, weathering intensity, rock strength, stratigraphic unit and rock mass classification [6].

This study proposes an approach to evaluate feature importance of MWD variables for the classification and predictive modelling of geotechnical properties. Unlike previous studies [18,28] that applied Principal Component Analysis (PCA) for this purpose, which can yield misleading results, the current research utilizes appropriate feature selection algorithms, Minimum Redundancy Maximum Relevance (MRMR), and ReliefF, in combination with ML techniques. The study examines geological traits of an orebody using MWD data from an open cut iron ore mine in the Pilbara region of Western Australia. It presents a method to assess the feature importance of input drilling variables for predictive geotechnical modelling using MWD data and includes a comparative analysis of various classification-based ML algorithms' predictive performance.

The findings of this study offer a more accurate representation of orebodies based on MWD data, resulting in an order of magnitude increase in spatial resolution compared to RC and diamond drill hole-based geological models. This advancement has been achieved without the need for additional exploration drilling. The proposed approach holds promise for mine technical services personnel seeking cost-effective and high-resolution delineation of subsurface rock conditions, thereby improving the efficiency and productivity of mining production.

2. Methods

The data used in this paper are the same as in Goldstein et al. which aimed to predict wireline geophysical measurements and geochemical assay values from the same MWD dataset [24,27]. For the sake of self-completeness, the site and data are briefed as below:

2.1 Mine Site

The Western Australian Pilbara area is a high-volume iron ore exporter. In the year 2021, the area was responsible for exporting 874 million tons of iron ore [29]. The focus of this study lies in the iron-ore deposits found in Marra Mamba and Brockman (*BR*) Formations of the Hammersley Group, recognized for their substantial contribution to the economically exploitable iron ore in Pilbara [30]. An interesting feature of these formations is their interlayering with Banded Iron Formation (BIF), a mineral-rich sequence from about 2.5 billion years ago, and shale layers [31]. The Brockman Iron Formation itself is composed of the Dales Gorge Member, overlaid by Whaleback Shale, which in turn is topped by the Joffre Member. The Hamersley Detrital units, which appear higher in the stratigraphic sequence, originate from weathered bedded ores [4].

The current work investigates a single pit within the geological characteristics of the Brockman Formation (*BR*). A combination of 12 diamond core drill holes and 211 RC drill holes were used to characterize the pit's subsurface geological conditions. The diamond and RC holes totaling 1089 and 16,880 drill meters, respectively, with an average depth of

90 meters and 80 meters per hole, respectively. Field observations were employed to log information concerning rock type, weathering profile, rock strength, stratigraphic unit, and Geological Strength Index (GSI). There was no need for further data engineering on the resource-definition data due to prior scrutiny of these datasets through the mining company's Quality Assurance and Quality Control (QA/QC) procedures.

2.2 Geotechnical Field Observation Categories

This research explores various field observations logged, encompassing aspects such as stratigraphic unit, rock type, weathering, rock strength and GSI. The general categories for rock types include BIF, shale (SHL), detrital (DET), and the hydrated zone of alteration (HYD). Table 1 depicts the classification of weathering using a method adapted from the International Society for Rock Mechanics (ISRM) conventions [32]. In addition, Table 2 describes the ISRM strength categories for both soil and rock [33]. GSI is a rock mass classification system to evaluate a combination of the estimated rock strength and persistence of structures into several classes [34].

Table 1. Rock weathering classes

Code	Type	Description
FR	Fresh	No visible sign of rock material weathering
SW	Slightly Weathered	Less than 5% of material altered
MW	Moderately Weathered	Less than 50% of rock is decomposed
HW	Highly Weathered	More than 50% of rock is decomposed
CW	Completely Weathered	100% decomposed with intact structure
RS	Residual Soil	All rock material converted to soil

Table 2. Soil strength classes S0-S6 and rock strength classes R0-R6

Class	Term	Field Identification
S1	Very soft clay	Easily penetrated several inches by fist
S2	Soft clay	Easily penetrated several inches by thumb
S3	Firm clay	Can be penetrated several inches by thumb with moderate effort
S4	Stiff clay	Readily indented by thumb but penetrated only with great effort
S5	Very stiff clay	Readily indented by thumbnail
S6	Hard clay	Indented with difficulty by thumbnail
R0	Extremely weak rock	Indented by thumbnail
R1	Very weak rock	Crumbles under firm blows with a geological hammer
R2	Weak rock	Shallow indentations made by firm blow of a geological hammer
R3	Medium strong rock	Can be fractured with a single firm blow of a geological hammer
R4	Strong rock	Requires more than one blow of a geological hammer to fracture
R5	Very strong rock	Requires several blows of a geological hammer to fracture
R6	Extremely strong rock	Only chipped with a geological hammer

2.3 MWD Drilling Systems

MWD data collection was conducted using a fleet of 22 rotary blast hole rigs fitted with Tungsten Carbide Insert bits. This fleet included ten Pit Viper 271 rigs by Atlas Copco (Epiroc), two Terex SKS 12 rigs, one Bucyrus SKS 13 rig, and two Sandvik 460 rigs, which were used for drilling production blast holes of 0.229m in diameter (Figure 1a). Furthermore, a Cubex QXR 920 rig, a Sandvik 560 rig, and five Atlas Copco (Epiroc) D65 drill rigs were employed for creating 0.165m wall control blast holes (Figure 1b). The height of the benches in the iron-ore pits under study varied between 8 and 12 meters, with sub-drilling reaching approximately 2 meters beneath the bench floor. On average, the spacing and burden between production blast holes were 8 meters and 7 meters, respectively.

The MWD system on the drill rigs collected various measurements, such as rate of penetration (*rop*; m/s), rotary pressure or torque (*tor*; Nm), force on bit (*fob*; kgf) – typically known as weight on bit, thrust or pulldown pressure, bit air pressure or flushing air medium (*bap*; kgf/cm), and rotary speed (rpm). However, since inconsistencies in the onboard sensor resulted in rpm data being available for only around a quarter of the sample points, these data were omitted from the drilling measurements. The process of collecting MWD values involved both manually operated rigs and semi-autonomous machines, with the latter being remotely monitored from a distant Operations Centre. The drilling system logged MWD time-series data at approximately 0.1-meter intervals throughout the depth of the blast hole.

This study focused on the MWD dataset from *BR* pit, including 75,470 blast holes totaling 844,855 meters. MWD data was analyzed from 2 meters beneath the hole collars to the bottom of the blast holes, as the first two meters of the borehole may not accurately reflect the in situ rock conditions due to potential toe charge effects from the blasting of the previous bench. In addition, the *BR* MWD dataset was observed to have a relatively high noise-to-signal ratio with no QA/QC performed on the data.

Figure 1. Representative drilling rigs employed in the collection of MWD data: a) Terex SKS 12, utilized for the drilling of 0.229m production blast holes and b) Epiroc D65, used in the creation of 0.165m wall control blast holes.

2.3.1 MWD Data Pre-processing

The reliability of MWD data can be influenced by various factors such as the fabric and composition of the subsurface rock, the management system of the drill rig, and external circumstances, which may cause abnormal response values [35]. This could potentially lead to incorrect MWD response values and misinterpretations of the data [36]. Therefore, the noise-to-signal ratio in the examined mining MWD dataset is high, given that the data had not undergone a comprehensive QA/QC process.

Hence, the MWD data in this investigation necessitated feature engineering. To minimize potential effect on the representation of in situ rock due to collaring effects at the beginning of the shaft and potential blast damage from previous holes, the initial MWD dataset excluded the first 2 meters of each drilling hole. Further, data points showing negative *rop*, *tor*, *fob*, or *bap* values were eliminated. Any gaps in the MWD data were filled using linear interpolation, quartile detection methods, and a 1.5-factor threshold. A Gaussian filter with a smoothing factor of 0.3 was applied to the data from the blast holes to mitigate the local impacts of noise.

The drilling datasets for blast-hole MWD and exploration hole were converted from drill hole interval formats to point data, which encompassed geospatial coordinates and corresponding dataset values for each data point. The point data for exploration geotechnical holes were generated using downhole wireline logged desurvey data, which registered the azimuth and dip of each hole every 10 meters until the final depth. In contrast, the blast hole MWD data were not desurveyed due to the production nature of the holes, and each point's location was determined by presuming a straight line from the hole's collar to its end. A K-Nearest Neighbor distance-based search technique was utilized to calculate the distance between each point in the MWD and exploration data for merging these two datasets. Each exploration drilling data point was linked with the nearest MWD data point to execute supervised machine learning. Horizontal and vertical distance thresholds were employed to further refine the results.

2.4 Feature Selection Methods

PCA has often been employed to determine the most important features in MWD data. However, this research opts for feature selection algorithms to ascertain the relative importance of each MWD variable identified for geotechnical categories such as rock type, weathering intensity, stratigraphic unit, and rock strength. For this purpose, non-parametric approaches, specifically MRMR and ReliefF, were utilized on the pre-processed *BR* dataset. These techniques refrain from making assumptions about the relationships between input and output variables and instead assess feature selection in different ways.

MRMR, a non-parametric approach to feature selection, decouples complex variable interactions via mutual information maximization [37]. It identifies crucial features by fitting the model iteratively with each feature both included and excluded, subsequently measuring the variation in performance. The MRMR algorithm evaluates and chooses the MWD input that brings the most substantial improvement in the model as the most important, formulated as follows for categorical variables:

$$I(x,y) = \sum_{i,j} p(x_i,y_j)\log\frac{p(x_i,y_j)}{p(x_i)p(y_j)} \quad [1]$$

where the mutual information, *I*, quantifies the relationship between two variables, *x* and *y*. This relationship is defined in the context of their joint probabilistic distribution, $p(x_i,y_j)$, and the corresponding marginal probabilities, $p(x_i)$ and $p(y_j)$. The mutual information essentially provides a measure to determine a comparative level of similarity among geotechnical classifications. In addition, the principle of minimum redundancy, aims to select outputs that are maximally dissimilar from each other. Minimal redundancy enhances the representational efficacy of the feature set with respect to the entire dataset. This not only makes the selected features a better representative of the full dataset, but it also determines the relative importance among MWD variables.

On the other hand, ReliefF is a filter-based feature selection algorithm that determines the weights of predictors for categorical variables. The algorithm penalizes predictors that yield dissimilar values for neighbors belonging to the same class, and contrastingly, rewards predictors that produce different values for neighbors from distinct classes [38]. The ReliefF methodology randomly samples a datapoint and then examines the impact of the neighbors of the datapoint. The technique then adjusts the weights of the drilling variables for that datapoint, with the adjustments being governed by the extent to which these features can effectively differentiate between neighboring datapoints. The algorithm follows this logic:

Assuming x_r and x_q belong to the same class, the following equation applies:

$$W_j^{\,i} = W_j^{\,i-1} - \frac{\Delta_j(x_r,x_q)}{m}\cdot d_{rq}. \quad [2]$$

If x_r and x_q are part of different classes, this equation applies:

$$W_j^{\,i} = W_j^{\,i-1} + \frac{p_{y_q}}{1-p_{y_r}}\cdot\frac{\Delta_j(x_r,x_q)}{m}\cdot d_{rq}. \quad [3]$$

where W_j^i represents the weight of predictor F_j at the *i* iteration step, p^{yr} and p^{yq} are the prior probabilities of the classes to which x_r and x_q belong, respectively, *m* is the number of iterations, $\Delta j(x_r,x_q)$ is the difference in the value of predictor F_j between observations x_r and x_q, x_{rj} is the value of *j* for observation x_r, and x_{qj} is the value of x_q at *j*.

2.5 Classification-Based ML Methods

Different classification-based ML models were tested for their ability to classify rock types in various contexts. For example, Neural Networks (NNs), a type of machine learning model, proved effective in classifying rock types in a coal deposit in Canada [23]. However, a more specific type of NNs, known as Back Propagation NNs, failed in classifying rock types in an iron-ore mine in the United States [21]. Furthermore, two other ML techniques, Logistic Regression and Random Forests (RFs), were successful in predicting marble quality classes in Norwegian quarry [19].

In contrast to these previous studies, this research explored the use of a variety of newer machine learning methods. These include Decision Trees (DTs), Support Vector Machines (SVMs), K-Nearest Neighbors (KNNs), Linear Discriminant Analysis (LDA), and Naïve Bayes (NB). This research also employed RFs, as previous research had shown this method to be effective. The advantages and disadvantages of each classification-based ML method are summarized in Table 3.

Table 3. Comparison of the employed classification-based ML methods employed.

ML Algorithm	Advantages	Drawbacks
Decision Trees [39]	Easy to understand and interpret Not sensitive to outliers	Prone to overfitting Biased with imbalanced datasets
Support Vector Machines [40]	Effective in high dimensional spaces Outlier impact is minimized due to the margin maximization It is memory efficient	Can be challenging to interpret Unsuitable for big data due to high training time Poor performance with overlapping classes
K-Nearest Neighbours [41]	Simple to implement No assumptions about the data Adaptable to multiclass classifications	Computationally expensive Sensitivity to irrelevant features and data scale Must determine the value of K
Linear Discriminant Analysis [42]	Reduces dimensionality Avoids overfitting	Assumes the data are normally distributed Assumes that all classes share the same covariance matrix
Naïve Bayes [43]	Simple and easy to implement Works well with high dimensions	Makes a strong assumption about the shape of your data distribution Assigns a zero probability if variable is in test data but not training data
Random Forests [44]	Handles higher dimensionality well Effective for regression and classification Robust to outliers and nonlinear data	Tends to overfit for some datasets with noisy classification tasks Model interpretability difficult due to many trees Longer training period compared to DTs

The predictive capacity of various classification-based ML algorithms, with computations executed on a high-performance computing system known as Pawsey Supercomputer Nimbus cloud, operating on an Ubuntu system, outfitted with 8 virtual CPUs and 32GB of memory. The *Classification Learner Toolbox* in *MATLAB* was used with default hyperparameters and no optimization for each respective classification-based ML method to generate models and assess prediction performance [45]. The available data was portioned into two sets, with 80% dedicated to training the models, and the remaining 20% used for evaluating their predictions. 10-fold cross-validation was used to evaluate the strength of the models' predictions on the training data.

The effectiveness of the various models was compared using three specific measures: Accuracy, Overall Misclassification Cost (OMC), and Training Duration (TD).

i. Accuracy - this measure indicates the proportion of successful predictions made by the classification model. It is determined by dividing the number of correct predictions by the total number of predictions made.
ii. OMC - this is the total cost accumulated from incorrect predictions made by the model, computed by combining the cost matrix of misclassification with the corresponding confusion matrix.
iii. TD - this denotes the length of time it takes for the model to complete training phase.

The criteria for these metrics are defined as follows:

$$Accuracy = \frac{TN+TP}{TN+FN+TP+FP} \quad [4]$$

where *TN* and *TP* represent True Negatives (instances that are accurately predicted as not belonging to the class) and True Positives (instances that are correctly predicted as belonging to the positive class), respectively. In contrast, False Positives (*FP*) and False Negatives (*FN*) refer to the accurate and inaccurate negative predictions, respectively.

The OMC is determined, as follows:

$$\text{OMC} = (CostM_i * ConfM_i) \quad [5]$$

where *CostM*$_i$ is the misclassification cost matrix and *ConfM*$_i$ is the confusion matrix for the respective model.

3. Results

3.1 Exploratory Data Analysis

A preliminary analysis was conducted on the gathered measurements of MWD measurements (rate of penetration, torque, flow outback pressure, and bit axial pressure) acquired from drill sensors to establish an understanding of the data's distribution and frequency of occurrence. Various factors, including irregularities in mining machinery, operator proficiency, drill bit wear, and the rock characteristics, among others, have been identified as potential contributors to observable differences in *rop* and the *fob* [46]. Hence, it is possible that a univariate study alone may not adequately capture the nonlinear relationships that exist between MWD responses and geotechnical classification characteristics. Consequently, multivariate analysis using all MWD response variables was employed to maximize the prediction performance of the ML models.

Figure 2a-d depicts a variety of skewed and bimodal distributions of the MWD data points. The *rop* (Figure 2a) and *tor* (Figure 2b) have right skewed and left skewed distributions, respectively. This inverse relationship is sensible, as when *tor* increases to drill through a zone of strong zone, the *rop* should correspondingly decrease. The distributions for *fob* (Figure 2c) and *bap* (Figure 2d) are both bimodal with two prevalent value ranges in each MWD variable. The mean, median, standard deviation, minimum and maximum values for *rop*, *tor*, *fob* and *bap* are presented in Table 4.

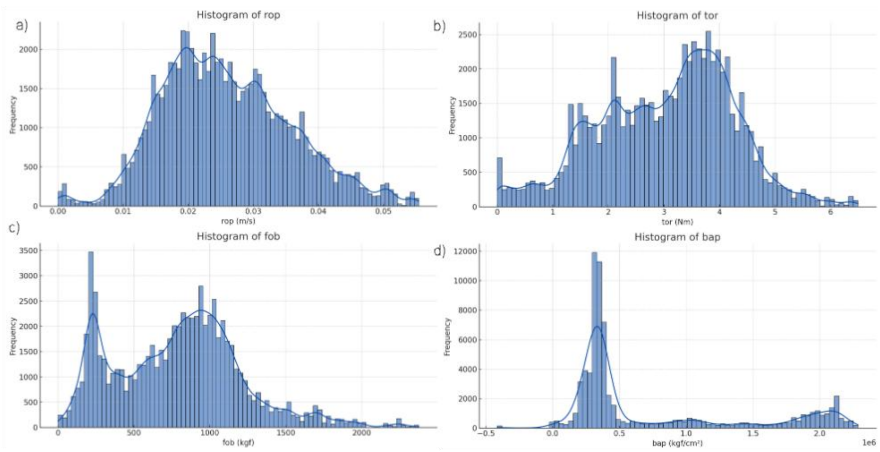

Figure 2. Distributions of MWD datapoints for a) *rop*, b) *tor*, c) *fob* and d) *bap*

Table 4: Statistical values for MWD data

	rop (m/s)	*tor* (Nm)	*fob* (kgf)	*bap* (kgf/cm$^{2)}$
Mean	0.026	3.05	793	738,147
Median	0.025	3.21	817	366,918
Standard Deviation	0.010	1.21	427	677,120
Minimum	0.000	0.00	0	-414,500
Maximum	0.055	6.49	2375	2,288,366

The observations of MWD data distributions suggest diverse data behaviors, underscoring the need for careful and nuanced analysis of the relationships between variables. As a result, a Pearson Correlation Coefficient plot for the MWD data is displayed in Figure 3. For instance, the correlation between *fob* and *tor* is approximately 0.57, indicating a very weak positive linear relationship. However, only linear relationships are displayed, which may not capture more intricate, non-linear relationships between variables.

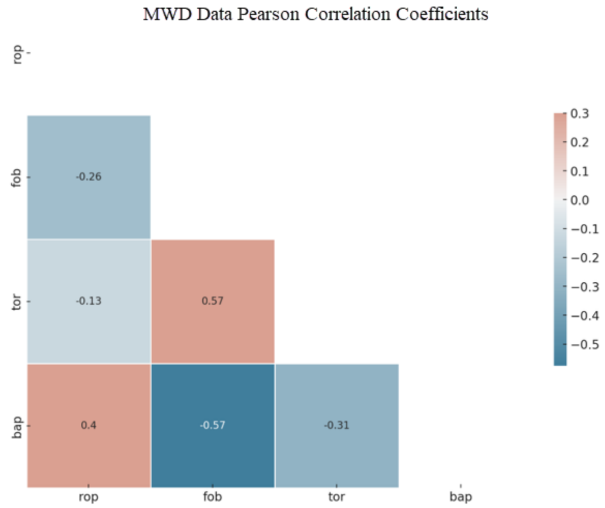

Figure 3. Pearson Correlation Coefficient plot for MWD data variables

Contrasting with the input MWD responses, the distributions of geotechnical class outputs reveal two distinct patterns (Figure 4). The Stratigraphic Unit and Rock Type exhibit a more even distribution across their respective categories. In contrast, Weathering Intensity, GSI, and Rock or Soil Strength predominantly feature a single category. This even distribution in the Stratigraphic Unit (Figure 4a) aligns with the stratified *BR* geological deposition observed in the pit: the DET unit overlays the DG3, DG2, and D1 units, which in turn rest atop the MCS [4].

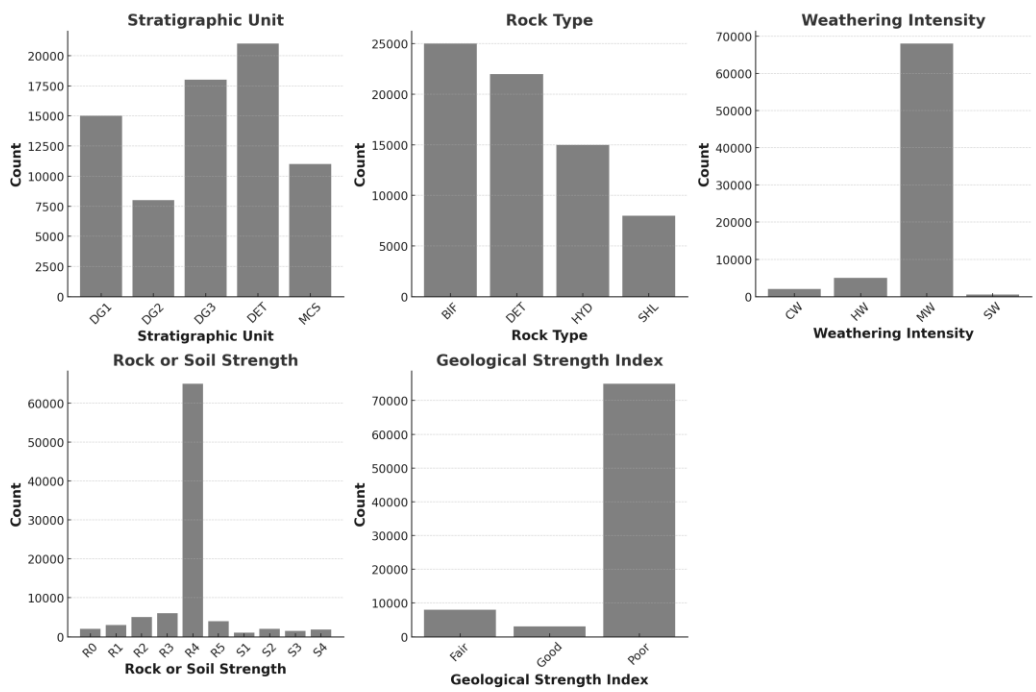

Figure 4. Distribution of investigated geotechnical categories.

Furthermore, the distribution within the Rock Type aligns with observed pit geology, where HYD alteration zones and SHL are less frequent compared to BIF and DET categories (Figure 4b). Conversely, the skewed distributions in Weathering, Rock or Soil Strength and GSI are consistent with the predominant features of the pit's *BR* geology, specifically favoring the MW, R3, and Poor categories (Figure 4c-e, respectively). Such a pronounced skewness towards a single category might influence the efficacy of predictive models, especially when these models rely on a limited set of infrequent categories for training and validation.

3.2 Feature Selection Results

The feature selection algorithms MRMR and ReliefF were applied to the four MWD response features to evaluate their significance in predicting five geotechnical categories: Rock Type, Strat. Unit, Strength, Weathering, and GSI. The percentages presented in were calculated by dividing the score of each MWD response in an experiment by the total of the four MWD responses in that respective experiment (Figure 5).

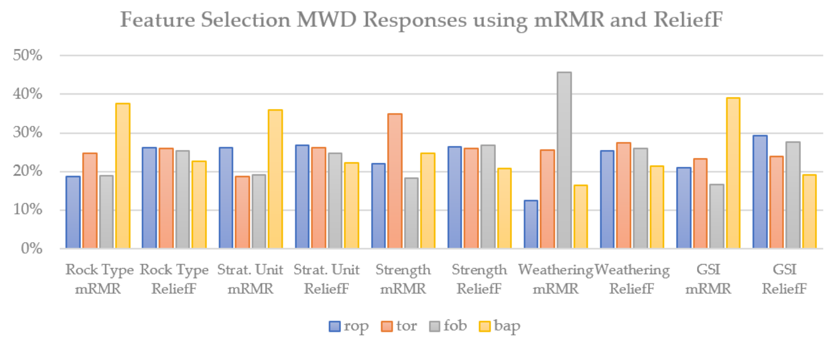

Figure 5. MRMR and ReliefF results for MWD response features.

MRMR consistently highlighted *bap* as the most influential feature in three out of five experiments, including Rock Type, Stratigraphic Unit and GSI underscoring its potential significance in these classification tasks. Conversely, ReliefF designated *rop* as the marginally leading feature for three experiments: Rock Type, Strat. Unit, and GSI. The prominence of *rop* in the ReliefF results underscores a divergent perspective on feature selection compared to MRMR. Notably, a stark difference was observed for the Strength classification. MRMR identified *tor* as the key feature, while ReliefF pinpointed *fob*. In the Weathering classification, MRMR and ReliefF again diverged, with *fob* and *tor* identified as the most influential features, respectively.

These discrepancies reflect the inherent differences in the methodologies of the two feature selection techniques. While MRMR focuses on maximizing relevance and minimizing redundancy, ReliefF emphasizes distinguishing capabilities between nearest neighbors of different classes. Such disparities emphasize the necessity of a comprehensive approach when selecting features, considering the inherent biases and strengths of each method. Importantly, since no features were identified as having zero or minimal influence, all four MWD responses will be included in predictive analysis.

3.3 Classification-Based ML Results

Various classification-based ML algorithms were applied to the geotechnical category datasets, including Stratigraphic Unit, Rock or Soil Strength, Rock Type, and Weathering, to compare model prediction performance using MWD data. For each model, five primary metrics were evaluated: 10 cross-fold Validation Accuracy, Testing Accuracy, Training Duration, Validation OMC, and Testing OMC. The results are listed in Table 5. While the KNN and RF had the consistently strongest Validation and Testing Accuracies of around 98%, the KNN model recurrently emerged as the strongest performing method due to lower Training Durations and Validation and Testing OMCs. Specifically, for GSI, Stratigraphic Unit, Rock or Soil Strength, and Rock Type classifications, the Fine KNN model consistently exhibited the highest Validation and Testing accuracies. In addition, in the Weathering classification, this model demonstrated the highest validation accuracy.

On the other hand, the other models had stronger performance in one aspect with weaker performance than KNN. For example, LDA consistently demonstrated the shortest training time across the Rock or Soil Strength and Weathering categories. However, the reduced training time came at the expense of Validation Accuracy, which was 10% lower than KNN's. In a similar example, the Gaussian NB model displayed the shortest training time for the GSI and Rock Type classifications.

However, the reduced training time for LDA did not translate to higher accuracy or lower costs than those of KNNs (Figure 6). In terms of OMC, the Fine KNNs model displayed the strongest performance versus training duration. For all five geotechnical classifications, KNN consistently showcased the lowest validation and testing costs. On the other hand, NB and LDA models had higher Validation costs despite shorter training times.

Table 5. Validation and Testing Accuracies, and Validation Costs for the ML algorithms

	ML Model	Decision Trees	Support Vector Machines	K-Nearest Neighbours	Random Forests	Linear Discriminant Analysis	Naïve Bayes
Geological Strength Index	Validation Accuracy (%)	98	98	98	98	97	97
	Testing Accuracy (%)	98	98	98	98	97	97
	Validation Cost	1,547	1,410	1,062	1,102	2,309	2,293
Stratigraphic Unit	Validation Accuracy (%)	50	83	96	33	32	96
	Testing Accuracy (%)	51	83	95	33	32	95
	Validation Cost	29,377	10,458	2,510	38,980	39,614	2,605
Rock or Soil Strength	Validation Accuracy (%)	87	93	95	95	85	85
	Testing Accuracy (%)	87	94	95	95	85	85
	Validation Cost	8,407	4,553	3,184	3,270	10,005	9,939
Rock Type	Validation Accuracy (%)	57	84	97	97	42	42
	Testing Accuracy (%)	59	85	97	97	42	43
	Validation Cost	22,784	8,428	1,626	1,720	30,821	30,651
Weathering	Validation Accuracy (%)	88	93	95	95	85	85
	Testing Accuracy (%)	88	93	95	95	85	85
	Validation Cost	7,693	4,411	3,100	3,257	9,851	9,841

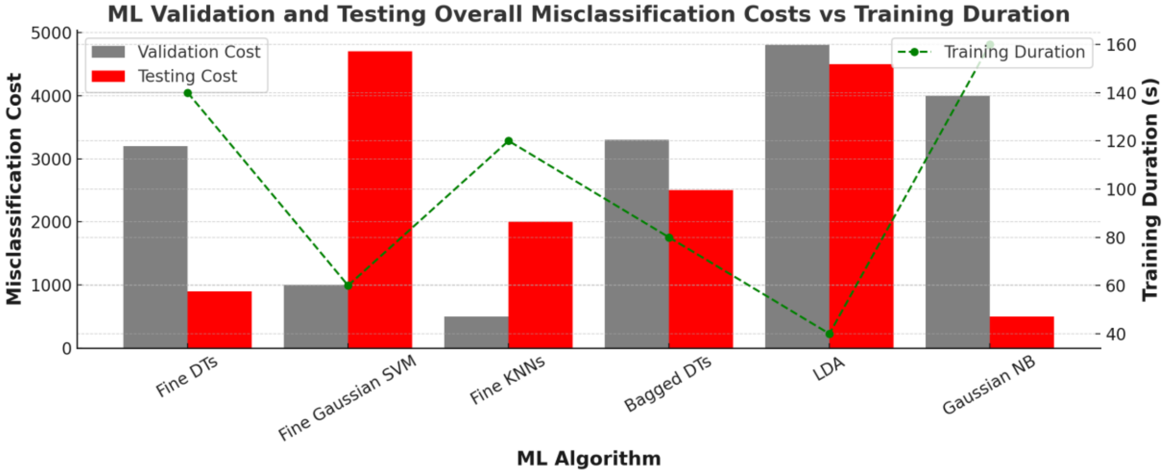

Figure 6. Validation and Testing Cost Scores versus Training Duration for the investigated classification-based ML algorithms.

Testing accuracies were further examined using confusion matrices to understand the pattern of correct and incorrect class predictions within a geotechnical dataset. For example, confusion matrices showing testing accuracies for Rock Type using the six ML algorithms are shown in Figure 7a. Across most models, the primary diagonal, which represents correct classifications, displays high values of more than 74.9% for the SVMs, KNNs and RFs (Figure 7b-d). This is indicative of the models' capability to correctly classify a vast majority of the samples. The strength and distinctiveness of the features associated with BIF and HYD likely contribute to this trend. On the other hand, DET, due to its more weathered nature and soil-like consistency, stands out as occasionally challenging for the models. Its weaker material strength, compared to BIF, HYD, and SH might be leading to these misclassifications. This underscores the importance of considering DET's unique geological history and characteristics when interpreting model results.

On the other hand, as BIF and HYD have a stronger material strength compared to SHL and DET, the models seem to have a relatively easier time distinguishing them. Their inherent robustness and resistance to geological processes impart them with features that machines can recognize with high accuracy. SHL, being stronger than DET but weaker than BIF and HYD, shows occasional overlaps with both groups in the DTs, LDA and NB (Figure 7a, 7e-f). This intermediate strength, combined with its rock-like nature, might cause it to share properties with both the stronger (BIF and HYD) and weaker (DET) materials, resulting in occasional misclassifications. Similar misclassifications were observed in the GSI, Stratigraphic Unit, Rock or Soil Strength and Weathering categories.

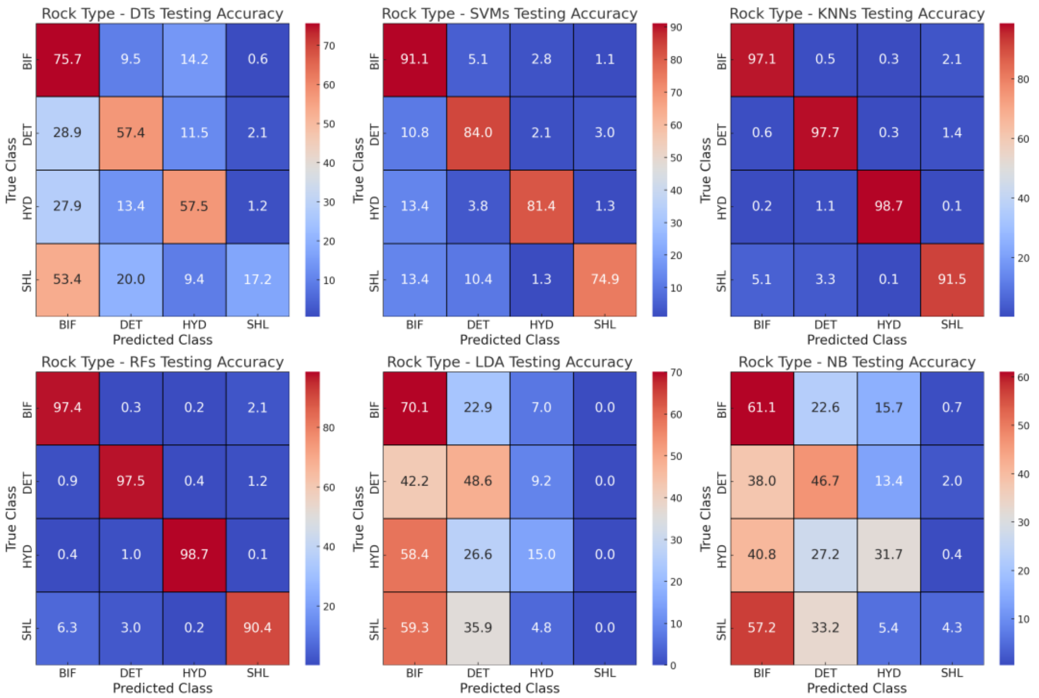

Figure 7. Confusion matrices showing testing accuracies (%) for Rock Type using a) DTs, b) SVMs, c) KNNs, d) RFs, e) LDA and f) NB

4. Discussion

This study demonstrates the effectiveness of classification-based ML techniques in estimating classes of geotechnical properties from MWD data, thereby increasing rock mechanics characterization beyond an order of magnitude with resource development drilling methods. Though the scope of this study was confined to five geotechnical data categories, including Stratigraphic Unit, Rock or Soil Strength, Rock Type, GSI and Weathering properties, it has the potential to be extended to other categorical orebody knowledge datasets. For example, higher resolution understandings of grade, trace contaminants, alteration intensity and mineralogy as well as other rock mass classifications systems, including Rock Mass Rating, Rock Quality Designation or Q, will greatly reduce uncertainty resulting in increased mining confidence.

This study departs from prior research by demonstrating the balanced influence of the four MWD variables. Earlier research emphasized *rop* and *tor*, utilizing PCA to determine the most important MWD measurements for rock type identification [13,16,18,21,23,47]. In contrast, both MRMR and ReliefF feature selection methods offer invaluable insights, yet their results can diverge based on their underlying methodologies. While MRMR highlighted the significance of the *bap* feature, ReliefF favored towards the *rop* feature. Such disparities emphasize the necessity of a comprehensive approach when selecting features, considering the inherent biases and strengths of each method. Future research might explore consensus-based approaches or further investigate the specific contexts where one method may be more appropriate than the other. However, both methods revealed a relatively balanced relationships between MWD measurements in which no features were identified as having zero or minimal influence.

This study also examined model prediction performance for approximating geotechnical categorical properties. The choice of the ML analytical model had a large effect on the ML prediction outcomes, demonstrated by higher Validation and Testing Accuracies, lower Training duration, Validation and Testing OMCs. DTs, LDA and NB performed the weakest across the five geotechnical datasets while KNN and RFs displayed the strongest results, consistently above 90% for Validation and Testing Accuracies for correct class identifications. Furthermore, KNN was quicker to train than RFs. For example, KNN, at 3s, was over 20 times faster than RFs, at 64s, for Rock Type. These results indicate that KNN is both the strongest and most computationally efficient model to predict geotechnical classification properties.

However, a great deal of the variance of accuracies and training durations can be traced to differences in class distributions between the five categories (Figure 5). Rock Type and Stratigraphic Unit had balanced distributions while the remaining categories were skewed to one class. The impact of this is observable in the consistently above 80% Accuracies for GSI, Rock or Soil Strength and Weathering prediction performance results. On the other hand, the Rock Type and Stratigraphic Unit, which had a wider spread of Accuracies, from 32% to 97%, depending on the ML algorithm. Moreover, similar physical properties may cause misclassification. For example, regarding Rock Type, SHL was observed to be misclassified as BIF and DET, because of its material strength lying between the relatively stronger BIF and weaker DET. This study demonstrated the success of classification-based ML technique for geotechnical classification problems but also supports the valuable role of subject matter expert oversight in complementing ML studies regarding instances of misclassification, especially concerning materials with close or overlapping properties.

5. Conclusions

The application of classification-based ML techniques in conjunction with innovative datasets, such as MWD data, has introduced fresh opportunities in the field of rock mechanics Characterisation. This work provides evidence for the efficacy of ML techniques in estimating geotechnical conditions. Additionally, it highlights the improvements in the characterization of rock mechanics properties beyond the scale achieved by traditional resource development methods. The MRMR and ReliefF feature selection methods support a balanced integration of the MWD features *rop*, *tor*, *fob*, and *bap* in multivariate analysis instead of depending solely on a single feature.

Moreover, a comprehensive assessment of diverse machine learning models yielded intricate observations regarding their predictive capabilities. The KNN and RFs algorithms demonstrated superior performance, routinely obtaining validation, and testing accuracies exceeding 90%. The short training duration for KNN compared with that of RFs highlights its remarkable computational efficiency. Nevertheless, it is important to acknowledge that these results are closely linked to the underlying data distributions within the geotechnical classifications.

The balanced distributions of classes in Rock Type and Stratigraphic Unit were in stark contrast to the other categories that exhibited a predominant skew towards a single class. This contrast was evident in the wide range of accuracies depending on the ML algorithm chosen in Rock Type and Stratigraphic Unit. Furthermore, the need for further examination arises from the misidentification of related materials, such as SHL with both BIF and DET. Future work should also include other Feature Importance algorithms, such as Shapley Values, that reveal the "black box" characteristics of ML techniques to improve explainability [48,49]. While the scope of this study was limited to five geotechnical data categories, the findings provide a solid basis for extrapolating these methods to other categorical datasets relevant to orebody knowledge.

Acknowledgments: One of the authors (DG) received support through the MRIWA Postgraduate Research Scholarship and the AusIMM Education Endowment Fund Postgraduate Scholarship during his doctoral studies at Curtin University. Furthermore, the research was enabled by the advanced computing resources provided by the Pawsey Supercomputing Research Centre in Perth, Australia.

Conflicts of Interest: The authors declare no conflict of interest.

References

1. Said, K.O.; Onifade, M.; Akinseye, P.; Kolapo, P.; Abdulsalam, J. A Review of Geospatial Technology-Based Applications in Mineral Exploration. *GeoJournal* **2023**, *88*, 2889–2911, doi:10.1007/s10708-022-10784-4.
2. Stebbins, S.A. *Cost Estimation Handbook for Small Placer Mines*; US Department of the Interior, Bureau of Mines, 1987; Vol. 9170;.
3. Silversides, K.; Melkumyan, A.; Wyman, D.; Hatherly, P. Automated Recognition of Stratigraphic Marker Shales from Geophysical Logs in Iron Ore Deposits. *Computers and Geosciences* **2015**, *77*, 118–125, doi:10.1016/j.cageo.2015.02.002.
4. Wedge, D.; Hartley, O.; McMickan, A.; Green, T.; Holden, E.J. Machine Learning Assisted Geological Interpretation of Drillhole Data: Examples from the Pilbara Region, Western Australia. *Ore Geology Reviews* **2019**, *114*, 103118–103118, doi:10.1016/j.oregeorev.2019.103118.
5. Potter, C.; Moussa, J.; Wilcox, A.; Gilbert, L.; Vargas, V. General Overview of Mobile Sources Used for Well Logging and Industrial Radiography Applications. **2022**.
6. Goldstein, D.M.; Aldrich, C.; O'Connor, L. A Review of Orebody Knowledge Enhancement Using Machine Learning on Open-Pit Mine Measure-While-Drilling Data. *Machine Learning and Knowledge Extraction* **2024**, *6*, 1343–1360, doi:https://doi.org/10.3390/ make6020063.
7. Barr, M.V. Instrumented Horizontal Drilling for Tunnelling Site Investigation. PhD, University of London: Imperial College of Science and Technology, 1984.
8. Hatherly, P.; Leung, R.; Scheding, S.; Robinson, D. Drill Monitoring Results Reveal Geological Conditions in Blasthole Drilling. *International Journal of Rock Mechanics and Mining Sciences* **2015**, *78*, 144–154, doi:10.1016/j.ijrmms.2015.05.006.
9. Kadkhodaie-Ilkhchi, A.; Monteiro, S.T.; Ramos, F.; Hatherly, P. Rock Recognition from MWD Data: A Comparative Study of Boosting, Neural Networks, and Fuzzy Logic. *IEEE Geoscience and Remote Sensing Letters* **2010**, *7*, 680–684, doi:10.1109/LGRS.2010.2046312.
10. Khorzoughi, M.B. Use of Measurement While Drilling Techniques for Improved Rock Mass Characterization in Open-Pit Mines. MSc, University of British Columbia: Vancouver, 2011.
11. Navarro, J.; Segarra, P.; Sanchidrián, J.A.; Castedo, R.; Fortes, A.P.P.; Natale, M.; López, L.M. Application of an In-House MWD System for Quarry Blasting.; Lulea, Sweden, 2018; pp. 203–210.
12. van Eldert, J.; Schunnesson, H.; Saiang, D.; Funehag, J. Improved Filtering and Normalizing of Measurement-While-Drilling (MWD) Data in Tunnel Excavation. *Tunnelling and Underground Space Technology* **2020**, *103*, 103467–103467, doi:10.1016/j.tust.2020.103467.
13. Galende-Hernández, M.; Menéndez, M.; Fuente, M.J.; Sainz-Palmero, G.I. Monitor-While-Drilling-Based Estimation of Rock Mass Rating with Computational Intelligence: The Case of Tunnel Excavation Front. *Automation in Construction* **2018**, *93*, 325–338, doi:10.1016/j.autcon.2018.05.019.
14. Klyuchnikov, N.; Zaytsev, A.; Gruzdev, A.; Ovchinnikov, G.; Antipova, K.; Ismailova, L.; Muravleva, E.; Burnaev, E.; Semenikhin, A.; Cherepanov, A.; et al. Data-Driven Model for the Identification of the Rock Type at a Drilling Bit. *Journal of Petroleum Science and Engineering* **2019**, *178*, 506–516, doi:10.1016/j.petrol.2019.03.041.
15. Peck, J.P. Performance Monitoring of Rotary Blasthole Drills. **1989**, 395.
16. Scoble, M.J.; Peck, J.; Hendricks, C. Correlation between Rotary Drill Performance Parameters and Borehole Geophysical Logging. **1989**, *8*, 301–312.
17. Segui, J.B.; Higgins, M. Blast Design Using Measurement While Drilling Parameters.; Hunter Valley, NSW, 2001; pp. 28–31.
18. Navarro, J.; Seidl, T.; Hartlieb, P.; Sanchidrián, J.A.; Segarra, P.; Couceiro, P.; Schimek, P.; Godoy, C. Blastability and Ore Grade Assessment from Drill Monitoring for Open Pit Applications. *Rock Mech Rock Eng* **2021**, *54*, 3209–3228, doi:10.1007/s00603-020-02354-2.

19. Akyildiz, O.; Basarir, H.; Vezhapparambu, V.S.; Ellefmo, S. MWD Data-Based Marble Quality Class Prediction Models Using ML Algorithms. *Math Geosci* **2023**, doi:10.1007/s11004-023-10061-1.
20. Basarir, H.; Wesseloo, J.; Karrech, A.; Pasternak, E.; Dyskin, A. The Use of Soft Computing Methods for the Prediction of Rock Properties Based on Measurement While Drilling Data. *Proceedings of the Eighth International Conference on Deep and High Stress Mining* **2017**, 537–551, doi:10.36487/acg_rep/1704_36_basarir.
21. Beattie, N. Monitoring-While-Drilling for Open-Pit Mining in a Hard Rock Environment. Master of Science, Queen's University: Kingston, Ontario, Canada, 2009.
22. Khushaba, R.N.; Melkumyan, A.; Hill, A.J. A Machine Learning Approach for Material Type Logging and Chemical Assaying from Autonomous Measure-While-Drilling (MWD) Data. *Math Geosci* **2021**, doi:10.1007/s11004-021-09970-w.
23. Martin, J. Application of Pattern Recognition Techniques to Monitoring-While- Drilling on a Rotary Electric Blasthole Drill at an Open-Pit Coal Mine. MSc, Queen's University: Kingston, Ontario, Canada, 2007.
24. Goldstein, D.; Aldrich, C.; O'Connor, L. Enhancing Orebody Knowledge Using Measure-While-Drilling Data: A Machine Learning Approach. *IFAC PapersOnLine* **2024**, *58*, 72–76.
25. Silversides, K.L.; Melkumyan, A. Multivariate Gaussian Process for Distinguishing Geological Units Using Measure While Drilling Data. In Proceedings of the Minig Goes Digitial; Taylor & Francis Group: London, 2019; pp. 94–100.
26. Silversides, K.L.; Melkumyan, A. Boundary Identification and Surface Updates Using MWD. *Mathematical Geosciences* **2020**, doi:10.1007/s11004-020-09891-0.
27. Goldstein, D.; Aldrich, C.; Shao, Q.; O'Connor, L. Unlocking Subsurface Geology: A Case Study with Measure-While-Drilling Data and Machine Learning. *Preprints* **2025**, doi:10.20944/preprints202501.2284.v1.
28. Schunnesson, H. Drill Process Monitoring in Percussive Drilling: A Multivariate Approach for Data Analysis. Licentiate, Lulea University of Technology: Lulea, Sweden, 1990.
29. Ker, P. Iron Ore Supply Slump as Rio Runs Late on New Mines. *Australian Financial Review* 2021.
30. De-Vitry, C.; Vann, J.; Arvidson, H. Multivariate Iron Ore Deposit Resource Estimation – a Practitioner's Guide to Selecting Methods. *Trans Inst Mining Metallurgy Sect B.* **2010**, *119*, 154–165.
31. Jones, H.; Walraven, F.; Knott, G. Natural Gamma Logging as an Aid to Iron Ore Exploration in the Pilbara Region of Western Australia.; Perth, Australia, 1973.
32. Brown, E. *Rock Characterization, Testing and Monitoring: ISRM Suggested Methods*; Pergamon Press, 1981;
33. International Society for Rock Mechanics (ISRM) Simple Field Identification Compressive Strength of Rock and Clay. *International Journal of Rock Mechanics and Mining Sciences* **1978**, *15*, 319–368.
34. Hoek, E. Strength of Jointed Rock Masses. *Géotechnique* **1983**, *33*, 187–223, doi:10.1680/geot.1983.33.3.187.
35. Khorzoughi, B.M.; Hall, R. Processing of Measurement While Drilling Data for Rock Mass Characterization. *International Journal of Mining Science and Technology* **2016**, *26*, 989–994, doi:10.1016/j.ijmst.2016.09.005.
36. van Eldert, J.; Schunnesson, H.; Johansson, D.; Saiang, D. Application of Measurement While Drilling Technology to Predict Rock Mass Quality and Rock Support for Tunnelling. *Rock Mechanics and Rock Engineering* **2020**, *53*, 1349–1358, doi:10.1007/s00603-019-01979-2.
37. Ding, C.; Peng, H. Minimum Redundancy Feature Selection from Microarray Gene Expression Data. *Journal of bioinformatics and computational biology* **2005**, *3*, 185–205.
38. Kira, K.; Rendell, L.A. A Practical Approach to Feature Selection. In *Machine learning proceedings 1992*; Elsevier, 1992; pp. 249–256.
39. Breiman, L.; Friedman, J.; Olshen, R.; Stone, C. *Classification and Regression Trees*; Wadsworth and Brooks/Cole Monterey, CA, USA, 1984;
40. Cortes, C.; Vapnik, V. Support-Vector Networks. *Machine learning* **1995**, *20*, 273–297.
41. Cover, T.; Hart, P. Nearest Neighbor Pattern Classification. *IEEE transactions on information theory* **1967**, *13*, 21–27.

42. Fisher, J.E.; Shakoor, A.; Watts, C.F. Comparing Discontinuity Orientation Data Collected by Terrestrial LiDAR and Transit Compass Methods. *Engineering Geology* **2014**, *181*, 78–92, doi:10.1016/j.enggeo.2014.08.014.
43. Duda, R.O.; Hart, P.E. Use of the Hough Transformation to Detect Lines and Curves in Pictures. *Communications of the ACM* **1972**, *15*, 11–15.
44. Breiman, L. Random Forests. *Machine Learning* **2001**, *45*, 5–32.
45. *Classification Learner Toolbox*; The MathWorks Inc.: Natick, Massachursetts, 2024;
46. Ghosh, R.; Schunnesson, H.; Kumar, U. Evaluation of Rock Mass Characteristics Using Measurement While Drilling in Boliden Minerals Aitik Copper Mine, Sweden. In *Mine Planning and Equipment Selection*; Drebenstedt, C., Singhal, R., Eds.; Springer International Publishing: Cham, 2014; pp. 81–91 ISBN 978-3-319-02677-0.
47. Ghosh, R.; Gustafson, A.; Schunnesson, H. Development of a Geological Model for Chargeability Assessment of Borehole Using Drill Monitoring Technique. *International Journal of Rock Mechanics and Mining Sciences* **2018**, *109*, 9–18, doi:10.1016/j.ijrmms.2018.06.015.
48. Aldrich, C. Process Variable Importance Analysis by Use of Random Forests in a Shapley Regression Framework. *Minerals* **2020**, *10*, 420, doi:https://doi.org/10.3390/min10050420.
49. Deng, S.; Aldrich, C.; Liu, X.; Zhang, F. Explainability in Reservoir Well-Logging Evaluation: Comparison of Variable Importance Analysis with Shapley Value Regression, SHAP and LIME. *IFAC PapersOnLine* **2024**, *58*, 66–71, doi:https://doi.org/10.1016/j.ifacol.2024.09.292.

Chapter 6: Paper D

Unlocking Subsurface Geology: A Case Study with Measure-While-Drilling Data and Machine Learning

Goldstein, D., Aldrich, C., Shao, Q., & O'Connor, L. (2025). Unlocking Subsurface Geology: A Case Study with Measure-While-Drilling Data and Machine Learning. *Minerals, 15(3),* 241. https://doi.org/10.3390/min15030241 *minerals*

Article

Unlocking Subsurface Geology: A Case Study with Measure-While-Drilling Data and Machine Learning

Daniel Goldstein [1,*], Chris Aldrich [1], Quanxi Shao [2] and Louisa O'Connor [1]

[1] Western Australia School of Mines, Curtin University, Kalgoorlie, WA 6430, Australia
[2] CSIRO Data61, P.O. Box 1130, Bentley, WA 6102, Australia
* Correspondence: daniel.goldstein@postgraduate.curtin.edu.au

Abstract: Bench-scale geological modeling is often uncertain due to limited exploration drilling and geophysical wireline measurements, reducing production efficiency. Measure-While-Drilling (MWD) systems collect drilling data to analyze mining blast hole drill rig performance. Early MWD studies focused on penetration rates to identify rock types. This paper investigates Artificial Intelligence (AI)-based regression models to predict geophysical signatures like density, gamma, magnetic susceptibility, resistivity, and hole diameter using MWD data. The machine learning (ML) models evaluated include Linear Regression (LR), Decision Trees (DTs), Support Vector Machines (SVMs), Random Forests (RFs), Gaussian Processes (GP), and Neural Networks (NNs). An analytical method was validated for accuracy, and a three-tier experimental method assessed the importance of MWD features, revealing no performance loss when excluding features with less than 2% importance. RF, DTs, and GPs outperformed other models, achieving R^2 values up to 0.98 with a low RMSE, while LR and SVMs showed lower accuracy. The NN's performance improved with larger datasets. This study concludes that the DT, RF, and GP models excel in predicting geophysical signatures. While ML-based methods effectively model relationships in the data, their predictive performance remains inherently constrained by the underlying geological and physical mechanisms. Model selection depends on computational resources and application needs, offering valuable insights for real-time orebody analysis using AI. These findings could be invaluable to geologists who wish to utilize AI techniques for real-time orebody analysis and prediction.

Keywords: measure-while-drilling (MWD); artificial intelligence (AI); machine learning (ML); geophysical; wireline; real-time orebody analysis; feature importance

Academic Editors: Yongzhang Zhou, Hui Yang, Xiaohui Ji and Amin Beiranvand Pour

Received: 29 January 2025
Revised: 24 February 2025
Accepted: 24 February 2025
Published: 26 February 2025

Citation: Goldstein, D.; Aldrich, C.; Shao, Q.; O'Connor, L. Unlocking Subsurface Geology: A Case Study with Measure-While-Drilling Data and Machine Learning. *Minerals* **2025**, *15*, 241. https://doi.org/10.3390/min15030241

1. Introduction

The geological profiling of orebodies must be accurate and precise to define and achieve a feasible grade and the tonnage requirements of mining production. Traditional methods of accomplishing this are frequently expensive due to their reliance on resource-definition drill holes. For example, the traditional method for profiling an iron ore deposit requires the use of an instrument on a wireline called a sonde to obtain geophysical response values in Reverse Circulation (RC) drill holes [1]. This method not only introduces inefficiencies due to a physical limitation of the sonde but also raises concerns for field personnel due to the potential exposure to radioactive sources from several sondes. Furthermore, the high costs of resource definition drilling leave gaps of approximately 50–100 m between drill holes, resulting in an inaccurate depiction of the subsurface due to interpolation [2]. As a result, a more cost-effective approach that allows for comprehensive data collection is required to enable the high-resolution delineation of subsurface geological conditions.

Measure-While-Drilling (MWD) technology provides an effective solution to this geological modeling uncertainty. It was originally developed for the petroleum sector before being integrated into open-pit mining blast hole drilling systems in the 1970s [3]. Continuous data gathering is enabled by installing a blast hole drill rig with MWD sensors, which provides insights into subsurface penetration performance [4]. In the context of operations involving repetitious drilling and blasting, such as open-pit mining, construction, and tunneling, a wealth of MWD data points can be generated [5–7]. For example, a high-output blast rig in an open-pit iron ore mine can generate approximately 10,000 MWD data points per day, and high-volume mines generate even more [8].

Historically, to interpret the complex, nonlinear correlations between drilling responses and subsurface composition from such abundant MWD data, manual methods were used [5,8–13]. Previous MWD research focused predominantly on rock type detection to improve blast fragmentation [5,8,10,12–14]. However, these findings do not adequately characterize smaller-scale geological conditions to optimize open-pit orebody characterization. In contrast to previous manual interpretation methods, recently, there have been attempts to apply Artificial Intelligence (AI) and Machine Learning (ML) approaches due to the improvements in computing power and availability [15–19]. Despite these advancements, only few studies have applied analytical methods to MWD data for geological boundary identification [20,21], but none have used a suitable method to evaluate the importance of each MWD metric for predicting geological features.

Principal Component Analysis (PCA) has been the sole method used to evaluate the feature importance of MWD values to determine rock type [14,22]. However, its application is problematic due to its inability to determine feature importance. PCA is a method that allows one to reduce the dimensionality of data by identifying the principal components responsible for most of the data variance [23]. Unfortunately, the most variable characteristics are not always the most important, resulting in an incorrect application of PCA to determine feature importance from MWD data [24]. Therefore, this study employs appropriate feature-importance-based algorithms, Multivariate Adaptive Regression Splines (MARSs), and Projection Pursuit Regression (PPR) on MWD data and ML techniques to determine the most important features and methods for predictive modeling.

The present investigation focuses on the geological characteristics of mineralized ore deposits at an open cut mine located in Pilbara, Australia, using MWD data. A method is presented to assess the feature importance of input drilling variables that will support feature selection for predictive geological modeling using MWD data. In addition, a comparative analysis of the predictive performance of various regression-based ML algorithms is included in this study. Through sophisticated analytics, such as an assessment of feature importance and machine learning predictive modeling, it is possible to derive a more accurate representation of an orebody from MWD data.

While achieving high predictive accuracy remains a challenge, this study contributes by systematically assessing feature importance and machine learning models for MWD-based geophysical predictions, setting a foundation for further refinement. However, ML-based models should be interpreted alongside geological principles, as purely data-driven approaches may misrepresent weak or non-existent correlations. In comparison to resource development RC drill hole-based geological models, the findings represent an order of magnitude increase in spatial resolution previously unavailable without significant additional RC drilling.

2. Methods

2.1. Mine Site

The Western Australian region of Pilbara is renowned for being the main exporter of iron ore in Australia. In 2021, the state exported a remarkable 874 million tons [25]. The iron ore deposits investigated in this study are in the Hammersley Group's Marra Mamba and Brockman Formations, which have been identified as important contributors to Pilbara's economically viable iron ore [26]. Approximately 2.5 billion years ago, extensive sequences of mineral-rich Banded Iron Formation (BIF) were interlayered with shale layers, resulting in these formations [27]. For example, the Marra Mamba Formation comprises the Mount Newman Member, which is overlain by the West Angelas Member, which is dominated by shales. In contrast, the Brockman Formation is made up of the mineralized Dales Gorge BIF and shale bands.

The current investigation focuses on two pits that reflect the geological features of the Marra Mamba and Brockman Formations. Resource development drillholes spaced 50 m apart were used to delineate the geological characteristics of each pit's orebody. The Brockman Pit (*BR*) consisted of 211 RC drill holes totaling 16,880 m and an average depth of 80 m per hole. On the other hand, the Marra Mamba Pit (*MM*) included 167 RC drill holes totaling 13,957 m and an average depth of 83 m per hole. To describe each pit's geology, wireline-based geophysical measurements of density (t/m^3), gamma (API), magnetic susceptibility (m^{3}kg^{-1}), resistivity (Ωm), and hole diameter (cm) were recorded at 0.01 m intervals in the *BR* and *MM* resource-definition RC holes. No additional data engineering was undertaken on the resource-definition data as the mining company's Quality Assurance and Quality Control (QA/QC) procedure had scrutinized these datasets.

2.2. Geological Qualities from Geophysical Measurements

This study considers various geophysical measurements, namely radioactive (gamma and density), electrical (resistivity and magnetic susceptibility), and physical (hole diameter), which are measured from their respective downhole sondes. The numbers of observations used after data processing are listed in Table 1.

Table 1. Number of observations used in each dataset after data processing.

Geophysical Measurement	Observations		
	BR	***MM***	***COM***
Density	45,813	5789	51,602
Gamma	71,126	7791	78,917
Magnetic Susceptibility	71,012	8261	79,273
Resistivity	3202	3798	7000
Caliper	61,666	7505	69,171

Gamma and density wireline logging uses an active radioactive source to assess the bulk densities of subsurface materials as well as their reactions to the *gamma* radiation emanating from a regulated source housed within the logging instrument [28]. These responses are used for several purposes. For example, density (*dens*) is predominantly used as a proxy for ore grade. It can also be employed to estimate the tonnage of overburden stripping or as a measure of porosity. In contrast, the prevalent association of *gamma* radiation with clay minerals has led to using *gamma* as an indicator of shale or clay.

Resistivity and magnetic susceptibility are types of electrical logging that measure the electrical attributes of a rock formation. Resistivity (*res*) defines its capacity to resist the flow of electric current. Alterations in the rock's electrical properties can be attributed to factors, such as the content of clay minerals, water content and porosity, temperature variations, and conductivity of water [29]. Consequently, resistivity logs assist in interpreting conductive material properties and are predominantly employed to estimate salinity and demarcate lithology for hydrogeological studies. Magnetic susceptibility (*magsus*) quantifies the magnetization level of the stratigraphy in a drill hole when exposed to a magnetic field using electromagnetic induction [30]. *magsus* data are useful for characterizing the degree of magnetization of subsurface material encountered in a drill hole exposure to differentiate and infer the mineralogy or lithology of a formation.

The caliper (*cal*) log, also referred to as the hole diameter log, is a physical measurement tool in which one or more tensioned mechanical arms measure the dimensions of the drill cavity [28]. Certain physical characteristics of the drill hole, for example, hole diameter, hole wall roughness, and drilling mud thickness, influence other geophysical measurements. By interrogating the drill hole wall, *cal* can be used in conjunction with other geophysical measures to gain an improved understanding of subsurface geology.

2.3. MWD Systems

This research employed the MWD method for data collection, using a total of 22 rotary blast hole drill rigs that were outfitted with Tungsten Carbide Insert bits. The drilling fleet comprised ten Atlas Copco (Epiroc) Pit Viper 271 rigs, two Terex SKS 12 rigs, a single Bucyrus SKS 13 rig, and two Sandvik 460 rigs. These were deployed to drill production blast holes with a diameter of 0.229 m (Figure 1a). In addition, one Cubex QXR 920 rig, one Sandvik 560 rig, and five Atlas Copco (Epiroc) D65 drill rigs were deployed for drilling 0.165 m wall control blast holes (Figure 1b). The bench heights in the studied iron ore pits ranged from 8 to 12 m, with sub-drilling extending roughly 2 m below the bench floor. The spacing and burden between production blast holes averaged at 8 m and 7 m, respectively.

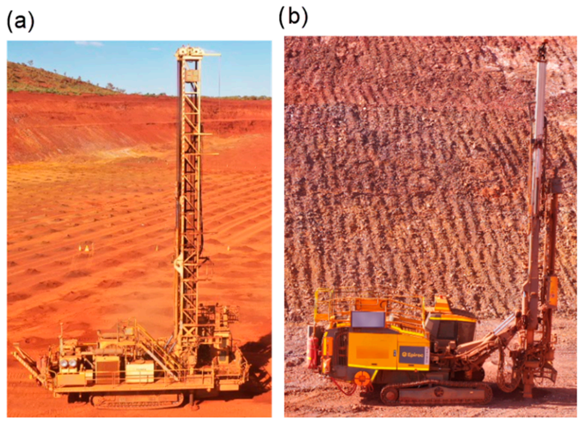

Figure 1. Representative drilling rigs employed in the collection of MWD data [31]: (**a**) Terex SKS 12, utilized for the drilling of 0.229 m production blast holes, and (**b**) Epiroc D65, used in the creation of 0.165 m wall control blast holes.

The MWD system on the drill rigs tracked metrics including the rate of penetration (*rop*; m/s), rotary pressure or torque (*tor*; Nm), force on bit (*fob*; kgf)—also called weight on bit, thrust, or pulldown pressure—bit air pressure or flushing air medium (*bap*; kgf/cm^2), and rotary speed (rpm). However, due to irregularities in the onboard sensor, the rpm data were only available for approximately a quarter of the sample points, leading to the exclusion of rpm from the drilling variables. The collection of MWD metrics was facilitated by a mix of manually operated rigs and semi-autonomous machines, with the latter being remotely overseen from an off-site operations center. The drilling system logged the MWD time-series data at about 0.1 m intervals along the blast hole depth.

MWD data were collected from two distinct pits, *BR* and *MM*, each characterized by unique geological conditions. The *BR* provided a dataset encompassing 75,470 blast holes totaling 844,855 m, while the *MM* pit contributed a dataset comprising 18,887 holes totaling 208,705 m. A combined dataset (*COM*) was generated using *BR* and *MM* data. Combining datasets from different pits improves the robustness of the analysis and ensures that predictive models are applicable across different geological settings. This study concentrated on MWD data ranging from 2 m below the hole collars to the bottom of the blast holes, as the initial two meters of the borehole may not accurately represent the in situ geochemical properties of the rock due to possible toe charge effects during the previous bench's blasting.

MWD Data Pre-Processing

The efficacy of MWD data is affected by a variety of factors, such as subsurface composition, drill rig management system, and external circumstances, which can result in abnormal response values [32]. Consequently, these discrepancies can potentially lead to inaccurate MWD response values and erroneous interpretations of the data [33]. Accordingly, the noise-to-signal ratio in the analyzed mining MWD dataset is substantial as the data had not been subjected to a thorough QA/QC process.

As a result, the MWD data in this study required feature engineering. Because collaring effects at the start of the shaft and potential blast damage from previous holes could skew the in situ rock representation, the initial MWD dataset omitted the first 2 m of each drilling hole. Then, any data points with negative *rop*, *tor*, *fob*, or *bap* values were removed. Using linear interpolation, interquartile range methods, and a 1.5-factor threshold, the voids in the MWD data were considered outliers and subsequently filled. The blasthole data were refined with a Gaussian filter smoothing factor of 0.3 to reduce the local impacts of noise.

The MWD features obtained after performing feature engineering on the first four MWD responses are shown in Table 2. These variables contain the original MWD features, derived ratios of the original features (e.g., *rop* divided by *tor*, indicated as *roptor*), and a moving standard deviation across 0.5 m for the original features (e.g., *ropS*).

Table 2. MWD features investigated in this study.

Type	**MWD Features**			
Recorded	***rop***	***tor***	***fob***	***bap***
Ratio	*roptor* *ropfob* *ropbap*	*torrop* *torfob* *torbap*	*fobrop* *fobtor* *fobbap*	*baprop* *baptor* *bapfob*
Standard Deviation	*ropS*	*torS*	*fobS*	*bapS*

The drilling datasets for blast hole MWD and the exploration hole were transformed from drill hole interval formats to point data, including geospatial coordinates and associated dataset values for each data point. The point data for exploration holes were generated utilizing downhole wireline logged desurvey data, which recorded the azimuth and dip of each hole every 10 m until the final depth. On the other hand, the blast hole MWD data were not desurveyed due to the production nature of the holes, and the location of each point was determined by presuming a straight line from the hole's collar to its end. To merge these two datasets, a K-Nearest Neighbor distance-based search technique was used to calculate the distance between each point in the MWD and exploration data. Each exploration drilling data point was associated with the nearest MWD data point to conduct supervised machine learning. Horizontal and vertical distance thresholds were utilized to further refine the outcomes.

2.4. Feature-Importance-Based Methods

PCA has frequently been used to determine the most important MWD features [14,17,19,22,34]. In contrast, this study employs feature importance algorithms to establish the relative importance of each MWD variable identified for geophysical measurements such as *dens*, *gamma, magsus*, *res*, and *cal*. Non-parametric approaches, such as MARS and PPR, were applied to the pre-processed and merged *BR*, *MM*, and *COM* datasets. Both techniques do not make any assumptions on the relationships between the input and output variables. However, they evaluate feature significance differently.

MARS, a non-parametric approach to regression, disentangles complex variable interactions through a succession of piecewise linear regressions [35]. It identifies crucial features by fitting the model iteratively with each feature, both included and omitted, and measuring the performance variation. MARS has been demonstrated as a valid feature importance methodology in other fields, including molecular biology, environmental science, and civil engineering [36–38]. The MARS algorithm selects the MWD input that leads to the greatest improvement in the model as the most important as follows:

$$\hat{f}(x) = \sum_{j=1}^{J} a_j B_j(x) \tag{1}$$

where $\hat{f}(x)$ is a spline approximation of the function of interest $f(x)$ given by respective constant coefficients, a_j, and a linear combination of basis functions, $B_j(x)$ for (j = 1, 2, . . ., J), which consist of a constant and a hinge function [36]. The earth package in R (v5.3.4), which uses the MARS technique, was used with default hyperparameters to generate models that match the data distribution and to assess the feature relevance of correlations between MWD variables [39].

On the other hand, PPR, a nonlinear regression technique, reveals the most informative data projections into a lower-dimensional subspace [40]. In contrast to MARS, it identifies the most influential characteristics by analyzing the impact of each variable on these projections and determining which variables contribute the most to informative estimates. PPR has been used extensively in other fields for feature importance, including geometallurgy, biochemistry, and economics [41–43]. The PPR formula is as follows:

$$\hat{f}(x) = \sum_{m=1}^{M} S_{\alpha m}\left(\sum_{i=1}^{n} \alpha_{im} x_i\right) \tag{2}$$

where $\alpha_{im} x_i$ denotes the inner product iteratively created in three steps: (1) initializing the residual to the response variable and the term counter M to zero; (2) using numerical optimization to determine the S values that maximize the figure of merit; and (3) eliminating the last term if the merit score falls below a particular threshold. The R package stats (v3.6.2) [44], which incorporates PPR, was used with default hyperparameters to determine the goodness of fit for each variable.

MARS and PPR were utilized to quantify the feature importance of drilling metrics with the goal of understanding the complex, multi-variate relationships between MWD features and in situ geochemical signatures. These feature-importance-based methods were applied to MWD data for both short and big n-terms (basic functions of 101 and 201 for MARS, and terms of 5 and up to 50 for PPR, respectively). Furthermore, the purpose was to determine whether complex models with larger n-terms would model links between geochemical assays and MWD data better than simpler models with smaller n-terms.

2.5. Regression-Based ML Methods

Neural Networks (NNs) are the only regression-based ML algorithms that have been used to address subsurface geophysical intensity with moderate success [19]. However, this study employed a variety of regression-based ML techniques, including Support Vector

Machines (SVMs), Random Forests (RFs), Gaussian Process Regression (GPR), Linear Regression (LR), and Decision Trees (DTs), to investigate the effectiveness of these models to correlate geophysical properties with MWD data, as shown in Table 3.

Table 3. The regression-based ML classes and subclasses utilized include Linear Regression (LR), Decision Trees (DTs), Support Vector Machines (SVMs), Random Forests (RFs), Gaussian Process Regression (GPR), and Neural Networks (NNs).

Class	Linear Regression (LR)	Decision Trees (DTs)	Support Vector Machines (SVMs)	Random Forests (RFs)	Gaussian Process Regression (GP)	Neural Networks (NNs)
Subclass	– Linear – Interactions – Robust – Stepwise	– Fine – Medium – Coarse	– Linear – Quadratic – Cubic – Fine Gaussian – Medium Gaussian – Coarse Gaussian	– Boosted – Bagged	– Squared Exponential – Matern 5/2 – Exponential – Rational Quadratic	– Narrow – Medium – Wide – Bilayered – Trilayered

Su et al. defined LR as a simple linear model that attempts to fit a line to a given dataset [45]. LR works well when the input and output variables are linearly related. However, LR algorithms may miss complex multivariate relationships. In contrast, DTs use recursive partitioning and key attributes to divide the data into smaller subgroups [46]. These trees can efficiently capture nonlinear interactions, but improper pruning may lead to overfitting. SVMs seek to determine the optimal hyperplane for classifying data [47]. They can effectively manage nonlinear relationships and high-dimensional data using kernel methods. Breiman defines RFs as a combination of several DTs to improve efficiency, prevent overfitting, and manage nonlinear relationships [48]. GPR examines the output variable as a Gaussian distribution to identify the function that most closely approximates the data [49]. The GPR method considers nonlinear interactions and provides a probabilistic prediction of the outcome. Bishop describes NNs as flexible nonlinear models because they are modeled after the human brain, consisting of interconnected layers of neurons [50]. NNs reflect complicated relationships and work well with high-dimensional data but are susceptible to overfitting if not adequately regulated.

This study evaluated the predictive ability of regression-based ML algorithms and performed the calculations on a Pawsey Supercomputer Nimbus cloud Ubuntu instance with 8 vCPUs and 32 GB of memory. The Regression Learner Toolbox in MATLAB (R2024A) was used with default hyperparameters and no optimization for each respective regression-based ML method to generate models and assess prediction performance [51]. The coefficient of determination (R^2) and root mean square error (RMSE) metrics were used to compare the performance of various models, defined by the following criteria:

$$R^2 = 1 - \frac{RSS}{TSS} = 1 - \left(\frac{\sum_{i=1}^{N} (y_i - f(x_i))^2}{\sum_{i=1}^{N} (y_i - \overline{y})^2} \right) \tag{3}$$

$$RMSE = \sqrt{\frac{1}{N} * \sum_{i=1}^{N} (y_i - f(x_i))^2} \tag{4}$$

where RSS is the sum of squares of residuals, TSS is the total sum of squares, N is the sample size, y_i is the measured value, $f(x_i)$ is the predicted value, and $\overline{y}$ is the mean.

3. Results

A preliminary investigation of the MWD features (*rop*, *tor*, *fob*, and *bap*) collected from sensors on the drills was conducted to comprehend the data's range and frequency. Significant variations in *rop* and *fob* can be attributed many factors, including inconsistencies in mining equipment, operator competence, bit degradation, and rock mass properties [52].

Therefore, a single variable analysis of these features may not adequately capture the nonlinear correlations between MWD and geophysical measurements.

Figure 2a–d depict the first four MWD datapoints from the *COM*, respectively. The *COM rop* displayed a balanced distribution, averaging 0.0248 m/s with a standard deviation of 0.010 m/s. Similarly, as shown in Figure 2b, the *COM tor* responses also have a typical distribution, with a mean of 3.41 Nm and a standard deviation of 1.06 Nm. On the other hand, Figure 2c depicts the skewed distribution of the *COM fob* with a mean of 97,945 kgf and a standard deviation of 78,524 kgf. Figure 2d displays a normal distribution for the *COM bap*, with values ranging from 230,300 kgf/cm^2 to 439,400 kgf/cm^2, a mean value of 335,550 kgf/cm^2, and a standard deviation of 49,384 kgf/cm^2.

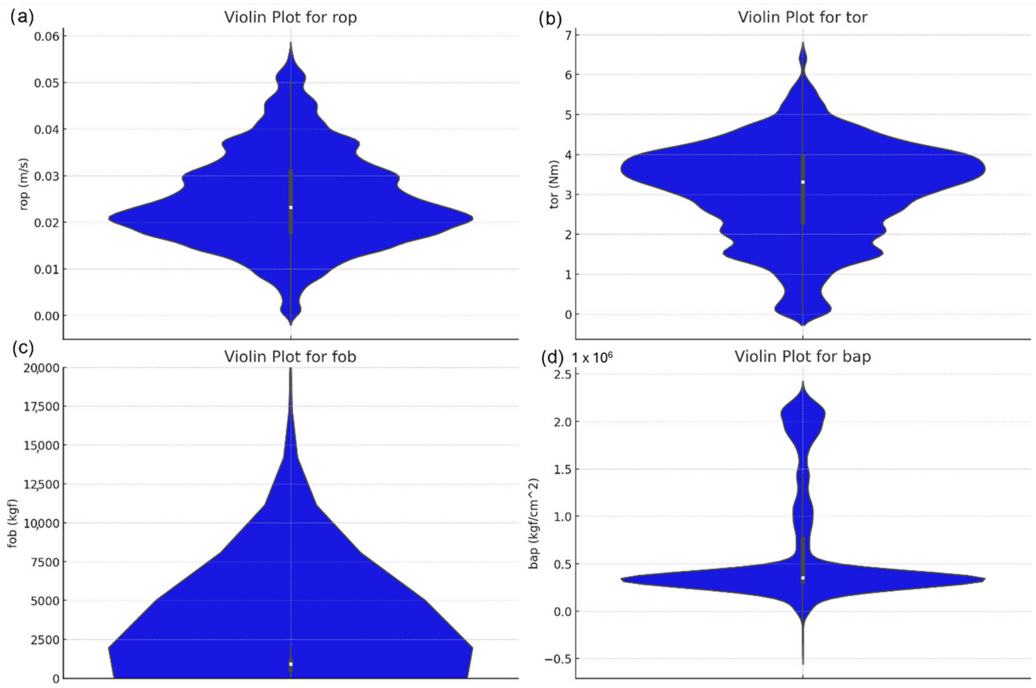

Figure 2. Violin plots showing frequencies and ranges of MWD data for (**a**) *COM rop*, (**b**) *COM tor*, (**c**) *COM fob*, and (**d**) *COM bap*.

Upon examination of the *COM* geophysical data presented through violin plots in Figure 3, distinct patterns were observed. The *COM dens* measurements exhibit a uniform distribution, suggesting consistent rock densities across the studied region. In contrast, the *COM res* data are notably skewed towards lower values, indicating predominant low resistivity, with occasional higher resistivity regions. In addition, the *COM gamma* and *COM magsus* measurements present more variable distributions, signifying a diverse range of rock properties. Lastly, the *COM cal* data demonstrate symmetry, indicating consistent borehole sizes. While certain measurements like *dens* and *cal* indicate uniformity, *gamma* and *magsus* highlight variability in subsurface geophysical conditions.

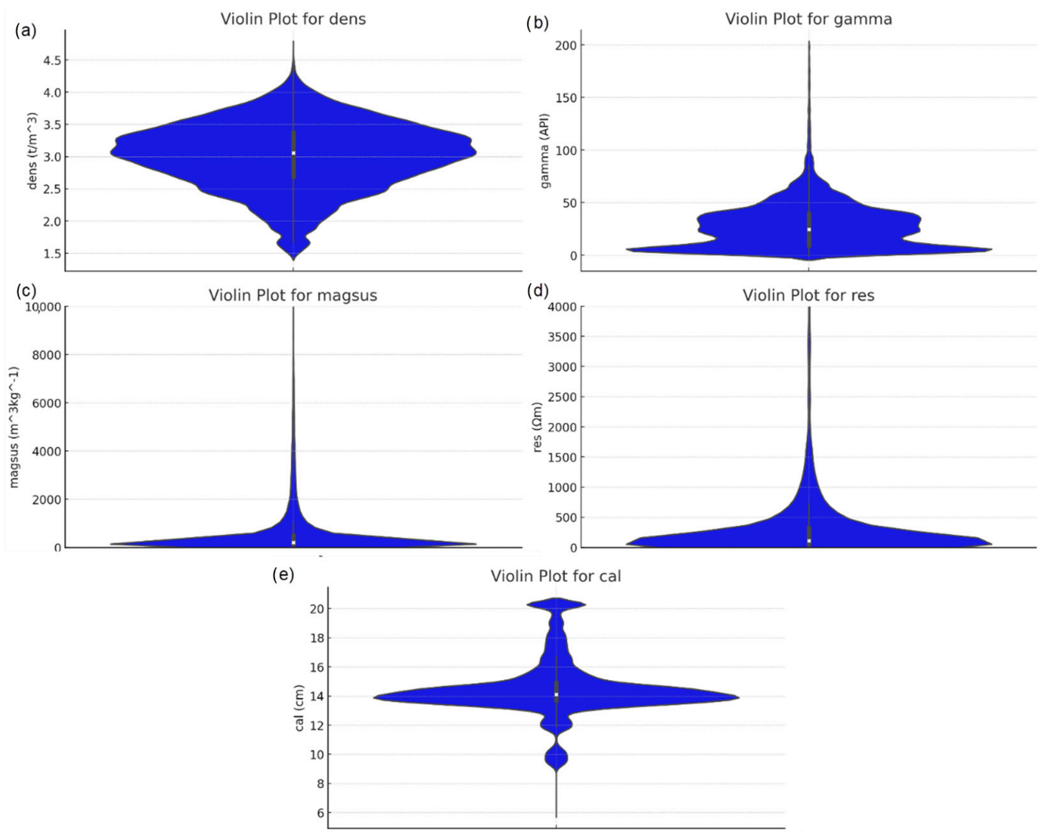

Figure 3. Violin plots showing frequencies and ranges of *COM* geophysical data for (**a**) *dens*, (**b**) *gamma*, (**c**) *magsus*, (**d**) *res*, and (**e**) *cal*.

3.1. Feature-Importance-Based Results

The importance of the investigated MWD response features in inferring geophysical measures was investigated. Small and large n-terms MARS and PPR models were developed to determine whether more complex ML methods would be advantageous during subsequent predictive modeling.

The percentages presented in Tables 4 and 5 were calculated by adding the relative weights of each attribute and dividing by the total for MARS and PPR, respectively. These percentages can be categorized into three different groups: (a) 0% relative feature importance, where MWD features were deemed irrelevant by MARS and PPR in predicting orebody quality measures; (b) greater than 0% but less than 5% relative feature importance (minor importance), indicating a slight influence on the prediction of orebody quality measures; and (c) exceeding 5% relative feature importance.

Table 4. MARS-derived feature importance of MWD measures in predicting *COM* geophysical values. Importance is expressed as relative percentage of cumulative value for each specific scenario. Scenarios considered include both small (101) and large (201) n-terms (basis functions).

MWD Feature	**Density**		**Gamma**		**Magnetic Susceptibility**		**Resistivity**		**Caliper**	
MARS n-Terms	**101 (%)**	**201 (%)**	**101 (%)**	**201 (%)**	**101 (%)**	**201 (%)**	**101 (%)**	**201 (%)**	**101 (%)**	**201 (%)**
rop	7	7	10	10	6	6	3	4	11	11
tor	7	7	9	9	8	8	8	7	0	0
fob	1	1	0	0	4	4	1	1	0	0
bap	5	4	2	2	0	0	10	10	0	0

Table 4. *Cont.*

MWD Feature	Density		Gamma		Magnetic Susceptibility		Resistivity		Caliper	
MARS n-Terms	**101 (%)**	**201 (%)**	**101 (%)**	**201 (%)**	**101 (%)**	**201 (%)**	**101 (%)**	**201 (%)**	**101 (%)**	**201 (%)**
roptor	7	7	7	7	6	6	9	9	18	18
ropbap	6	6	7	7	0	0	8	10	0	0
ropfob	6	6	5	5	1	0	6	5	0	0
torrop	7	7	8	8	10	10	4	8	2	2
torbap	8	8	5	5	5	5	12	12	0	0
torfob	6	6	4	4	13	13	5	5	7	7
baprop	10	9	8	8	9	9	3	3	15	15
baptor	4	4	9	9	10	10	6	8	0	0
bapfob	2	1	0	0	9	9	0	0	0	0
fobrop	1	1	0	0	0	0	1	1	14	14
fobtor	6	5	5	5	4	4	6	5	7	7
fobbap	9	9	8	8	2	2	10	2	10	10
ropS	0	0	7	7	0	0	0	0	0	0
torS	3	6	6	6	6	6	6	9	5	5
fobS	3	3	0	0	2	2	0	0	12	12
bapS	3	2	0	0	5	5	0	0	0	0

Table 5. PPR-derived feature importance of MWD measures in predicting *COM* geophysical values. Importance is expressed as relative percentage of cumulative value for each specific scenario. Scenarios considered include both small (5) and large (<50) n-terms (basis functions).

MWD Feature	Density		Gamma		Magnetic Susceptibility		Resistivity		Caliper	
PPR n-Terms	**5 (%)**	**<50 (%)**	**5 (%)**	**<50 (%)**	**5 (%)**	**<50 (%)**	**5 (%)**	**<50 (%)**	**5 (%)**	**<50 (%)**
rop	0	0	0	0	0	0	0	0	0	0
tor	0	0	0	0	0	0	0	0	0	0
fob	16	18	11	17	21	21	4	8	3	9
bap	7	4	7	8	5	8	1	18	3	9
roptor	0	0	0	0	0	0	0	0	0	0
ropbap	0	0	0	0	0	0	0	0	0	0
ropfob	0	0	0	0	0	0	0	0	0	0
torrop	19	2	25	9	18	5	9	3	21	12
torbap	0	0	0	0	0	0	0	0	0	0
torfob	0	0	0	0	0	0	0	0	0	0
baprop	28	5	29	6	13	12	11	11	49	6
baptor	7	4	8	4	8	4	7	4	7	19
bapfob	4	8	3	13	7	10	19	16	3	24
fobrop	11	12	4	33	14	28	11	20	6	14
fobtor	5	37	8	6	9	9	34	1	3	5
fobbap	0	0	0	0	0	0	0	0	0	0
ropS	0	0	0	0	0	0	0	0	0	0
torS	0	0	0	0	0	0	0	0	0	0
fobS	3	9	2	3	5	1	2	17	1	1
bapS	0	1	4	2	1	1	2	2	3	1

The findings suggest that the relative importance of features remains stable across models with both small and large term counts. Despite the apparent consistency in both n-term models, MARS and PPR analyses assigned varying degrees of importance to different features. For instance, when using the *COM* dataset, the MARS method identified 15 out of 20 of the MWD measures as crucial in inferring *dens* (Figure 4a), with the exceptions being *fob*, *bapfob*, *fobrop*, *fobS* and *bapS*. Most features were identified as important due to the MARS method, which involves searching for relationships between variables. Conversely, the PPR approach determined that only half of the MWD features were important, with only five variables being greater than or around ten percent: *fobrop*, *fob*, *bapfob*, *torrop*, and *bap*. (Figure 4b). PPR implies that the remaining MWD features exert minimal to no influence on the prediction of orebody quality, possibly due to the lack of consideration for nonlinear interaction among features in the PPR model. Thus, to encompass all potential significant MWD features, MARS and PPR methodologies were employed.

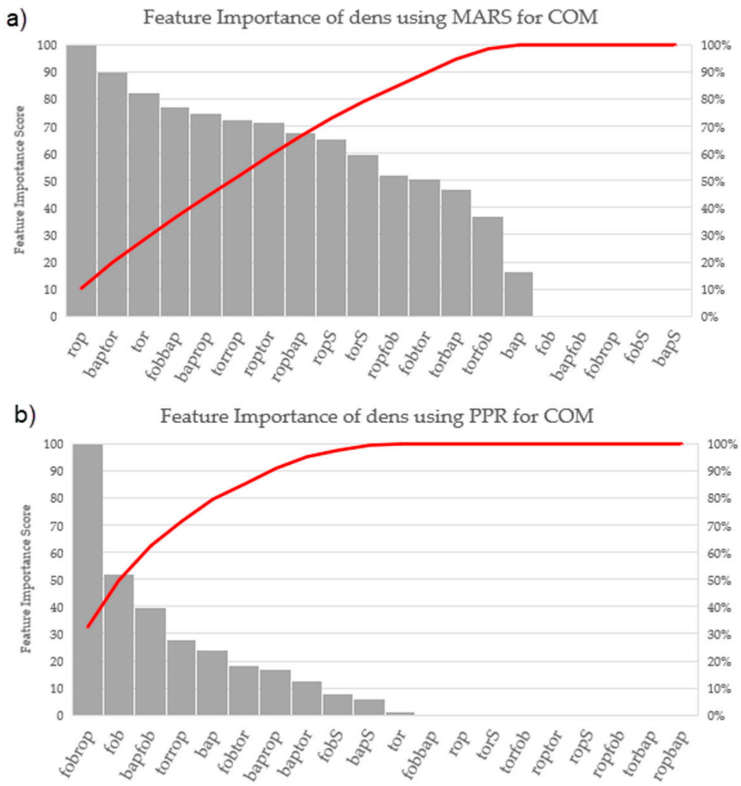

Figure 4. Feature importance scores of MWD features for *COM dens* values employing (**a**) MARS and (**b**) PPR. Total percentages of feature importance are graphically presented as red lines.

Figure 5 provides a comparative analysis of the significance of the MWD features for *gamma*, *dens*, *magsus*, *res*, and *cal COM* dataset, as determined by the MARS and PPR methodologies. These results correspond to the top ten most important MWD features discovered in the *dens* analysis (Figure 4). The MWD characteristic *fobrop* routinely emerges as highly important in this study's datasets, along with *bapfob*, *baprop*, *fob*, *bap*, and *fobtor*. It is important to note, however, that this does not diminish the importance of other MWD features; rather, it highlights those that are frequently identified as important.

As shown in Tables 4 and 5, the importance of features for evaluating *dens* varies across different datasets when the MARS and PPR methodologies are applied. The six MWD variables deemed most important for predicting den from the analyzed BIF deposits are *fobrop*, *fobtor*, *bapfob*, *torrop*, *baprop*, and *baptor*, in accordance with the peak importance findings (Figure 5). This result generally corresponds to the importance of MWD features identified for *gamma*, *magsus*, *res*, and *cal* (Figure 4). The ratios *fobrop*, *fobtor*, *bapfob*, *torrop*, *baprop*, and *baptor* carried more importance than the primary *rop* and *tor* variables, the *rop*-influenced ratios *roptor*, *ropbap*, and *ropfob*, as well as the variability-related metrics *ropS*, *torS*, and *bapS*. On the other hand, *fob* was identified as highly important from PPR but was very low or missing in the MARS rankings.

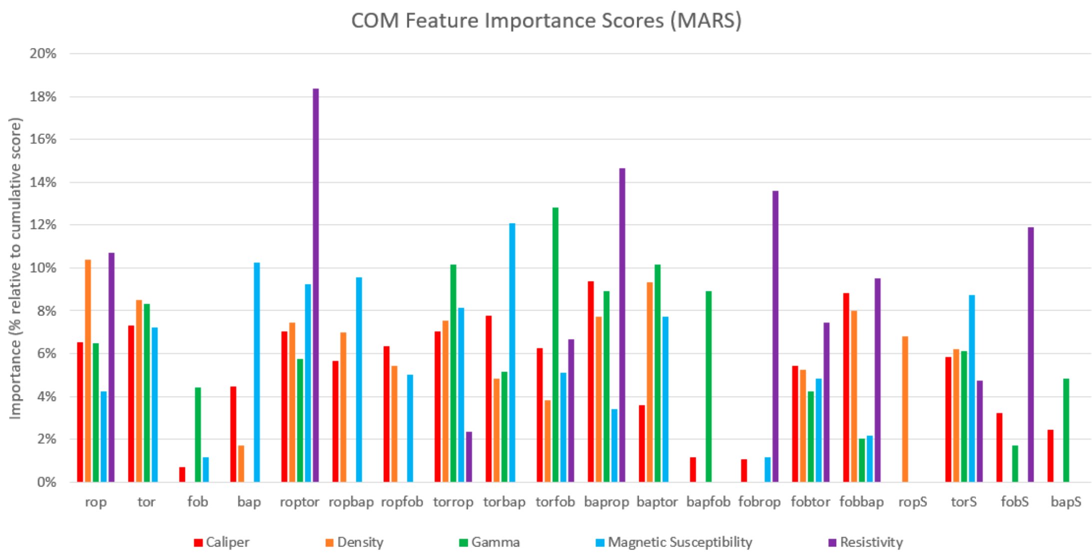

Figure 5. Feature-importance-based ML results of MWD variables for the *COM* dataset in predicting geophysical measurements, namely *cal*, *dens*, *gamma*, *magsus*, and *res*, as determined by the MARS approach. The *y*-axis represents the importance score as a percentage of the overall value for MARS. The MWD features are graphed along the *x*-axis.

3.2. Regression-Based ML Analytical Prediction Results

The following sections evaluate the prediction strength of several kinds of regression-based ML regression models for predicting geophysical measurements of an orebody. The investigated geophysical measurements included *dens*, *gamma*, *magsus*, *res*, and *cal*, and they were predicted based on the MWD input features described in Table 2. This analysis required validating the proposed ML analytical procedure with a variety of geophysical signatures to establish theoretical precision.

A 10-fold cross-validation technique revealed the training dataset's prediction strength. The datasets were split into 80% for training and 20% for testing. The testing results are reported as RMSE value, with the R^2 value being the average of the 10 folds during cross-validation. In addition, a threshold of twenty-four hours of computation time was established due to practical limitations regarding calculation speed for real-time analysis. Consequently, several GP-based analyses were prematurely terminated and categorized as nonapplicable (N/A). Moreover, scatter plots are useful for visualizing individual predictions but may not effectively convey comparative model performance across multiple geophysical parameters. Tables provide a comprehensive view of RMSE and R^2 across different models, allowing for a direct evaluation of their relative strengths and weaknesses.

A preliminary investigation was conducted using the Coarse DT method to determine whether additional MWD features beyond *rop*, *tor*, *fob*, and *bap* would strengthen the prediction performance of regression-based ML models. The results are listed in Table 6. Based on these results showing that 14 out of 15 models performed better with the additional features, the decision was made to incorporate the ratio and moving standard deviation (Table 2) MWD features in all of the investigated predictive ML models. The *res* models did not improve as much as the others, possibly due to smaller numbers of observations due to this geophysical sonde not being used in every drillhole.

Table 6. Prediction performance of DT models using only 4 measured MWD features and all 20 investigated MWD features. Higher performing models are in **bold**.

Geophysical Measurement	*BR*				*MM*				*COM*			
	Measured		Additional		Measured		Additional		Measured		Additional	
	RMSE	R^2	RMSE	R^2	RMSE	R^2	RMSE	R^2	RMSE	R^2	RMSE	R^2
dens	0.33	0.57	**0.29**	**0.68**	0.37	0.51	**0.34**	**0.59**	0.34	0.56	**0.30**	**0.66**
gamma	15.47	0.50	**14.01**	**0.59**	13.62	0.65	**10.67**	**0.78**	15.53	0.51	**13.67**	**0.62**
magsus	848	0.70	**701**	**0.80**	389	0.24	**376**	**0.29**	845	0.68	**680**	**0.79**
res	582	0.27	**554**	**0.34**	**697**	**0.31**	705	0.29	650	0.29	**631**	**0.33**
cal	1.12	0.68	**0.93**	**0.78**	1.19	0.61	**1.03**	**0.70**	1.16	0.66	**0.94**	**0.78**

3.2.1. Density and Gamma Prediction

The regression results for estimating *dens* and *gamma* values using ML models such as LR, DTs, SVMs, RFs, GP, and NNs are detailed in Tables 7 and 8, respectively. The R^2 values of models utilizing *BR* data to predict *dens* and *gamma* were marginally superior to those utilizing *MM* and *COM* datasets. This discrepancy may be attributable to the *BR* and *MM* datasets containing different quantities of data.

Table 7. R^2 and RMSE results of regression-based ML models to predict *dens* values from MWD data. Highest performing model results are in **bold**. All 20 MWD features were incorporated into models. Standard deviations (std) from 10-fold cross-validation are reported for RMSE and R^2.

Regression-Based ML Class	Regression-Based ML Suclass	*BR*		*MM*		*COM*	
		RMSE (t/m^3)	R^2	RMSE (t/m^3)	R^2	RMSE (t/m^3)	R^2
LR	Linear	0.49	0.06	0.49	0.13	0.50	0.05
	Interactions	0.55	0.00	0.45	0.28	0.79	0.00
	Robust	0.49	0.06	0.50	0.13	0.50	0.04
	Stepwise	**0.48**	**0.12**	**0.44**	**0.32**	**0.49**	**0.09**
DTs	**Fine**	**0.22**	**0.81**	**0.27**	**0.74**	**0.23**	**0.80**
	Medium	0.25	0.76	0.29	0.69	0.25	0.75
	Coarse	0.29	0.68	0.34	0.59	0.30	0.66
SVMs	Linear	0.49	0.05	0.50	0.12	0.50	0.04
	Quadratic	0.46	0.17	0.41	0.40	0.48	0.13
	Cubic	0.37	0.46	0.31	0.66	0.56	0.00
	Fine Gaussian	**0.31**	**0.63**	**0.25**	**0.77**	**0.32**	**0.61**
	Medium Gaussian	0.40	0.39	0.37	0.50	0.43	0.28
	Coarse Gaussian	0.48	0.09	0.48	0.18	0.49	0.07
RFs	Boosted	0.46	0.19	0.41	0.41	0.47	0.16
	Bagged	**0.21**	**0.83**	**0.24**	**0.80**	**0.21**	**0.82**
GPs	Squared Exponential	0.28	0.70	0.23	0.81	0.27	0.72
	Matern 5/2	0.27	0.72	0.22	0.82	0.26	0.73
	Exponential	0.22	0.82	**0.19**	**0.87**	0.22	0.81
	Rational Quadratic	**0.20**	**0.84**	0.20	0.86	**0.22**	**0.82**
NNs	Narrow	0.44	0.24	0.35	0.56	0.45	0.21
	Medium	0.38	0.42	0.29	0.69	0.41	0.36
	Wide	**0.32**	**0.61**	**0.24**	**0.79**	**0.34**	**0.55**
	Bilayered	0.41	0.36	0.33	0.62	0.43	0.29
	Trilayered	0.40	0.38	0.31	0.65	0.42	0.33

Table 8. R^2 and RMSE results of regression-based ML models used to predict *gamma* values from MWD data. Highest performing model results are in **bold**. 20 All MWD features were used in these models. Standard deviations (std) from 10-fold cross-validation are reported for RMSE and R^2.

Regression-Based ML Class	Regression-Based ML Suclass	*BR*		*MM*		*COM*	
		RMSE (API)	R^2	RMSE (API)	R^2	RMSE (API)	R^2
LR	Linear	21.30	0.06	20.52	0.20	**21.53**	**0.06**
	Interactions	21.53	0.04	17.81	0.40	22.38	0.00
	Robust	21.47	0.04	22.83	0.01	21.71	0.04
	Stepwise	**20.75**	**0.11**	**16.23**	**0.50**	N/A	N/A
DTs	**Fine**	**10.24**	**0.78**	**0.80**	**0.88**	**10.00**	**0.80**
	Medium	11.90	0.71	8.79	0.85	11.58	0.73
	Coarse	14.01	0.59	10.67	0.78	13.67	0.62
SVMs	Linear	21.49	0.04	22.02	0.08	21.71	0.04
	Quadratic	20.39	0.14	15.45	0.55	20.70	0.13
	Cubic	18.33	0.30	10.05	0.81	27.88	0.00
	Fine Gaussian	**16.13**	**0.46**	**7.56**	**0.89**	**16.02**	**0.48**
	Medium Gaussian	18.63	0.28	12.76	0.69	19.19	0.25
	Coarse Gaussian	20.96	0.09	21.03	0.16	21.24	0.08
RFs	Boosted	19.92	0.18	13.86	0.63	20.03	0.18
	Bagged	**9.65**	**0.81**	**7.04**	**0.91**	**9.43**	**0.82**
GPs	Squared Exponential	14.31	0.58	6.73	0.91	13.30	0.64
	Matern 5/2	13.72	0.61	6.52	0.92	**13.24**	**0.64**
	Exponential	**10.93**	**0.75**	**6.32**	**0.92**	N/A	N/A
	Rational Quadratic	N/A	N/A	6.51	0.92	N/A	N/A
NNs	Narrow	19.70	0.20	11.61	0.74	19.98	0.19
	Medium	18.17	0.32	8.87	0.85	18.61	0.30
	Wide	**16.03**	**0.47**	**6.88**	**0.91**	**16.22**	**0.47**
	Bilayered	18.92	0.26	9.34	0.83	19.19	0.25
	Trilayered	18.84	0.26	9.41	0.83	19.28	0.24

Among all *COM* models, those employing LR and SVMs consistently produced the least accurate predictions for *dens* and *gamma* with R^2 values below 0.50 (Tables 7 and 8). In contrast, models constructed with DTs, RFs, and GP yielded the highest R^2 values for *dens* and *gamma* predictions, with both achieving 0.80. These high-performing DTs, RFs, and GP models yielded an average RMSE of approximately 0.21 t/m^3 for *dens* and 9.42 API for *gamma*. GP displayed the most accurate predictions, with R^2 values of 0.87 and 0.92 and RMSEs of less than 0.19 t/m^3 and 6.32 API for *MM dens* and *gamma*, respectively.

Within each ML algorithm class, significant differences were observed between the subclasses of ML outlined in Table 3. As an example, the Bagged (Bootstrapped Aggregate) Tree method outperformed the Boosted Tree RFs in predicting densities and *gamma*, with an R^2 value of approximately 0.82 for both geophysical measurements. Similarly, Wide NNs consistently outperformed other NN types, with peak R^2 values of 0.54 and 0.43 for *dens* and *gamma*, respectively, and the lowest RMSE values of 0.35 t/m^3 for *dens* and 16.68 API for *gamma*. Lastly, a Fine Tree DT correlation value of 0.80 for both *dens* and *gamma* was obtained, which is superior to those of the Medium and Fine parameters.

Figure 6a–f depict the ML analytical prediction results compared to actual wireline measured *dens* values for the best-performing LR, DTs, SVMs, RFs, GP, and NNs models. The Bagged RF models had the strongest correlation with an R^2 value of 0.82. The DT models generated a slightly weaker R^2 value of 0.80. However, the training speed of the DT models was over 10 times that of the Bagged RF models, at around 400 with

35 observations per second, respectively. Furthermore, although density is often considered a relatively stable parameter, its prediction using MWD data remains complex due to inherent sensor noise, operational variability, and small-scale geological heterogeneity. The errors observed in Figure 6 reflect these real-world challenges, reinforcing the need for further data integration approaches.

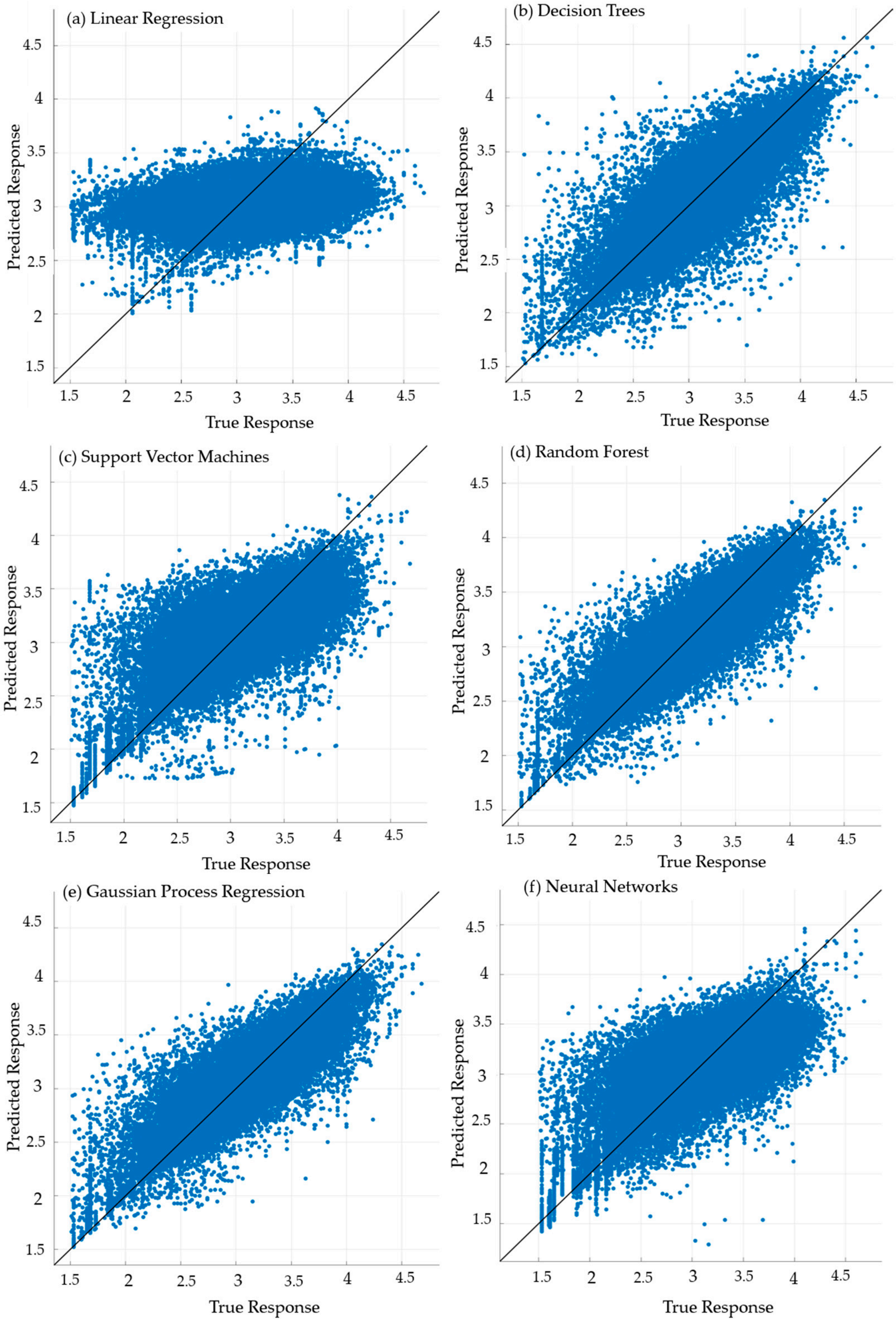

Figure 6. Actual versus predicted R^2 values for *dens* predictions using various machine learning analytical methods, including (**a**) LR, (**b**) DTs, (**c**) SVMs, (**d**) RFs, (**e**) GP, and (**f**) NNs.

In addition, a series of three-level experiments with variable input parameters were conducted to correspond to the three primary levels of relative feature significance determined by MARS and PPR in Section 3.1, namely 0%, less than 5%, and over 5%. The objective of this method was to determine the effect of omitting MWD features deemed to be of minimal importance. The experimental design included (1) all 20 MWD features, including those with 0% relative importance, (2) the exclusion of MWD features identified as having 0% relative importance, and (3) the removal of MWD features classified as having less than 5% importance, which was designated as minor importance.

Interestingly, the elimination of minor importance features had no effect on prediction performance when compared to the use of all features (Figure 7). With the *gamma COM* dataset, most instances exhibited less than a 0.05 decrease in R^2, whereas the Fine Tree and Medium Tree DT techniques demonstrated 0.19 and 0.06 enhancements in R^2, respectively. Nonetheless, there was a consistent increase in training speed for *dens* and *gamma* DTs, as well as *dens* NNs, when marginally significant features were used over all features (Figure 7). In contrast, when utilizing all features, *gamma* NNs models demonstrated faster training rates and higher R^2 values. This anomaly may be due to the inherent dynamics of the NN method, which has difficulty establishing relationships between these datasets using marginally significant features, resulting in lower R^2 values.

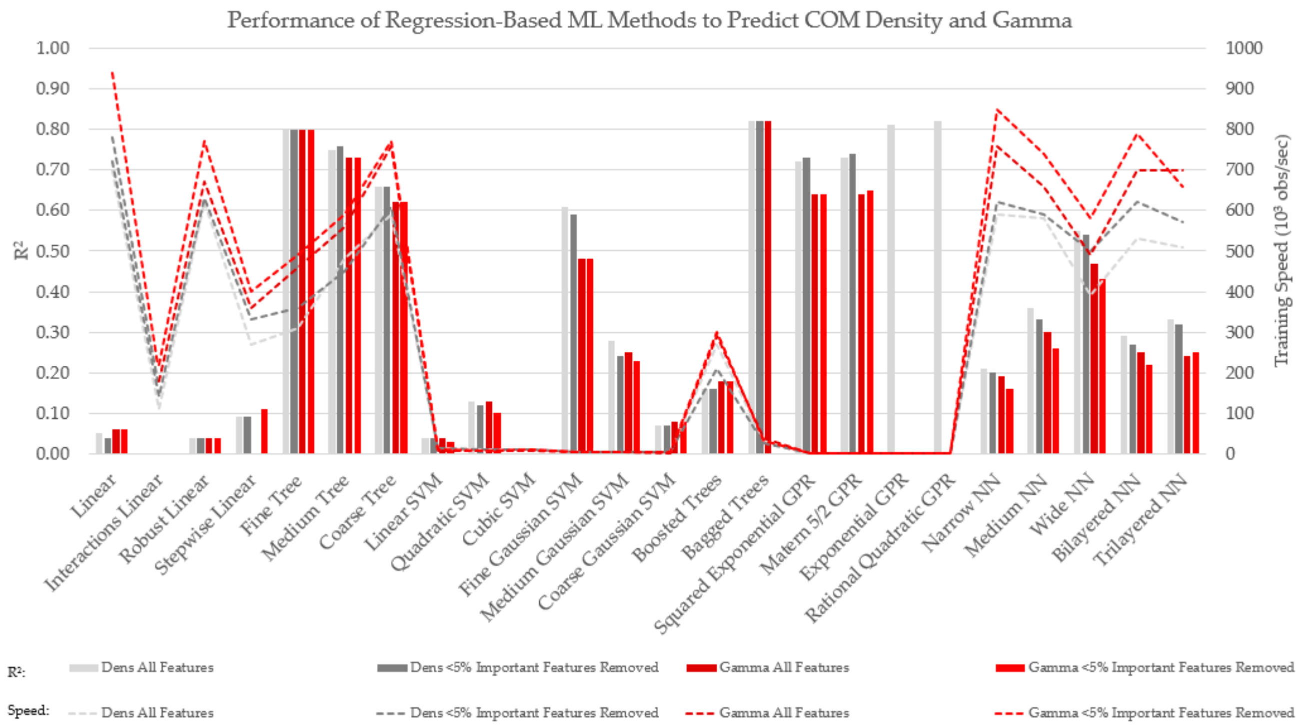

Figure 7. R^2 (columns) and training speeds (lines) of investigated regression-based ML methods used to predict *dens* and *gamma* orebody geophysical values using MWD features in *COM*.

3.2.2. Magsus and Res Prediction

The prediction results of *magsus* and *res* geophysical measurements using various ML models, including LR, DTs, SVMs, RFs, GP, and NNs, are presented in Tables 9 and 10. Interestingly, the DT models showed consistent performance across the *BR*, *MM*, and *COM* datasets, with R^2 variances of less than 0.02 between them. In contrast, the NN models demonstrated a notable performance improvement on the *MM* dataset. This divergence aligns with the observations made for *dens* and *gamma* (see Section 3.2.1) and could be attributed to the disparity in data volume between the *BR* and *MM* datasets, a point that requires more investigation.

Table 9. R^2 and RMSE results of regression-based ML models used to predict *magsus* values from MWD data. Highest performing model results are in **bold**. All 20 MWD features were used in these models. Standard deviations (std) from 10-fold cross-validation are reported for RMSE and R^2.

Regression-Based ML Class	Regression-Based ML Suclass	*BR*		*MM*		*COM*	
		RMSE (m^3kg^{-1})	R^2	RMSE (m^3kg^{-1})	R^2	RMSE (m^3kg^{-1})	R^2
LR	Linear	1505	0.06	435	0.05	1446	0.05
	Interactions	1490	0.08	**388**	**0.24**	1464	0.03
	Robust	1625	0.00	453	0.00	1552	0.00
	Stepwise	**1450**	**0.13**	N/A	N/A	**1387**	**0.13**
DTs	**Fine**	**518**	**0.89**	**260**	**0.66**	**499**	**0.89**
	Medium	564	0.87	291	0.57	542	0.87
	Coarse	701	0.80	375	0.29	680	0.79
SVMs	Linear	1606	0.00	450	0.00	1537	0.00
	Quadratic	1498	0.07	443	0.01	1468	0.03
	Cubic	1306	0.30	389	0.24	1403	0.11
	Fine Gaussian	**1081**	**0.52**	**375**	**0.29**	**1105**	**0.45**
	Medium Gaussian	1366	0.23	438	0.03	1403	0.11
	Coarse Gaussian	1576	0.00	450	0.00	1517	0.00
RFs	Boosted	1171	0.43	298	0.55	1134	0.42
	Bagged	**486**	**0.90**	**253**	**0.68**	**457**	**0.91**
GPs	Squared Exponential	668	0.82	**252**	**0.68**	646	0.81
	Matern 5/2	667	0.82	254	0.68	590	0.84
	Exponential	504	0.90	N/A	N/A	**471**	**0.90**
	Rational Quadratic	**483**	**0.90**	N/A	N/A	484	0.89
NNs	Narrow	1093	0.51	307	0.53	1114	0.44
	Medium	1019	0.57	287	0.59	1030	0.52
	Wide	**865**	**0.69**	**262**	**0.66**	**902**	**0.63**
	Bilayered	997	0.59	295	0.56	1012	0.54
	Trilayered	971	0.61	276	0.62	986	0.56

The DT approaches produced R^2 values ranging from 0.79 to 0.89 when applied to *COM magsus* data. However, the *res COM* DT models were remarkably lower than the *magsus* data, ranging from 0.32 to 0.58. This discrepancy could be due to the *res* dataset having around 10 times less data due to inconsistent wireline logging practices, as *res* was not measured on the same number of holes as *magsus*. Moreover, the relatively weak prediction performance of *res* can be attributed to the lack of intrinsic correlation between drilling parameters and resistivity in formations devoid of conductive minerals. Since *res* primarily depends on pore fluid content rather than mechanical drilling forces, ML models face inherent challenges in accurately modeling this relationship.

Certain ML subclasses outperformed others within the same ML class, a pattern consistent with those discovered for *dens* and *gamma*. For example, Fine DTs consistently outperformed Medium and Coarse DTs in both the *COM magsus* and *res* datasets. Moreover, in the predictions for *magsus* and *res*, Bagged RFs performed better than Boosted Tree RFs. Likewise, Wide NNs consistently outperformed other NN subclasses, with the R^2 values for *magsus* and *res* reaching maximums of 0.63 and 0.49, respectively. Fine Gaussian SVMs achieved R^2 values greater than 0.44 for *magsus* and Cubic SVMs of 0.22 for *res*, demonstrating a wide range of outcomes. In contrast, the R^2 values of Linear and Coarse Gaussian SVMs were all 0.00.

With R^2 values exceeding 0.60 for electrical geophysical predictions, GPs consistently generated reliable results across all GP subclasses. Nonetheless, as shown in Figure 8, GP models required a prolonged computation time than methods such as DTs, RFs, and NNs. However, no significant decrease in prediction performance was observed when models excluded features with less than 5% importance in comparison to models that included all features. Certain models, including most created with Stepwise LR, Exponential GPR, and Rational Quadratic GPR, had to be stopped after 24 h; therefore, their results are not included here.

Table 10. R^2 and RMSE results of regression-based ML models used to predict *res* values from MWD data. Highest performing model results are in **bold**. All 20 MWD features were used in these models. Standard deviations (std) from 10-fold cross-validation are reported for RMSE and R^2.

Regression-Based ML Class	Regression-Based ML Suclass	*BR*		*MM*		*COM*	
		RMSE (Ωm)	R^2	RMSE (Ωm)	R^2	RMSE (Ωm)	R^2
LR	Linear	21.30	0.06	20.52	0.20	**21.53**	**0.06**
	Interactions	21.53	0.04	17.81	0.40	22.38	0.00
	Robust	21.47	0.04	22.83	0.01	21.71	0.04
	Stepwise	**20.75**	**0.11**	**16.23**	**0.50**	N/A	N/A
DTs	**Fine**	**10.24**	**0.78**	**0.80**	**0.88**	**10.00**	**0.80**
	Medium	11.90	0.71	8.79	0.85	11.58	0.73
	Coarse	14.01	0.59	10.67	0.78	13.67	0.62
SVMs	Linear	21.49	0.04	22.02	0.08	21.71	0.04
	Quadratic	20.39	0.14	15.45	0.55	20.70	0.13
	Cubic	18.33	0.30	10.05	0.81	27.88	0.00
	Fine Gaussian	**16.13**	**0.46**	**7.56**	**0.89**	**16.02**	**0.48**
	Medium Gaussian	18.63	0.28	12.76	0.69	19.19	0.25
	Coarse Gaussian	20.96	0.09	21.03	0.16	21.24	0.08
RFs	Boosted	19.92	0.18	13.86	0.63	20.03	0.18
	Bagged	**9.65**	**0.81**	**7.04**	**0.91**	**9.43**	**0.82**
GPs	Squared Exponential	14.31	0.58	6.73	0.91	13.30	0.64
	Matern 5/2	13.72	0.61	6.52	0.92	**13.24**	**0.64**
	Exponential	**10.93**	**0.75**	**6.32**	**0.92**	N/A	N/A
	Rational Quadratic	N/A	N/A	6.51	0.92	N/A	N/A
NNs	Narrow	19.70	0.20	11.61	0.74	19.98	0.19
	Medium	18.17	0.32	8.87	0.85	18.61	0.30
	Wide	**16.03**	**0.47**	**6.88**	**0.91**	**16.22**	**0.47**
	Bilayered	18.92	0.26	9.34	0.83	19.19	0.25
	Trilayered	18.84	0.26	9.41	0.83	19.28	0.24

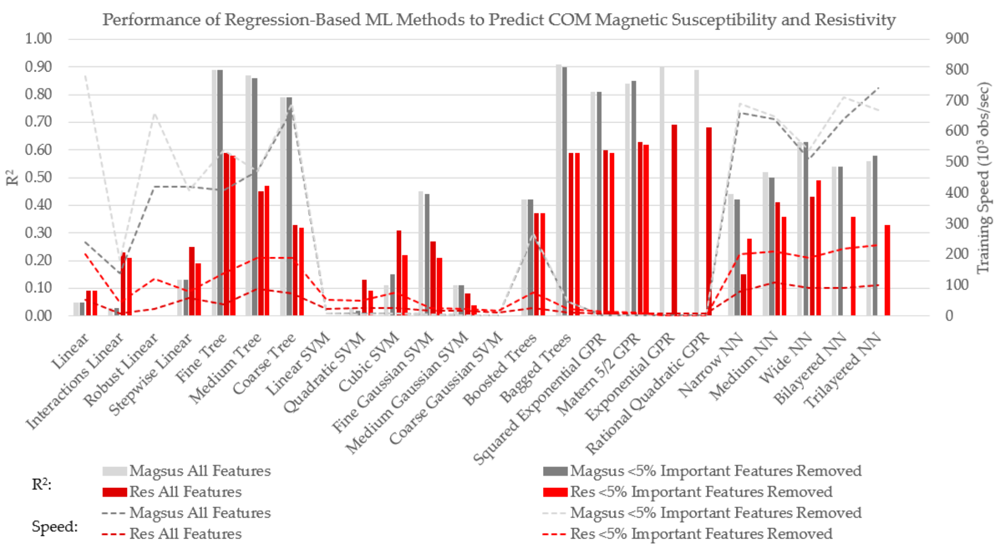

Figure 8. R^2 (columns) and training speeds (represented by lines) demonstrating performance of regression-based ML methods using *COM* MWD data to predict *magsus* and *res*.

3.2.3. Caliper Predictions

Table 11 displays the results of *cal* prediction using the LR, DT, SVM, RF, GP, and NN models. The *BR*, *MM*, and *COM* models all had relatively consistent R^2 and RMSE values. These results contrast with the differences between the *BR* and *MM* observed in the *dens*, *gamma*, *magsus*, and *res* results, indicating the need for an additional investigation to understand the differences between the *BR* and *MM* results.

Table 11. R^2 and RMSE results of regression-based ML models used to predict *cal* values from MWD data. Highest performing model results are in **bold**. All 20 MWD features were used in these models. Standard deviations (std) from 10-fold cross-validation are reported for RMSE and R^2.

Regression-Based ML Class	Regression-Based ML Suclass	*BR*		*MM*		*COM*	
		RMSE (cm)	R^2	RMSE (cm)	R^2	RMSE (cm)	R^2
LR	Linear	1.92	0.07	1.70	0.20	1.92	0.06
	Interactions	2.56	0.00	1.57	0.31	3.81	0.00
	Robust	2.00	0.00	1.75	0.15	1.99	0.00
	Stepwise	**1.85**	**0.14**	**1.40**	**0.45**	**1.84**	**0.14**
DTs	**Fine**	**0.76**	**0.85**	**0.71**	**0.86**	**0.76**	**0.85**
	Medium	0.79	0.84	0.81	0.82	0.80	0.84
	Coarse	0.93	0.78	1.03	0.70	0.94	0.78
SVMs	Linear	1.98	0.01	1.76	0.14	1.97	0.01
	Quadratic	1.82	0.17	1.34	0.50	1.85	0.13
	Cubic	1.47	0.46	0.97	0.74	1.91	0.07
	Fine Gaussian	**1.08**	**0.71**	**0.70**	**0.86**	**1.12**	**0.68**
	Medium Gaussian	1.58	0.37	1.19	0.61	1.70	0.26
	Coarse Gaussian	1.94	0.05	1.67	0.22	1.94	0.05
RFs	Boosted	1.77	0.21	1.34	0.50	1.79	0.19
	Bagged	**0.71**	**0.87**	**0.62**	**0.89**	**0.70**	**0.87**
GPs	Squared Exponential	0.85	0.82	0.63	0.89	0.83	0.82
	Matern 5/2	0.83	0.83	0.61	0.90	0.81	0.83
	Exponential	**0.71**	**0.87**	**0.53**	**0.92**	**0.70**	**0.88**
	Rational Quadratic	0.75	0.86	0.58	0.91	0.75	0.86
NNs	Narrow	1.67	0.30	1.15	0.63	1.74	0.23
	Medium	1.47	0.45	0.91	0.77	1.57	0.37
	Wide	**1.09**	**0.70**	**0.68**	**0.87**	**1.21**	**0.63**
	Bilayered	1.57	0.37	1.03	0.70	1.64	0.32
	Trilayered	1.50	0.43	1.02	0.71	1.58	0.37

Examining the predictive performance of these models reveals that all variants of LR models, including Linear, Interactions, Robust, and Stepwise, consistently underperformed with R^2 values lower than 0.45. In contrast, models built with SVMs, RFs, GP, and NNs provided more accurate predictions, with maximum R^2 values of 0.86, 0.89, 0.92, and 0.87, respectively, and an average RMSE of approximately 0.63 cm.

Among these models, Bagged RFs and Wide NNs delivered the best predictive results within their respective ML classes, with RMSEs of 0.62 cm and 0.68 cm, respectively. On the *COM* dataset, DTs produced R^2 values of 0.76, 0.80, and 0.94 for the Coarse, Medium, and Fine parameters, respectively. SVMs displayed the most variable results based on the chosen method, with Fine Gaussian achieving an R^2 value of up to 0.86 and Linear, Cubic, and Coarse Gaussian yielding R^2 values below 0.50 and a 1.34 cm RMSE.

Experiments that excluded features with less than 5% (minor) importance had no appreciable impact on the *cal* prediction accuracy. Compared to the trials that included all

MWD features, as shown in Figure 9, this feature exclusion sped up the model training times. DTs and NNs emerged as the quickest training methods with around 600,000 observations per second, whereas GP computations were around 300× more time-consuming with around 2000 observations per second. The models utilizing Exponential GPR (for *BR* < 5% and *MM* < 5%) and Rational Quadratic GPR (for *BR* < 5%, *MM* < 5%, *COM* all, and *COM* < 5%) were discontinued after 24 h, and their results are therefore not presented.

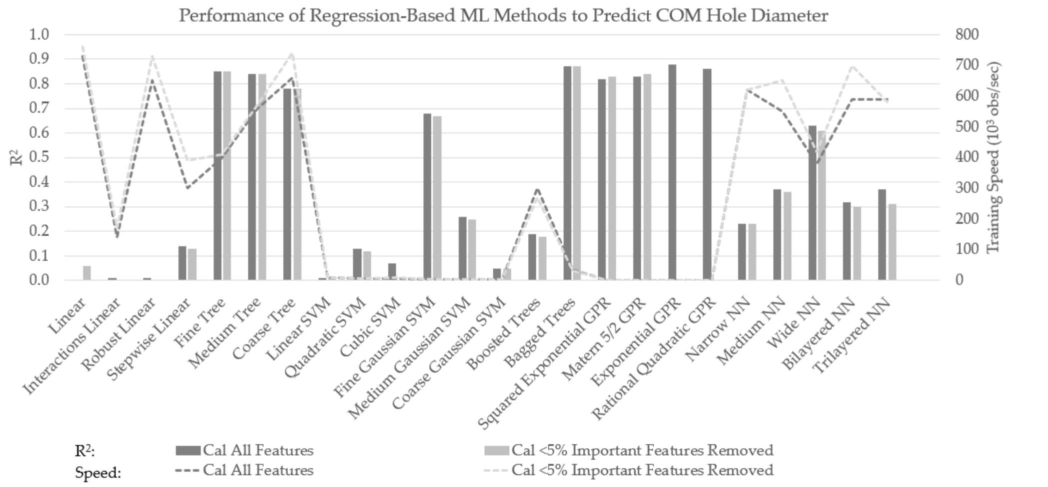

Figure 9. R^2 (columns) and training speeds (represented by lines) demonstrating performance of regression-based ML methods using *COM* MWD data to predict *cal*.

4. Discussion

This study demonstrates the effectiveness of feature-importance-based methods and regression-based ML techniques in estimating subterranean geophysical signatures from MWD data, thereby increasing orebody knowledge. Tables 4 and 5 reveal that the success of predictive modeling of the five investigated geophysical properties depends primarily on two factors: the characteristics of the on-site host rock, as represented by MWD data, and its distribution across various mining locations, as well as the quantity of data. While the absolute predictive accuracy of some models remains limited, this study provides crucial insights into which MWD variables contribute the most to predictive performance. These findings can guide future work in refining data preprocessing, feature selection, and hybrid modeling approaches that integrate geophysical constraints.

The impact of data volume (Table 1) is particularly significant, as greater amounts of MWD data improve the robustness and generalizability of regression-based ML models. Conversely, in scenarios with lower data availability or reduced data resolution, model performance may degrade, raising the question of whether alternative approaches might be more suitable. Future work should investigate the minimum viable amount of MWD data required for this approach to remain effective, particularly in settings where data sparsity is a constraint. Moreover, for parameters like resistivity, where intrinsic geological correlation with MWD features is weak, ML models struggled to achieve high predictive accuracy. This highlights the necessity of incorporating domain knowledge when interpreting ML outputs.

Though the scope of this study was confined to five geophysical properties, it has the potential to be extended to other measurements such as acoustic, neutron porosity, dip-meter, spontaneous potential, or nuclear magnetic resonance. This study departs from prior research by showing the importance of MWD ratio features, such as *fobrop*, *fobtor*, *bapfob*, *torrop*, *baprop*, and *baptor*, in addition to *fob*. Earlier research emphasized *rop* and *tor*, utilizing PCA to determine the most important MWD measurements for rock type identification [9,12,14,17,19,34]. In contrast with the PCA-based feature selection in MWD data, feature-importance-based ML methodologies, such as MARS and PPR, revealed previously unobserved complex relationships between MWD features and rock mass characteristics such as those derived from *bap*.

The differences in feature importance evaluations between MARS and PPR result from the underlying mechanics of these algorithms. The MARS technique evaluates the correlation between MWD features and geophysical signatures, therefore expanding the range of relevant MWD features (Table 4). On the other hand, PPR evaluates the influence of each feature on data projections and determined that half of the drilling features were not important (Table 5).

Moreover, when compared to their smaller equivalents, larger n-term MARS and PPR models did not offer a more robust depiction of correlations between MWD data and geophysical measurements [53]. The consistent performance of DTs and Bagged RFs, with R^2 prediction values exceeding 0.80 across most ML models, as shown in Tables 7–11, suggests that complex ML models may not always provide superior predictive capabilities. Furthermore, more complex models like SVMs struggle with non-scaled features and imbalanced datasets where one class of features dominates. In this case, the drill rig type and hole diameter may be two factors, as the larger rigs drilled more wider-diameter production holes than smaller rigs drilling narrower holes for wall control.

This study also examined regression-based ML model prediction performance when minor importance features were eliminated for approximating geophysical signatures. It was found that discarding MWD features of minor significance could increase the processing speed without significantly compromising prediction accuracy. The predictive performance of most models remained stable when less important features were omitted. Despite a slight decline in predictive performance, the accelerated training durations for larger datasets suggest that excluding less important features is advantageous.

In addition, the choice of the regression-based ML analytical model, whether GP, NNs, or RFs, had little effect on the ML prediction outcomes, indicating that the predictive accuracy was primarily dependent on the quality of the extracted features. This observation is consistent with the findings, which observed comparable prediction abilities among diverse ML models for rock types and geochemical assay results [8,18,31]. In particular, the prediction accuracy of geophysical measurement estimates for *dens*, *gamma*, *magsus*, *res*, and *cal* using DTs, SVMs, RFs, GPs, and NNs models in the *BR* dataset was much higher than in the *MM* or *COM* datasets. A great deal of these variances can be traced to differences in data volume between the two datasets. The differences in geological composition between the Brockman and Marra Mamba Formations may also account for the residual differences in predictive power between *BR* and *MM* studies.

5. Conclusions

This study introduced a method for evaluating subsurface geophysical characteristics by applying feature-importance-based methods and regression-based ML algorithms to MWD data. The ability of feature-importance-based methods to unveil the "black box" nature of ML methods enable greater interpretation and acceptance of these models. A framework was developed to assess the importance of MWD data features in estimating the geophysical properties of an orebody, including density, *gamma*, magnetic susceptibility, resistivity, and hole diameter. Through MARS and PPR feature importance analyses, MWD features were grouped based on their importance as negligible (0%), minor (<5%), or significant (>5%). Notably, several previously unrecognized MWD attributes, such as *fob*, and ratios derived from MWD features—*fobrop*, *fobtor*, *bapfob*, *torrop*, *baprop*, and *baptor*—were found to have significant importance in determining geophysical attributes. Future work will also be extended to the use of other feature importance algorithms, such as Shapley value regression, which are increasingly used as tools in variable importance analysis in other fields [54,55].

Considering the varying importance of MWD features, we compared the prediction performance of various regression-based ML analytical methodologies, omitting specific features at distinct levels, considering the varying importance of the MWD features. The results indicate that omitting MWD attributes classified as having zero to minor importance does not significantly diminish prediction accuracy. Therefore, the elimination of features with low importance can reduce computation time without compromising the accuracy of the ML model's estimates. In addition, empirical data revealed correlations as high as 0.91 between MWD attributes and orebody geophysical predictive values when RF was employed, validating the effectiveness of the proposed method.

Despite limitations in prediction accuracy, this study establishes a foundation for MWD-based geophysical modeling, demonstrating the feasibility of ML applications while identifying areas requiring further refinement. Future advancements in feature engineering and hybrid modeling approaches may enhance practical applicability. While this study highlights that ML provides powerful predictive capabilities, its utility is maximized when combined with geological expertise to validate and interpret results appropriately.

These findings have significant implications for the mining industry. By utilizing these models, mining professionals can estimate precise and reliable short-term ore and waste tonnages. This predictive comprehension of orebody geophysical characteristics is crucial for mining operations as it guides extraction and processing decisions. The high-resolution geological data derived from these models enable the recovery of high-grade ore containing economically valuable minerals. Through the high-resolution orebody representation afforded by the methodologies outlined in this study, mining geologists could better distinguish between high-grade, low-grade, and waste components. As a result, mining engineers can develop optimal excavation strategies that minimize the amount of waste material incorporated into processing facilities.

Author Contributions: Conceptualization, D.G.; methodology, D.G.; software, D.G.; validation, D.G.; formal analysis, D.G.; investigation, D.G.; resources, D.G.; data curation, D.G.; writing—original draft preparation, D.G.; writing—review and editing, D.G., C.A., Q.S. and L.O.; visualization, D.G.; supervision, C.A., Q.S. and L.O.; project administration, D.G. All authors have read and agreed to the published version of the manuscript.

Funding: This research received no external funding.

Data Availability Statement: The data used in this study is not publicly available due to confidentiality agreements with the organization that supplied it. Access to the data is restricted to comply with contractual obligations and proprietary considerations. As such, the dataset cannot be shared or disclosed.

Acknowledgments: One of the authors (D.G.) received support through the MRIWA Postgraduate Research Scholarship and the AusIMM Education Endowment Fund Postgraduate Scholarship during his doctoral studies at Curtin University. Furthermore, this research was enabled by the advanced computing resources provided by the Pawsey Supercomputing Research Centre in Perth, Australia.

Conflicts of Interest: The authors declare no conflicts of interest.

References

1. Silversides, K.; Melkumyan, A.; Wyman, D.; Hatherly, P. Automated Recognition of Stratigraphic Marker Shales from Geophysical Logs in Iron Ore Deposits. *Comput. Geosci.* **2015**, *77*, 118–125. [CrossRef]
2. Wedge, D.; Hartley, O.; McMickan, A.; Green, T.; Holden, E.J. Machine Learning Assisted Geological Interpretation of Drillhole Data: Examples from the Pilbara Region, Western Australia. *Ore Geol. Rev.* **2019**, *114*, 103118. [CrossRef]

3. Barr, M.V. Instrumented Horizontal Drilling for Tunnelling Site Investigation. Ph.D. Thesis, University of London, Imperial College of Science and Technology, London, UK, 1984.
4. Hatherly, P.; Leung, R.; Scheding, S.; Robinson, D. Drill Monitoring Results Reveal Geological Conditions in Blasthole Drilling. *Int. J. Rock Mech. Min. Sci.* **2015**, *78*, 144–154. [CrossRef]
5. Khorzoughi, M.B. Use of Measurement While Drilling Techniques for Improved Rock Mass Characterization in Open-Pit Mines. Master's Thesis, University of British Columbia, Vancouver, BC, Canada, 2011.
6. Navarro, J.; Sanchidrian, J.A.; Segarra, P.; Castedo, R.; Paredes, C.; Lopez, L.M. On the Mutual Relations of Drill Monitoring Variables and the Drill Control System in Tunneling Operations. *Tunn. Undergr. Space Technol.* **2018**, *72*, 294–304. [CrossRef]
7. van Eldert, J.; Schunnesson, H.; Johansson, D.; Saiang, D. Application of Measurement While Drilling Technology to Predict Rock Mass Quality and Rock Support for Tunnelling. *Rock Mech. Rock Eng.* **2020**, *53*, 1349–1358. [CrossRef]
8. Kadkhodaie-Ilkhchi, A.; Monteiro, S.T.; Ramos, F.; Hatherly, P. Rock Recognition from MWD Data: A Comparative Study of Boosting, Neural Networks, and Fuzzy Logic. *IEEE Geosci. Remote Sens. Lett.* **2010**, *7*, 680–684. [CrossRef]
9. Galende-Hernández, M.; Menéndez, M.; Fuente, M.J.; Sainz-Palmero, G.I. Monitor-While-Drilling-Based Estimation of Rock Mass Rating with Computational Intelligence: The Case of Tunnel Excavation Front. *Autom. Constr.* **2018**, *93*, 325–338. [CrossRef]
10. Klyuchnikov, N.; Zaytsev, A.; Gruzdev, A.; Ovchinnikov, G.; Antipova, K.; Ismailova, L.; Muravleva, E.; Burnaev, E.; Semenikhin, A.; Cherepanov, A.; et al. Data-Driven Model for the Identification of the Rock Type at a Drilling Bit. *J. Pet. Sci. Eng.* **2019**, *178*, 506–516. [CrossRef]
11. Peck, J.P. Performance Monitoring of Rotary Blasthole Drills. Ph.D. Thesis, McGill University, Montreal, QC, Canada, 1989.
12. Scoble, M.J.; Peck, J.; Hendricks, C. Correlation between Rotary Drill Performance Parameters and Borehole Geophysical Logging. *Min. Sci. Technol.* **1989**, *8*, 301–312. [CrossRef]
13. Segui, J.B.; Higgins, M. *Blast Design Using Measurement While Drilling Parameters*; Fragblast: Hunter Valley, NSW, Australia, 2001; pp. 28–31.
14. Navarro, J.; Seidl, T.; Hartlieb, P.; Sanchidrián, J.A.; Segarra, P.; Couceiro, P.; Schimek, P.; Godoy, C. Blastability and Ore Grade Assessment from Drill Monitoring for Open Pit Applications. *Rock Mech. Rock Eng.* **2021**, *54*, 3209–3228. [CrossRef]
15. Akyildiz, O.; Basarir, H.; Vezhapparambu, V.S.; Ellefmo, S. MWD Data-Based Marble Quality Class Prediction Models Using ML Algorithms. *Math. Geosci.* **2023**, *55*, 1059–1074. [CrossRef]
16. Basarir, H.; Wesseloo, J.; Karrech, A.; Pasternak, E.; Dyskin, A. The Use of Soft Computing Methods for the Prediction of Rock Properties Based on Measurement While Drilling Data. In Proceedings of the Eighth International Conference on Deep and High Stress Mining, Perth, WA, Canada, 16–18 November 2017; pp. 537–551. [CrossRef]
17. Beattie, N. Monitoring-While-Drilling for Open-Pit Mining in a Hard Rock Environment. Master's Thesis, Queen's University, Kingston, ON, Canada, 2009.
18. Khushaba, R.N.; Melkumyan, A.; Hill, A.J. A Machine Learning Approach for Material Type Logging and Chemical Assaying from Autonomous Measure-While-Drilling (MWD) Data. *Math. Geosci.* **2021**, *54*, 285–315. [CrossRef]
19. Martin, J. Application of Pattern Recognition Techniques to Monitoring-While-Drilling on a Rotary Electric Blasthole Drill at an Open-Pit Coal Mine. Master's Thesis, Queen's University, Kingston, ON, Canada, 2007.
20. Silversides, K.L.; Melkumyan, A. Multivariate Gaussian Process for Distinguishing Geological Units Using Measure While Drilling Data. In *Minig Goes Digitial*; Taylor & Francis Group: London, UK, 2019; pp. 94–100.
21. Silversides, K.L.; Melkumyan, A. Boundary Identification and Surface Updates Using MWD. *Math. Geosci.* **2020**, *53*, 1047–1071. [CrossRef]
22. Schunnesson, H. Drill Process Monitoring in Percussive Drilling: A Multivariate Approach for Data Analysis. Licentiate Thesis, Lulea University of Technology, Lulea, Sweden, 1990.
23. Wold, S.; Esbensen, K.; Geladi, P. Principal Component Analysis. *Chemom. Intell. Lab. Syst.* **1987**, *2*, 37–52. [CrossRef]
24. Goldstein, D.M.; Aldrich, C.; O'Connor, L. A Review of Orebody Knowledge Enhancement Using Machine Learning on Open-Pit Mine Measure-While-Drilling Data. *Mach. Learn. Knowl. Extr.* **2024**, *6*, 1343–1360. [CrossRef]
25. Ker, P. Iron Ore Supply Slump as Rio Runs Late on New Mines. Available online: https://www.afr.com/companies/mining/rio-tinto-iron-ore-takes-300m-inflation-hit-20210716-p58a8l (accessed on 15 January 2025).
26. De-Vitry, C.; Vann, J.; Arvidson, H. Multivariate Iron Ore Deposit Resource Estimation—A Practitioner's Guide to Selecting Methods. *Trans. Inst. Min. Metall. Sect. B* **2010**, *119*, 154–165. [CrossRef]
27. Jones, H.; Walraven, F.; Knott, G.G. Natural gamma logging as an aid to iron ore exploration in the Pilbara region of Western Australia. In Proceedings of the Australasian Institute of Mining and Metallurgy Annual Conference, Perth, Australia, 24–25 May 2023; pp. 53–60.
28. Tittman, J.; Wahl, J.S. The Physical Foundations of Formation Density Logging (Gamma-Gamma). *Geophysics* **1965**, *30*, 284–294. [CrossRef]
29. Yang, Q.; Tan, M.; Zhang, F.; Bai, Z. Wireline Logs Constraint Borehole-to-Surface Resistivity Inversion Method and Water Injection Monitoring Analysis. *Pure Appl. Geophys.* **2021**, *178*, 939–957. [CrossRef]

30. Elsayed, M.; Isah, A.; Hiba, M.; Hassan, A.; Al-Garadi, K.; Mahmoud, M.; El-Husseiny, A.; Radwan, A.E. A Review on the Applications of Nuclear Magnetic Resonance (NMR) in the Oil and Gas Industry: Laboratory and Field-Scale Measurements. *J. Pet. Explor. Prod. Technol.* **2022**, *12*, 2747–2784. [CrossRef]
31. Goldstein, D.; Aldrich, C.; O'Connor, L. Enhancing Orebody Knowledge Using Measure-While-Drilling Data: A Machine Learning Approach. *IFAC-PapersOnLine* **2024**, *58*, 72–76. [CrossRef]
32. Khorzoughi, B.M.; Hall, R. Processing of Measurement While Drilling Data for Rock Mass Characterization. *Int. J. Min. Sci. Technol.* **2016**, *26*, 989–994. [CrossRef]
33. van Eldert, J.; Schunnesson, H.; Saiang, D.; Funehag, J. Improved Filtering and Normalizing of Measurement-While-Drilling (MWD) Data in Tunnel Excavation. *Tunn. Undergr. Space Technol.* **2020**, *103*, 103467. [CrossRef]
34. Ghosh, R.; Gustafson, A.; Schunnesson, H. Development of a Geological Model for Chargeability Assessment of Borehole Using Drill Monitoring Technique. *Int. J. Rock Mech. Min. Sci.* **2018**, *109*, 9–18. [CrossRef]
35. Friedman, J.H. Multivariate Adaptive Regression Splines. *Ann. Stat.* **1991**, *19*, 1–67. [CrossRef]
36. Shao, Q.; Traylen, A.; Zhang, L. Nonparametric Method for Estimating the Effects of Climatic and Catchment Characteristics on Mean Annual Evapotranspiration: Nonparametric Method for Mean Annual Evapotranspiration. *Water Resour. Res.* **2012**, *48*, 1–13. [CrossRef]
37. Kaveh, A.; Hamze-Ziabari, S.M.; Bakhshpoori, T. Estimating Drying Shrinkage of Concrete Using a Multivariate Adaptive Regression Spline Approach. *Int. J. Optim. Civ. Eng.* **2018**, *8*, 181–194.
38. Menon, R.; Bhat, G.; Saade, G.R.; Spratt, H. Multivariate Adaptive Regression Splines Analysis to Predict Biomarkers of Spontaneous Preterm Birth. *Acta Obstet. Gynecol. Scand.* **2014**, *93*, 382–391. [CrossRef]
39. *Earth: Multivariate Adaptive Regression Splines*, version 5.3.4; Stephen Milborrow: Cape Town, South Africa, 2023.
40. Friedman, J.H.; Stuetzle, W. Projection Pursuit Regression. *J. Am. Stat. Assoc.* **1981**, *76*, 817–823. [CrossRef]
41. Sepulveda, E.; Dowd, P.A.; Xu, C.; Addo, E. Multivariate Modelling of Geometallurgical Variables by Projection Pursuit. *Math. Geosci.* **2017**, *49*, 121–143. [CrossRef]
42. Yu, X.; Liu, B.; Lai, Y. Monthly Pork Price Prediction Applying Projection Pursuit Regression: Modeling, Empirical Research, Comparison, and Sustainability Implications. *Sustainability* **2024**, *16*, 1466. [CrossRef]
43. Du, H.; Wang, J.; Zhang, X.; Yao, X.; Hu, Z. Prediction of Retention Times of Peptides in RPLC by Using Radial Basis Function Neural Networks and Projection Pursuit Regression. *Chemom. Intell. Lab. Syst.* **2008**, *92*, 92–99. [CrossRef]
44. R Core Team. *R Stats Package*; R Foundation for Statistical Computing: Indianapolis, IN, USA, 2022.
45. Su, X.; Yan, X.; Tsai, C.-L. Linear Regression. *WIREs Comput. Stat.* **2012**, *4*, 275–294. [CrossRef]
46. Kotsiantis, S.B. Decision Trees: A Recent Overview. *Artif. Intell. Rev.* **2013**, *39*, 261–283. [CrossRef]
47. Hearst, M.A.; Dumais, S.T.; Osuna, E.; Platt, J.; Scholkopf, B. Support Vector Machines. *IEEE Intell. Syst. Their Appl.* **1998**, *13*, 18–28. [CrossRef]
48. Breiman, L. Random Forests. *Mach. Learn.* **2001**, *45*, 5–32. [CrossRef]
49. Schulz, E.; Speekenbrink, M.; Krause, A. A Tutorial on Gaussian Process Regression: Modelling, Exploring, and Exploiting Functions. *J. Math. Psychol.* **2018**, *85*, 1–16. [CrossRef]
50. Bishop, C.M. Neural Networks and Their Applications. *Rev. Sci. Instrum.* **1993**, *65*, 1803–1832. [CrossRef]
51. *Regression Learner Toolbox*; The MathWorks Inc.: Natick, MA, USA, 2024.
52. Ghosh, R.; Schunnesson, H.; Kumar, U. Evaluation of Rock Mass Characteristics Using Measurement While Drilling in Boliden Minerals Aitik Copper Mine, Sweden. In *Mine Planning and Equipment Selection*; Drebenstedt, C., Singhal, R., Eds.; Springer International Publishing: Cham, Switzerland, 2014; pp. 81–91. ISBN 978-3-319-02677-0.
53. Roe, K.D.; Jawa, V.; Zhang, X.; Chute, C.G.; Epstein, J.A.; Matelsky, J.; Shpitser, I.; Taylor, C.O. Feature Engineering with Clinical Expert Knowledge: A Case Study Assessment of Machine Learning Model Complexity and Performance. *PLoS ONE* **2020**, *15*, e0231300. [CrossRef]
54. Aldrich, C. Process Variable Importance Analysis by Use of Random Forests in a Shapley Regression Framework. *Minerals* **2020**, *10*, 420. [CrossRef]
55. Deng, S.; Aldrich, C.; Liu, X.; Zhang, F. Explainability in Reservoir Well-Logging Evaluation: Comparison of Variable Importance Analysis with Shapley Value Regression, SHAP and LIME. *IFAC-PapersOnLine* **2024**, *58*, 66–71. [CrossRef]

Chapter 7: Paper E

Enhancing Orebody Knowledge using Measure-While-Drilling Data: A Machine Learning Approach

Goldstein, D. M., Aldrich, C., & O'Connor, L. (2024). Enhancing Orebody Knowledge using Measure-While-Drilling Data: A Machine Learning Approach. *IFAC-PapersOnLine, 58(22)*, 72-76. https://doi.org/10.1016/j.ifacol.2024.09.293.

Available online at www.sciencedirect.com

ScienceDirect

IFAC PapersOnLine 58-22 (2024) 72–76

Enhancing Orebody Knowledge using Measure-While-Drilling Data: A Machine Learning Approach

D. Goldstein*, C. Aldrich**, L. O'Connor***

*Western Australian School of Mines: Minerals, Energy and Chemical Engineering, Curtin University, GPO Box U1987, Perth, WA 6845, Australia. (*e-mail: daniel.goldstein@postgraduate.curtin.edu.au; **e-mail: chris.aldrich@postgraduate.curtin.edu.au); ***email: louisa.oconnor@curtin.edu.au*

Abstract: Due to limited resource definition and grade control drilling, conventional bench-scale geochemical exploration is frequently plagued by uncertainty, resulting in diminished processing plant efficiencies. The Measure-While-Drilling (MWD) system comprises a set of sensors designed to gather data pertaining to the performance of mining blast hole drill rigs. Previous MWD research primarily relied on penetration rate to identify rock type and estimate grade. This investigation uses Data Fusion and Machine Learning (ML) algorithms to characterize geochemical orebody quality values, such as iron percentage, phosphorous, sulfur, alumina, and silica content, based on MWD data collected at the field-scale, thereby facilitating efficient mine planning and excavation. Feature importance algorithms identified novel significant MWD variables, such as force on bit and ratio of bit air pressure to penetration rate, which provide valuable insights into subsurface geochemical properties. The performance of various ML algorithms was compared, with the Random Forest algorithm demonstrating the highest coefficients of determination (up to 0.96), indicating accurate field or laboratory results prediction. As a result, this work demonstrates that MWD data can be used to obtain high-resolution orebody knowledge prior to mining, improving subsurface geochemistry prediction. This knowledge can optimize the excavation of high-grade material by minimizing dilution from lower-grade or waste rock entering the processing plant.

Keywords: Measurement-While-Drilling (MWD), Orebody knowledge, Open pit, Feature importance, Machine learning, Grade estimation

1. INTRODUCTION

The precise geochemical characterization of an orebody is critical for achieving mine production grade targets. However, traditional characterization methods necessitate intensive testing of drill hole cuttings, in which gaps between datapoints can be hundreds of meters (Sommerville et al., 2014). One technique that could resolve the geochemical uncertainty is MWD technology. It originated in the petroleum industry and was later adopted for open pit mining blast hole drilling systems in the 1970s, offers potential benefits (Barr, 1984). The technique outfits a blast hole drill rig with MWD sensors that collect continuous data and provide insight into subsurface penetration performance (Hatherly et al., 2015).

Artificial Intelligence (AI) methods have been used to understand the intricate, nonlinear relationships between drill responses and subsurface composition from the vast quantities of MWD data (Basarir et al., 2017; Beattie, 2009; Galende-Hernández et al., 2018; Kadkhodaie-Ilkhchi et al., 2010; Khorzoughi, 2011; Klyuchnikov et al., 2019; Martin, 2007; Navarro et al., 2021; Peck, 1989; Scoble et al., 1989; Segui and Higgins, 2001). Previous AI research using Machine Learning (ML) methods, has primarily focused on rock type detection to improve blast fragmentation, which does not adequately characterize geochemical conditions to optimize open pit orebody characterization. In contrast, only a few studies have used analytical methods on MWD responses to assess variations in subsurface geochemical conditions (Khushaba et al., 2021; Lahat et al., 2019; Schunnesson, 1990). Moreover, there were no studies using a suitable method to assess the individual importance of each MWD metric in predicting geochemical features.

This study evaluated orebody characteristics of mineralized deposits in a Pilbara open pit mine using MWD data sourced from an Australian iron ore mine. A novel method is introduced that determines the feature importance of MWD input metrics, aiding in the selection of critical features for predictive orebody and grade modelling. This study also incorporates a comparative analysis of the predictive performance of various ML algorithms. Sophisticated analytics, such as the assessment of feature importance and ML predictive modelling, might yield a more accurate portrayal of an orebody from MWD data, superseding the current precision offered by resource development scale Reverse Circulation (RC) and blast-hole chip assays for short-term grade-control models.

2. METHODS

2.1 Mine Site

The Pilbara region of Western Australia, recognized as Australia's primary source of exported iron ore, generated a substantial 874 million tons of iron ore in 2021 (Ker, 2021). The Brockman Formation deposit of the Hammersley Group Banded Iron Formation (BIF) was scrutinized in this study, esteemed as the most substantial sources of commercially

10.1016/j.ifacol.2024.09.293

viable Pilbara iron ore (De-Vitry et al., 2010). The Brockman Pit (BR) consisted of 211 RC holes, spanning a total depth of 16,880 meters and averaging 80 meters per hole. The resource development data acquired from the BR holes was derived from laboratory assays of RC rock chips, reported geochemical properties. These include aluminum oxide (Al_2O_3), calcium oxide (CaO), iron (Fe), total loss of ignition (LOI), magnesium oxide (MgO), manganese (Mn), phosphorus (P), sulfur (S), silica oxide (SiO_2), and titanium oxide (TiO_2) at 2-metre intervals. This resource development dataset has undergone the mining company's Quality Assurance and Quality Control (QA/QC) procedure, eliminating the need for further data engineering.

2.2 Orebody Qualities

This analysis considers several orebody qualities including Fe, P, S, Al_2O_3, and SiO_2. Fe stands as a key determinant of ore quality, regulating its classification into high-grade ore, low-grade ore, or waste rock. Meanwhile, Al_2O_3, P, S and SiO_2 are classified as impurities that could potentially disrupt the steelmaking process in a blast furnace. P and S are regarded as primary impurities, with S causing a reduction in steel's mechanical properties and resulting in red-shortness or brittleness when heated. P, on the other hand, escalates the metal's propensity to become cold-short, or brittle under low temperatures (Lu et al., 2013). Al_2O_3 and SiO_2 are identified as secondary impurities, their impact on steelmaking deemed less significant than phosphorus and sulfur. Laboratory assays of rock chips report these orebody qualities.

2.3 Drilling System

In this work, MWD data was collected using 22 rotary blast hole rigs that were equipped with tricone Tungsten Carbide Insert bits (Figure 1). Bench heights in the iron-ore pits studied ranged from 8 to 12 meters, with sub-drilling occurring approximately 2 meters below the bench floor. The burden and spacing between production blast holes was approximately 7 meters and 8 meters, respectively.

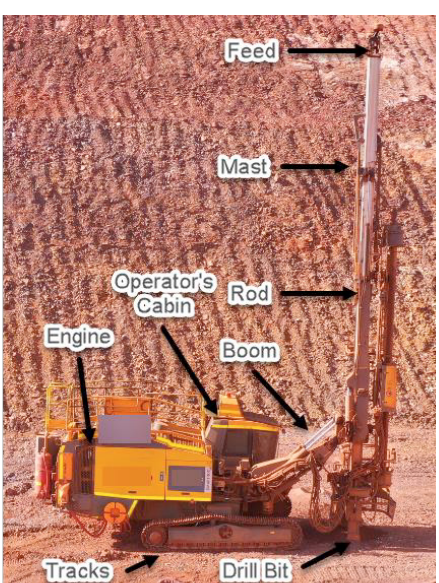

Figure 2. Typical layout of a surface mining blast drill rig (Type: Epiroc D65)

The drills were equipped with a MWD system, which facilitated the monitoring of several measurements including the rate of penetration, (rop; m/s), torque or rotary pressure (tor; Nm), force on bit (fob; kgf), also known as weight on bit, thrust or pulldown pressure, bit air pressure or flushing air medium (bap; kgf/cm), and rotary speed (rpm). Due to inconsistencies with the onboard sensor, rpm data was only available for about a quarter of the sample points, prompting the decision to remove rpm from the drilling variables. The time-series data from the MWD system was recorded by the drilling system. at intervals of approximately 0.1 meter along the blast hole depth.

The BR pit's MWD dataset included 75,470 blast holes spanning 844,855 meters. Because the initial two meters of the borehole are likely not representative of the rock's in-situ geochemical values due to potential impacts from the toe charge during the previous bench's blasting, MWD data analysis for this study spanned from 2 meters below the hole collars to the bottom of the blast holes. The resulting number of datapoints for Fe, P, S, Al_2O_3, and SiO_2 were 87385, 81583, 81583, 81583 and 87385, respectively.

2.3.1 MWD Data Preprocessing

Variations in subsurface composition, drill rig management system, and external influences affect the performance of MWD data, resulting in abnormally high and low response values (Khorzoughi and Hall, 2016). These variables can potentially lead to imprecision in MWD response values and erroneous interpretations of MWD data (van Eldert et al., 2020). As a result, the mining MWD dataset analyzed for the investigation exhibits a high noise-to-signal ratio.

Since the MWD data points had not been subjected to a thorough Quality Assurance and Quality Control (QA/QC) process, this research required feature engineering. Data within the first two meters of each blast drillhole were first removed from the original MWD data as it may not accurately represent the in-situ host rock due to collaring effects at the hole's beginning and potential blast damage from the previous bench's holes. Then, any data points with negative values for rop, tor, fob or bap were removed. The missing MWD data points were then reconstructed using linear interpolation, the quartile detection method, and a 1.5-factor threshold. Finally, to reduce the localized influence of noise, the blast hole data was smoothed using a Gaussian filter with a smoothing factor of 0.3.

A set of derived variables was calculated using rop, tor, fob and bap. These derived variables include ratios of the original variables (e.g., rop divided by tor, denoted as roptor) and a moving standard deviation across 0.5 meters for the initial values (e.g., the moving standard deviation for rop denoted as ropS).

2.4 Feature Importance

This study engaged purposeful feature importance methods to ascertain the relative significance of each MWD variable on the geochemical values of Fe, S, P, Al_2O_3, and SiO_2. Feature importance techniques, namely Multivariate Adaptive Regression Splines (MARS). MARS is a non-parametric algorithm that makes no assumptions regarding the relationships between input and output variables. The technique explicates intricate interactions among variables by implementing a series of piecewise linear regressions (Friedman, 1991). It identifies critical features by iteratively fitting the model with each feature included and excluded, assessing the performance variation.

2.5 ML Methods

This study evaluated the predictive capabilities of a variety of ML techniques, including Gaussian Support Vector Machines (SVMs), Bagged Random Forests (RFs), Exponential Gaussian Process Regression (GPR), Stepwise Linear Regression (LR), Fine Decision Trees (DTs), and Wide Neural Networks (NNs) to forecast the orebody geochemical values of Fe, S, P, Al_2O_3, and SiO_2 based on the MWD responses. The data was partitioned into 80% for training and 20% for testing, Models were trained using 10-fold cross validation. These computations were conducted on a Pawsey Supercomputer Nimbus cloud Ubuntu instance with 8 vCPUs and 32GB of Memory using MATLAB 2023b. The comparative evaluation of the models was conducted by utilizing the coefficient of determination (R^2) and Root Mean Square Error (RMSE).

3. RESULTS

3.1 Feature Importance

This section investigates the significance of various MWD response characteristics in predicting geochemical values (Fe, S, P, Al_2O_3, and SiO_2) to determine the influence of each MWD variable on geochemical characteristics. According to the highest importance results in Table 1, the six MWD metrics most important in predicting Fe from the studied BIF deposit are fob, baprop, baptor, fobrop, ropS and torS. Results vary from the feature importance of Al_2O_3, P, S and SiO_2 (Table 1).

Table 1. MARS derived feature importance (%) of MWD features in predicting geochemical assays.

	Fe	S	P	Al_2O_3	SiO_2
rop	2%	0%	16%	9%	2%
tor	0%	0%	0%	4%	8%
fob	9%	43%	0%	1%	3%
bap	6%	13%	5%	5%	0%
roptor	8%	13%	9%	8%	0%
ropbap	4%	0%	9%	6%	6%
ropfob	0%	0%	0%	0%	0%
torrop	4%	13%	8%	8%	11%
torbap	1%	0%	0%	0%	1%
torfob	7%	0%	9%	8%	9%
baprop	9%	9%	0%	5%	13%
baptor	9%	7%	0%	4%	8%
bapfob	0%	0%	0%	6%	0%
fobrop	9%	2%	8%	0%	10%
fobtor	0%	0%	8%	8%	0%
fobbap	0%	0%	0%	0%	0%
ropS	9%	0%	0%	7%	9%
torS	9%	0%	9%	7%	10%
fobS	5%	0%	12%	8%	7%
bapS	7%	0%	8%	6%	6%

In the case of Fe, the fobrop, baprop, torrop, baptor, and fobtor ratios were deemed more significant than the original rop and tor variables, the rop-influenced ratios roptor, ropbap, and ropfob, and additionally the variability-related metrics ropS, torS, bapS.

3.2 ML Analytical Prediction Results

This section evaluates the performance of various ML regression models in predicting orebody qualities such as Fe, P, S, Al_2O_3, and SiO_2 based on MWD data. Validation of the proposed ML analytical method utilizing a collection of geochemical variables to establish conceptual accuracy.

Figure 2a-f depicts the ML analytical prediction results compared to actual laboratory Fe values for the best-performing LR, DTs, SVMs, RFs, GP, and NNs models. The RFs model, with an R^2 value of 0.96 and an RMSE of 6.75% Fe, had the strongest correlation with the laboratory observations. The GP and DT models generated slightly weaker R^2 values of 0.93 and 0.90, and RMSE values of 7.77 and 6.75, respectively.

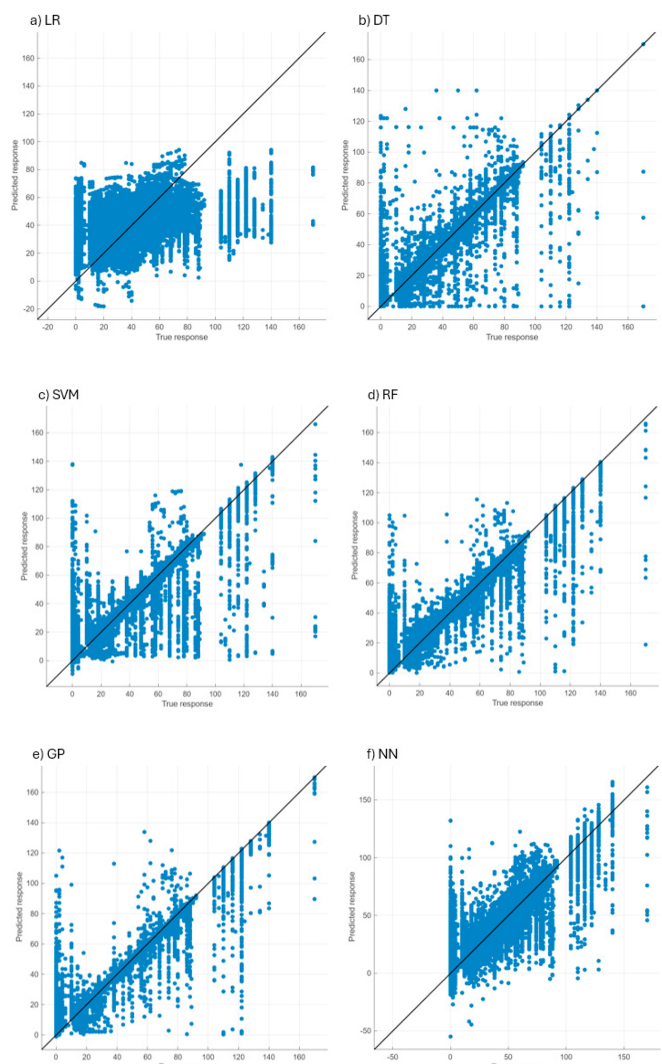

Figure 2. Actual versus predicted training values for %Fe predictions using various ML methods, including a) LR, b) DTs, c) SVMs, d) RFs, e) GP and f) NNs

Table 2 displays the results of Fe, P, S, Al_2O_3 and SiO_2 content prediction using LR, DTs, SVMs, RFs, GP, and NNs models. Among these models for Fe, DTs, RFs, and GPR delivered the best predictive results between the ML classes, with RMSEs of 7.15% Fe, 6.35% Fe and 6.79%, respectively.

Table 2. The 10-fold cross-validation training and testing R^2 and RMSE testing results of ML analyses for Fe, P, S, Al_2O_3 and SiO_2 content prediction in the BR dataset.

		LR	DT	SVM	RF	GPR	NN
Fe	RMSE (%)	29.4	10.2	15.3	9.38	8.08	16
	R^2 (train)	0.16	0.88	0.75	0.9	0.93	0.74
	R^2 (test)	0.15	0.9	0.77	0.91	0.94	0.75
P	RMSE (%)	16.8	6.06	8.64	5.63	4.49	8.97
	R^2 (train)	0.08	0.88	0.77	0.90	0.93	0.74
	R^2 (test)	0.06	0.88	0.75	0.90	0.93	0.73
S	RMSE (%)	0.42	0.11	0.40	0.13	0.2	0.34
	R^2 (train)	-0.01	0.84	0.08	0.82	0.63	0.37
	R^2 (test)	-0.01	0.93	0.07	0.90	0.61	0.36
Al_2O_3	RMSE (%)	11.9	4.28	6.30	4.02	3.50	6.99
	R^2 (train)	0.08	0.86	0.75	0.89	0.91	0.70
	R^2 (test)	0.09	0.88	0.75	0.90	0.92	0.69
SiO_2	RMSE (%)	32.3	10.1	16.0	9.31	7.68	17.0
	R^2 (train)	0.06	0.88	0.75	0.90	0.93	0.74
	R^2 (test)	0.06	0.91	0.77	0.92	0.95	0.74

Those models employing LR consistently produced the worst predictions for P and S, with R^2 values lower than 0.12 (Table 2). Models built with DTs, RFs, and GPR, on the other hand, produced the highest R^2 values of 0.97 and 0.98 for P and S predictions, respectively. These top-performing DTs, RFs, and GP models resulted in an average RMSE of approximately 3.07% for P and 0.18 % for S.

As shown in Table 2, LR models consistently underperformed in their ability to predict Al_2O_3 and SiO_2. RFs and GPR models had the highest R^2 values, exceeding 0.96. Conversely, SVMs and NNs had lower R^2 values (0.79 and 0.71, respectively).

4. DISCUSSION

This study demonstrates the capability of ML algorithms to predict subsurface geochemical variables from MWD data, thereby informing orebody geochemistry. Although this methodology was only applied to five quality indicators in this study, it has the potential to be extended to other variables such as CaO, LOI, MgO, Mn, and TiO_2. As suggested by Table 1, the accuracy of predictive modelling is primarily dependent on the features of the in-situ rock and the volume of MWD data.

In contrast to previous research, the derived ratio MWD variables fobrop, baprop, torrop, baptor, and fobtor, in addition to fob, demonstrated significant feature importance in this study. Prior studies (Beattie, 2009; Galende-Hernández et al., 2018; Ghosh et al., 2018; Martin, 2007; Navarro et al., 2021; Scoble et al., 1989) emphasized rop and tor using Principal Component Analysis (PCA) to identify the most important MWD measures for rock type identification. In comparison to this predominant PCA-based feature selection employed in MWD analysis, feature importance methods, such as MARS, exhibited intricate relationships between the MWD variables and orebody characteristics, such as those derived from bap, which had not been observed.

In addition, the choice of the ML analytical model, whether GP, NNs, or RFs, did not significantly influence the ML prediction results, indicating that the predictive accuracy was primarily determined by the quality of the extracted features. This result is consistent with the findings of Kadkhodaie-Ilkhchi et al. (2010) and Khushaba et al. (2021), who observed comparable prediction abilities among diverse ML models for rock types and geochemical assay results.

5. CONCLUSION

This study presents a proof-of-concept method for evaluating orebody quality by analyzing MWD data with ML algorithms. A framework was developed to determine the significance of MWD data features in predicting orebody quality indicators such as Fe, S, P, Al_2O_3, and SiO_2. The MARS feature importance analyses allowed MWD variables to be classified as having zero (0%), marginal (2%), or significant (>2%) importance. Importantly, several previously overlooked MWD features, such as fob, and derived ratios of MWD features—fobrop, baprop, torrop, baptor, and fobtor—were found to have substantial predictive value for estimating orebody quality. Because of the varying importance of MWD features, a comparison of prediction performance across various ML analytical techniques was conducted. In addition, empirical results demonstrated correlations as high as 0.97 between MWD characteristics and orebody quality values when using RF. The proposed methodology can also be applied to forecast geomechanical properties, which would improve blasting fragmentation and add value in crushing and milling.

These discoveries have far-reaching implications for the mining industry. Applying these models can allow miners to determine accurate and precise short-term geochemical estimations. Predictive knowledge of orebody geochemistry is crucial for mining, as it will inform decisions for extraction and processing phases. The availability of geochemical data produced from these models with high downhole resolution aids in the recovery of high-grade ore containing economically viable mineral content for extraction. Mining geologists can increase the granularity with which they differentiate high-grade, low-grade, and waste elements by leveraging the high-definition depiction of the orebody provided by the methodologies presented in this study. As a result, mining engineers can plan optimal excavations to minimize the dilution of waste material in a processing plant.

6. ACKNOWLEDGEMENTS

The author[1] received support through the Minerals Research Institute of Western Australia's Postgraduate Research Scholarship and the Australasian Institute of Mining and Metallurgy's Education Endowment Fund Postgraduate Scholarship during their doctoral studies at Curtin University. Furthermore, the research was enabled by the advanced computing resources provided by the Pawsey Supercomputing Research Centre.

REFERENCES

Barr, M.V. (1984). Instrumented Horizontal Drilling for Tunnelling Site Investigation (PhD). University of London, Imperial College Science and Technology

Basarir, H., Wesseloo, J., Karrech, A., Pasternak, E., Dyskin, A. (2017). The use of soft computing methods for the prediction of rock properties based on measurement while drilling data. Proceedings of the Eighth International Conference on Deep and High Stress Mining 537–551. https://doi.org/10.36487/acg_rep/1704_36_basarir

Beattie, N. (2009). Monitoring-While-drilling for Open-Pit Mining in a Hard Rock Environment (Master of Science). Queen's University, Kingston, Canada.

De-Vitry, C., Vann, J., Arvidson, H. (2010). Multivariate iron ore deposit resource estimation – a practitioner's guide to selecting methods. *Trans Inst Mining Metallurgy Sect B*. 119, 154–165.

Friedman, J.H. (1991). Multivariate Adaptive Regression Splines. *The Annals of Statistics* 19, 1–67.

Galende-Hernández, M., Menéndez, M., Fuente, M.J., Sainz-Palmero, G.I. (2018). Monitor-While-Drilling-based estimation of rock mass rating with computational intelligence: The case of tunnel excavation front. Automation in Construction 93, 325–338. https://doi.org/10.1016/j.autcon.2018.05.019

Ghosh, R., Gustafson, A., Schunnesson, H. (2018). Development of a geological model for chargeability assessment of borehole using drill monitoring technique. *International Journal of Rock Mechanics and Mining Sciences* 109, 9–18. https://doi.org/10.1016/j.ijrmms.2018.06.015

Hatherly, P., Leung, R., Scheding, S., Robinson, D. (2015). Drill monitoring results reveal geological conditions in blasthole drilling. *International Journal of Rock Mechanics and Mining Sciences* 78, 144–154. https://doi.org/10.1016/j.ijrmms.2015.05.006

Kadkhodaie-Ilkhchi, A., Monteiro, S.T., Ramos, F., Hatherly, P. (2010). Rock recognition from MWD Data: A comparative study of boosting, neural networks, and fuzzy logic. IEEE Geoscience and Remote Sensing Letters 7, 680–684. https://doi.org/10.1109/LGRS.2010.2046312

Ker, P. (2021). Iron ore supply slump as Rio runs late on new mines. Australian Financial Review.

Khorzoughi, B.M., Hall, R. (2016). Processing of measurement while drilling data for rock mass characterization. *International Journal of Mining Science and Technology* 26, 989–994. https://doi.org/10.1016/j.ijmst.2016.09.005

Khorzoughi, M.B. (2011). Use of Measurement While Drilling Techniques for Improved Rock Mass Characterization in Open-Pit Mines (MSc). University of British Columbia, Vancouver.

Khushaba, R.N., Melkumyan, A., Hill, A.J. (2021). A Machine Learning Approach for Material Type Logging and Chemical Assaying from Autonomous Measure-While-Drilling Data. *Math Geosci*. https://doi.org/10.1007/s11004-021-09970-w

Klyuchnikov, N., Zaytsev, A., Gruzdev, A., Ovchinnikov, G., Antipova, K., Ismailova, L., Muravleva, E., Burnaev, E., Semenikhin, A., Cherepanov, A., Koryabkin, V., Simon, I., Tsurgan, A., Krasnov, F., Koroteev, D. (2019). Data-driven model for the identification of the rock type at a drilling bit. *Journal of Petroleum Science and Engineering* 178. https://doi.org/10.1016/j.petrol.2019.03.041

Liaghat, S., Gustafson, A., Johansson, D., Schunnesson, H. (2019). Ore grade prediction using informative features of MWD data. Mining Goes Digital - Proceedings of the 39th international symposium on Application of Computers and Operations Research in the Mineral Industry, APCOM 2019 226–234. https://doi.org/10.1201/9780429320774-26

Lu, L., Devasahayam, S., Sahajwalla, V. (2013). Evaluation of coal for metallurgical applications, in: The Coal Handbook: Towards Cleaner Production.

Martin, J. (2007). Application of Pattern Recognition Techniques to Monitoring-While- Drilling on a Rotary Electric Blasthole Drill at an Open-Pit Coal Mine (MSc). Queen's University, Kingston, Canada.

Navarro, J., Seidl, T., Hartlieb, P., Sanchidrián, J.A., Segarra, P., Couceiro, P., Schimek, P., Godoy, C. (2021). Blastability and Ore Grade Assessment from Drill Monitoring for Open Pit Applications. *Rock Mech Rock Eng* 54, 3209–3228. https://doi.org/10.1007/s00603-020-02354-2

Peck, J.P. (1989). Performance Monitoring of Rotary Blasthole Drills 395.

Schunnesson, H. (1990). Drill Process Monitoring in Percussive Drilling: A Multivariate Approach for Data Analysis (Licentiate). Lulea University of Technology, Lulea, Sweden.

Scoble, M.J., Peck, J., Hendricks, C. (1989). Correlation between Rotary Drill Performance Parameters and Borehole *Geophysical Logging* 8, 301–312.

Segui, J.B., Higgins, M. (2001). Blast Design Using Measurement While Drilling Parameters. Presented at EXPLO 2001, Hunter Valley, NSW, pp. 28–31.

Sommerville, B., Boyle, C., Brajkovich, N., Savory, P., Latscha, A.-A. (2014). Mineral resource estimation of the Brockman 4 iron ore deposit in the Pilbara region. *Applied Earth Science* 123, 135–145. https://doi.org/10.1179/1743275814Y.0000000038

van Eldert, J., Schunnesson, H., Saiang, D., Funehag, J., (2020). Improved filtering and normalizing of Measurement-While-Drilling (MWD) data in tunnel excavation. *Tunnelling and Underground Space Technology* 103, 103467–103467. https://doi.org/10.1016/j.tust.2020.103467

Chapter 8: Discussion and Conclusion

8.1 Contributions

This research has applied a widely recognized generic ML workflow to the domain of MWD-based orebody characterization but with adaptations that address the unique challenges of mining data. While the sequential stages of data preparation, feature selection, model training, and validation are common to many ML applications, this work contributes a domain-specific implementation that accounts for the irregular and multi-resolution nature of geological datasets, the operational variability of drill rig sensors, and the need for geologically meaningful feature engineering from raw drilling signals.

In Paper B, Gaussian filtering was parameterised by iteratively selecting a smoothing window that reduced high-frequency drilling noise while preserving transitions associated with genuine rock property changes; the resulting kernel bandwidth of approximately 0.3-0.5 m produced stable outcomes across holes. Three-dimensional proximity was defined using a spatial tolerance consistent with local variogram ranges (typically 10-15 m), ensuring that MWD samples and reference labels were matched only where geological continuity was expected. Correlation analysis showed strong pairwise relationships among several MWD variables (e.g., rop/tor, wob/bap), reinforcing the need for feature-selection or importance techniques to prevent redundancy-driven model bias.

These adaptations include bespoke spatial alignment methods for high-frequency operational MWD readings with sparse geotechnical, geophysical, and geochemical reference data, integration of model-independent and model-derived feature importance methods to suit analysis before and after modelling and systematic evaluation of model performance across three domains using production-scale, operationally sourced datasets. The COM dataset refers to the combined dataset incorporating records from both pits to increase the representativeness and robustness of the geophysical modelling. Feature importance values for each geophysical property were computed independently and then synthesised in the discussion.

The contribution of this thesis lies in demonstrating how a standardized ML framework using can be operationalized for MWD data, identifying where generic methods suffice and where domain-specific treatment is required. This distinction provides both a replicable pipeline for other mining contexts and a benchmark for assessing the readiness of ML workflows using MWD data for deployment in production operations.

Theoretically, it advances the use of interpretable ML frameworks for feature importance and predictive modelling using production-scale mining data. Practically, it introduces a modular analytical workflow that can be deployed on existing MWD systems with minimal infrastructure overhead.

The following contributions have been made:

- A general, model-agnostic unified framework was developed to integrate MWD data with supervised ML algorithms across diverse output types and domains.
- Feature importance insights through identification and ranking of key MWD variables, which influenced subsurface predictions, aiding interpretability and improving trust in ML models.
- High-resolution subsurface modelling produced by the framework resulting in accurate prediction of rock strength, geological domains, gamma response and elemental composition at sub-meter resolution.
- Multivariate-based predictive models were validated across geotechnical, geophysical and geochemical properties using industry data, supporting the robustness of the approach.
- Publications in five peer-reviewed journal articles across Q1 and Q2 journals, advancing the academic literature on digital mining and ML applications.

Several methodological questions raised by the examiner relate to operational constraints embedded within the dataset.

- The definition of three-dimensional proximity reflects the maximum spatial separation at which exploration labels remain representative of the MWD interval, typically governed by local geological continuity.

- Gaussian filtering parameters were selected to smooth high-frequency sensor noise without distorting underlying drilling responses, following standard signal-processing practice.
- Correlations between MWD variables and target properties are driven by physical interactions between drilling mechanics and rock mass behaviour, and are therefore expected to vary between geotechnical, geophysical and geochemical domains.

Moreover, where feature importance results are presented for only one method in the published papers, this reflects either the most stable or most interpretable output for the domain under study. The thesis does not revise these published figures but provides additional narrative context here to clarify interpretation.

Taken together, the results across all papers demonstrate a consistent behavioural pattern of the dominant MWD predictors (rop, tor, wob, bap) retaining predictive relevance across geotechnical, geophysical and geochemical domains, although their relative importance shifts with the underlying physics of each target property. This convergence indicates that the drilling system encodes a common mechanical response to subsurface conditions that generalises across domains. At the same time, domain-specific divergences, such as higher sensitivity of geochemical predictions to bap/rop ratios, highlight the value of combining general-purpose MWD signals with targeted feature-engineering. This cross-domain consistency supports the validity and scalability of the unified analytical framework developed in this thesis.

8.2 Limitations

Despite the strong predictive performance and practical potential of the framework, several limitations were identified during this research. One key constraint is the specificity of the dataset. All modelling and validation were performed using data from a single iron ore deposit in the Pilbara region, which may limit the generalizability of the results. Applying the framework to different geological settings or commodities, such as copper, gold or coal would likely require retraining the models and adapting to new lithological and geomechanical conditions.

Another limitation stems from sensor variability. MWD tools across different drill rigs can vary in calibration, resolution and data quality. These inconsistencies can introduce systematic bias or noise into the input data, potentially degrading model performance when transferred across rigs or operations. Ensuring standardization in sensor configuration and calibration would be necessary for broader deployment.

Furthermore, model performance across all studies was influenced by several practical limitations. MWD data exhibit variability due to rig-specific behaviour, bit condition, and transient drilling states, introducing noise that cannot be fully removed. The exploration datasets used as labels, particularly laboratory geochemical assays and UCS measurements, are spatially sparse relative to MWD density, constraining generalisation in regions with limited reference data. Data confidentiality also restricts the ability to release open-source datasets that would otherwise promote benchmarking and reproducibility. These constraints are typical of operational mining environments and must be considered when deploying predictive systems.

Additionally, the availability of ground-truth reference data remains a challenge. Geotechnical parameters such as UCS and laboratory-based geochemical assays are typically collected at sparse intervals. This limits the density and spatial resolution of supervised labels available for training and evaluation, potentially affecting model reliability in heterogeneous zones.

Finally, operational constraints must be considered for real-time implementation. While the models developed here are suitable for post-processing and batch analysis, deploying them in real-time settings would require optimization for computational efficiency. This includes streamlining data ingestion, reducing model complexity and adapting inference to edge computing environments typically found on or near drill rigs.

8.3 Future Work

The findings and limitations of this study point to several opportunities for future research. These areas build on the foundation of real-time, data-driven subsurface modelling and seek to extend it across geological settings, modelling techniques, deployment architectures and integrated mine planning systems.

8.3.1 Expansion to Different Geological Settings and Commodities

An important area for future extension is the adaptability of this framework across geological contexts, as outlined below.

- Apply the framework to different deposit types, such as porphyry copper, hard rock gold and stratified sedimentary basins, to assess its adaptability and generalizability beyond the single iron-ore operation in the Pilbara used in this thesis
- Evaluate the impact of varying lithology, mineralogy and structural complexity, such as complex faulted terrains or high alteration zones on the relationship between MWD responses and subsurface properties.
- Retrain or fine-tune models where geological conditions introduce nonlinear or discontinuous behaviors in MWD data.

8.3.2 Exploration of Deep Learning Techniques

Beyond the classical ML approaches trialed in this thesis, there is significant scope to investigate Deep Learning (DL) methods tailored to the unique properties of MWD data. Convolutional Neural Networks (CNNs) could be applied to spectrograms or other time-frequency representations of drilling signals (e.g., torque, vibration, air pressure) to capture localized patterns indicative of lithological changes (Zhao et al., 2023). Recurrent Neural Networks (RNNs), particularly Long Short-Term Memory (LSTM) architectures, are well suited to sequential MWD datasets, allowing the model to learn temporal dependencies in drilling behavior and material transitions along the borehole (Cheng et al., 2023). Transformer-based architectures, with their self-attention mechanisms, offer potential advantages over RNNs for modelling longer drilling sequences and integrating multi-rig datasets, as demonstrated in analogous applications in directional drilling and well-logging (Romanenkova et al., 2020).

Future work should also explore hybrid models that integrate domain knowledge into DL workflows, such as physics-informed neural networks or architectures constrained by known drilling mechanics. This could improve generalization across deposits while retaining geological plausibility in predictions. Furthermore, applying advanced explainability techniques, such as Gradient-weighted Class Activation Mapping (Grad-CAM), could enhance trust in DL models by highlighting the drilling intervals or sensor patterns that drive predictions (Selvaraju et al., 2017). These interpretability methods have shown promise in geoscientific modelling contexts and could help address industry concerns over “black box” AI adoption (Herwig & Borghesani, 2023).

In addition to data-driven architectures, physics-informed neural networks and hybrid models constrained by known drilling mechanics represent a promising direction. Embedding physical principles into model structure may reduce overfitting, improve interpretability and enhance generalisation across rigs, lithologies and operating conditions.

Combining these DL methods with rigorous benchmarking against the best-performing classical ML models from this study would provide a robust assessment of whether the increased complexity of deep learning architectures delivers a commensurate operational benefit.

8.3.3 Real-Time Deployment and Automation

Operationalizing this framework in real-time environments introduces several technical challenges. These include data latency, edge inference limitations and integration with existing drill rig infrastructure.

- Develop lightweight model architectures optimized for real-time inference on edge devices deployed at the drill rig.
- Integrate MWD-based predictions into drilling control systems or onboard monitoring platforms.
- Automate data ingestion, preprocessing and result delivery workflows for seamless integration with autonomous or semi-autonomous drilling operations.
- Pilot real-time prediction systems in production environments to evaluate feedback latency, decision impact and operational reliability.

8.3.4 Integration with Digital Twin and Mine-to-Mill Optimization

Future implementations may benefit from integration with digital twin environments and dynamic mine-to-mill optimization platforms.

- Incorporate MWD-based predictions of rock properties into digital twin models to simulate drilling, blasting, fragmentation and downstream processing.

- Enable real-time updating of short-term schedules and blast designs based on predicted lithology and strength profiles.
- Interface with fleet management and shovel allocation systems to adjust dig strategies in response to changing ground conditions.
- Support adaptive mine-to-mill optimization by providing continuous, drill-aligned data streams on ore quality and rock behavior.

8.3.5 Bit Wear Effect

An important avenue for future research is the systematic study of drill-bit wear and its influence on MWD responses. Bit degradation alters drilling mechanics and can confound both feature-importance rankings and predictive performance. A controlled field study integrating bit-wear metrics with MWD signals would provide valuable insights and improve robustness of MWD-based predictive models.

8.4 Conclusion

The contributions presented in this thesis (Section 8.1) establish a foundation for real-time, MWD-based subsurface characterization using interpretable machine learning. When considered alongside the future research opportunities (Section 8.3), they illustrate a pathway toward digital orebody intelligence that is robust, scalable and integrated across the mining value chain. Continued research into model generalization, automation and deep learning integration will further strengthen the operational viability and strategic impact of this approach.

This thesis has demonstrated that MWD data, when analyzed using ML, can improve orebody characterization and mine planning. By addressing key research gaps in feature importance, geotechnical, geophysical and geochemical prediction, this study provides a scalable and cost-effective enhancement to traditional resource-definition drilling. The findings hold significant implications for academic research and mining industry practice, contributing to AI-enhanced subsurface modeling, digital mine planning and real-time decision-making. While challenges remain in data integration, model deployment and industry adoption, this research paves the way for the next generation of AI-driven geotechnical and geochemical analysis in mining. Future research should focus on expanding the AI framework to different commodities, testing real-time deployment strategies and integrating AI-driven MWD analysis into autonomous mining systems. Through continued innovation, AI-enhanced MWD models have the potential to transform the way orebody knowledge is acquired, interpreted and applied in modern mining operations.

Taken together, the five studies demonstrate that MWD data, when analysed using interpretable ML methods, can serve as a unified, multi-domain surrogate for traditional subsurface characterization techniques. The collective findings establish a coherent framework that links geotechnical, geophysical and geochemical prediction, providing a scalable pathway toward real-time orebody intelligence in open-pit mining operations.

References

Ahsan, N., Scheding, S., Monteiro, S. T., Leung, R., McHugh, C., & Robinson, D. (2015). Adaptive sampling applied to blast-hole drilling in surface mining. *International Journal of Rock Mechanics and Mining Sciences*, *75*, 244-255. https://doi.org/10.1016/j.ijrmms.2015.01.009

Akyildiz, O., Basarir, H., Vezhapparambu, V. S., & Ellefmo, S. (2023). MWD Data-Based Marble Quality Class Prediction Models Using ML Algorithms. *Mathematical Geosciences*. https://doi.org/10.1007/s11004-023-10061-1

Aldrich, C. (2020). Process Variable Importance Analysis by Use of Random Forests in a Shapley Regression Framework. *Minerals*, *10*(5), 420. https://doi.org/10.3390/min10050420

Barr, M. V. (1984). *Instrumented Horizontal Drilling for Tunnelling Site Investigation* [PhD]. University of London.

Barr, M. V., & Brown, E. T. (1983). A Site Exploration Trial using Instrumented Horizontal Drilling. *Essai de Forage Instrumente Pour La Reconnaissance de Terrain Versuchsbohrung Am Ort Mit Hilfe Yon Einem Mit Messgeraten Versehenen Horizontalbohrer*, 51-58.

Barton, N., Lien, R., & Lunde, J. (1974). Engineering classification of rock masses for the design of tunnel support. *Rock Mechanics*, *6*, 189-236.

Basarir, H., & Karpuz, C. (2016). Preliminary estimation of rock mass strength using diamond bit drilling operational parameters. *International Journal of Mining, Reclamation and Environment*, *30*(2), 145-164. https://doi.org/10.1080/17480930.2015.1025561

Basarir, H., Wesseloo, J., Karrech, A., Pasternak, E., & Dyskin, A. (2017). The use of soft computing methods for the prediction of rock properties based on measurement while drilling data. *Proceedings of the Eighth International Conference on Deep and High Stress Mining*, *Vynne 1997*, 537-551. https://doi.org/10.36487/acg_rep/1704_36_basarir

Beattie, N. (2009). *Monitoring-While-drilling for Open-Pit Mining in a Hard Rock Environment* [Master of Science]. Queen’s University.

Bieniawski, Z. T. (1989). Geomechanics Classification (Rock Mass Rating System). In *Engineering rock mass classifications: A complete manual for engineers and geologists in mining, civil, and petroleum engineering*. Wiley-Interscience.

Bishop, C. M. (1993). Neural networks and their applications. *Review of Scientific Instruments*, *65*.

Breiman, L. (2001). Random Forests. *Machine Learning*, *45*, 5-32.

Breiman, L., Friedman, J., Olshen, R., & Stone, C. (1984). *Classification and Regression Trees*. Wadsworth and Brooks/Cole Monterey, CA, USA.

Brown, E. (1981). *Rock Characterization, Testing and Monitoring: ISRM Suggested Methods*. Pergamon Press.

Brown, E. T., & Barr, M. V. (1978). Instrumented Drilling as an Aid to Site Investigations. *Proceedings of the 3rd International Congress of the International Association of Engineering Geology*, 21-28.

Cheng, X., Tang, H., Wu, Z., Liang, D., & Xie, Y. (2023). BILSTM-Based Deep Neural Network for Rock-Mass Classification Prediction Using Depth-Sequence MWD Data: A Case Study of a Tunnel in Yunnan, China. *Applied Sciences*, *13*(10), 6050. https://doi.org/10.3390/app13106050

Classification Learner Toolbox (Version 24.1.0 (R2024a)). (2024). The MathWorks Inc. http://www.mathworks.com

Cortes, C., & Vapnik, V. (1995). Support-vector networks. *Machine Learning*, *20*, 273-297.

Costamagna, E., Oggeri, C., & Vinai, R. (2021). Damage and contour quality in rock excavations for quarrying and tunnelling: Assessment for properties and solutions for stability. *IOP Conf. Ser.: Earth Environ. Sci.* 833 012137. doi:10.1088/1755-1315/833/1/012137

Cover, T., & Hart, P. (1967). Nearest neighbor pattern classification. *IEEE Transactions on Information Theory*, *13*(1), 21-27.

Deere, D. U. (1963). Technical Description of Rock Cores.pdf. *Rock Mechanics and Engineering Geology*, *I*(1), 18-22.

Deng, S., Aldrich, C., Liu, X., & Zhang, F. (2024). Explainability in Reservoir Well-logging Evaluation: Comparison of Variable Importance Analysis with Shapley Value Regression, SHAP and LIME. *IFAC PapersOnLine*, *58*(22), 66-71. https://doi.org/10.1016/j.ifacol.2024.09.292

De-Vitry, C., Vann, J., & Arvidson, H. (2010). Multivariate iron ore deposit resource estimation - a practitioner's guide to selecting methods. *Trans Inst Mining Metallurgy Sect B.*, *119*(3), 154-165.

Ding, C., & Peng, H. (2005). Minimum redundancy feature selection from microarray gene expression data. *Journal of Bioinformatics and Computational Biology*, *3*(02), 185-205.

Du, H., Wang, J., Zhang, X., Yao, X., & Hu, Z. (2008). Prediction of retention times of peptides in RPLC by using radial basis function neural networks and projection pursuit regression. *Chemometrics and Intelligent Laboratory Systems*.

Duda, R. O., & Hart, P. E. (1972). Use of the Hough transformation to detect lines and curves in pictures. *Communications of the ACM*, *15*(1), 11-15.

Elbaz, S., Crawford, D., & Tuck, M. (2016). A method to assess rock strength and excavability of diamondiferous kimberlite ore through in-situ rock testing. *Geotechnical and Geophysical Site Characterisation 5*. 2016 Australian Geomechanics Society, Sydney, Australia. https://doi.org/10.1007/978-3-319-07713-0

Elsayed, M., Isah, A., Hiba, M., Hassan, A., Al-Garadi, K., Mahmoud, M., El-Husseiny, A., & Radwan, A. E. (2022). A review on the applications of nuclear magnetic resonance (NMR) in the oil and gas industry: Laboratory and field-scale measurements. *Journal of Petroleum Exploration and Production Technology*, *12*(10), 2747-2784. https://doi.org/10.1007/s13202-022-01476-3

Fang, Y., Wu, Z., Sheng, Q., Tang, H., & Liang, D. (2020). Tunnel Geology Prediction Using a Neural Network Based on Instrumented Drilling Test. *Applied Sciences*, *11*(1), 217. https://doi.org/10.3390/app11010217

Finfinger, G., Peng, S., Gu, Q., Wilson, G., & Thomas, B. (2000). An Approach to Identifying Geological Properties from Roof Bolter Drilling Parameters. *Proc. 19th Conf. on Ground Control in Mining*, 1-12.

Fisher, J. E., Shakoor, A., & Watts, C. F. (2014). Comparing discontinuity orientation data collected by terrestrial LiDAR and transit compass methods. *Engineering Geology*, *181*, 78-92. https://doi.org/10.1016/j.enggeo.2014.08.014

Friedman, J. H. (1991). Multivariate Adaptive Regression Splines. *The Annals of Statistics*, *19*(1), 1-67.

Friedman, J. H., & Stuetzle, W. (1981). Projection Pursuit Regression. *Journal of the American Statistical Association*, *76*, 817-823.

Galende-Hernández, M., Menéndez, M., Fuente, M. J., & Sainz-Palmero, G. I. (2018). Monitor-While-Drilling-based estimation of rock mass rating with computational intelligence: The case of tunnel excavation front. *Automation in Construction*, *93*(April), 325-338. https://doi.org/10.1016/j.autcon.2018.05.019

Ghosh, R. (2017). *Assessment of Rock Mass Quality and its Effects on Chargeability Using Drill Monitoring Technique* [PhD]. Lulea University of Technology.

Ghosh, R., Gustafson, A., & Schunnesson, H. (2018). Development of a geological model for chargeability assessment of borehole using drill monitoring technique. *International Journal of Rock Mechanics and Mining Sciences*, *109*(July 2017), 9-18. https://doi.org/10.1016/j.ijrmms.2018.06.015

Ghosh, R., Schunnesson, H., & Kumar, U. (2014). Evaluation of Rock Mass Characteristics Using Measurement While Drilling in Boliden Minerals Aitik Copper Mine, Sweden. In C. Drebenstedt & R. Singhal (Eds.), *Mine Planning and Equipment Selection* (pp. 81-91). Springer International Publishing. https://doi.org/10.1007/978-3-319-02678-7_9

Goldstein, D. M., Aldrich, C., & O'Connor, L. (2024a). A Review of Orebody Knowledge Enhancement Using Machine Learning on Open-Pit Mine Measure-While-Drilling Data. *Machine Learning and Knowledge Extraction*, *6*, 1343-1360. https://doi.org/10.3390/ make6020063

Goldstein, D., Aldrich, C., & O'Connor, L. (2024b). Enhancing Orebody Knowledge using Measure-While-Drilling Data: A Machine Learning Approach. *IFAC PapersOnLine*, *58*(22), 72-76.

Goldstein, D., Aldrich, C., Shao, Q., & O'Connor, L. (2025a). Unlocking Subsurface Geology: A Case Study with Measure-While-Drilling Data and Machine Learning. *Minerals*, 15(3), 241. https://doi.org/10.3390/min15030241

Goldstein, D., Aldrich, C., Shao, Q., & O'Connor, L. (2025b). A Machine Learning Classification Approach to Geotechnical Characterization Using Measure-While-Drilling Data. *Geosciences*, 15(3), 93. https://doi.org/10.3390/geosciences15030093

Goldstein, D., Aldrich, C., Shao, Q., & O'Connor, L. (2025c). A Field-Scale Framework for Assessing the Influence of Measure-While-Drilling Variables on Geotechnical Characterization Using a Boruta-SHAP Approach. *Mining*, 5(1), 20. https://doi.org/10.3390/mining5010020

Gupta, I., Tran, N., Devegowda, D., Jayaram, V., Rai, C., Sondergeld, C., & Karami, H. (2020). Looking Ahead of the Bit Using Surface Drilling and Petrophysical Data: Machine-Learning-Based Real-Time Geosteering in Volve Field. *SPE Journal*, *25*(02), 990-1006. https://doi.org/10.2118/199882-PA

Hatherly, P., Leung, R., Scheding, S., & Robinson, D. (2015). Drill monitoring results reveal geological conditions in blasthole drilling. *International Journal of Rock Mechanics and Mining Sciences*, *78*, 144-154. https://doi.org/10.1016/j.ijrmms.2015.05.006

Hearst, M. A., Dumais, S. T., Osuna, E., Platt, J., & Scholkopf, B. (1998). Support Vector Machines. *IEEE Intelligent Systems and Their Applications*, *13*(4), 18-28.

Herwig, N., & Borghesani, P. (2023). Explaining deep neural networks processing raw diagnostic signals. *Mechanical Systems and Signal Processing*, *200*. https://doi.org/10.1016/j.ymssp.2023.110584.

Hjelme, J. G. (2010). *Drill parameter analysis in the Løren tunnel* [Masters]. University of Oslo.

Hoek, E. (1983). Strength of jointed rock masses. *Géotechnique*, *33*(3), 187-223. https://doi.org/10.1680/geot.1983.33.3.187

Hoek, E., & Brown, E. T. (1997). Practical estimates of rock mass strength. *International Journal of Rock Mechanics and Mining Sciences*, *34*(8), 1165-1186.

Howarth, D. F., & Rowlands, J. C. (1987). Quantitative assessment of rock texture and correlation with drillability and strength properties. *Rock Mechanics and Rock Engineering*, *20*(1), 57-85. https://doi.org/10.1007/BF01019511

International Society for Rock Mechanics (ISRM). (1978). Simple Field Identification Compressive Strength of Rock and Clay. *International Journal of Rock Mechanics and Mining Sciences*, *15*(6), 319-368.

Jones, H., Walraven, F., & Knott, G. (1973). *Natural gamma logging as an aid to iron ore exploration in the pilbara region of western australia*. Australasian Institute of Mining and Metallurgy Annual Conference, Perth, Australia.

Kadkhodaie-Ilkhchi, A., Monteiro, S. T., Ramos, F., & Hatherly, P. (2010). Rock recognition from MWD Data: A comparative study of boosting, neural networks, and fuzzy logic. *IEEE Geoscience and Remote Sensing Letters*, *7*(4), 680-684. https://doi.org/10.1109/LGRS.2010.2046312

Kahraman, S., Rostami, J., & Naeimipour, A. (2016). Review of Ground Characterization by Using Instrumented Drills for Underground Mining and Construction. *Rock Mechanics and Rock Engineering*, *49*(2), 585-602. https://doi.org/10.1007/s00603-015-0756-4

Kaveh, A., Hamze-Ziabari, S. M., & Bakhshpoori, T. (2018). Estimating Drying Shrinkage of Concrete Using a Multivariate Adaptive Regression Spline Approach. *International Journal of Optimization in Civil Engineering*, *8*(2), 181-194.

Ker, P. (2021, July 16). Iron ore supply slump as Rio runs late on new mines. *Australian Financial Review*. https://www.afr.com/companies/mining/rio-tinto-iron-ore-takes-300m-inflation-hit-20210716-p58a8l

Khorzoughi, B. M., & Hall, R. (2016). Processing of measurement while drilling data for rock mass characterization. *International Journal of Mining Science and Technology*, *26*(6), 989-994. https://doi.org/10.1016/j.ijmst.2016.09.005

Khorzoughi, M. B. (2011). *Use of Measurement While Drilling Techniques for Improved Rock Mass Characterization in Open-Pit Mines* [MSc]. University of British Columbia.

Khorzoughi, M. B., Hall, R., & Apel, D. (2018). Rock fracture density characterization using measurement while drilling (MWD) techniques. *International Journal of Mining Science and Technology*, *28*(6), 859-864. https://doi.org/10.1016/j.ijmst.2018.01.001

Khushaba, R. N., Melkumyan, A., & Hill, A. J. (2021). A Machine Learning Approach for Material Type Logging and Chemical Assaying from Autonomous Measure-While-Drilling (MWD) Data. *Mathematical Geosciences*. https://doi.org/10.1007/s11004-021-09970-w

King, R. L., Hicks, M. A., & Signer, S. P. (1993). Using unsupervised learning for feature detection in a coal mine roof. *Engineering Applications of Artificial Intelligence*, *6*(6), 565-573. https://doi.org/10.1016/0952-1976(93)90053-Z

Kira, K., & Rendell, L. A. (1992). A practical approach to feature selection. In *Machine learning proceedings 1992* (pp. 249-256). Elsevier.

Klyuchnikov, N., Zaytsev, A., Gruzdev, A., Ovchinnikov, G., Antipova, K., Ismailova, L., Muravleva, E., Burnaev, E., Semenikhin, A., Cherepanov, A., Koryabkin, V., Simon, I., Tsurgan, A., Krasnov, F., & Koroteev, D. (2019). Data-driven model for the identification of the rock type at a drilling bit. *Journal of Petroleum Science and Engineering*, *178*, 506-516. https://doi.org/10.1016/j.petrol.2019.03.041

Kotsiantis, S. B. (2013). Decision trees: A recent overview. *Artificial Intelligence Review*, *39*, 261-283.

Kursa, M. B., & Rudnicki, W. R. (2010). Feature Selection with the Boruta Package. *Journal of Statistical Software*, *36*(11). https://doi.org/10.18637/jss.v036.i11

Leighton, J. C. (1982). *Development of a correlation between rotary drill performance and controlled blasting powder factors* [MSc]. University of British Columbia.

Leung, R., & Scheding, S. (2015). Automated coal seam detection using a modulated specific energy measure in a monitor-while-drilling context. *International Journal of Rock Mechanics and Mining Sciences*, *75*, 196-209. https://doi.org/10.1016/j.ijrmms.2014.10.012

Liaghat, S., Gustafson, A., Johansson, D., & Schunnesson, H. (2019). Ore grade prediction using informative features of MWD data. *Mining Goes Digital - Proceedings of the 39th International Symposium on Application of*

Computers and Operations Research in the Mineral Industry, APCOM 2019, *2010*, 226-234. https://doi.org/10.1201/9780429320774-26

Litvinenko, V. S., Dvoinikov, M. V., & Saint Petersburg Mining University. (2019). Justification of the technological parameters choice for well drilling by rotary steerable systems. *Journal of Mining Institute*, *235*(1), 24-29. https://doi.org/10.31897/pmi.2019.1.24

Liu, H., & Yin, K. K. (2001). Analysis and interpretation of monitored rotary blasthole drill data. *International Journal of Surface Mining, Reclamation and Environment*, *15*(3), 177-203. https://doi.org/10.1076/ijsm.15.3.177.3410

Liu, J. (2021). *Study on Intelligent Prediction Models of Geological Conditions ahead of Tunnel Face using Measurement-While-Drilling Data* [PhD]. Nagasaki University.

Liu, J., Jiang, Y., Han, W., & Sakaguchi, O. (2021). Optimized ANN model for predicting rock mass quality ahead of tunnel face using measure-while-drilling data. *Bulletin of Engineering Geology and the Environment*, *80*(3), 2283-2305. https://doi.org/10.1007/s10064-020-02057-6

Liu, J., Jiang, Y., Ishizu, S., & Sakaguchi, O. (2020). Estimation of tunnel support pattern selection using artificial neural network. *Arabian Journal of Geosciences*, *13*(9), 321. https://doi.org/10.1007/s12517-020-05311-z

Liu & Jiankang. (2021). *Study on Intelligent Prediction Models of Geological Conditions ahead of Tunnel Face using Measurement-While-Drilling Data*.

Liu, W., Rostami, J., Ray, A., & Elsworth, D. (2020). Statistical Analysis of the Capabilities of Various Pattern Recognition Algorithms for Fracture Detection Based on Monitoring Drilling Parameters. *Rock Mechanics and Rock Engineering*, *53*(5), 2265-2278. https://doi.org/10.1007/s00603-019-01965-8

Liu, X., & Aldrich, C. (2022). *Assessing the Influence of Operational Variables on Process Performance in Metallurgical Plants by Use of Shapley Value Regression*.

Loh, W.-Y., & Zhou, P. (2021). Variable Importance Scores. *Journal of Data Science*, *19*(4), 569-592. https://doi.org/DOI 10.6339/21-JDS1023

Lu, L., Devasahayam, S., & Sahajwalla, V. (2013). Evaluation of coal for metallurgical applications. In *The coal handbook: Towards cleaner production* (pp. 352-386).

Lucifora, D. J., & Rafezi, H. (2013). *State of the Art Review: Monitoring-While-Drilling for Mining Applications*. *4*.

Lundberg, S., & Lee, S.-I. (217 C.E.). *A Unified Approach to Interpreting Model Predictions*. 1-10. https://doi.org/10.48550

Manzoor, S., Liaghat, S., Gustafson, A., Johansson, D., & Schunnesson, H. (2019). Rock Mass Characterization Using MWD Data and Photogrammetry. *Mining Goes Digital - Proceedings of the 39th International Symposium on Application of Computers and Operations Research in the Mineral Industry, APCOM 2019*, 217-225. https://doi.org/10.1201/9780429320774-25

Martin, J. (2007). *Application of Pattern Recognition Techniques to Monitoring-While- Drilling on a Rotary Electric Blasthole Drill at an Open-Pit Coal Mine* [MSc]. Queen's University.

MATLAB (Version 24.1.0 (R2024a)). (2024). The MathWorks Inc. http://www.mathworks.com

Menon, R., Bhat, G., Saade, G. R., & Spratt, H. (2014). Multivariate adaptive regression splines analysis to predict biomarkers of spontaneous preterm birth. *Acta Obstetricia et Gynecologica Scandinavica*.

Millborrow, S. (2023). *Package 'earth'* (Version 5.3.2) [R]. https://cran.r-project.org/web/packages/earth/index.html

Navarro, J., Sanchidrián, J. A., Segarra, P., Castedo, R., Costamagna, E., & López, L. M. (2018). Detection of potential overbreak zones in tunnel blasting from MWD data. *Tunnelling and Underground Space Technology*, *82*(September), 504-516. https://doi.org/10.1016/j.tust.2018.08.060

Navarro, J., Sanchidrian, J. A., Segarra, P., Castedo, R., Paredes, C., & Lopez, L. M. (2018). On the mutual relations of drill monitoring variables and the drill control system in tunneling operations. *Tunnelling and Underground Space Technology*, *72*(October 2017), 294-304. https://doi.org/10.1016/j.tust.2017.10.011

Navarro, J., Schunnesson, H., Ghosh, R., Segarra, P., Johansson, D., & Sanchidrián, J. Á. (2019). Application of drill-monitoring for chargeability assessment in sublevel caving. *International Journal of Rock Mechanics and Mining Sciences*, *119*(November 2018), 180-192. https://doi.org/10.1016/j.ijrmms.2019.03.026

Navarro, J., Segarra, P., Sanchidrián, J. A., Castedo, R., Fortes, A. P. P., Natale, M., & López, L. M. (2018). *Application of an in-house MWD system for quarry blasting*. 203-210.

Navarro, J., Segarra, P., Sanchidrián, J. A., Castedo, R., & López, L. M. (2019). Assessment of drilling deviations in underground operations. *Tunnelling and Underground Space Technology*, *83*(September 2018), 254-261. https://doi.org/10.1016/j.tust.2018.10.003

Navarro, J., Seidl, T., Hartlieb, P., Sanchidrián, J. A., Segarra, P., Couceiro, P., Schimek, P., & Godoy, C. (2021). Blastability and Ore Grade Assessment from Drill Monitoring for Open Pit Applications. *Rock Mechanics and Rock Engineering*, *54*(6), 3209-3228. https://doi.org/10.1007/s00603-020-02354-2

Navarro Miguel, J. (2018). *The Use of Measure While Drilling for Rock Mass Characterization and Damage Assessment in Blasting* [PhD]. Universidad Politechnica de Madrid.

Palleske, C., Kalenchuk, K., Hume, C., & Bawden, W. (2017). *Strategic use of geotechnical data for maximised value added*. 511-520. https://doi.org/10.36487/ACG_rep/1704_33_Palleske

Peck, J. P. (1989). *Performance Monitoring of Rotary Blasthole Drills*. 395.

Peng, S. (2004). *Evaluation of Roof Bolting Requirements Based on In-Mine Roof Bolter Drilling* (DE-FC26-01NT41056). West Virgina University.

Potter, C., Moussa, J., Wilcox, A., Gilbert, L., & Vargas, V. (2022). *General Overview of Mobile Sources Used for Well Logging and Industrial Radiography Applications.*

R Core Team. (2022). *R Stats Package* (Version 4.3.0) [Vienna, Austria]. R Foundation for Statistical Computing. https://stat.ethz.ch/R-manual/R-devel/library/stats/html/stats-package.html

Rai, P., Schunesson, H., Lindqvist, P. A., & Kumar, U. (2015). An Overview on Measurement-While-Drilling Technique and its Scope in Excavation Industry. *Journal of The Institution of Engineers (India): Series D*, *96*(1), 57-66. https://doi.org/10.1007/s40033-014-0054-4

Rajesh Kumar, B., Vardhan, H., Govindaraj, M., & Vijay, G. S. (2013). Regression analysis and ANN models to predict rock properties from sound levels produced during drilling. *International Journal of Rock Mechanics and Mining Sciences*, *58*, 61-72. https://doi.org/10.1016/j.ijrmms.2012.10.002

Regression Learner Toolbox (Version 24.1.0 (R2024a)). (2024). The MathWorks Inc. http://www.mathworks.com

Roe, K. D., Jawa, V., Zhang, X., Chute, C. G., Epstein, J. A., Matelsky, J., Shpitser, I., & Taylor, C. O. (2020). Feature engineering with clinical expert knowledge: A case study assessment of machine learning model complexity and performance. *PLOS ONE*, *15*(4), e0231300. https://doi.org/10.1371/journal.pone.0231300

Romanenkova, E., Zaytsev, A., Klyuchnikov, N., Gruzdev, A., Antipova, K., Ismailova, L., Burnaev, E., Semenikhin, A., Koryabkin, V., Simon, I., & Koroteev, D. (2020). Real-Time Data-Driven Detection of the Rock-Type Alteration During a Directional Drilling. *IEEE Geoscience and Remote Sensing Letters*, *17*(11), 1861-1865. https://doi.org/10.1109/LGRS.2019.2959845

Rostami, J., Kahraman, S., Naeimipour, A., & Collins, C. (2015). Rock characterization while drilling and application of roof bolter drilling data for evaluation of ground conditions. *Journal of Rock Mechanics and Geotechnical Engineering*, *7*(3), 273-281. https://doi.org/10.1016/j.jrmge.2015.01.006

Said, K. O., Onifade, M., Akinseye, P., Kolapo, P., & Abdulsalam, J. (2023). A review of geospatial technology-based applications in mineral exploration. *GeoJournal*, *88*(3), 2889-2911. https://doi.org/10.1007/s10708-022-10784-4

Schulz, E., Speekenbrink, M., & Krause, A. (2018). A tutorial on Gaussian process regression: Modelling, exploring, and exploiting functions. *Journal of Mathematical Psychology*, *85*, 1-16.

Schunnesson, H. (1990). *Drill Process Monitoring in Percussive Drilling: A Multivariate Approach for Data Analysis* [Licentiate]. Lulea University of Technology.

Schunnesson, H. (1996). RQD predictions based on drill performance parameters. *Tunnelling and Underground Space Technology*, *11*(3), 345-351. https://doi.org/10.1016/0886-7798(96)00024-7

Schunnesson, H. (1997). *Drill process monitoring in percussive drilling for location of structural features, lithological boundaries and rock properties, and for drill productivity evaluation* [PhD]. Lulea University of Technology.

Schunnesson, H. (1998). Rock characterisation using percussive drilling. *International Journal of Rock Mechanics and Mining Sciences*, *35*(6), 711-725. https://doi.org/10.1016/S0148-9062(97)00332-X

Scoble, M. J., & Peck, J. (1987). *A technique for ground characterization using automated production drill monitoring*. *5265*. https://doi.org/10.1080/09208118708944101

Scoble, M. J., Peck, J., & Hendricks, C. (1989). *Correlation between Rotary Drill Performance Parameters and Borehole Geophysical Logging*. *8*, 301-312.

Segui, J. B., & Higgins, M. (2001). *Blast Design Using Measurement While Drilling Parameters*. 28-31.

Sepulveda, E., Dowd, P. A., Xu, C., & Addo, E. (2017). Multivariate Modelling of Geometallurgical Variables by Projection Pursuit. *Mathematical Geosciences*, *49*(1), 121-143. https://doi.org/10.1007/s11004-016-9660-z

Shao, Q., Traylen, A., & Zhang, L. (2012). Nonparametric method for estimating the effects of climatic and catchment characteristics on mean annual evapotranspiration: NONPARAMETRIC METHOD FOR MEAN

ANNUAL EVAPOTRANSPIRATION. *Water Resources Research*, *48*(3). https://doi.org/10.1029/2010WR009610

Silversides, K. L., Ball, A., & Melkumyan, A. (2020). BIF-hosted deposit unit differentiation using multivariate Gaussian processes on measure while drilling data. *Applied Earth Science: Transactions of the Institute of Mining and Metallurgy*, *129*(4), 164-175. https://doi.org/10.1080/25726838.2020.1829253

Silversides, K. L., & Melkumyan, A. (2019). Multivariate Gaussian process for distinguishing geological units using measure while drilling data. *Minig Goes Digitial*, 94-100.

Silversides, K. L., & Melkumyan, A. (2020). Boundary Identification and Surface Updates Using MWD. *Mathematical Geosciences*. https://doi.org/10.1007/s11004-020-09891-0

Silversides, K. L., & Melkumyan, A. (2022). Machine learning for classification of stratified geology from MWD data. *Ore Geology Reviews*, *142*, 104737. https://doi.org/10.1016/j.oregeorev.2022.104737

Silversides, K., Melkumyan, A., Wyman, D., & Hatherly, P. (2015). Automated recognition of stratigraphic marker shales from geophysical logs in iron ore deposits. *Computers and Geosciences*, *77*, 118-125. https://doi.org/10.1016/j.cageo.2015.02.002

Sommerville, B., Boyle, C., Brajkovich, N., Savory, P., & Latscha, A.-A. (2014). Mineral resource estimation of the Brockman 4 iron ore deposit in the Pilbara region. *Applied Earth Science*, *123*(2), 135-145. https://doi.org/10.1179/1743275814Y.0000000038

Statistics and Machine Learning Toolbox (Version 24.1.0 (R2024a)). (2024). The MathWorks Inc. http://www.mathworks.com

Stebbins, S. A. (1987). *Cost estimation handbook for small placer mines* (Vol. 9170). US Department of the Interior, Bureau of Mines.

Su, X., Yan, X., & Tsai, C.-L. (2012). Linear regression. *WIREs Computational Statistics*, *4*, 275-294.

Teale, R. (1965). The concept of specific energy in rock drilling. *International Journal of Rock Mechanics and Mining Sciences And*, *2*(1), 57-73. https://doi.org/10.1016/0148-9062(65)90022-7

Tittman, J., & Wahl, J. S. (1965). The Physical Foundations of Formation Density Logging (Gamma-Gamma). *GEOPHYSICS*, *30*(2), 284-294. https://doi.org/10.1190/1.1439574

Utt, W. K. (1999). Neural network technology for strata strength characterization. *IJCNN'99. International Joint Conference on Neural Networks. Proceedings (Cat. No.99CH36339)*, *6*, 3806-3809. https://doi.org/10.1109/IJCNN.1999.830760

Van Eldert, J. (2018). *Analysis of Excavation Damage , Rock Mass Characterisation and Rock Support Design using Drilling Monitoring* [Licentiate]. Lulea University of Technology.

Van Eldert, J. (2020). *Drill Monitoring for Rock Mass Assessment in Tunnelling* [PhD]. Lulea University of Technology.

van Eldert, J., Funehag, J., Schunnesson, H., & Saiang, D. (2021). Drill Monitoring for Rock Mass Grouting: Case Study at the Stockholm Bypass. *Rock Mechanics and Rock Engineering*, *54*(2), 501-511. https://doi.org/10.1007/s00603-020-02279-w

van Eldert, J., Schunnesson, H., Johansson, D., & Saiang, D. (2020). Application of Measurement While Drilling Technology to Predict Rock Mass Quality and Rock Support for Tunnelling. *Rock Mechanics and Rock Engineering*, *53*(3), 1349-1358. https://doi.org/10.1007/s00603-019-01979-2

van Eldert, J., Schunnesson, H., Saiang, D., & Funehag, J. (2020). Improved filtering and normalizing of Measurement-While-Drilling (MWD) data in tunnel excavation. *Tunnelling and Underground Space Technology*, *103*(December 2019), 103467-103467. https://doi.org/10.1016/j.tust.2020.103467

Van Eldert & Jeroen. (2018). *Analysis of Excavation Damage , Rock Mass Characterisation and Rock Support Design using Drilling Monitoring*.

Vezhapparambu, V. S., Eidsvik, J., & Ellefmo, S. L. (2018). Rock classification using multivariate analysis of measurement while drilling data: Towards a better sampling strategy. *Minerals*, *8*(9). https://doi.org/10.3390/min8090384

Vezhapparambu, V. S., Eidsvik, J., & Ellefmo, S. L. (2018). Rock classification using multivariate analysis of measurement while drilling data: Towards a better sampling strategy. *Minerals*, 8(9). https://doi.org/10.3390/min8090384

Vezhapparambu, V. S., & Ellefmo, S. L. (2020). Estimating the blast sill thickness using changepoint analysis of MWD data. *International Journal of Rock Mechanics and Mining Sciences*, *134*, 104443. https://doi.org/10.1016/j.ijrmms.2020.104443

Wedge, D., Hartley, O., McMickan, A., Green, T., & Holden, E. J. (2019). Machine learning assisted geological interpretation of drillhole data: Examples from the Pilbara Region, Western Australia. *Ore Geology Reviews*, *114*(September), 103118-103118. https://doi.org/10.1016/j.oregeorev.2019.103118

Wei, P., Lu, Z., & Song, J. (2015). Variable importance analysis_ A comprehensive review. *Reliability Engineering and System Safety*, *142*, 399-432. https://doi.org/10.1016/j.ress.2015.05.018

Wold, S., Esbensen, K., & Geladi, P. (1987). Principal Component Analysis. *Chemometrics and Intelligent Laboratory Systems*, *2*(1-3), 37-52.

Yang, Q., Tan, M., Zhang, F., & Bai, Z. (2021). Wireline Logs Constraint Borehole-to-Surface Resistivity Inversion Method and Water Injection Monitoring Analysis. *Pure and Applied Geophysics*, *178*(3), 939-957. https://doi.org/10.1007/s00024-021-02674-6

Yu, X., Liu, B., & Lai, Y. (2024). Monthly Pork Price Prediction Applying Projection Pursuit Regression: Modeling, Empirical Research, Comparison, and Sustainability Implications. *Sustainability*, *16*(4), 1466.

Zachos, D., Alamanis, N., Papageorgiou, G., Chrysanidis, T., Zafoulis, N., & Paschalis, E. (2023). Calculation of penetration depth of a support retaining system anchored on the top, for underground network and buried energy pipelines. *Energy Systems*, 15, 1511-1526. https://doi.org/10.1007/s12667-023-00613-z

Zhang, W., Li, H., Li, Y., Liu, H., Chen, Y., & Ding, X. (2021). Application of deep learning algorithms in geotechnical engineering: A short critical review. *Artificial Intelligence Review*. https://doi.org/10.1007/s10462-021-09967-1

Zhao, R., Shi, S., Li, S., Guo, W., Zhang, T., Li, X., & Lu, J. (2023). Deep Learning for Intelligent Prediction of Rock Strength by Adopting Measurement While Drilling Data. *International Journal of Geomechanics*, *23*(4), 04023028. https://doi.org/10.1061/IJGNAI.GMENG-8080

Zhong, R., Johnson, R. L., & Chen, Z. (2019). Using machine learning methods to identify coals from drilling and logging-while-drilling LWD data. *SPE/AAPG/SEG Asia Pacific Unconventional Resources Technology Conference 2019, APUR 2019*. https://doi.org/10.15530/ap-urtec-2019-198288

Zhou, H., Hatherly, P., Monteiro, S. T., Ramos, F., Oppolzer, F., Nettleton, E., & Scheding, S. (2012). Automatic rock recognition from drilling performance data. *Proceedings - IEEE International Conference on Robotics and Automation*, 3407-3412. https://doi.org/10.1109/ICRA.2012.6224745

Appendix

Paper A: Peer Review Comments and Responses

Goldstein, D. M., Aldrich, C., & O’Connor, L. (2024). A Review of Orebody Knowledge Enhancement Using Machine Learning on Open-Pit Mine Measure-While-Drilling Data. *Machine Learning and Knowledge Extraction*, *6(2),* 1343-1360. https://doi.org/10.3390/make6020063

Reviewer 1

Comment 1: *It was a pleasure to read your paper.*

Response 1: The authors appreciate the comment of the reviewer.

Reviewer 2

This article focuses on the use of Machine Learning (ML) to enhance orebody knowledge through Measure-While-Drilling (MWD) data in open-pit mining. It highlights the transition from manual to computerized data acquisition and interpretation to determine lithological boundaries more efficiently. The research underlines the high prediction accuracy (>90%) achieved by artificial intelligence algorithms, such as Neural Networks and Gaussian Processes, in recognizing subsurface conditions like rock types from MWD data. However, it also points out the underutilization of methods like Principal Component Analysis in evaluating the significance of each MWD feature.

Strengths

- Innovative Approach: The article presents a forward-thinking approach by integrating ML with MWD data to predict subsurface conditions accurately, a significant leap forward in mining exploration and operational efficiency.

- High Prediction Accuracy: Demonstrating over 90% prediction accuracy in identifying subsurface conditions using ML algorithms is a compelling outcome that underscores the potential of this technology in enhancing orebody knowledge.

- Extensive Data Analysis: The use of a comprehensive array of sensors for data collection and the subsequent application of ML for data interpretation effectively leverages the vast amounts of data generated during drilling operations.

Weaknesses:

- Limited Methodology Exploration: While the success of Neural Networks and Gaussian Processes is highlighted, the paper does not extensively explore or compare other ML methodologies that might offer additional insights or efficiencies.

- Feature Importance Evaluation: The article mentions the underutilization of certain analytical methods (like Principal Component Analysis) for evaluating feature importance, suggesting that further work could enhance the model's predictive capabilities.

- Data Collection Constraints: The paper briefly touches on the challenges associated with the substantial volume of data requiring manual analysis but does not delve into potential solutions or ways to streamline this process further.

Critical Remarks:

Comment 1: *- Literature Review: The review of existing literature appears to be thorough, but the article could benefit from a more detailed comparison with recent studies to ensure the utilization of the latest ML methodologies and data processing techniques.*

Response 1: The paper was updated to include some of the most recent studies, specifically focusing on deep learning methods. This is reflected in Table 1 (as highlighted) and discussion in the text.

Comment 2: *- Future Developments: While the article successfully outlines the current application of ML in MWD data analysis, it could provide a clearer roadmap for future research, particularly in addressing the highlighted weaknesses and exploring the integration of additional ML algorithms.*

Response 2: More discussion was added to section 5.2, highlighting trends in the adoption of deep learning models that are better able to deal with unstructured data, such as vibrational signals and borehole images. A second future direction relates to the development of explainable models that can be interrogated to determine possible causes or reasons for specific model predictions.

Comment 3: *- Application and Impact: A deeper discussion on the practical implications of this technology in mining operations, including cost savings, efficiency improvements, and potential environmental benefits, would offer a more holistic view of its value.*

Response 3: Cost savings are difficult to quantify, except to note that the drive towards real-time information would in general enable more efficient process operation associated with significant cost savings.

Comment 4*: Conclusion: The article presents a significant advancement in using ML to interpret MWD data, offering high prediction accuracies and showcasing the potential to revolutionize subsurface characterization in mining. While there are areas for improvement, particularly in exploring additional ML methodologies and addressing data collection challenges, the* *research provides a solid foundation for future exploration and application in the field.*

Response 4: The authors appreciate the comment and trust that the revised version improves significantly on the areas that have been outlined by the reviewer.

Reviewer 3 (Round 1)

Comment 1: *I read the paper carefully. The topic is interesting and deserves to be published in Make after making some major modifications as follows:*

The abstract must be written. Please give us much more detailed results.

Response 1: The abstract was comprehensively revised to better reflect the contents and results of the study.

Comment 2: *Along with using Google Scholar, I would suggest using other database, such as Scopus, Web of Science, and So on.*

Response 2: This was done, the main ones included being Scopus, ScienceDirect, Wiley and IEEE Xplore. Where applicable additional references have been included in the revised paper, specifically in Table 1 and also in references in the concluding sections of the paper.

Comment 3: *Which parameter have been considered in the papers? For instance, how many blast holes were considered in each work/ average? You must clarify them in proper flowcharts/tables for describing the input parameters! For instance, the types of geological settings must be classified in a table or flowchart based on the iron type.*

Response 3: The authors have tried to fit this in as best as possible in Table 1, although this information was not readily available in all the investigations reported in the literature.

Comment 4: *You mentioned that you used PCA for analysing the data. I'd like to see that.*

Response 4: Since the authors have not actually analysed any data with PCA in this investigation themselves, the sentence in the text have been rephrased to clarify this.

Comment 5: *That would be great if you could add a brief section for each ML methods which have been used and compare them together.*

Response 5: The authors have added more comment on the ML methods in the paper, such as in section 2. However, the authors have not compared them directly, as there are multiple studies elsewhere dealing with the comparison of ML methods, but more importantly, it would be very difficult to generalise any of the results regarding MWD data.

Reviewer 3 (Round 2)

This is the re-review manuscript entitled "A Review of Orebody Knowledge Enhancement using Machine Learning on Open Pit Mine Measure-While-Drilling Data". I read the revised article carefully, However, I am not yet convinced that the article deserves to be published in Makes. I would like to give the authors a second chance to address major issues.

Comment 1: *1- Q2 from the initial review remains unaddressed. The authors haven't clarified which parameters were considered in the reviewed papers. This includes details like the number of blast holes analysed per study (averages would be helpful). A well-structured table or flowchart outlining these input parameters, including geological setting classifications based on iron type (e.g., a table showing different iron types), would be highly beneficial.*

Response 1: The authors have tried to fit this in as best as possible in Table 1, although this information was not readily available in all the investigations reported in the literature. Table 1 includes the number of holes in each study, as well as the rock type. Where indicated in the literature, a subtype for iron ore, e.g.' BIF' was included, but most investigations simply refer to the rock type as 'iron' or 'coal' for example, without providing specific detail.

Comment 2: *2-The paper's organisation needs improvement. Identifying keyword clusters is an excellent approach to highlighting research hotspots. I recommend incorporating this strategy into the discussion section. I am afraid to say that the current structure makes it difficult to follow the main topic.*

Response 2: The authors have revisited the discussion section of the revised paper to make it easier to follow the main topic. This includes a diagram (Fig. 5) that was based on a keyword analysis of the publications available in the Scopus database. It is not necessarily as sophisticated an analysis as could be done with bibliometric software, but hopefully this would give some indication of the methods that have been used to analyse MWD data over the last decade.

Comment 3: 3-I strongly recommend adding sub-sections such as "reviewing the highly cited articles" and "top leading institutions, top 10 articles in the field, journals, publishers" to the review section. What were your criteria for filtering the articles? Which type of articles were excluded from your final list, for instance, review papers? Which guidelines did you follow to conduct your review? Which exact keywords? Which categories were excluded from your review.

Response 3: The method of selection is covered in Section 2 of the revised paper, “Literature Sources and Dissemination”. A progressively narrower focus on keywords was subsequently introduced in Section 2, as indicated in Figure 2, specifically focusing on papers related to open pit mining identified by the keywords “Measure While Drilling”, “Measure While Drilling” AND “Rock Characterization”, as well as “Measure While Drilling” AND “Rock Characterization” AND “Machine Learning” compared on an annual basis in a bar chart (Fig. 2). Moreover, the authors have indicated that Australia and Canada are at the centre of these areas of research. In addition, the journals Mathematical Geosciences and Minerals contain some 22% of the papers considered in this review.

Highly cited articles, review papers or “Top 10 articles in the field” were not considered as such, but were implicitly included in the review instead. The authors trust that the approach they have used in the selection of papers is clear, although not necessarily the same as the approach suggested by the reviewer.

Paper B: Peer Review Comments and Responses

Goldstein, D., Aldrich, C., Shao, Q., & O’Connor, L. (2025). A Field-Scale Framework for Assessing the Influence of Measure-While-Drilling Variables on Geotechnical Characterization Using a Boruta-SHAP Approach. *Mining*, 5(1), 20. https://doi.org/10.3390/mining5010020

Reviewer 1

Thank you for your constructive and encouraging review of our manuscript, *"Unlocking Subsurface Geology: A Case Study with Measure-While-Drilling Data and Machine Learning."* We greatly appreciate your insights which have helped us refine the manuscript. Below, we address each of your comments and outline the changes made.

Comment 1: *The authors have captured a useful review of existing literature that is pertinent to the study. The critique of PCA is acceptable and the use of MARS and PPR on MWD data seems appropriate. I would encourage to authors to identify any prior works that have suggested such an approach previously that would further support the approach taken. However, the reason for the approach has been justified.*

Response 1: We appreciate this suggestion and have reviewed the literature further to identify any prior works that have explored similar approaches. We have strengthened our justification for using MARS and PPR by explicitly stating that PCA has been the only method identified that has previously attempted feature importance (line 65-66). This highlights the novelty of our approach while acknowledging existing methods. We have added a short selection of papers using MARS (lines 229-231) and PPR (lines 244-245) for feature importance in other fields.

Comment 2: *Can the authors consider using a different coloured font/location to depict a)/b) in Figure 1, as it would be near impossible to read in greyscale.*

Response 2: We acknowledge the readability issue and have made modifications to improve accessibility. We have moved the location of the a) and b) labels in Figure 1 (line 175) off of the images to improve readability in greyscale."

Comment 3: *The method implemented is sound. The additional implementation of regression-based ML methods was an insightful way to expand the viability of using MARS and PPR on the MWD data to produce positive results.*

The results of the approach are exciting. Again, the authors should be commended on the output of the approach! However, I would like to see in the discussion a short reflection of the impact of the amount of data available *on results. For example, with more data, the regression ML Methods used would likely significantly improve. Therefore, is there a minimum amount of MWD data required for this approach to be viable? It appears as though there would be perhaps other approaches may be better to implement in those scenarios of lower amounts of data or data resolution.*

Response 3: We agree that data availability plays a critical role in ML performance and have now explicitly discussed this aspect in the Discussion section. We have added a reflection on the impact of data quantity and resolution on model performance (lines 638-641). This addition provides insights into data requirements and highlights potential limitations of the approach in low-data environments.

Comment 4: The conclusions identified are sound. I'm excited to see if this work will be implemented commercially as I believe there is a lot of value there.

I also believe future work into other approaches will be useful to bolster up and further extend the (notably already) success of this existing approach.

Response 4: We sincerely appreciate your thoughtful review and constructive suggestions. We hope these revisions adequately address your concerns and further improve the clarity and impact of our work. Please let us know if any additional modifications are needed.

Reviewer 2 (Round 1)

We appreciate your thoughtful review and constructive feedback on our manuscript, "Unlocking Subsurface Geology: A Case Study with Measure-While-Drilling Data and Machine Learning." Your comments have helped refine our discussion, particularly regarding the role of machine learning (ML) in geophysical predictions and its relationship with underlying physical mechanisms as well as the predictive performance of the models and practical applicability of our approach. Below, we outline the revisions made in response to your concerns.

Comment 1: *This paper presents a well-structured study on using ML models to predict geophysical properties from MWD data. The methodology is solid, experiments are thorough, and results are well-analyzed. The discussion on model selection is practical and informative.*

However, the main weakness is the lack of innovation. The use of ML for MWD data analysis is well-established, and the study does not introduce novel methodologies, models, or insights beyond existing work. While the comparisons are useful, the research mainly reinforces known conclusions rather than advancing the field.

1. *Machine learning is merely a tool for extracting patterns from data; it cannot create relationships that do not inherently exist. The paper focuses too much on ML models while neglecting the underlying physical mechanisms governing the relationships between the measured parameters.*

Response 1: Yes, we agree that ML has been used for MWD data analysis. In this paper, we overcome the issues in the current use of ML: (1) existing research used ML without feature selection (by assuming that the importance features are known, which is not true) or improper feature selection tool (i.e., CPR which cannot select importance features), (2) existing research adopted a single ML model without proper comparison, resulting sub-optimal choice of ML tools. To clarify this, we have made changes. We added a statement in the abstract to acknowledge the constraints of ML when modeling geophysical relationships (lines 22-24) and revised the final paragraph of the introduction to emphasize the importance of validating ML outputs with geological knowledge (lines 86-87).

Moreover, we agree on the black-box issues about ML. It will be an important research opportunity to develop structured ML using geophysical knowledge. This paper is just a starting point to harvesting the rich ML tools for MWD data analysis. To clarify this, we have made changes. As above, we included a statement in the conclusion emphasizing that ML should be used alongside geological knowledge in the conclusion (lines 714-718).

We agree that ML should be presented as a tool that models existing relationships rather than establishing causality.

Comment 2: *For example, consider the correlation between ROP, torque, weight on bit , and resistivity. In formations without conductive minerals, resistivity is primarily influenced by pore fluid content rather than mechanical drilling parameters. Given this weak intrinsic correlation, it is unsurprising that the model struggles to predict resistivity accurately. This fundamental issue is overlooked in the analysis, leading to poor prediction performance.*

Response 2: We acknowledge that our initial discussion did not sufficiently highlight the limitations of ML models in predicting resistivity due to its weak correlation with drilling parameters. To address this, we have added a paragraph to Section 3.2.1 explicitly discussing why resistivity predictions performed poorly (lines 551-555) and reworded the first paragraph of the Discussion section to acknowledge that weak intrinsic correlations limit ML's predictive ability (lines 641-644).

Comment 3: *2. While the paper provides detailed experiments and analyses, the actual predictive performance is quite poor. The only scatter plot presented (Figure 6) for density shows significant errors, even though density has a relatively narrow range and should be one of the easier parameters to* *predict. Other key properties, such as gamma ray, resistivity, and magnetic susceptibility, are only summarized in tables, with results that appear similarly weak. If the models fail to achieve meaningful accuracy, their practical applicability is questionable. This further highlights the lack of innovation—if the approach does not lead to usable results, what is the real contribution of this study?*

Response 3: We acknowledge that, although our results showed significant improvement in comparison with previous studies, some of the model predictions, particularly for density and resistivity, exhibit significant errors. However, the primary contribution of this study is not solely in achieving perfect predictive accuracy but rather: a) benchmarking machine learning models for geophysical property estimation using MWD data, b) identifying which MWD features are most influential in predicting geophysical parameters and c) providing insights into the limitations of ML in geological applications and suggesting pathways for improvement.

To clarify these contributions and address concerns about accuracy, we have made the following revisions:

- Explicitly state in the Introduction that the study's value lies in feature importance analysis and model benchmarking, rather than just achieving high predictive accuracy (lines 83-85).
- Acknowledge in Section 3.2 the challenge of predicting density despite its relatively narrow range, attributing errors to operational variability, sensor noise, and geological heterogeneity (lines 477-481.
- Explain in Section 3.2 why additional scatter plots were not included and why tabulated results were chosen for a clearer comparative analysis (lines 407-410).
- Emphasize in the Discussion that while model accuracy is limited, the study still provides valuable insights into ML applicability and feature selection for MWD-based predictions (lines 630-634).
- Highlight in the Conclusion that the study establishes a benchmark for future ML research in MWD-based geophysical modeling (lines 712-714)

Minor Issues

Comment 4: *1. The reported rock density range (1.5 to 4.5 t/m³) appears questionable. Typically, rock densities rarely exceed 3 t/m³. The authors should verify the accuracy of their data to ensure it aligns with geological expectations.*

Response 4: Thank you for your comment. The reported rock density range (1.5 to 4.5 t/m³) is based on site-specific geological data and aligns with observed variations in mineral composition. Figure 3a’s y-axis include 4.5 t/m^3 but very few samples were in this range. Most samples were less than 4.0 t/m^3. High-grade banded iron formations (BIF) containing significant hematite enrichment often exhibit densities approaching and sometimes exceeding 4.0 t/m^3 due to the high specific gravity of hematite (5.26 t/m^3). When hematite is intergrown with dense shale components, bulk densities over 4.0 t/m^3 are plausible.

For validation, we have reviewed density measurements from drill core samples and compared them with literature values. Studies such as Guo 2023 (doi: 10.3934/geosci.2023003) report similar density ranges for high-grade hematite-rich BIFs.

Comment 5: *2. The clarity of the figures is suboptimal, making it difficult to interpret key results. The authors should enhance the resolution and readability of all figures.*

Response 5: Thank you for your feedback. We acknowledge that the figures are relatively small. However, they remain legible and provide the necessary details to interpret key results. The current formatting ensures that all relevant data is presented concisely within the constraints of the manuscript.

To improve readability, we will enhance the resolution of the figures and, where feasible, adjust their size to optimize clarity without exceeding layout limitations. Additionally, we will refine the labeling and contrast further to aid interpretation. We appreciate your suggestion and will ensure that the figures are as clear as possible in the revised version.

Comment 6: *3. Figure 9 should be in color to maintain consistency with previous figures and improve visual clarity.*

Response 6: Thank you for your comment. We acknowledge the suggestion to present Figure 9 in color. However, we have intentionally used different shades of grey to maintain consistency with other figures. Specifically, the first variable (caliper in this case) is displayed in varying shades of grey for both the full 20-variable experiments and the reduced-feature experiments, following the same approach used for density (dens) in the density and gamma plot and magnetic susceptibility (magsus) in the magsus and resistivity plot.

This consistent formatting ensures uniformity across all figures while preserving clarity in differentiating the experimental conditions. However, to enhance readability, we will refine the contrast in Figure 9 to further distinguish between data groups while maintaining the established grayscale scheme. We appreciate your feedback and will make minor adjustments to optimize visual clarity.

Comment 7: *4. Furthermore, the authors should provide scatter plots similar to Figure 6 for other predicted parameters to give a clearer visualization of model performance.*

Response 7: Thank you for your suggestion. We agree that additional scatter plots could provide further insights into model performance. However, including scatter plots for all predicted parameters would significantly increase the length of the manuscript. Instead, we have provided an example scatter plot for density (dens) in Figure 6 to demonstrate model performance. This example is representative of the general trends observed across other parameters. We appreciate your feedback on the matter of balancing transparency while maintaining conciseness.

Comment 8: *In its current state, the paper does not meet the quality required for publication, particularly due to the two major issues highlighted. The authors need to critically rethink the purpose of their research rather than treating ML modeling as a data-driven exercise without meaningful scientific insight. However, given the substantial effort invested, I recommend a major revision. The authors should make fundamental improvements, refocusing on the core research questions, to bring the paper up to the necessary standard for publication.*

Response 8: We sincerely appreciate your feedback, which has helped refine our presentation of the study's contributions. We hope these revisions adequately address your concerns and improve the clarity of our work. Please let us know if any further clarifications are needed.

Reviewer 2 (Round 2)

Comment 1: *The authors have not adequately addressed all the comments.*

1. *First, the claim of innovation in feature selection is unconvincing. Feature engineering, including feature selection, is a standard practice in machine learning. The use of MARS for feature selection only adds some interpretability to the data, but the experimental results show that the inclusion of these features has minimal impact on the model's computation time. Additionally, using variance and ratio as features is unconventional. In theory, such features, like ratios, could be learned by more complex neural network architectures.*

Response 1: We respectfully disagree with the assertion that our feature selection approach lacks innovation. While feature engineering is a standard practice in machine learning, the application of Multivariate Adaptive Regression Splines and Projection Pursuit Regression for feature selection in Measure-While-Drilling data is novel within the context of geophysical parameter prediction. Prior studies have predominantly relied on Principal

Component Analysis or expert judgment, which do not provide an objective, data-driven assessment of feature importance. MARS and PPR offer an interpretable means of evaluating the contribution of each feature, allowing us to systematically determine which variables enhance prediction accuracy and which can be omitted to improve computational efficiency.

Regarding the concern about the impact of feature selection on computation time, we clarify that the importance of feature selection is not solely for reducing computation time. Rather, it serves to identify the most relevant input features for predictive modeling, reducing dimensionality and increasing the generalizability of models in real-world applications. Furthermore, the use of variance and ratio features is grounded in domain knowledge, reflecting established physical relationships in rock mechanics. While deep learning models might theoretically learn these relationships, the primary goal here is to use transparent and explainable methods that allow for interpretability, which is critical for practical deployment in mining operations.

Comment 2: Second, while the authors compare several machine learning models, the models chosen are outdated and perform poorly. This comparison lacks meaningful insights, as the models do not represent the state-of-the-art in machine learning, making it difficult to draw any substantial conclusions from the results.

Response 2: The reviewer suggests that the models chosen are outdated and perform poorly. However, our model selection was deliberate and based on the practical considerations of mining operations, where interpretability, computational efficiency, and robustness matter more than using the latest deep learning techniques.

Decision Trees, Random Forests, Support Vector Machines, Gaussian Process Regression, and Linear Regression are widely used in industrial settings because they provide explainable and verifiable results. Unlike black-box neural networks, they allow operators and geologists to understand the relationships between input features and predictions. Neural Networks were also evaluated, demonstrating that larger datasets improve their performance, but their lack of interpretability limits their practical adoption in mining applications.

The claim that our results lack meaningful insights overlooks the fact that comparing various models under different feature selection strategies is crucial for evaluating their effectiveness in geophysical prediction. Rather than aiming to chase state-of-the-art AI models, this study focuses on developing a practical, transparent framework applicable to the mining industry.

Furthermore, we emphasize that high model performance alone does not justify the adoption of a technique in mining. The need for real-time implementation, domain interpretability, and resistance to overfitting in sparse datasets outweighs marginal gains in predictive accuracy achieved by deep learning.

Comment 3: *It's from the Response3.*
Benchmarking Issue: The claim that the dataset represents a benchmark for machine learning models in geophysical property estimation is problematic. In addition to the dataset not being widely used and it seems not open source, the feature selection process also deviates from common practices. These issues, combined with the use of non-mainstream methods, make it difficult to justify this study as a benchmark.
Lack of Insights: The greatest issue with the paper is the lack of meaningful insights. The results are not analyzed deeply, and simply comparing poor model performances over time does not provide valuable insights. The models fail to capture the underlying relationships within the data, and comparing multiple suboptimal models does not lead to any significant conclusions or improvements in understanding. Without a deeper analysis of the results, the claims about the insights gained from this work are unsubstantiated.

Response 3: We acknowledge that the dataset used in this study is not publicly available due to confidentiality agreements with the mining company that provided it and have removed the benchmark term from the manuscript to avoid doubt. Therefore, we do not claim that this dataset represents a formal benchmark for the broader machine learning community. However, within the context of MWD-based geophysical prediction, this dataset serves as a valuable reference point for evaluating feature importance and model performance in real-world mining applications.

The dataset consists of high-resolution, real-world MWD data from active mine sites, capturing operational complexities that are absent in publicly available datasets. While we do not claim this as an industry-wide benchmark, the methodology and results provide insights that can guide future work in geophysical parameter estimation using MWD data. The feature selection framework and model comparisons remain relevant for both research and industrial applications, even if the dataset is proprietary.

The assertion that our feature selection approach "deviates from common practices" is also misplaced. Traditional feature selection methods such as PCA have inherent limitations in determining variable significance in nonlinear relationships. By using MARS and PPR, we offer a more robust approach that allows domain experts to validate model behavior.

Comment 4: *The authors continue to avoid addressing the poor performance of the prediction models. The results lack sufficient analysis, and based on my rough estimation from GAMA, the best RMSE reported in Table 8 is* *around 10. From Figure 3, it appears that the majority of GAMA values fall within the range of 10, with others ranging from 20 to 40. Doing a rough calculation, the error percentage is approximately 30%, which still represents the best performance among all models. I believe this approach is insufficient for reliably predicting geophysical parameters. How can such performance be considered a benchmark?*

Response 4: The reviewer claims that our results lack sufficient analysis and that the model performances are poor. We argue the analysis provided is already extensive, covering multiple models, feature selection techniques, and real-world mining datasets. The detailed comparisons of feature importance and model performance provide significant insights into the role of MWD data in geophysical prediction. Moreover, the assertion that the models fail to capture underlying relationships is incorrect. The results demonstrate that geophysical parameter prediction is inherently complex, and that traditional mining sensors may not always capture relationships with sufficient precision. Furthermore, the RMSE values and performance metrics have been rigorously analyzed, and we acknowledge the inherent difficulty of geophysical property prediction. However, the reviewer's calculation of a 30% error without considering the scale of the problem, geological variability, and sensor noise is an oversimplification. The prediction performance should be evaluated within the context of mining applications, where even partial improvements in geophysical modeling can yield substantial operational benefits.

Comment 5: *Additionally, the authors justify the limited number of figures by citing page restrictions, but given that only eight figures are included, this explanation seems insufficient. Most journals would not impose such strict limits.*

Response 5: We reiterate that our selection of figures was intentional and aimed at focusing on the most critical aspects of the study. While additional figures could be added, the current ones effectively illustrate the key findings without unnecessary redundancy.

Comment 6: The authors' overall revision mainly consists of statements and clarifications, without substantial improvements. The experiments involve a lot of comparisons regarding feature selection and the performance of outdated models, which do not offer meaningful insights. I suggest the authors test these models on simpler, open-source prediction tasks, where the results would be more trustworthy. Predicting geophysical well log data from MWD is inherently a complex problem and attempting to solve it with such basic models is not convincing.

Response 6: We acknowledge the reviewer's suggestion to test on simpler, open-source prediction tasks. However, we stand by our decision to focus on real-world MWD data, as it is more relevant to the mining industry. Open-source datasets do not typically capture the unique challenges of mining geophysical predictions, including drilling inconsistencies, sensor noise and geological heterogeneity. Moreover, this study is not intended to develop a general-purpose ML method applicable to all domains but rather to refine and assess ML methods for a highly specialized and critical industrial application.

We appreciate the reviewer's critical perspective, but we maintain that our approach is valid, practical and relevant for mining applications. The study's contributions lie in:

1. Applying MARS and PPR for feature selection in MWD data, providing an interpretable and systematic evaluation of feature importance.
2. Foundational MWD analysis using traditional ML models in a real-world mining context, where interpretability and efficiency are paramount.
3. Demonstrating the feasibility of using ML for geophysical prediction despite inherent data limitations, highlighting both the challenges and opportunities for future research.

We do not claim that the dataset represents a universal benchmark for geophysical prediction in machine learning, but rather a real-world case study that informs future research and industry applications.

Reviewer 3

Comment 1: This is an interesting paper that should be of value to the community.

Response 1: Thank you.

Comment 2: Why the data from two mine sites were combined should be explained.

Response 2: The data from Brockman pit and Marra Mamba pit were combined to enhance the robustness and generalizability of the predictive models. By integrating data from different geological formations, we ensured that the machine learning models captured a wider range of variability, increasing their applicability across diverse mining conditions. This clarification has been added to the Methods section (lines 183-184).

Comment 3: Are artificial intelligence (AI) regression models same as the machine learning models?

Response 3: In the Introduction, we have clarified that machine learning is a subset of artificial intelligence. The study specifically employs ML-based regression techniques, such as decision trees, random forests and Gaussian processes, to model geophysical relationships from drilling data.

Comment 4: In line 198, what is quartile detection methods and 1.5-factor threshold?

Response 4: The quartile detection method is a statistical approach used to identify and remove outliers. In this study, we applied the interquartile range method, where any values lying beyond 1.5 times the IQR were considered outliers and removed. This explanation has been expanded in the data preprocessing section (lines 200-201).

Comment 5: *In lines 298 and 300, the equations should be consistent. Is f(x_{i})^{2} the value predicted from the model? if so, x_{i} in Equation (4) should use the same notation.*

Response 5: We have corrected the notation inconsistency in Equation (4), ensuring that f(xi)^2 correctly refers to the predicted value and that xi is used consistently throughout the text.

Comment 6: Please clarify the statement in lines 404 to 406.

Response 6: We have reworded this section to clearly state that the types of geophysical outputs predicted from the MWD input variables.

Paper C: Peer Review Comments and Responses

Goldstein, D., Aldrich, C., Shao, Q., & O'Connor, L. (2025). A Machine Learning Classification Approach to Geotechnical Characterization Using Measure-While-Drilling Data. *Geosciences*, 15(3), 93.
https://doi.org/10.3390/geosciences15030093

Reviewer 1

Comment 1: *Better to include deep learning algorithms to see the accuracy of the results. Includes ANN and CNN.*

Response 1: We appreciate the reviewer's suggestion to incorporate deep learning algorithms such as Artificial Neural Networks and Convolutional Neural Networks to evaluate their predictive accuracy. While ANN and CNN are powerful techniques, our study primarily focuses on interpretable machine learning models suitable for geotechnical applications. Many mining operations require transparent models that provide clear feature importance and decision-making rationale, which is a key limitation of deep learning models, often regarded as "black-box" approaches.

However, we acknowledge the value of deep learning methods in geotechnical classification and will explore them in future work. Specifically, ANN models could be used for handling non-linear relationships in MWD data, while CNNs, which are typically applied to spatial and image-based data, may be less suitable for tabular MWD datasets. Future work will compare ANN models with traditional ML approaches to assess their viability in high-resolution geotechnical characterization.

To clarify the scope of this study, we have added the following statement in the Discussion section:
"While this study focuses on conventional ML approaches due to their interpretability and practical application in mining operations, future research may explore deep learning models such as Artificial Neural Networks and Convolutional Neural Networks to enhance classification performance. While these models can capture complex, non-linear relationships in datasets, which may further refine classification accuracy, deep learning models often function as "black boxes," limiting their practical use in mining operations where explainability is critical. Therefore, while deep learning approaches hold potential, the trade-off between accuracy and interpretability remains a key consideration for re-al-time geotechnical decision-making."

Reviewer 2

The paper "A Machine Learning Classification Approach to Geotechnical Characterisation using Measure-While-Drilling Data" presents a novel framework for classifying geotechnical properties (e.g., stratigraphic unit, rock/soil strength, rock type, Geological Strength Index and weathering intensity) using data collected from Measure-While-Drilling (MWD) systems. The authors compare several machine learning (ML) classifiers—including Decision Trees, Support Vector Machines, K-Nearest Neighbors, Random Forests, Linear Discriminant Analysis and Naïve Bayes—along with two feature selection algorithms (MRMR and ReliefF) to identify the most influential drilling parameters. The topic is interesting, with significant contributions to industry. There are a few major gaps in the paper:

Comment 1: *The proposed method, which derives key geological attributes solely from MWD data, raises concerns about its potential misuse as a substitute for comprehensive testing. It appears designed to deliver immediate responses, which might encourage users to forgo additional, necessary tests that capture the intricate interplay among various geological factors. To prevent this risk, the authors should clearly define the boundaries and conditions under which their machine learning approach is valid. Emphasizing that the method is intended to supplement not replace traditional testing will help ensure that critical synergies among influencing factors are not overlooked.*

Response 1: We fully acknowledge the importance of ensuring that our ML approach is not perceived as a replacement for traditional geotechnical testing. Our methodology is intended to enhance the spatial resolution of geotechnical classification while working alongside established field and laboratory testing methods. A new statement has been added to the Discussion section: "This machine learning approach is intended to complement, rather than replace, traditional geotechnical testing. While the models can improve spatial resolution and provide real-time insights, they should be used in conjunction with conventional methods such as laboratory strength tests, geophysical wireline logging and geological mapping. Ensuring a balanced approach between AI-driven insights and field validation is crucial for robust geotechnical characterization." (lines 455-461)

Comment 2: *Based on the reviewer's experience, incorporating the XGBoost method could be a valuable addition to the study. XGBoost, known for its robustness and efficiency in handling structured data, might deliver results that are as good as or even superior to those obtained using KNN and Decision Trees. Could the authors run an additional XGBoost model ?*

Response 2: We appreciate the reviewer's suggestion to incorporate XGBoost. However, we have deliberately focused on a selection of interpretable ML models suited for practical geotechnical applications. While XGBoost is a powerful algorithm, it introduces additional complexity, such as extensive hyperparameter tuning and a reduction in interpretability compared to models like Decision Trees and Random Forests. In mining operations, explainability and traceability of predictions are critical for geotechnical decision-making, making simpler models more suitable.

Additionally, our study primarily investigates classification-based ML approaches that can be readily implemented in mining operations without requiring extensive computational resources. XGBoost, while effective, is optimized for large-scale datasets with complex interactions, whereas our dataset is structured and relatively low-dimensional. Given these factors, we have opted not to include XGBoost in this study.

Comment 3: *As shown in Figure 4, the skewed or nonnormal class distributions of data were observed, especially in weathering intensity, rock or soil strength, geological strength index. The model may become biased toward predicting the majority class. This can reduce accuracy for underrepresented classes and lead to misleadingly high overall accuracy. The evaluation framework currently focuses mainly on accuracy, which might not fully capture the nuances of prediction errors. Please consider add AUC, F1-score as indices.*

Response 3: We acknowledge the concern regarding class imbalance and appreciate the suggestion to include additional evaluation metrics. However, we have chosen to focus on accuracy and misclassification cost as primary evaluation metrics due to their direct relevance to practical geotechnical decision-making.

The primary reason for not including AUC is that it is best suited for binary classification tasks and imbalanced datasets where distinguishing between positive and negative classes is critical. In contrast, our study involves multi-class classification problems, where overall prediction accuracy and misclassification cost are more meaningful indicators of model performance. Additionally, F1-score is most useful when precision and recall trade-offs are a primary concern (e.g., in medical diagnostics or fraud detection), but in our case, the primary objective is to achieve high spatial resolution of geotechnical properties using MWD data rather than minimizing false positives or false negatives in a specific category.

To address class imbalance, we have instead ensured that the dataset was partitioned in a manner that prevents overfitting to majority classes and we have explicitly discussed model misclassifications where they occur.

Comment 4: *In addition to the filter-based approaches (MRMR and ReliefF) shown in Figure 5, Could author derive model-based feature importance from the best-performing tree-based classifiers such as XGBoost and Decision*

Trees to see whether their internal rankings align with the earlier results (See https://doi.org/10.1680/jenge.22.00181). Please add the modeling workflow in this study.

Response 4: We appreciate the reviewer's suggestion to further validate feature selection results using model-based feature importance. However, our study focuses on the feature selection methods MRMR and ReliefF due to their independence from specific machine learning models and their ability to rank features based on relevance and redundancy rather than model-specific biases. These methods are well-established in feature selection, where maintaining model-agnostic feature rankings is important for broad applicability.

Furthermore, incorporating model-based feature importance from tree-based classifiers would introduce dependency on a specific algorithm, potentially skewing feature selection towards the internal mechanics of that model. Since the primary objective of this study is to evaluate general feature importance across multiple classifiers, we have deliberately focused on MRMR and ReliefF rather than deriving feature importance from individual machine learning models.

Reviewer 3

Comment 1: *The article is suitable for publication in "Geosciences," but some minor revisions should be made. Lines 128-129: Were these blast holes evenly spaced, according to a specific pattern or ore deposition, or randomly? Please explain.*

Response 1: The blast holes were not randomly distributed. They were arranged according to a specific drilling pattern based on mine design and orebody geometry. Production blast holes followed an 8m × 7m spacing pattern to ensure efficient fragmentation, while wall control holes were spaced more closely to maintain pit slope stability. This information has been clarified in the manuscript as follows: The blast holes were arranged in a structured drilling pattern. Production holes followed an 8 meter by 7 meter grid pattern, while wall control holes had closer spacing to maintain slope stability. This spacing was designed to optimize fragmentation and minimize overbreak.

Comment 2: *Lines 149-150: What could cause data points with negative values for rate of penetration, torque, force on bit, or bit axial pressure? Please explain.*

Response 2: Negative values in the MWD dataset are typically the result of sensor errors, calibration issues, or data transmission anomalies rather than physical drilling conditions. These may arise due to sudden rig shutdowns, incorrect zeroing of sensors, or temporary signal loss. We have expanded on this explanation in the manuscript by including “Negative values for MWD features are likely caused by sensor calibration issues, temporary signal loss, or data logging errors rather than actual negative drilling responses. Such anomalies can occur due to sudden rig stoppages, incorrect zeroing of sensors, or transient fluctuations in the onboard MWD data acquisition system.”

Comment 3: *Lines 154-156: How many exploration holes were drilled? Please characterize raw rock parameter data (before use of the K-Nearest Neighbor distance-based search technique).*

Response 3: We appreciate the reviewer’s request for further clarification regarding the number and type of exploration holes. This information is already provided in the Methods section (Lines 87-89), which details that 12 diamond core drill holes and 211 reverse circulation (RC) drill holes were used for geological characterization.

Regarding the characterization of raw rock parameter data, we regret that we are unable to provide the original raw geotechnical data due to confidentiality agreements with the mining company. However, the manuscript includes all data relevant to the MWD data analysis results, ensuring transparency in the study’s methodology and findings.

Comment 4: *Line 289: The scale in Fig. 3 should have the same range for positive and negative numbers.*

Response 4: We acknowledge the discrepancy in the scale range of Figure 3. The figure has been revised to ensure that the positive and negative ranges are balanced for consistency.

Comment 5: *Lines 292-293: Do the presented data concern raw rock parameter data (from exploration holes), or are these already data merged to blast holes? Please explain.*

Response 5: The data presented in this section correspond to merged data after the K-Nearest Neighbor distance-based search technique was applied. However, we acknowledge that this distinction was not explicitly stated and have clarified it in the manuscript by including “The presented data correspond to the merged dataset after applying the K-Nearest Neighbor distance-based search technique to integrate exploration hole geotechnical observations with blast hole MWD measurements. The original raw exploration data were independently logged before this merging process." (lines 293-297)

Comment 6: *Lines 336-358: Please provide the values of the most important hyperparameters for selected machine learning algorithms.*

Response 6: We agree that providing hyperparameter values will improve the clarity of our methodology. We have added a column to Table 3 in the Methods section (line 229) summarizing the key hyperparameters used for the each algorithm in the study for classification-based ML models

Paper D: Peer Review Comments and Responses

Goldstein, D., Aldrich, C., Shao, Q., & O'Connor, L. (2025). Unlocking Subsurface Geology: A Case Study with Measure-While-Drilling Data and Machine Learning. *Minerals, 15(3),* 241. https://doi.org/10.3390/min15030241

Reviewer 1

Dear Authors,

The estimation of geotechnical properties using MWD data and ML techniques requests proper sampling, techniques for survey and appropriate application fileds (excavation, mass properties, geostructural data restitution). Algorithms can help to provide a pattern of joints that can be compared with results in terms of blast efficiency, contour quality and joint behaviour.

Comment 1: *Too many keywords, some are generic: Artificial Intelligence (AI); Machine Learning (ML); Geotechnical Engineering;*

Response 1: We have revised the keyword list to focus on more specific terms directly related to the study's scope. Generic keywords such as "Artificial Intelligence (AI)," "Machine Learning (ML)," and "Geotechnical Engineering" have been removed. We have replaced with more precise descriptors including: Measure-While-Drilling (MWD) Geotechnical Characterization, Boruta-SHAP Feature Importance, Rock Mass Prediction, Machine Learning in Mining and Subsurface Geotechnical Modeling.

Comment 2: *Some points should be clarified: for example at line 491-492 the concept expressed should be more detailed.*

Response 2: We have expanded the discussion at lines 491-492 to provide additional details on the methodology and interpretation of results. The revision clarifies how Boruta-SHAP ensures statistical robustness in feature selection and its advantages over traditional methods.

The text added is as follows: Unlike PCA-based feature selection, which primarily identifies directions of maximum variance without necessarily ranking feature importance for predictive modeling, Boruta-SHAP ensures statistical robustness by comparing real MWD variables against shadow features. The method's reliance on Shapley values allows for the quantification of nonlinear feature interactions, preserving only the most informative variables while eliminating redundant or weak predictors. This enhances model interpretability, enabling the reliable identification of key MWD parameters that govern geotechnical conditions, ultimately supporting more effective decision-making in mine planning and slope stability assessments.

Comment 3: *Too many acronyms along the text, some should be omitted to let more fluent the paper.*

Response 3: We have reviewed and reduced the use of acronyms throughout the manuscript, ensuring clarity and readability. Unnecessary abbreviations have been replaced with full terms.

Comment 4: *Captions of fig. 12-13-14 - 15 should be extended*

Response 4: The captions for Figures 10-15 have been expanded to provide more explanatory detail, including descriptions of key trends, variables and implications for geotechnical characterization.

Comment 5: *Comment more about feasibility on GSI estimation, as Authors of the classification method have been cautious in the past year literature.*

Response 5: A dedicated response in the Discussion section on the feasibility of GSI estimation using MWD data has been added. We acknowledge caution include a critical evaluation of the limitations and potential applications of our approach.

The text added is as follows: The feasibility of estimating GSI, a calculated property, using Measure-While-Drilling data presents both opportunities and challenges. MWD variables, particularly bit air pressure, torque-to-penetration ratio and force-on-bit, exhibit correlations with GSI, offering potential for real-time, high-resolution rock mass characterization. However, GSI is inherently a visual classification system, making direct numerical mapping challenging, especially when structural features like joint spacing and weathering are not explicitly captured by drilling responses. Additionally, bit wear, operational variability and differences in spatial resolution between MWD datasets and traditional geotechnical logging introduce uncertainty in predictive models. To improve reliability, MWD-based GSI estimates should be validated against mapped discontinuities and geophysical data, with site-specific calibration of machine learning models. Despite these limitations, integrating MWD-derived GSI predictions into mine planning and slope stability models could enhance geotechnical decision-making by providing continuous, large-scale assessments of rock mass conditions.

Comment 6: *Porosity and UCS of rock: how can be evaluated and how they influence behaviour of joints?*

Response 6: We have expanded the discussion on how porosity and rock strength can be estimated using indirect MWD parameters. Additionally, we describe their influence on joint behavior.

The text added is as follows: Porosity and UCS significantly influence rock mass behavior and joint stability and while traditionally measured via core testing, they can be indirectly estimated using Measure-While-Drilling variables. High porosity typically correlates with lower rock strength, as increased void space weakens rock cohesion, often reflected in lower torque, penetration rate and force-on-bit values. Conversely, low-porosity, high-strength rocks exhibit greater resistance, requiring higher drilling energy. These variations impact joint behavior, with porous, low-UCS rocks developing persistent, open joints prone to shear failure, while high-UCS formations exhibit tighter, more discontinuous fractures. By integrating MWD-derived estimates with geophysical data and site-specific calibration, mine operators can improve geotechnical risk assessments and slope stability management, enhancing excavation efficiency and safety.

Comment 7: *Few references following the editorial rules, to focus on applications and importance of preliminary detection of properties also thanks to equipment performances:*

(a) Rock Classification Using Multivariate Analysis of Measurement While Drilling Data: Towards a Better Sampling Strategy, by Veena S. Vezhapparambu, in Minerals, DOI: 10.3390/min8090384

from the cited Madrid school of mining:

(b) Damage and contour quality in rock excavations for quarrying and tunnelling: Assessment for properties and solutions for stability, by Costamagna, E., in proceedings EUROCK 2021, doi 10.1088/1755-1315/833/1/012137

Response 7: The reference list has been updated to include the suggested papers:
(a) *Rock Classification Using Multivariate Analysis of Measurement While Drilling Data: Towards a Better Sampling Strategy* by Veena S. Vezhapparambu (DOI: 10.3390/min8090384).
(b) *Damage and Contour Quality in Rock Excavations for Quarrying and Tunneling: Assessment for Properties and Solutions for Stability* by Costamagna, E. (EUROCK 2021, DOI: 10.1088/1755-1315/833/1/012137).

These references have been cited in relevant sections to strengthen the discussion on the application of MWD data for preliminary geotechnical assessments.

Reviewer 2

Comment 1: *This study presents an application of Boruta-SHapley Additive ExPlanations (Boruta-SHAP) for geotechnical characterization using Measure-While-Drilling (MWD) data, enabling a more interpretable and statistically rigorous assessment of feature importance. Pit-scale Measure-While-Drilling (MWD) data was used to characterize geotechnical properties* *via regression-based algorithms. The results are plausible, confirming that MWD data could provide a high-resolution description of geotechnical conditions prior to mining leading to a more confident prediction of subsurface geotechnical properties. Therefore, the fragmentation from blasting as well as downstream operational phases, such as digging, hauling and crushing, could be improved effectively. Useful conclusions arise.*

Nevertheless, before it is accepted for publication some issues described below have to be answered.

Response 1: We acknowledge the reviewer’s comments and have incorporated clarifications, expanded explanations and additional references where needed. The revisions improve the clarity, rigor and comprehensiveness of our study.

Comment 2: It is written:

“The data used in this paper are the same as in Goldstein et al. [27,49,50] which aimed to predict wireline geophysical measurements, geochemical assay values and geotechnical categories from the same MWD dataset.”

Please answer the following questions:

Why were these data used and chosen?

Why not choose other data?

Explain this in detail.

It is written:

“The Marra Mamba Formation and Brockman Formation of the Hammersley Group were the deposits analyzed in this study, as they are the greatest sources of economic Pilbara iron ore [52].”

Please answer the following questions:

Why were these deposits chosen?

Why not choose other deposits, too apart from those two?

Explain this in detail.

Response 2: The dataset used in this study, derived from Goldstein et al. [27,49,50], was chosen as it was part of the first author's PhD project, which focused on enhancing orebody knowledge using Measure-While-Drilling data. This dataset was selected due to its high spatial resolution, extensive geotechnical characterization and the availability of validated ground-truth datasets (wireline geophysics, geochemical assays and geotechnical categories). These factors allowed for robust validation of MWD-based predictive models.

Additionally, this dataset was sourced from an active mining operation, ensuring its relevance to industry applications. Alternative datasets from other mining regions were not selected due to the lack of consistent geotechnical validation data or differences in drilling system configurations, which could introduce additional uncertainties. Given that this study is a continuation of the first author's PhD research, it builds on prior analyses and extends the methodology to improve geotechnical characterization through advanced feature importance techniques.

The Marra Mamba Formation and Brockman Formation were selected because they are among the primary sources of economic iron ore in the Pilbara region, representing distinct geotechnical domains within the Hammersley Group. These formations provide a well-characterized, high-volume dataset with contrasting rock strength and fracturing characteristics, making them ideal for testing feature selection methodologies. While including additional deposits could broaden the study's scope, this initial work aims to validate the methodology within a well-understood geological setting before expanding to more variable deposits.

Comment 3: *It is written:*

"The burden and spacing of the production blast holes averaged 7 meters and 8 meters, respectively."

Please answer the following questions:

Why 7 and 8 meters?

Why not other burden and spacing?

Explain this in detail.

Response 3: The burden (7m) and spacing (8m) were selected by the mine operator based on mine operational standards for optimizing blast fragmentation while minimizing overbreak. These values align with best-practice guidelines for iron ore mining in similar rock masses, balancing explosive energy distribution and excavation efficiency. Alternative spacing configurations were not considered in this study, as they require site-specific optimization beyond the scope of this research.

Comment 4: *It is written:*

"The results of this comparison (Table 2) demonstrate all models performed better with

the Engineered features, increasing R^2 by 10-40% and reducing RMSE by up to 40%."

Please answer the following questions:

Why did this happen with the Engineered features?

Why not with the Measured features?

Explain this in detail.

Change the following phrase to:

"Boruta-SHAP is derived from cooperative game theory, where the contribution of each

feature is computed as the marginal contribution across all possible feature ***subsets [47].****"*

Include the above changes accordingly, as they are proposed with the bold letters

Response 4: The following detailed explanation has been added in the section prior to Table 2:

Engineered features incorporate additional interactions between drilling parameters (e.g., torque-to-penetration ratios), which improve the predictive model's ability to capture non-linear relationships. The measured features alone do not fully describe rock variability, while engineered features reduce noise and enhance feature differentiation, improving model accuracy.

The suggested changes have been included with regard to bold letters.

Comment 5: *Change the following phrase to:*

"The similar skewness in both ***formations*** *suggests variable penetration resistance, likely due to bit wear, operator variability and changing rock properties along the borehole."*

Include the above changes accordingly, as they are proposed with the bold letters.

Response 5: This change has been incorporated as per the reviewer's request.

Comment 6: *It is written:*

"fob and tor are stronger predictors in BR, implying fractures are more mechanically induced, while in MM, structural factors likely dominate."

Please answer the following questions:

Why is this happening?

Why in MM structural factors likely dominate?

Explain this in detail.

Response 6: The following text has been added as an explanation to 3.1 MWD Exploratory Data Analysis in the Results section:

The Marra Mamba formation is characterized by a greater presence of pre-existing structural discontinuities (e.g., bedding planes, joints), which influence rock mass behavior more than mechanical drilling resistance. In contrast, the Brockman Formation has more competent, homogeneous rock where mechanical resistance dictates fracture behavior.

Comment 7: *Please answer the following questions:*

Are there any more publications to support that apart from those referred already?

Especially throughout the whole paper, there are matters referring to soils and drilling, in

which the following publication, since it seems to be relevant and helpful, should be used,

too:

- *https://doi.org/10.1007/s12667-023-00613-z*

Response 7: This reference (https://doi.org/10.1007/s12667-023-00613-z) has been reviewed and incorporated where relevant, particularly in discussions on drilling-based geotechnical characterization.

Comment 8: *It is written:*

"iii. bap emerged as the most significant raw feature, reinforcing the role of flushing pressure in geotechnical characterization."

Please answer the following questions:

Why has bap emerged as the most significant raw feature?

Why not other features be more significant?

Explain this in detail.

Response 8: A detailed explanation has been included in the discussion section, as follows:

Furthermore, bit-air-pressure was identified as a consistently high ranking important feature. This drilling variable plays a crucial role in clearing cuttings from the borehole, reducing friction and maintaining drilling efficiency. Variations in bap correlate strongly with rock mass competency, influencing both penetration efficiency and fracture response.

Comment 9: *Figure 10.*

At the X axis, what do the minus values represent compared to the positive values?

E.g. what does -20 value represent compared to +20 value?

Response 9: The following text has been added to section 3.1 to explain interpretation of SHAP values:

Negative SHAP values indicate that the corresponding feature reduces the predicted value of the target variable, while positive SHAP values increase the predicted outcome. The magnitude of SHAP values reflects the strength of influence on the model’s prediction.

Comment 10: *Figure 11*

At the X axis, what do the minus values represent compared to the positive values?

E.g. what does -15 value represent compared to +15 value?

Response 10: As indicated in Response 9, an explanation has been added to the text to explain interpretation of SHAP values.

Comment 11: *Figure 12*

At the X axis, what do the minus values represent compared to the positive values?

E.g. what does -4 value represent compared to +4 value?

Response 11: As indicated in Response 9, an explanation has been added to the text to explain interpretation of SHAP values.

Comment 12: *Figure 13*

At the X axis, what do the minus values represent compared to the positive values?

E.g. what does -2 value represent compared to +2 value?

Response 12: As indicated in Response 9, an explanation has been added to the text to explain interpretation of SHAP values.

Comment 13: *It is written:*

“The role of interaction-based variables further underscores these contrasting fracture behaviors.”

Please answer the following questions:

Why is this happening?

Why does the role of interaction-based variables further underscore these contrasting fracture behaviors?

Explain this in detail.

Response 13: The following explanation has been added to section 3.1.2 Feature Importance Boruta-SHAP - FPM:

Fracture behavior is influenced by the combined effects of multiple drilling variables rather than individual metrics alone. In the Brockman Formation, torque-related interactions (e.g., torque-to-penetration ratio) are dominant due to the rock's competency, where fractures develop primarily through mechanical resistance. In contrast, in the Marra Mamba Formation, interactions involving fob and rop play a larger role, as pre-existing structural discontinuities such as bedding planes and joints govern fracture propagation. These findings emphasize the non-linearity in fracture formation, while individual features provide some predictive power, their interactions enhance explanatory capability by capturing localized rock heterogeneity and stress redistribution. This supports previous research indicating that fracture initiation is a function of both drilling resistance and geological structure.

Comment 14: *Figure 14*

At the X axis, what do the minus values represent compared to the positive values?

E.g. what does -6 value represent compared to +6 value?

Response 14: As indicated in Response 9, an explanation has been added to the text to explain interpretation of SHAP values.

Comment 15: *Figure 15*

At the X axis, what do the minus values represent compared to the positive values?

E.g. what does -5 value represent compared to +5 value?

Response 15: As indicated in Response 9, an explanation has been added to the text to explain interpretation of SHAP values.

Comment 16: *Table 3*

Please answer the following questions:

- *Which software has been used for the regression analyses?*
- *Which model do the authors consider as better taking into account both R^2 and time?*

Response 16: The regression analyses were performed using MATLAB's Regression Learner Toolbox, as described in section 2.6 Regression-based ML Methods.

The following text was added to section 3.2 Regression-based ML Overview:

Considering both R^2 and computational efficiency, Random Forest was selected as the most balanced model, offering high accuracy with moderate computational time, making it suitable for operational deployment.

Comment 17: *Table 4*

Please answer the following questions:

- *Which software has been used for the regression analyses?*
- *Which model do the authors consider as better taking into account both R^2 and time?*

Response 17: As indicated in Response 16, the regression analyses were performed using MATLAB's Regression Learner Toolbox, as described in section 2.6 Regression-based ML Methods. Moreover, as in Response 16, a section has been added to explain the selection of Random Forest as the most balanced model.

Comment 18: *Table 5*

Please answer the following questions:

- *Which software has been used for the regression analyses?*
- *Which model do the authors consider as better taking into account both R^2 and time?*

Response 18: As indicated in Response 16, the regression analyses were performed using MATLAB's Regression Learner Toolbox, as described in section 2.6 Regression-based ML Methods. Moreover, as in Response 16, a section has been added to explain the selection of Random Forest as the most balanced model.

Paper E: Peer Review Comments and Responses

Goldstein, D. M., Aldrich, C., & O'Connor, L. (2024). Enhancing Orebody Knowledge using Measure-While-Drilling Data: A Machine Learning Approach. *IFAC-PapersOnLine, 58(22)*, 72-76. https://doi.org/10.1016/j.ifacol.2024.09.293.

Reviewer 1

Comment 1: *1.- In the caption of the figure, it should read 'Actual versus predicted values for...' instead of 'Actual versus predicted R2 values for...' to accurately reflect the content of the figure.*

Response 1: The authors appreciate the correction and have updated the figure caption as recommended.

Comment 2: *2.- The R2 values presented do not seem to align with the results depicted in Figure 2. Please review and ensure consistency between the reported R2 values and the corresponding data in the figure.*

Response 2: The authors appreciate this and have double checked the R^2 values against the figure. A correction was inserted for one of the figure's plot.

Comment 3: *3.-It would be beneficial to include more detailed information about the dataset used in the study, such as the number of samples and the partition used for training the models.*

Response 3: The authors have included number of datapoints in section 2.3 and the training vs testing split and cross-fold validation methods in section 2.5 as well as including testing R^2 results in Table 2.

Comment 4: *4.- It would be valuable to discuss the potential application of the proposed methodology for estimating geomechanical characteristics of the ore.*

Response 4: The authors have included a brief discussion of the value from forecasting geomechanical properties of rock using the techniques outlined in this study. Separate work focusing on this application is being prepared for publication.

Reviewer 2

Comment 1: *A discription of the structure of the ML models would be* *beneficial, or a description of the tools used to determine, for example, the number of nodes, layers, activation functions for NN the NN model. However the same would be useful for DT, SVM etc.*

Response 1: The authors appreciate the requested detail and have included a description of the ML model sub-type in section 2.5, such as Bagged Random Forests and Stepwise Linear Regression Models.

Comment 2: *It would also be useful if the data were split into training and testing datasets, so that the model performance could be validated using data that is not part of the training dataset.*

Response 2: The authors have included the training vs testing split and cross-fold validation methods in section 2.5 as well as including testing R^2 results in Table 2.